Collected Papers by H.G Midgley on the Mineralogy of Silicate Building Materials with additional papers

H.G Midgley

Ph.D.

1967

Collected papers by H.G. Midgley on the mineralogy of silicate building materials, with additional papers.

Paper No.

3. A Serpentine mineral from Kennack Cove, Lizard, Cornwall. H.G. Midgley. Mineral. Mag., 29, (212), 526-530, 1951.

4. Chalcedony and Flint. H.G. Midgley. Geol. Mag., 88 (3), 179-184, 1951.

5. The mineralogy of Blast furnace slag. R.W. Nurse and H.G. Midgley. Silicate Industriels, 16, (7), 211-217, 1951.

7. Mellilite from high alumina cement. H.G. Midgley. 3rd International Symposium on the Chemistry of Cement, Cement and Concrete Association, London, 515-516, 1952.

8. Composition of beta dicalcium silicate from a Dorset clinker. H.G. Midgley in R.W. Nurse. 3rd International Symposium on the Chemistry of Cement, Cement and Concrete Association, London, 75-76, 1952.

9. The Ferrite phase. H.G. Midgley. 3rd International Symposium on the Chemistry of Cement, Cement and Concrete Association, London, 140-141, 1952.

10. Studies on the Mellilite Solid Solutions. R.W. Nurse and H.G. Midgley. Journ. Iron and Steel Inst., 174, 121-131, 1953.

11. Thermal reactions of smectites. H.G. Midgley and K.A. Gross. Clay Min. Bull., 3, (16), 79-90, 1957.

12. A compilation of X-ray powder diffraction data of cement minerals. H.G. Midgley. Mag. Conc. Res., 9, (25), 17-24, 1957.

13. The composition of the ferrite phase in Portland cement. H.G. Midgley. Mag. Conc. Res. 10, (28), 13-16, 1958.

15. The staining of concrete by pyrite. H.G. Midgley. Mag. Conc. Res., 10, (29), 75-78, 1958.

16. A Sepiolite from Mullion, Cornwall. H.G. Midgley. Mag. Conc. Res., 12, (29), 75-78, 1958.

17. The mineralogy of some commercial vermiculites. H.G. Midgley and C.M. Midgley. Clay Min. Bull., 4, (23), 142-150, 1960.

18. Hydrothermal reactions in the lime rich part of the system $CaO-SiO_2-H_2O$. H.G. Midgley and S.K. Chopra. Mag. Concr. Res., 12, (34), 19-26, 1960.

19. Hydrothermal reactions between lime and aggregate fines. H.G. Midgley and S.K. Chopra. Mag. Conc. Res., 12, (35), 73-82, 1960.

22. X-ray diffraction examination of Portland cement clinker. H.G. Midgley, D. Rosaman and K.E. Fletcher. 4th International Symposium on the Chemistry of Cement, Bureau of Standards, Washington. 6[illegible]-74, 1962.

23. The composition of ettringite in set Portland Cement, H.G. Midgley and D. Rosaman. 4th International Symposium on the Chemistry of Cement, Bureau of Standards, Washington. 25[illegible]-262, 1962.

24. The mineralogical examination of set Portland cement. H.G.Midgley. 4th International Symposium on the Chemistry of Cement. Bureau of Standards, Washington. 47[illegible]-4[illegible], 1962.

25. The role of alumina and magnesia in the polymorphism of tricalcium silicate. H.G. Midgley and K.E. Fletcher. Trans.Brit. Cer. Soc., 62, (4), 917-937, 1963.

26. The formation and phase composition of Portland cement clinker. H.G. Midgley. Chapter 3, The Chemistry of Cement. Editor. H.F.W. Taylor, Academic Press, London, 1964.

27. Optical microscopy. H.G. Midgley and H.F.W. Taylor. Chapter 20, The Chemistry of Cement. Editor.H.F.W.Taylor, Academic Press, London, 1964.

28. The identification and determination of alite in Portland cement clinker. H.G. Midgley, K.E. Fletcher and A.G. Cooper. Analysis of Calcareous materials. Soc. Chem. Indust., monograph 18, 3[illegible]2-371, 1964.

29. Data on the binary system $3CaO.Al_2O_3$ - $Na_2O.8CaO.3Al_2O_3$ within the system $CaO-Al_2O_3$ - Na_2O. K.E. Fletcher, H.G. Midgley and A.E. Moore. Mag. Conc. Res., 17, 171-176, 1965.

30. D.t.a. - Contribution to discussion H.G. Midgley. Analysis of Calcareous materials. Soc.Chem.Ind., Monograph 18, 442,443, 1964.

31. Microscopic examination of cement clinker, contribution to discussion. H.G. Midgley. Analysis of Calcareous materials. Soc.Chem. Ind., Monograph 18, 390, 1964.

1. The Geology and Petrology of the Cockburn Law Intrusion Berwickshire. H.G. Midgley. Geol.Mag., 83, (2), 49-6[illegible], 1946.

2. An Upper Eocene Outlier at St.Ann's Hill, Chertsey. H.G. Midgley. Geol. Mag., 87, (4), 29[illegible]-[illegible]02, 1950.

6. A quick method of determining the density of liquid mixtures. H.G. Midgley. Acta Cryst., 4, (6), 565, 1951.

14. A further occurrence of phosgenite. H.G. Midgley. Mineral Mag., 31, (241) [illegible], 195[illegible].

20. A mineralogical examination of suspended solids from nine English rivers. R.F. [illegible], D. Rosaman and H.G. Midgley. Clay Min.Bull., 4, (25), 23[illegible]-242, 1961.

21. On the occurrence of [illegible] in Thames river gravel. H.G. Midgley. Amer.Min., 47, 404-40[illegible], 1962.

The Geology and Petrology of the Cockburn Law Intrusion, Berwickshire

BY

H. G. MIDGLEY

Reprinted from the GEOLOGICAL MAGAZINE, Vol. LXXXIII, No. 2.
March–April, 1946.

The Geology and Petrology of the Cockburn Law Intrusion, Berwickshire

By H. G. Midgley

1. Introduction

THE Cockburn Law intrusion is situated in that part of Scotland where many intrusions of both Caledonian and Carboniferous age form the Laws of the Lammermuirs. The intrusion has been known for many years and may have been visited by Playfair and Hall during the time of the controversy between the Plutonists and the Neptunists. Cockburn Law, one of the " Caledonian Granite " intrusions of the Southern Uplands, lies at the junction of Sheets 33 and 34 of the Geological Survey of Scotland, about three miles north of Duns. The intrusion forms the two hills of Cockburn Law 1,066 ft. O.D. and Stoneshiel Hill 723 ft. O.D. The hills are separated by a gorge formed by a meander in the Whiteadder Water.

The first good description is given by Stevenson (1849), he noticed the variability of the granite and even at that early date attributed the " marginal ' syenites ' (= diorites) to greywackes fused by the agency of the molten granite ". F. Walker in two papers (1925) and (1928) described the Cockburn Law intrusion together with other Southern Upland Intrusions. He describes the various rock types present, including a central basic hornblende-biotite-granodiorite, an intermediate ' monoclinic-pyroxene-diorite " and a marginal " quartz-hypersthene-porphyrite ". In one paper (1928) F. Walker gave two analyses for the granodiorite and the quartz-biotite-hypersthene-porphyrite. No detailed description of the petrography or of the field relationship of the various rock types is given.

The area has been mapped on a 6 in. to 1 mile scale, the mass is not well exposed, in places there are no exposures, being covered with grassland or ploughed land. The best exposures are to be found in the river cliffs of the Whiteadder Water, where it is possible to collect specimens showing the gradual transition of rock types on passing out from the centre of the intrusion. The hybrids are well exposed north of Law Plantation and on the summit of Cockburn Law. There are also fair exposures on the west side of Stoneshiel Hill. The rest is badly exposed, there being only

occasional weathered boulders surrounded by grass and heathland. It is nowhere possible to see the transitions in any one exposure.

The junction between the intrusion and the Llandovery country rock is not exposed, but it is possible to obtain evidence of the nature of the contact.

The intrusion can be divided into two broad groups :—

1. The uncontaminated acid intrusive rocks, adamellite, granite, and granophyric microgranite.

2. The hybrid diorites, resulting from contamination.

After consolidation of the main intrusion, continuation of igneous activity produced dykes in the surrounding Silurian rocks, and aplite veins in the main intrusion itself.

In this paper the method of formation of the hybrids is indicated, their age in relation to the main body of the intrusion fixed, and the source of material suggested. Variation of the uncontaminated part in relation to the cooling processes of the magma is also explained.

II. Adamellite and Granite

The adamellite and granite which form the core of the intrusion occur in the valley of the Whiteadder Water, flanking the sides of Cockburn Law to a height of about 650 ft. O.D.

The adamellite occurs in the bank of the Whiteadder Water near the southward bend of the river.

The granite forms the lower slopes of Cockburn Law and the slopes of Stoneshiel Hill.

1. *The Adamellite.*

In hand specimen the adamellite varies from coarse to medium in grain size, is red in colour, with some dark patches, chiefly hornblende.

Thin sections show it to be composed essentially of plagioclase, orthoclase, quartz, hornblende, and biotite.

The bulk of the plagioclase has a composition of approximately $Ab_{70}An_{30}$ (oligoclase-andesine), optically biaxial, positive. It occurs as euhedral and subhedral crystals, not large, about 2·0 mm. × 0·7 mm., showing repeated albite twinning. The orthoclase is badly decomposed, but occurs as euhedral crystals of about the same size as the plagioclase crystals. Some of the orthoclase crystals show Carlsbad twinning, but the majority show only badly decomposed cores, rimmed with clear orthoclase. The quartz is interstitial with few inclusions, and there is quartz around some of the feldspars showing crystal continuity. Biotite is abundant, pleochroic with X yellow, Y brown, Z vandyke brown, with a noticeable absence of haloes. The biotite is frequently decomposed to chlorite, which is pleochroic X yellow, Y pale green, Z green, biaxial. Hornblende is present as the green variety, X dark green, Y medium green, Z pale green, optically biaxial, positive Z : c 11°, 2V medium.

In this and all other rocks the accessory minerals were determined by crushing the rocks and separating with heavy liquids. The most common accessory mineral is apatite, some of which is green. All the grains are short and show crystal terminations. Zircon, showing good crystal shape,

occurs occasionally, but not so frequently as apatite. Very occasionally tourmaline is present.

The texture is best described as hypidiomorphic granular. Biotite and hornblende, which crystallized first, have been " eaten into " by some of the feldspars which have themselves crystallized with good euhedral forms, while quartz, which crystallized last, fills in the interstices.

There is a variation in the quantity of coloured mineral present in different parts of the adamellite intrusion, but an average composition by volume (determined by Shand's recording micrometer) is as follows: quartz 31·8 per cent, orthoclase 36·0 per cent, plagioclase 24·3 per cent, hornblende and biotite 18·2 per cent.

The name adamellite is based on the definition of Johannsen (1937), namely a rock with more than 5 per cent visible quartz, with orthoclase and plagioclase ratios ranging from 35 : 65 to 65 : 35, with coloured minerals. Such a rock compares with the tonalite of Gardiner and Reynolds (1932), who describe a tonalite as consisting of quartz with plagioclase, subordinate orthoclase, and biotite.

2. *The Granite.*

Hand specimens of the granite are very similar to those of the adamellite, but of a duller red colour, with less marked patches of coloured mineral.

In thin section the granite is composed essentially of orthoclase, plagioclase, quartz, biotite, and a little hornblende.

Orthoclase shows much decomposition, chiefly from the centre, but there are some euhedral crystals up to 2·6 mm. × 1·2 mm. The plagioclase is very acid and has a composition of $Ab_{90}An_{10}$ (oligoclase), there is some plagioclase with a composition near $Ab_{95}An_5$ (albite). The feldspar occurs as euhedral crystals up to 1·2 mm. × 0·4 mm., showing twinning on both albite and Carlsbad laws. Quartz is plentiful, clear with few inclusions, and occurs chiefly in the interstices between the plagioclase and orthoclase. The biotite is plentiful, pleochroic with X yellow, Y brown, Z almost black. The biotite frequently is replaced by chlorite, which is pleochroic with X pale yellow, Y pale green, Z green. There is also a little hornblende, X green, Y medium green, Z yellow, optically biaxial, positive Z : c 14°.

The most noticeable accessory mineral is zircon, which occurs as moderately well-shaped crystals about 0·1 mm. long, with a very high birefringence. Apatite is present, but sporadic. Some good apatite crystals can be seen enclosed in quartz. The occasional presence of tourmaline is noteworthy, indicating pneumatolysis.

The granite differs from the adamellite in containing an increased amount of orthoclase, and in the diminution of hornblende as an important coloured mineral, biotite being the more important coloured mineral in the granite.

The texture in the granite is similar to the adamellite, but as stated previously the orthoclase has formed larger euhedral crystals which are set in a mixture of euhedral and subhedral crystals of plagioclase, biotite, and hornblende, with interstitial quartz. An average composition of the granite is as follows: Quartz 15·7 per cent, orthoclase 64·6 per cent, plagioclase 4·2 per cent, coloured minerals 15·5 per cent.

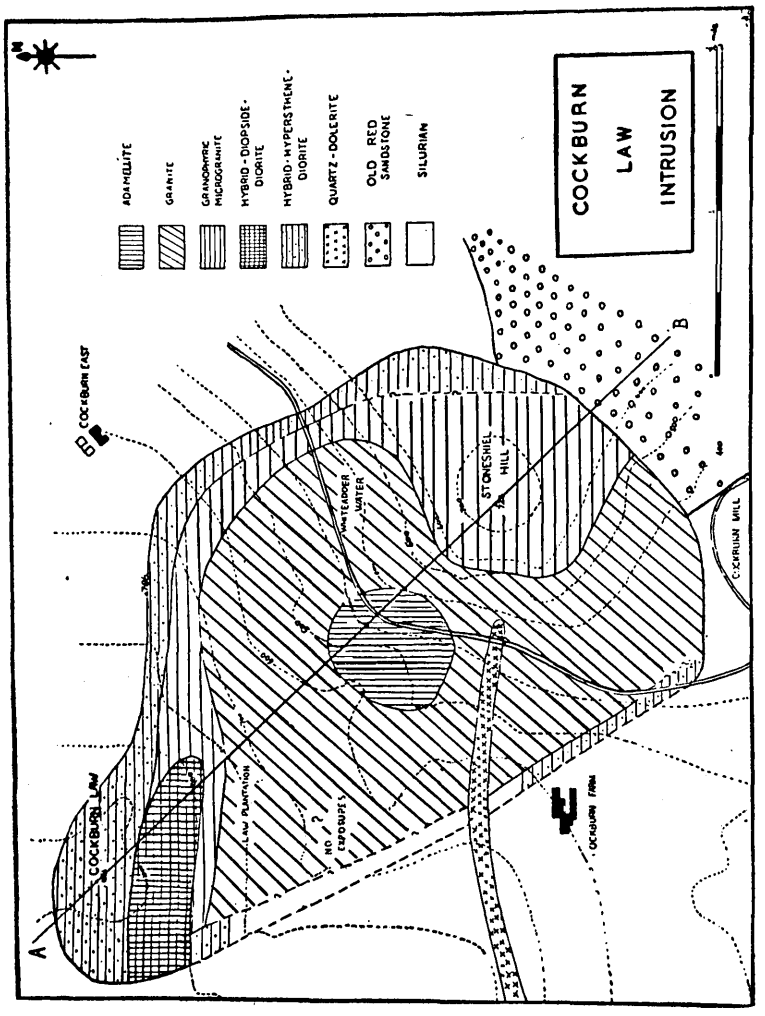
COCKBURN LAW INTRUSION
ADAMELLITE
GRANITE
GRANODIORITE MICROGRANITE
HYBRID - DIOPSIDE - DIORITE
HYBRID - HYPERSTHENE - DIORITE
QUARTZ - DOLERITE
OLD RED SANDSTONE
SILURIAN
COCKBURN EAST
COCKBURN LAW
STONESHIEL HILL
WHITEADDER WATER
COCKBURN MILL
A
B

TEXT-FIG. 1.

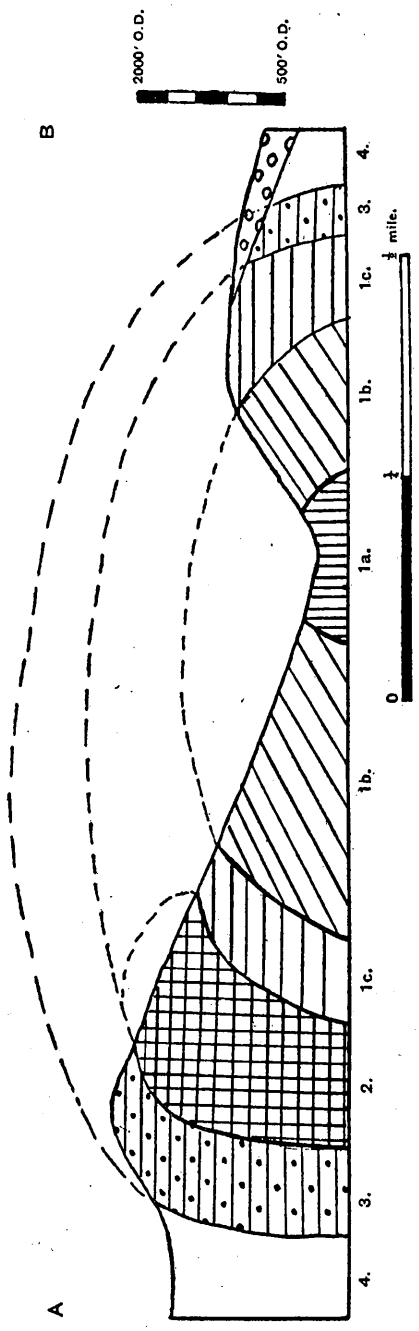

TEXT-FIG. 2.—Section through Cockburn Law and Stoneshiel Hill.

1a = Adamellite, 1b = Granite, 1c = Granophyric Microgranite, 2 = Hybrid Diopside Diorite, 3 = Hybrid Hypersthene Diorite, 4 = Silurian.

III. Granophyric Microgranite

The granophyric microgranite forms the cover and marginal parts of the uncontaminated igneous material. It is exposed at about 850 ft. O.D. on Cockburn Law and at about 625 ft. O.D. on Stoneshiel Hill, forming an arc round the north-eastern part of the granite.

In hand specimen the granophyric microgranite is medium-grained, pale brown to grey in colour, and shows abundant biotite.

In thin section it is composed essentially of quartz, orthoclase, plagioclase, and biotite.

The biotite occurs in what might be termed " skeletal " crystals, pleochroic with X yellow brown, Y brown, Z vandyke brown. Some of the biotite has decomposed to green chlorite, which often shows brown staining and is frequently acicular. The crystals of biotite show no sign of magmatic corrosion and may represent the phase where building up of the crystals was stopped by lack of material. Since the eutectic for quartz and feldspar had been reached the magma would be cooling rapidly. If the magma had been cooling more slowly the biotite crystals formed first might have been redissolved in the magma and then recrystallized as better developed crystals. In the granophyric microgranite the cooling was rapid and there was no time for re-solution, so the biotite had to remain as " skeletal " crystals.

The quartz occurs filling in the spaces between the decomposed subhedral orthoclase crystals. The plagioclase, composition about $Ab_{90}An_{10}$ (oligoclase), occurs as euhedral phenocrysts about 0·9 mm. × 0·4 mm., and there are smaller crystals of similar composition in the groundmass. There are also a few small crystals of hornblende, pleochroic with X green, Y medium green, Z yellow, Z : c 14°.

The accessory minerals are similar to those present in the granite, consisting of euhedral zircon up to 0·14 mm. in length, with some rounded grains enclosing " negative crystals ". Apatite, about 0·04 mm. in length, occurs, occasionally green in colour.

The texture is granophyric, though not the texture of a typical granophyre, since no good micropegmatite has been produced, but the occurrence of most of the quartz as scattered parts of large crystals all of which are crystallographic units, suggests that the rock is very near to a true granophyre.

IV. The Hybrid Rocks

There has been considerable contamination of the igneous magma by both igneous and sedimentary rocks, so that it is possible to classify the hybrids produced under two main headings, namely :—

1. Those due to contamination by igneous rocks and distinguished by the presence of xenoliths of a basic igneous rock, and by the occurrence of monoclinic pyroxene, diopside, such rocks hereafter being referred to as hybrid diopside diorites.

2. Those due to contamination by sediments and characterized by the occurrence of sedimentary xenoliths, " porphyroblastic " feldspars, and the orthorhombic pyroxene, hypersthene, such rocks being described as the hybrid hypersthene diorites. There is also a zone of rocks found

chiefly along the junction of the two main types, these rocks possessing characters common to types 1 and 2, i.e. showing both clino- and ortho-pyroxene. These rocks are referred to as hybrid pyroxene diorites. The name hybrid diorite has been used in preference to others, since it indicates the nature of the rock.

1. *Hybrid Diopside Diorite.*

The contamination of the original magma by basic igneous rock has produced varying types of rock, but all are characterized by the presence of clino-pyroxene. The hybrid diopside diorite forms a small outcrop just below the summit of Cockburn Law. In hand specimen they are pale grey, fine to medium in grain size, with a variable amount of coloured mineral, the latter usually prominent. The contaminating basic material appears to be represented by xenoliths occurring in the hybrid diorite, and these are described below.

(*a*) *The Xenoliths.*—The xenoliths are chiefly remnants of a basic igneous rock, seen in the hand specimen as black clots, which on microscopic examination are found to be aggregates, recognizable as being of primary igneous rock structure. There are also detached and corroded crystals (xenocrysts) which are in a partial stage of absorption by the " parent magma ".

The xenoliths consist of well-formed crystals of titaniferous augite, with a little olivine, biotite, and plagioclase. The augite occurs as semi-prismatic crystals, with rounded corners, often with an outer rim of pale green " augite " flecked with magnetite. The augite is of a pale plum colour, optically biaxial, positive, Z : c 40°. It occasionally contains a core of colourless clino-pyroxene. The olivine is colourless and decomposed along cracks. Plagioclase is not present in any large amount, but shows lamellar twinning.

The above rock assemblage suggests an original basic rock of composition approximately that of a picrite or gabbro according to the original feldspar content which is indeterminable from the relic material. Since the composition of the original basic rock might have varied it is not possible to suggest a composition for the original " parent magma " which has suffered contamination.

(*b*) *Petrology of the Hybrid Diopside Diorite.*—In thin section the hybrid diopside diorite shows biotite, clino-pyroxene (diopside), hornblende, and plagioclase as porphyritic crystals, the groundmass consisting of epidote and quartz together with coloured minerals and feldspar.

The biotite occurs as small crystals, pleochroic with X yellow, Y brown, Z vandyke brown ; some being particularly ferriferous, often associated with magnetite, and in this case the biotite has X red-brown, Y brown, Z vandyke brown. Biotite is frequently replaced by green chlorite. Biotite also occurs as the third component of coronas, consisting of pyroxene, hornblende, and biotite.

The clino-pyroxene, which occurs as well-formed prismatic crystals elongated along c axis, is usually colourless or very pale green, non-pleochroic, optically biaxial, positive, Z : c 42°, a diopside, probably malacolite.

The hornblende occurs chiefly as small crystals about 0·2 mm. in size,

but these may form aggregates up to 1·2 mm., and may also form aggregates around the pyroxene.

The plagioclase phenocrysts show good euhedral form, with twinning on both albite and pericline laws. They have an average composition of approximately $Ab_{55}An_{45}$ (labradorite). Optically biaxial and positive. Laths of feldspar of similar composition, but very much smaller, occur in the groundmass.

Quartz occurs in the groundmass as small grains associated with the feldspars. Grains of epidote also occur, being probably derived from the hornblende.

Accessory minerals include zircon, usually well shaped but occasionally rounded, and apatite, some of which may be dark cored.

The rock is essentially medium grained and porphyritic. The presence of the diopside together with the quartz and feldspar is curious, but in view of the occurrence of augite in the xenoliths the origin of the diopside and the other minerals might be accounted for by reactions such as those indicated below :—

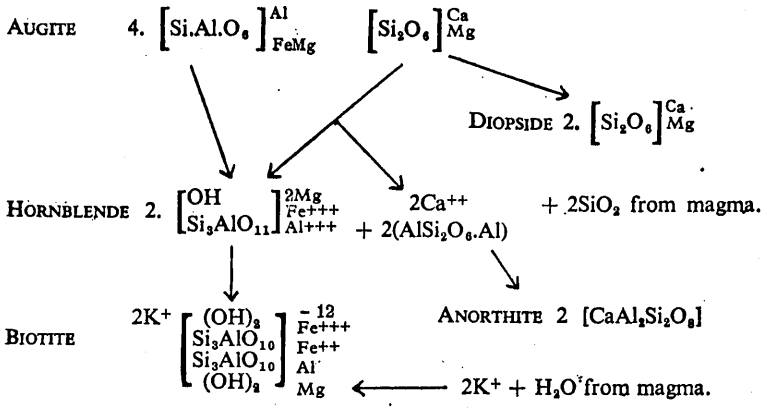

These reactions are comparable with the latter half of the discontinuous reaction series of Bowen (1928).

The net result is the addition of Ca^{++} and Al^{+++} to the "parent-magma", which loses potential K^+ to the biotite, thus Ca^{++} and Al^{+++} are available to produce the anorthite molecule $CaAl_2Si_2O_8$. The loss of potential K^+ in the magma means a decrease in the quantity of potential orthoclase that can be formed. Plagioclase will therefore replace orthoclase in the rock produced from the parent-magma. SiO_2 will be required from the magma to build up the plagioclase with the material released from the augite, and so there will be less silica available in the "mixed-magma" for the formation of free quartz.

Thus it may be assumed that part of the hybrid diopside diorite is produced by the pure assimilation of a basic igneous rock, where augite and olivine have given rise to the diopside, hornblende, and biotite, while the plagioclase together with the plagioclase formed from the coloured

minerals form the potential plagioclase in the " mixed-magma " ; a plagioclase more basic than that which would have been formed by the original " parent-magma ", and more acid than that of the original basic rock.

2. *Hybrid Hypersthene Diorite.*

Contamination of igneous magma by sediments has been much more widespread than contamination by igneous rock. The hybrid hypersthene diorite forms a narrow outcrop around the circumference of the intrusion.

In hand specimen it is almost black and very difficult to distinguish from the surrounding biotite cordierite hornfels of the country rock. It contains occasional xenoliths of sedimentary origin, usually larger than the basic igneous xenoliths found in the hybrid diopside diorite. Smaller included fragments, described below, too small to be seen with the naked eye, are revealed in thin section and these xenoliths, large and small, suggest the nature of the contaminating material, viz. biotite cordierite hornfels.

(*a*) *The Xenoliths.*—In thin section these consist of spinel, cordierite, and biotite, with occasional plagioclase.

Biotite is the most plentiful mineral, occurring as small plates ; associated with green spinel, probably pleonaste. This spinel occurs occasionally as well-formed crystals, showing octahedron and cube faces, and also as geniculate twins apparently twinned on the octahedron. Most of the spinel, however, occurs as small rounded grains set in the biotite and cordierite. Cordierite is common, clear, and occasionally shows sector twinning. These xenoliths correspond with Class 3*a* of the silica-poor derivatives of Tilley (1924).

The marginal portions of the xenoliths are composed of cordierite and biotite alone. The absence of spinel in the proximity of the igneous rock seems to indicate that SiO_2 has passed from the magma to the xenoliths.

There are also many clots of small red biotite grains, which, although not large enough to be called xenoliths, and being aggregates cannot be called xenocrysts, must be attributed to the incorporation of biotite hornfels.

(*b*) *Petrology of the Hybrid Hypersthene Diorite.*—In thin section the hybrid hypersthene diorite consists of hypersthene, hornblende, biotite, plagioclase, epidote, and quartz.

The plagioclase is of three types : zoned phenocrysts, up to 1·8 mm. × 0·8 mm., small crystals in the groundmass, and what may be called " porphyroblastic feldspars ".

The plagioclase phenocrysts have an average composition about $Ab_{70}An_{30}$ (oligoclase-andesine), and are often zoned. They are optically biaxial, negative. The crystals frequently show elongation by secondary growth forming longer crystals, with the limits of the original crystal clearly defined. None of the secondary growths show zoning.

The plagioclase in the groundmass occurs as small lath-shaped crystals showing lamellar twinning. The composition of the crystals is similar to that of the phenocrysts.

The " porphyroblastic " plagioclase crystals are of interest as they seem to represent crystals which have grown from the included sedimentary

material. They are generally irregular in outline, some showing poor twinning, but some grains better shaped show twinning good enough to indicate the nature of the feldspar. In these feldspars the composition varies from $Ab_{60}An_{40}$ (andesine) to $Ab_{50}An_{50}$ (labradorite). They always contain included crystals, frequently aligned parallel to the pinacoids. These small inclusions consist chiefly of biotite, a pale green pyroxene (noted by Gardiner and Reynolds (1932) in the Loch Doon Granite area, Galloway), magnetite, and finely divided opaque material. Other feldspars contain some of the above inclusions together with sillimanite needles.

Some well-shaped " porphyroblastic " plagioclase crystals have granular cores, as if an aggregate of plagioclase crystals had formed a nucleus for a plagioclase crystal to grow. These may or may not contain included crystals.

Hypersthene usually occurs as prismatic crystals. It is pleochroic, X pink, Y yellow, Z green, optically biaxial, negative 2V large.

Hornblende occurs in small irregular patches, chiefly as granular aggregates, mainly associated with biotite, but also around the hypersthene.

Biotite occurs as small crystals, irregular in shape, pleochroic, X yellow, Y brown, Z dark brown.

Epidote occurs as small crystals, probably as a decomposition product from hornblende.

The groundmass consists of an aggregate of quartz and plagioclase, the size of the grains ranging from 0·25 mm. to 0·1 mm. in length.

Among the accessory minerals, apatite and a few rounded zircon crystals are the commonest.

The texture is that of a porphyritic medium-grained rock. The phenocrysts consist of both coloured minerals and plagioclase. The coloured minerals often show coronas representing components of a reaction series, with hypersthene as the core, surrounded by successive rims of hornblende and biotite. This type of structure, together with the patchy nature of the rock, is evidence of rapid cooling (cf. Read, 1935).

The production of the hybrid hypersthene diorite follows the process of granitization as set out by MacGregor (1938). The hypersthene has been produced from the metamorphosed clay-grade material. The " porphyroblastic " plagioclase crystals in the hybrid are probably the product of the assimilation of the cordierite present in the biotite cordierite hornfels country rock. The composition of the latter is described in a later section of the paper.

3. *Hybrid Pyroxene Diorite.*

The rocks at the junction of the two main types of hybrids contain both diopside and hypersthene, and combine the characters of the two main hybrids.

The fact that three types of hybrids occur, one a transition type between the other two, suggests that assimilation happened once only and this is confirmed by the lack of evidence of either type of hybrid being included in the other.

The process of assimilation which produced the various hybrid rocks is shown diagrammatically as follows :—

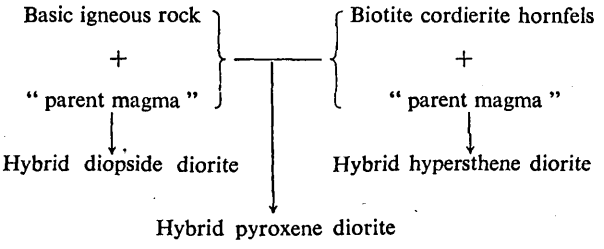

Plagioclase Present in the Igneous Rocks.

Adamellite	$Ab_{70}An_{30}$
Granite	$Ab_{90}An_{10}$
Granophyric microgranite .	$Ab_{90}Ab_{10}$
Hybrid diopside diorite . .	$Ab_{55}An_{45}$
Hybrid hypersthene diorite .	$Ab_{70}An_{30}$

As is to be expected, the plagioclase in the adamellite is more calcic than the plagioclase of the granite and granophyric microgranite. The hybrid hypersthene diorite contains plagioclase of similar composition, but the hybrid diopside diorite contains a very much more calcic plagioclase. This appears to support the suggestion that the hybrid diopside diorite is the product of basic rock assimilation.

V. Metamorphism of the Country Rock

In the vicinity of the intrusion there is a progressive change in the grade of metamorphism of the Silurian shales and greywackes, which constitute the country rock. The normal Silurian rock is a pelite in which the only clastic mineral represented is quartz, which occurs as very small grains, the remainder consisting of a fine-grained mass of scales of white mica and what Harker (1919) refers to as " paste " or " base ", which may be regarded as kaolin with some chlorite. The white mica can be assumed to be sericite. The greywacke consists of grains of quartz set in a matrix of chlorite and green mica and fine " silty " material of similar composition to the pelite.

The lowest grade of metamorphism is found about three or four hundred yards away from the intrusion. This grade consists of anhedral grains of quartz, of two sizes, 0·2 mm. and 0·005 mm., rounded patches of cordierite in a mixture of chlorite and green mica (biotite). It is the product of pure thermal (or contact) metamorphism with no addition of material from the magma, since the biotite and chlorite present in larger crystals than in the shale or greywacke, could be produced from the white mica (sericite), chlorite, and iron ore present in the original rock. The kaolin in the base, together with some of the chlorite, produced cordierite, while the remaining mineral, quartz, could have been produced from the recrystallization of the excess of silica (either from the pelite or from the quartz grains in the greywacke) by means of the heat supplied from the intrusion.

On passing inwards from this low-grade metamorphic zone there is an increase in grade shown by the following stages :—

(*a*) Production of ordinary brown biotite as small rounded grains, together with quartz and cordierite.

(*b*) Biotite becoming larger and lath-shaped and showing cleavage.

(*c*) An increase in the quantity of biotite and cordierite at the expense of quartz.

(*d*) Formation of a biotite-cordierite rock consisting of many small grains of biotite set in clear patches of cordierite, the outline of the latter being determined by the larger biotite crystals. In this rock there is a conspicuous absence of quartz. It must represent a stage not far removed from mobilization. All the rocks of stages *a-d* may be termed biotite cordierite hornfels.

This progressive change in metamorphic grade from biotite cordierite hornfels to a rock consisting of biotite and cordierite, veined with igneous material, which then grades into hybrid hypersthene diorite (a diorite of abnormal type inasmuch as it contains much hypersthene) containing numerous xenoliths of hornfels, suggests that in a narrow region round the intrusion there has been " mechanical mixing " of country rock and igneous magma indicating granitization of the Llandovery country rock.

VI. The Structure of the Intrusion

1. *Structural Features.*

The exposed portion of the intrusion is only about three-quarters of a square mile in area. It is roughly triangular in shape, with the apex pointing north-west.

The form of the intrusion is best seen in the valley of the Whiteadder Water near to Cockburn East. Although there is no sharp line of demarcation between the country rock and the intrusion here, the progressive change from one to the other can be demonstrated between 600 ft. O.D. and 400 ft. O.D. on both sides of the Whiteadder Water. In the river bank west of Cockburn Mill the Llandovery greywackes can be seen in contact with the granite, and here the junction is almost vertical. From this it is apparent that the junction is steep-sided and so the intrusion may be called a boss, but owing to the " layered " succession the intrusion has the appearance of a sheeted mass. Since there is no evidence of the presence or the absence of a floor, it seems best to assume that the intrusion is a steep-sided boss, made up of sheets around a central core.

In the few exposures in the Llandovery rocks which surround the boss on three sides there is no sign of any lifting of the sediments, as the " cleavage " of the beds, where seen, is always parallel to the margin of the intrusion. This is to be expected if the outer ring of the intrusion is the product of assimilation of country rock by acidic magma.

The boss has been little disturbed since its injection in " Caledonian " times, but it may have been tilted a little since Upper Old Red Sandstone times. This is suggested by the following facts : the Old Red Sandstone conglomerates in the bank of the Whiteadder Water, opposite Cockburn Mill, are dipping south, as are the Upper Old Red Sandstone beds around Preston, where, however, the dip is less. This dipping of the Upper Old

Red Sandstone beds suggests that the boss, together with the country rock, has been slightly tilted southwards since its intrusion.

2. *Jointing.*

There is no large scale jointing in the igneous rocks, but some very minor joints can be seen. They are best exposed in the granophyric microgranite which is found west of Law plantation and also half a mile due south of Cockburn East, on either side of the Whiteadder Water. In some rock masses the joints are seen occurring at right angles, often at $10\frac{1}{2}$ in. intervals ; and this has led to the production of some roughly cuboidal masses such as are found on Cockburn Law. Vertical jointing is seen on a larger scale in the adamellite, and these joints have been invaded by products of later pneumatolytic activity, such as greisen, described later. The small scale jointing in the blocks found on Cockburn Law is roughly aligned in direction with the strike of the Silurian sediments around the intrusion so that the jointing observed seems to form part of a concentric and radiating system. This may be due to the cooling of the hybrids, partly induced by contact with the cold sediments.

3. *Order of Intrusion.*

It seems probable that the major intrusion began with the injection of a basic rock which consolidated in place. This was followed by the intrusion of the main acid magma, which by assimilation produced the hybrid diorites, and by slow cooling produced the adamellite, granite, and granophyric microgranite. The assimilation of the country rock to give the hybrid hypersthene diorite was the result of the stoping of the roof and walls of the boss. This action, i.e. the breaking up of the country rocks and their flotation in the intruding magma, has produced a zone of " mobilization " (see MacGregor (1938)) round the margin of the intrusion. This conclusion follows from the evidence of the progressive granitization of the Silurian sediments to produce the hybrid hypersthene diorite. The heat lost in warming the surrounding sediments and fusing the material assimilated by the magma would cool the outer margin of the magma in the intrusion rapidly and considerably ; thereby chilling the margin of the igneous rock sufficiently to solidify it. Such rapid cooling is borne out by the nature of the rocks present round the margin of the boss, which are all medium-grained and also by the " patchy " nature of the rock together with the coronas described earlier in this paper. This chilling would only affect the thin skin of the magma next to the roof and walls of the boss, and so the major portion of the magma below would be able to cool under more normal conditions, and produce rocks of coarser grain.

4. *Variations in Composition.*

The variation of the rock types of Cockburn Law may be summed up as follows :—

(*a*) The centre of the intrusion is a hornblende adamellite, which represents a more basic type than : —

(*b*) The granite which surrounds the adamellite and forms the major part of the intrusion.

(*c*) The granophyric microgranite, which forms the outer part of the uncontaminated rock suite.

(*d*) The hybrids, which form the outer ring of the whole intrusion, and were formed first.

After the hybrids were formed, the main part of the magma began to cool slowly. The adamellite would be formed, by gravity separation, as the lowest portion. As shown by the outcrops there is a progressive acidification of rock types from the adamellite through granite to granophyric microgranite, which is largely an eutectic mixture of quartz and feldspar.

VII. Probable Relationship to other " Caledonian " Granites

The Cockburn Law intrusion is one of the " Caledonian " intrusions of the Southern Uplands, and it probably represents a cupola from a bathylith belonging to a series of deep-seated igneous masses which extend south-west or west, perhaps under much of the Southern Uplands and possibly into Ireland. The similarity of the intrusion to those of Priestlaw, Criffel-Dalbeattie, Loch Dee, Cairnsmore of Carsphairn, Dhoon (Isle of Man), and Newry, is marked and is described below.

Priestlaw, the nearest intrusion to Cockburn Law, described by Geikie (1910), pp. 22–3, consists of biotite granite, hornblende biotite granite (? adamellite), and fine-grained more basic varieties (= hybrid diorite) near its margins.

Criffel-Dalbeattie, the largest of the Southern Uplands intrusions, described in great detail by MacGregor (1937), consists of a tonalite with a marginal quartz diorite, the latter being ascribed by MacGregor to assimilation of country rock in the " parent magma ". In his description of xenoliths MacGregor states that many are of undoubted sedimentary origin, but for some he does not suggest a composition, and from the description of these xenoliths, which appear to be similar to the igneous rock xenoliths described in this paper, it may well be that they represent relic material from a basic rock.

The Loch Dee (or Loch Doon) granite also provides evidence for the presence of basic rock, as Gardiner and Reynolds (1932) describe norite which crops out in the north-west of the complex, which has produced a quartz norite by contaminating the " sub-magma ". Contamination of this " sub-magma " by sediments has produced a marginal tonalite, which is crowded with sedimentary xenoliths. The " hybrid " tonalite also contains " porphyroblastic " feldspar crystals with many inclusions besides corona-structures and a patchy nature regarded as evidence of quick cooling. The central core of the intrusion is acid intrusive rock, while corresponding to the hybrid diopside diorite and hybrid hypersthene diorite of Cockburn Law are quartz norite and tonalite.

W. A. Deer (1935), in his description of the Cairnsmore of Carsphairn igneous complex, refers to a basic rock, gabbro, as having been contaminated to produce hybrids, but suggests an intermediate stage, quartz norite, which he considers to have been produced from the gabbro by addition of SiO_2 and Al_2O_3. Pyroxene-biotite-hybrids he regards as

having been then produced from the quartz norite by further contamination.

The Dhoon (Isle of Man) intrusion consists of a microgranite which has been injected into a gabbro to produce intermediate hybrid rocks, and Nockolds (1931), having evidence of the gabbro, has suggested that the hybrid intermediate rocks are the products of contamination of the invading granite magma by the gabbro and sediments already present before intrusion.

Newry has furnished great opportunity for investigation of the methods of formation of hybrids, and D. L. Reynolds (1934) has described the occurrence of ultrabasic rocks, peridotite, and biotite-pyroxenite. Augite biotite diorite, augite monzonite, and hypersthene monzonite, found near the western border of the Newry complex, are similar to the hybrids of Cockburn Law. The main mass of the Caledonian intrusion is a granodiorite.

A. G. MacGregor (1930) describes the Distinkorn complex in detail. He finds a central pink or red granodiorite, surrounded by " altered dioritic rock " ; which consists of dioritic rocks with fresh monoclinic pyroxene, diorite with fresh rhombic and monoclinic pyroxene, and suggests that these diorites have been magmatically metamorphosed by the granodiorite, and were therefore present previous to the intrusion of the granodiorite. He suggests that the rocks present before the intrusion of the granodiorite were also diorites.

The similarity of Cockburn Law to each of these intrusions is apparent, the hybrids which are produced being similar if not identical in type. Some variation would be expected since the contaminating basic and sedimentary rocks are not the same in each case. The basic rock known at Dhoon and Cairnsmore of Carsphairn is a gabbro ; at Newry a peridotite and biotite pyroxenite ; at Loch Dee a norite, and at Distinkorn a diorite. It is possible that some of the quartz-norite of Cairnsmore of Carsphairn may represent a similar stage as the hybrid-diopside-diorite of Cockburn Law, since at Cairnsmore of Carsphairn the contamination by gabbro produced hypersthene whereas at Cockburn Law contamination by basic rock produced diopside.

Moreover, in all the above cases there is a general resemblance in structure and products, namely an acid magma rising and being contaminated by basic (or ultrabasic) rock and by sediments to produce an outer zone of contaminated or hybrid intermediate rock, and a central mass or core of acid rock.

Whatever the age of the basic rock, its occurrence in so many areas preceding the intrusion of acid material suggests a common source for both basic and acid magma, and this has suggested to A. G. MacGregor (1930) the occurrence of a large bathylith or series of bathyliths in a Caledonian direction from Newry to the Firth of Forth.

It should be pointed out that one of the largest " Caledonian " intrusions of the Southern Uplands, i.e. Cairnsmore of Fleet, does not resemble any of the above complexes. The Cairnsmore of Fleet granite which invaded Llandovery sediments, as described by Gardiner and Reynolds (1937), shows no evidence of contamination by basic material.

The Cheviot mass resembles the above complexes in part, since it

consists of a central core of granite surrounded by a shell of granophyre, succeeded by hybrid rocks which Jhingran (1943) believes to be due to contamination of acid magma by Silurian sediments.

VIII. The Age of the Intrusion

It is not possible to date the intrusion exactly, but its age can be fixed within certain limits. The granite was intruded into Silurian rocks, since it has metamorphosed sediments of Llandovery age. It is therefore post-Llandovery. The rocks next in the stratigraphical succession found in the area are the Upper or Great Conglomerates of the Upper Old Red Sandstone, which are seen resting on the boss just north-east of Cockburn Mill. The intrusion is therefore pre-Upper Old Red Sandstone age. Confirmatory evidence is provided by the fact that these conglomerates contain numerous pebbles of the granite, especially the conglomerates near Preston, a point noted by Geikie (1910).

There are no lavas, but such may have existed and since been eroded, since the boss must have been exposed to denudation before Upper Old Red Sandstone times.

Later minor intrusions can be found cutting only the Silurian, so that the whole of the cycle was complete before the deposition of the Upper Old Red Sandstone. By analogy with other intrusions it is likely that the Cockburn Law intrusion belongs to the Lower Old Red Sandstone period.

IX. Minor Intrusions and Late Stages of Igneous Activity

There was considerable activity after the consolidation of the main plutonic mass. This activity falls into three main classes :—

1. Pneumatolytic effects in the intrusion and surrounding sediments.
2. Formation of aplite veins in the intrusion.
3. Intrusion of dykes into the surrounding sediments.

1. *Pneumatolytic Activity.*

Pneumatolysis is seen chiefly in the products which are found in the numerous vertical joints occurring in the adamellite. These products include barytes, associated with quartz, in veins running W.S.W.–E.N.E. The granite has itself been acted upon a little, as shown by the presence of tourmaline in the heavy mineral separations, but the action was very slight, since no tourmaline has been seen in any of the thin sections examined. Stevenson (1849) refers to galena and copper-pyrites which were found in the intrusion near the top of Stoneshiel Hill, and these minerals are probably products of pneumatolytic action.

Other evidence of pneumatolytic activity is found in the Silurian sediments. This activity is difficult to trace, but copper lodes and mines are known to have existed, the evidence being place names on Ordnance Survey maps, which indicate the localities of some of the old copper mines. A mine is marked on the map published by Stevenson (1849) and in the text he refers to the occurrence of malachite. The original copper ore was probably associated with the late-stage activity accompanying the consolidation of the intrusion.

Of great interest is some of the material found in a vertical joint in the

adamellite in the bank of the Whiteadder Water, near its southward bend. This joint contains a vein about 2 inches wide, consisting of a hard reddish-brown rock, of two parts, the outer a mixture of quartz and limonite ; and the inner portion a curious assemblage of minerals, comprising quartz, colourless mica, and a little topaz and limonite. The colourless mica occurs as whisps showing good cleavage, very often pseudomorphed by the quartz, which has taken on the original basal cleavage of the mica. The quartz also occurs as anhedral grains set in the groundmass, the latter consisting of small quartz grains and a felted mass of colourless mica. The topaz is not common, occurring as rounded colourless grains optically biaxial and positive. This rock, consisting of quartz and colourless mica with a little topaz, could be called a greisen and so regarded as a definite product of pneumatolysis.

2. *The Aplite Veins.*

The plutonic intrusion has been invaded by many small veins of aplite ranging from veins about 0·004 in. up to 3 in. in width, the majority being about 0·3 in. These are most common in the hybrids near the summit of Cockburn Law, where they occur aligned parallel to the minor joint planes.

In hand specimen the aplite is medium-grained and of a pale pinkish yellow, weathering pink. In thin section it consists of quartz and orthoclase with a very little dark mica. In the larger veins some sections show a complete absence of any coloured mineral. The orthoclase is decomposed while the quartz is clear with few inclusions.

Often associated with the aplite veins are veins of clear crystalline quartz, some of which may be traced up to 20 inches in length, usually parallel to a joint plane. These quartz veins probably represent the residuum from the magma which produced the suite of rocks in the major plutonic intrusion.

3. *Minor Intrusions.*

The minor intrusions can be divided into two main groups, the acid intrusives and the lamprophyres. The acid intrusions are represented by quartz porphyries. They occur as dykes with a general N.E.–S.W. trend, this direction following the folding and strike of the Silurian, but nowhere do they cut the boss.

It is probable that the lamprophyres, also dykes with similar strike, represent material differentiated from the magma which gave rise to the aplite veins.

Cutting the intrusion and running east-west for about a mile, from Cockburn Dean to the Whiteadder Water, is a quartz dolerite dyke, but this by analogy with other quartz dolerite dykes is of Carboniferous age and is therefore not dealt with in this paper.

X. Summary

The Cockburn Law intrusion is a small sheeted boss of late Caledonian age, intruded into Silurian rocks of Llandovery age.

The following are the chief stages in its formation :—

1. The earliest igneous activity was the intrusion of basic rock, now only found as xenoliths. This intrusion was followed at some later stage by—

2. The main plutonic magma which assimilated the basic rock and country rock to produce the following hybrids—

(*a*) Hybrid hypersthene diorite, from contamination by the Silurian pelites and greywackes.

(*b*) Hybrid diopside diorite, from contamination by the basic rock.

(*c*) Hybrid pyroxene diorite, from contamination by material from both basic igneous and sedimentary rocks.

3. After the consolidation of the marginal hybrids the main body of the magma began to solidify, but had time to differentiate in place to give a composition ranging from adamellite through granite to granophyric microgranite.

4. The heat from the intrusion metamorphosed the Silurian sediments to biotite cordierite hornfels which grade insensibly into the hybrid hypersthene diorite.

5. Following the consolidation of the plutonic mass there was considerable activity by vapours to form pneumatolytic products, while differentiation of the residual magma produced the aplitic, acidic, and lamprophyric dykes.

The intrusion may form a cupola from a bathylith, which may possibly belong to a series of bathyliths lying in a Caledonian direction from Newry to the Firth of Forth.

XI. List of Works to which Reference is Made

Bowen, N. 1928. *The Evolution of the Igneous Rocks.* Princeton. p. 60.

Deer, W. A. 1935. The Cairnsmore of Carsphairn Igneous Complex. *Quart. Journ. Geol. Soc.*, xci, 47.

Gardiner, C. I., and Reynolds, S. H. 1932. The Loch Doon Granite Area, Galloway. *Quart. Journ. Geol. Soc.*, lxxxviii, 1.

—— —— 1937. Cairnsmore of Fleet Granite and Metamorphic Aureole. *Geol. Mag.*, lxxiv, 289.

Geikie, and others. 1910. The Geology of East Lothian. *Mem. Geol. Surv. Scotland.*

Harker, A. 1919. *Petrology for Students.* 7th edn. p. 219. Cambridge.

Jhingran, A. G. 1942. The Cheviot Granite. *Quart. Journ. Geol. Soc.*, xcviii, 241.

Johannsen, A. 1937. *Petrography*, II. p. 208. University of Chicago Press.

MacGregor, A. G. 1930. Chap. III and IV *in* The Geology of North Ayrshire. *Mem. Geol. Surv. Scotland.*

MacGregor, M. 1937. The Western part of the Criffel-Dalbeattie Igneous Complex. *Quart. Journ. Geol. Soc.*, xciii, 457.

—— 1938. The Evolution of the Criffel-Dalbeattie Quartz-diorite. A study in Granitization. *Geol. Mag.*, lxxv, 481.

Nockolds, S. R. 1931. The Dhoon (Isle of Man) granite. *Min. Mag.*, xxii, 494.

Read, H. H. 1935. The Gabbros and associated Xenolithic Complexes of the Haddo House District, Aberdeenshire. *Quart. Journ. Geol. Soc.*, xci, 601.

Reynolds, D. L. 1934. The Eastern End of the Newry Complex. *Quart. Journ. Geol. Soc.*, xc, 585.

Stevenson, W. 1849. The Geology of Cockburnlaw and the adjoining District in Berwickshire. *Trans. Roy. Soc. Edinb.*, xvi, 33.

Tilley, C. E. 1924. Contact Metamorphism in the Comrie area. *Quart. Journ. Geol. Soc.*, lxxx, 58.

Walker, F. 1925. Four Granitic Intrusions in South-Eastern Scotland. *Trans. Edinb. Geol. Soc.*, xi, 357–365.

—— 1928. The Plutonic Intrusions of the Southern Uplands East of the Nith Valley. *Geol. Mag.*, lxv, 153–162.

CONTENTS

of Vol. LXXXIII, No. 2

STEPHEN AUSTIN & SONS, LTD.
1 FORE STREET, HERTFORD, HERTS

Reprinted from the GEOLOGICAL MAGAZINE
Vol. LXXXVII, No. 4, July–August, 1950, pp. 253–262.

Reprinted from the GEOLOGICAL MAGAZINE,
Vol. LXXXVII, No. 4, July–August, 1950, pp. 279–284.

An Upper Eocene Outlier at St. Ann's Hill, Chertsey

By H. G. MIDGLEY

ABSTRACT

An outlier of the Bagshot Series occurs at St. Ann's Hill, Chertsey, where beds of the Bagshot, Bracklesham, and Barton sub-divisions are exposed. The division into these beds by pebble bed junctions is suggested. Heavy mineral analyses using percentages of fresh and abraded grains of three indicator minerals, viz. tourmaline, rutile, and zircon, suggests that the divisions postulated are justified.

INTRODUCTION

ST. ANN'S HILL shows an almost complete section of the beds formerly known as the " Bagshot Series " as it is found in north-west Surrey. When the section was described by Woodward (1909) it was difficult to recognize all the strata listed by Prestwich (1847), as the section was much disturbed by slipping and so was obscured. In 1940 the demand for sand led to the opening of the pits on the north-east side of St. Ann's Hill. This paper deals with the data obtained from a study of these new openings and of the old sections as now visible. No fossils have been found in these beds, but it is possible to divide them into three groups, with prominent pebble beds as junctions, by a study of the variations of the heavy minerals. It has not yet been possible to correlate these divisions with the Bagshot, Bracklesham, and Barton of the type localities.

THE SUCCESSION

St. Ann's Hill is an outlier of the " Bagshot Series " surrounded by Thames river gravels. The summit rises to approximately 220 feet O.D., and is about 160 feet above the surrounding country. Although the London Clay is not seen in any of the sections at or near St. Ann's Hill, it is known to be present below.

The succession exposed at St. Ann's Hill can be summarized as follows :—

Pleistocene	1. A thin capping of gravels	0–5 feet
Barton	2. Brown sands with a pebble bed at the base	10 feet
Bracklesham	3. Green and brown sands with clays	60 feet
	4. Glauconitic sand 5. Pebble bed 6. Glauconitic sand	2 ft. 6 in.
Bagshot	7. White and yellow sands	15 feet
	8. Yellow fine-grained sands with two clay bands	6 feet
	9. Green, very fine-grained sands seen to 6 feet.	

Pleistocene

This gravel is probably of Pleistocene age and consists of black flint pebbles. The pebbles are well rounded and average 1½ in. by 1 in. by ½ in. Rolled chert pebbles have been recorded by Irving (1887). These probably came from the Lower Greensand and their presence seems to indicate that the Wealden dome had been denuded as far as the Hythe Beds when these gravels were deposited. This bed compares with the capping found on the surrounding heights, e.g. St. Georges Hill, Oxshott Heath, etc.

Barton

The Barton Beds consist of medium-grained sand (average diameter 0·5 mm.) with a pebble bed at the base. The sand consists of rounded, iron-stained, brown quartz grains, with some rounded white quartz grains and a few grains of glauconite. The pebble bed, about 18 inches thick, consists chiefly of rounded black flint pebbles with a few sub-angular ones. The matrix consists chiefly of a medium-grained brown sand consisting chiefly of rounded, iron-stained quartz grains (average diameter 0·5 mm.), and a fine fraction consisting of angular quartz grains of diameter 0·05 mm. A few angular flint fragments (average diameter 5·0 mm.), rounded flint grains (average diameter 1·0 mm.), angular quartz grains (average diameter 0·25 mm.), sub-angular quartz grains (average diameter 3·0 mm.) also occur. There are also a few grains of glauconite in the matrix, which is probably resorted Bracklesham material. The pebbles of the pebble bed are sometimes cemented together.

Bracklesham

The Bracklesham beds consist of sands and clays with a pebble bed near the base. The sandy beds are composed of medium-grained, reddish sand (average grain size 0·25 mm. to 0·5 mm. diameter), containing a few glauconite grains, a few flint chips, and also numerous clear, glassy quartz grains, which may be as large as 2·0 mm. in diameter. The numerous clay beds may be as thick as 4 inches and weather red. These clay bands are important. One forms the floor of the dingle, which was at one time a pit, but is now a public park near the top of St. Ann's Hill. This clay bed holds up water to form a lake on the pit floor.

The clay beds do not consist entirely of clay material but contain a very small percentage of coarser particles, up to 0·25 mm. in diameter. At the base of the Bracklesham is a pebble bed about 26 inches thick, with a thin glauconitic sand bed above and below. The glauconitic sands contain a very high percentage of glauconite and are dark green in colour. The sand is of medium grain size (0·25 mm. to 0·5 mm.

diameter), with a small amount of fine material (0·1 mm. diameter). There is a little iron staining of some of the fine material. A number of clear, glassy quartz grains occur, some of which are angular.

The pebble bed consists of a partly consolidated conglomerate composed of about equal proportions of rounded pebbles and pebbles which were rounded but have since been split in two. There are also many small fragments of flint which show no sign of rounding. All the pebbles examined were of flint, some being light in colour. The sandy matrix is of medium grain size and light brown in colour. The pebble bed and glauconitic sands appear to be resting in hollows cut into the Bagshot beds below.

Bagshot

The Bagshot beds consist of fine-grained pale coloured sands with very fine-grained green sands at the base. There are occasional clay bands throughout. Two prominent clay bands, about 3 feet apart, occur about 16 feet below the pebble bed at the base of the Bracklesham. The topmost bed, about 15 feet thick, consists of white to pale yellow fine-grained sands with an average grain size of between 0·1 mm. and 0·05 mm. diameter. There are some clear, glassy angular quartz grains and a few iron-stained quartz grains but no glauconite. The sand between the prominent clay bands is a fine-grained white sand (average diameter 0·1 mm.) consisting chiefly of white quartz grains, i.e. not iron-stained. A few of these are clear and glassy. The clay bands are persistent and are composed of a stiff white clay (pipe clay). The lower clay band is thicker than the higher one, and it may be as thick as 4 inches in places. This clay band contains a few ironstone nodules, consisting mostly of ochreous material. A few fragments of a hard ironstone occur, consisting of sand grains cemented by limonite. This occurrence of ironstone in the lower clay band suggests that it was formed by iron-rich solutions held up by the impervious clay band. In the sands a few specimens of lignite were found ; they were rounded, showed little structure, and had apparently suffered some wear before deposition. The basal fine-grained sand, seen to 6 feet, consists of a white fine-grained sand with a high proportion of silt (grain size from 0·1 mm. to 0·05 mm. diameter). The grains are mainly angular, and there are many clear, glassy quartz grains.

Stratigraphy

The " Bagshot Series " of St. Ann's Hill district was divided into Upper, Middle, and Lower by Prestwich (1847). The correlation of the subdivisions with beds found in other areas is difficult owing to the paucity of fossil evidence. Some of the sands of the Middle series of St. Ann's Hill area were shown to be of Bracklesham age by

Monkton (1883). The top pebble bed was classed as Bartonian by Woodward (1909), who wrote: "At St. Ann's Hill . . . an outlier of Bracklesham beds is shown on the map; this is capped by 10 feet or more of flint shingle, forming a pebble bed which is sometimes cemented to form a puddingstone. It rests on the Bracklesham Beds and is now grouped at the base of the Barton Beds."

There was in the past some difficulty in deciding the stratigraphical position of the pebble beds. Woodward (1909) thought that there was only one pebble bed, assuming that the pebble bed found in the pits on the north-east side of St. Ann's Hill—i.e. the pebble bed here placed at the base of the Bracklesham beds—was the upper pebble bed slipped down the hillside. Also it is not clear how much of the beds exposed at St. Ann's Hill, if any, should be classed as Bracklesham. In any case any divisions that may be decided upon petrological evidence alone may not be equivalent to the divisions of Bagshot, Bracklesham, and Barton as defined on fossil evidence.

Petrography of the Beds

In order to ascertain if petrological evidence would throw any light on the stratigraphical problems involved, the heavy minerals of the sands of the Bagshot Series were examined. The following minerals were found to be present: zircon, rutile, tourmaline, kyanite, amphibole, staurolite, anatase, brookite, monazite, epidote, iron-ores, and glauconite. The relative frequency of occurrence of the commoner minerals in certain beds was determined by counting the various grains in a number of microscopic fields, and the results are shown in Table 1.

Table 1.—Percentage of Heavy Minerals in the "Bagshot Series" of St. Ann's Hill

		Zircon.	*Rutile.*	*Tourmaline.*	*Kyanite.*	*Amphibole.*	*Staurolite.*	*Anatase.*	*Iron Ores.*	*No. of Grains counted.*
	Barton sands . .	32·8	5·7	1·2	1·5	2·6	0·4	0	55·8	751
	Pebble-bed at base of Barton Beds .	53·1	5·6	0·9	0·5	0·5	0·1	0	39·0	815
	Bracklesham sands .	17·5	5·8	3·1	0·7	0·1	0·1	0	72·7	800
	Glauconitic sand at base of Brackles-ham . . .	31·7	8·1	0·9	1·6	0·7	1·3	0	55·7	557
	Pebble-bed at base of Bracklesham Beds.	25·8	9·1	1·0	1·3	2·1	1·3	0	59·4	585
Bagshot.	Yellow sands .	35·0	7·1	2·7	1·2	0·4	0	2·5	51·1	752
	Sands and clays .	30·5	3·7	0·7	0·7	2·3	0	1·6	48·7	960
	Fine-grained sands . .	44·5	3·6	2·0	0·7	0·9	1·1	2·2	45·0	573

From these frequencies it can be seen that there is no consistently marked change in the frequency of occurrence of the different minerals from bed to bed on the three series.

Recourse was therefore made to a study of the shape shown by certain grains. It was found that the commonest non-opaque heavy minerals, zircon, rutile, and tourmaline could be divided into two classes :—

(*a*) Fresh, euhedral, and subhedral grains.

(*b*) Abraded and rounded grains.

Each mineral was dealt with separately and counts of the two classes were made. For each mineral the counts made of the two types were expressed as percentages of the total number of grains of that mineral. For simplicity only the percentages of the fresh grains are recorded in the Table 2. As in some cases only a few grains were counted, the total number of grains counted is also given in Table 2.

It can be seen from these results that the Bagshot Beds contain a high percentage of fresh grains of rutile and tourmaline and a low percentage of fresh grains of zircon ; while in the beds above, Bracklesham and Barton, there is a low percentage of fresh grains of rutile and tourmaline and a high percentage of fresh grains of zircon.

The percentages of fresh grains of zircon, rutile, and tourmaline also show sympathetic variation, that is, the minor fluctuations of the frequency of occurrence of the fresh grains all show the same variations

TABLE 2.—PERCENTAGES OF FRESH GRAINS

	Tourmaline		Rutile		Zircon	
	No. of grains counted.	Per cent of fresh grains.	No. of grains counted.	Per cent of fresh grains.	No. of grains counted.	Per cent of fresh grains.
Barton sands . . .	15	14	70	3	89	52
Pebble bed at base of Barton . . .	10	0	100	2	192	34
Bracklesham sands . .	30	13	41	5	118	42
Glauconitic sand at base of Bracklesham . .	10	0	48	0	227	37
Pebble bed at base of Bracklesham . .	11	9	32	15	123	50
Bagshot yellow sands .	15	80	32	78	228	10
Bagshot sands and clays .	38	66	70	64	232	4
Bagshot fine-grained sands	17	64	26	76	134	20

from bed to bed, i.e. when the percentage of fresh grains of zircon increases so do the percentages of the other two minerals.

LIST OF WORKS TO WHICH REFERENCE IS MADE

IRVING, A., 1887. The Physical History of the Bagshot Beds of the London Basin. *Quart. Journ. Geol. Soc.*, xliii, 377.

MONKTON, H. W., 1883. Bagshot Beds of London Basin. *Quart. Journ. Geol. Soc.*, xxxix, 348.

PRESTWICH, J., 1847. The Probable Age of the Bagshot Sands. *Quart. Journ. Geol. Soc.*, iii, 383.

WOODWARD, H. B., 1909. The Geology of the London District. *Mem. Geol. Surv.*, 43.

A serpentine mineral from Kennack Cove, Lizard, Cornwall

BY

H. G. MIDGLEY, Ph.D., M.Sc., F.G.S.

MINERALOGY SECTION, BUILDING RESEARCH STATION, DEPARTMENT OF SCIENTIFIC AND INDUSTRIAL RESEARCH

[Reprinted from the *Mineralogical Magazine*, London, March 1951, Vol. XXIX, No. 212, pp. 526–530.]

MINERALOGICAL SOCIETY

Officers and Council for 1950–51

PRESIDENT

Prof. C. E. TILLEY, B.Sc., Ph.D., F.R.S.

PAST-PRESIDENTS

L. J. SPENCER, C.B.E., B.Sc., M.A., Sc.D., F.R.S. (1936–39).

Sir ARTHUR RUSSELL, Bart., M.B.E. (1939–42).

Lt.-Col. W. CAMPBELL SMITH, C.B.E., M.C., T.D., M.A., Sc.D., F.G.S. (1945–48).

VICE-PRESIDENTS

A. F. HALLIMOND, M.A., Sc.D., F.G.S.

S. J. SHAND, D.Sc., Ph.D., F.G.S.

TREASURER

E. H. BEARD, B.Sc.

Mineral Resources Division, Imperial Institute, South Kensington, London, S.W. 7

GENERAL SECRETARY

G. F. CLARINGBULL, B.Sc., Ph.D., F.G.S.

British Museum (Natural History), Cromwell Road, London, S.W. 7

FOREIGN SECRETARY

L. J. SPENCER, C.B.E., B.Sc., M.A., Sc.D., F.R.S.

EDITOR OF THE JOURNAL

L. J. SPENCER, C.B.E., B.Sc., M.A., Sc.D., F.R.S.

111 *Albert Bridge Road, London, S.W.* 11

MANAGING TRUSTEES

Prof. C. E. TILLEY, B.Sc., Ph.D., F.R.S.

Lt.-Col. W. CAMPBELL SMITH, C.B.E., M.C., T.D., M.A., Sc.D., F.G.S.

ORDINARY MEMBERS OF COUNCIL

S. O. AGRELL, B.A., Ph.D., F.G.S.

F. A. BANNISTER, M.A., Sc.D., F.Inst.P.

H. G. DINES, A.R.S.M., F.G.S.

G. S. GOWING, M.A., F.G.S.

G. E. HOWLING, B.Sc.

J. PHEMISTER, M.A., D.Sc., F.R.S.E., F.G.S.

H. M. POWELL, M.A., B.Sc.

H. P. ROOKSBY, B.Sc., F.Inst.P.

P. A. SABINE, A.R.C.S., F.G.S.

F. H. STEWART, B.Sc., Ph.D., F.G.S.

S. I. TOMKEIEFF, M.Sc., D.Sc., F.G.S.

A. K. WELLS, D.Sc., F.G.S.

CLAY MINERALS GROUP

Chairman: Prof. A. L. ROBERTS, Ph.D.
Fuel Dept., The University, Leeds, 2

Hon. Secretary: R. C. MACKENZIE, B.Sc., Ph.D.
Macaulay Institute for Soil Research, Craigiebuckler, Aberdeen

---

Bankers and Custodian Trustee.—Messrs. Coutts & Co., 15 *Lombard Street, London, E.C.* 3

A serpentine mineral from Kennack Cove, Lizard, Cornwall.[1]

By H. G. Midgley, Ph.D., M.Sc., F.G.S.

Mineralogy Section, Building Research Station, Department of Scientific and Industrial Research.

[Read June 8, 1950.]

Introduction.—A white soapy mineral which could not easily be identified in the hand-specimen was collected from a vein in the serpentine rock at Kennack Cove, Lizard, in April 1949. From a preliminary optical examination the mineral was thought to be saponite, and therefore of interest to clay mineralogists. Chemical analysis, X-ray, thermal, and optical investigations were carried out at the Building Research Station.

Occurrence and optical data.—The mineral occurs in a vertical vein cutting the serpentine rock on the north-east side of Kennack Sands. The vein is about 2–3 inches wide and shows up very white against the dark serpentine rock. The mineral is pure white in colour, soapy to the touch, and soft (H. 2). It is an irregular aggregate of small crystals, which are for the most part hexagonal plates. In thin section the mineral is seen to have a distinct basal cleavage and a birefringence of about 0·01. Microscopical examination of powder specimens shows the plate-like habit of the grains, and also the presence of a second mineral which is probably talc. The plates, when lying flat, give a centred uniaxial negative interference figure. The mineral has ϵ 1·545 and ω 1·555, $\omega-\epsilon$ 0·01. These optical properties may be easily confused with those of saponite. Chemical analysis (table II) or X-ray examination (table III) will, however, distinguish between these two minerals. Table I gives the optical properties, with those of saponite, chrysotile, and antigorite for comparison.

Table I. Comparison of optical data.

		Serpentine mineral.	Saponite.	Chrysotile.	Antigorite.
ϵ ...	...	1·545	—	α 1·493–1·546	α 1·555–1·564
ω ...	...	1·555	1·555	β 1·504–1·550	β 1·562–1·573
$\omega-\epsilon$	...	0·01	0·01±	γ 1·517–1·557	γ 1·562–1·573
2V	...	0°	0°	0–50°	20–90°
Sign	...	negative	negative	positive	negative

Chemical analysis.—The analysis (table II) calculated on the basis of 10 oxygens gives the formula $Mg_{5\cdot6}(Si,Al)_4O_{10}(OH)_{7\cdot9}$. Making allowance for the talc impurity, it is probable that the mineral is analogous to either chrysotile or antigorite $Mg_6Si_4O_{10}(OH)_8$, and so should be regarded as a serpentine mineral.

TABLE II. Chemical analysis of serpentine mineral from Kennack, Lizard. (Analyst, L. J. Larner.)

SiO_2	44·49	CaO	0·03
Al_2O_3	2·26	TiO_2	0·03
MgO	40·27	Fe_2O_3	0·48
H_2O+	12·80		
			100·36

Thermal analysis.—A differential thermal analysis of a small sample was carred out by D. B. Honeyborne of the Building Research Station, and the resultant curve is reproduced as fig. 1. The curve is very like others obtained from some magnesium silicate minerals, for example antigorite.[1]

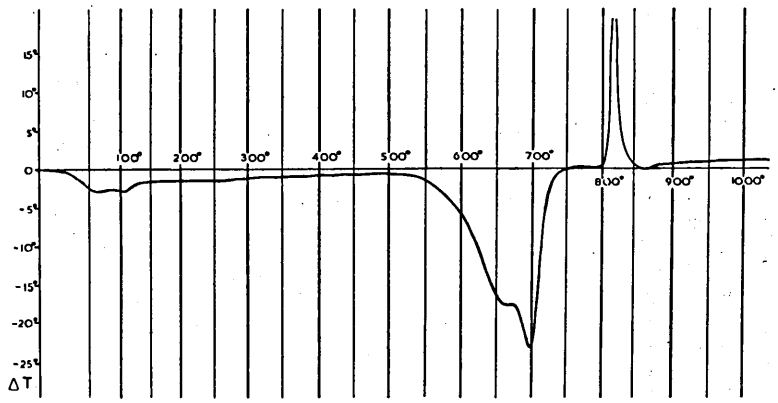

FIG. 1. Differential thermal analysis of serpentine mineral.

X-ray investigations.—Powder photographs and single-crystal rotation photographs of the serpentine mineral were taken. The powder photographs were taken on a 10-cm. camera using filtered Cu-$K\alpha$ radiation, λ 1·542 Å. The measurements of spacings are given in table III. A powder photograph of a sample of saponite[2] from the Lizard (kindly

[1] S. Caillère and S. Hénin, Ann. Agronom. Paris, 1947, n. ser., vol. 17, p. 23. [M.A. 11–175.]

[2] This material is white or stained red, soft (H. 2) and soapy to the touch. It forms a granular mass of micro-crystals with refractive index about 1·555.

supplied by Dr. G. F. Walker) was also taken, and the spacings for this mineral are given for comparison, together with the spacings for chrysotile and antigorite as recorded by Selfridge.[1] It can be seen that there is no resemblance between the serpentine mineral and the saponite; and that there is some resemblance between the chrysotile, antigorite, and the serpentine mineral, but not complete agreement.

TABLE III. Comparison of X-ray powder spacings and intensities.

Serpentine mineral		Chrysotile*		Antigorite*		Saponite	
d_{hkl} Å.	*I.*	d_{hkl} Å.	*I.*	d_{hkl} Å.	*I.*	d_{hkl} Å.	*I.*
(9·4	5)†	—		—		18·8	10
7·51	10	7·364	9	7·355	8½	9·1	5
5·20	½	—		—		6·05	1
4·59	5	4·431	6	4·668	4	4·54	5
3·94	½	—		—		3·605	5
3·73	10	3·658	9½	3·641	9	3·00	4
3·105	3	—		—		—	
2·75	1	—		—		—	
2·635	1	—		—		2·605	6
2·580	1	2·571	8	—		—	
2·490	9	2·424	8	2·558	10	2·48	3
2·420	1	—		—		—	
2·29	½	—		—		2·26	2
2·205	½	—		—		—	
2·14	5	2·089	6	2·186	7	2·00	1
1·814	1	—		1·845	3	—	
1·780	3	—		1·794	4	—	
1·725	1	1·729	6	—		1·733	4
1·686	1	—		—		—	
1·657	½	—		—		—	
1·550	½	—		1·583	7½	—	
1·525	5	1·522	10	1·553	7½	1·533	7
1·497	5	—		—		—	
1·450	1	—		—		—	
1·407	½	—		—		—	
1·322	½	—		—		1·318	4
1·300	3	1·301	7	1·326	6	—	
1·268	3	—		1·273	4	1·268	2
1·238	½	—		—		—	
1·208	½	—		—		—	
1·159	2	1·187	½	1·160	2	—	
1·099	1	—		1·061	3½	—	
1·068	2	—		—		—	
1·051	2	1·039	2	—		—	

* Data from G. C. Selfridge, 1936 (loc. cit.). † Line due to talc impurity.

Since the mineral occurs as small flakes with distinct basal cleavage,

[1] G. C. Selfridge, Amer. Min., 1936, vol. 21, p. 463. [M.A. 6–476.]

it was possible to pick out individual flakes, one of which was mounted and used for rotation photographs. A 6-cm. single-crystal camera was used with filtered Cu-$K\alpha$ radiation, λ 1·542 A. The flake was set up to give *a*, *b*, and *c* rotation photographs. The films produced are marred by the fact that some of the spots are extended into Debye powder lines. On indexing, however, it was found that the *hk*0 reflections were always spots, while *hkl* reflections were Debye powder lines. This suggests that there is preferred orientation of the layers.

The mineral was found to have a monoclinic unit cell with *a* 5·29, *b* 9·18, *c* 7·45 kX; β 91·4°; this cell leads to a calculated density of 2·52 g./c.c. The density determined by suspension in a bromoform-benzene mixture was 2·56 g./c.c.

In *h*0*l* planes *h* is always even, in *hkl* planes *h* plus *k* is always even, indicating that the monoclinic cell is centred on 001, and that the probable space-group is *C*2/*m*, *Cm*, or *C*2.

The cell dimensions of chrysotile and antigorite have been given by Aruja[1] as:

Antigorite . . . *a* 43·39, *b* 9·238, *c* 7·265 kX; β 91·4°.
Chrysotile . . . *a* 5·32, *b* 9·2, *c* 14·62 kX; β 93·2°.

The serpentine mineral from Kennack has a smaller unit cell than antigorite, but since the ratio of the *a*-axes is about one-eighth and the other dimensions are similar it is possible that the two minerals have a similar structure. Using the kaolinite-like sheet structure suggested by Aruja for antigorite as a basis, the intensities of the various reflections were calculated. It was necessary to adjust the *z*-coordinates of the ions to allow for the difference between the *c*-axes of antigorite (7·265 kX) and serpentine mineral (7·45 kX). The calculated intensities for the reflections falling on the equators of the *a* and *b* rotation photographs are given in table IV, and it can be seen that there is reasonable agreement.

Conclusions.—The white mineral from Kennack with a formula of $Mg_6Si_4O_{10}(OH)_8$ has a monoclinic unit cell with *a* 5·29, *b* 9·18, *c* 7·45 kX, β 91·4°, probable space-group *Cm*, *C*2, or *C*2/*m*. It probably has a kaolinite-like sheet structure with all the octahedral positions filled with magnesium ions and so is the magnesium analogue of kaolinite. It is probably a variety of antigorite with very little iron substitution and thus has optical properties (uniaxial, negative ϵ 1·545, ω 1·555, $\omega-\epsilon$ 0·01) different from those usually associated with antigorite.

[1] E. Aruja, Ph.D. thesis, Cambridge, 1943; Min. Mag., 1945, vol. 27, p. 65

TABLE IV.

Equator of a rotation photograph.

2 sin θ (calc.)	hkl.	F^2 (calc.)	Int. (obs.)	2 sin θ (obs.)
0·205	001	165·0	10	0·205
0·340	020	17·0	4	0·34
0·394	021	5·4	9	0·405
0·410	002	48		
0·533	022	7	—	—
0·615	003	18	3	0·615
0·680	040	1	1	0·680
0·704	023	3		
0·710	041	3	—	—
0 795	042	0	—	—
0 820	004	2	½	0·85
0 914	024	0	—	—
0·918	043	2	—	—
1·020	060	33	9	1·01
1·025	005	9		
1·040	061	6		
1·070	025	0	—	—
1·090	044	1	½	1·06
1·100	062	1	1	1·10
1·190	063	3		
1·230	006	3	½	1·27
1·233	045	0	—	—
1·27	026	0	—	—
1·325	064	0	—	—
1·360	080	1	—	—
1·400	046	0	—	—
1·435	007	1	—	—
1·470	027	0	—	—
1·58	047	0	—	—
1·64	008	0	—	—
1·67	028	0	—	—

Equator of b rotation photograph.

2 sin θ (calc.)	hkl.	F^2 (calc.)	Int. (obs.)	2 sin θ (obs.)
0·205	001	165	10	0·205
0·410	002	48	8	0·42
0·580	200	28	3	0·58
0·615	003	18	10	0·615
	201	75		
	20$\bar{1}$	39		
0·705	202	8	3	0·71
0·715	20$\bar{2}$	2		
0·82	004	2	1	0·84
0·83	203	1		
0·86	20$\bar{3}$	3	2	0·86
1·019	204	6	3	1·025
1·025	005	9		
1·040	20$\bar{4}$	7		
1·17	205	1	2	1·16
1·18	400	3		
1·19	20$\bar{5}$	3	3	1·19
	401	5		
1·20	40$\bar{1}$	9	2	1·20
1·23	006	3	½	1·23
	402	0	—	—
1·25	40$\bar{2}$	3	½	1·255
1·32	403	3	½	1·32
1·34	40$\bar{3}$	1	—	—
1·35	206	0	—	—
1·37	20$\bar{6}$	1	—	—
1·43	007	2	½	1·43
1·53	207	1	—	—
1·56	20$\bar{7}$	0	—	—
1·64	008	1	—	—
1·73	208	0	—	—
1·74	600	5	2	1·75
1·75	20$\bar{8}$	0	1	1·76
	601	2		
	60$\bar{1}$	1		
1·78	602	1	½	1·79
1·80	60$\bar{2}$	0	—	—
1·84	603	2	1	1·83
1·845	009	2	—	—
1·86	60$\bar{3}$	3	½	1·86

MINERALOGICAL SOCIETY PUBLICATIONS

The Publisher is Geoffrey Cumberlege, Oxford University Press, *Amen House, Warwick Square, London, E.C.* 4.

Mineralogical Magazine.—Current Numbers price 12*s.* net each. Annual Subscription for four Numbers post free 40*s.*, payable in advance to the Publisher, either direct or through any bookseller. Since 1920 (No. 88, Vol. XIX) the numbers have been issued quarterly, and include a separately-paged appendix of *Mineralogical Abstracts.*

Back Numbers.—The following numbers are out of print: 17–23, 73, 75, 77–9, 89, 90–5, 98–9, and 121–2. Moreover, certain numbers, the stock of which is low, are reserved for purchasers of part sets of the Magazine, and can only be sold as part of such sets. With the above exceptions, all numbers can be supplied at the following rates: Nos. 1–87 (Vols. I–XVIII, 1876–1919), No. 12* (Geological Map of the Shetland Islands, mounted and folded, which was issued as an addition to Vol. II), and the General Indexes to Vols. I–X and XI–XX, price 5*s.* each net. (To Members less 20% discount.) Nos. 88 onwards (Vols. XIX onwards, 1920–) at 12*s.* each net, or 40*s.* per annual issue of four numbers.

Mineralogical Abstracts (Vol. I, Nos. 1–12, 1920–22, issued with Vol. XIX of the Magazine) are also sold separately. Price 5*s.* net each number. Later numbers are issued only as part of the Magazine.

Bye-Laws and List of Members (1950). Price 2*s.* 6*d.* net.

Inquiries from Members of the Society concerning publications should be addressed to the General Secretary and not to the Publisher.

GENERAL NOTICES

Candidates for Election as Ordinary Members should obtain a nomination form from the General Secretary, Dr. G. F. Claringbull, *British Museum (Natural History), Cromwell Road, London, S.W.* 7. Candidates must be proposed by two Members of the Society, one, at least, of whom shall have personal knowledge of the candidate. There is an entrance fee of one guinea and the annual subscription is one guinea; the latter can be compounded for by a single payment of thirty pounds (£30). New Members, on the payment of their first subscription, receive all the numbers of the Magazine for the year for which the subscription is paid.

There are at least four meetings of the Society each year, on Thursdays, in January, March, June, and November. They are held (by kind permission) in the Apartments of the Geological Society, Burlington House, Piccadilly, London, W. 1. Titles of papers to be read at these meetings, with a view to subsequent publication in the Magazine, and of exhibits, should be sent with a short abstract to the General Secretary at least *three* weeks before the meeting. Authors alone are responsible for the views set forth in their respective papers. They are allowed, free of charge, fifty separate copies of their papers published in the Magazine.

MINERALOGICAL MAGAZINE

CONTENTS OF No. 212

(March 1951)

MINERALOGICAL ABSTRACTS

(Vol. 11, No. 4, pp. 181–252)

Authors of papers abstracted.—Adams, 235, Agrawal 203, Ahrens 224, 226, Alberman 228, Alcock 239, Anderson 228, Arnott 228, Backström 206, Bacon 235, Bairsto 233, Barrer 194, Barshad 218, 221, Bárta 207, 222, Bassett 193, Bateman 184, Bates 221, Beard 189, Beck 216, Berdesinski 192, Berg 185, Berry 240, Bertolani 249, Bertrand 245, Beus 190, Bhatnagar 204, Biljon 204, Blumenthal 215, Borland 218, Bracewell 251, Brasseur 194, Brenet 238, Brooks 239, Buerger 232–4, Burri, 181, Byström 237–8, Caillère 190, 210, 220, Čáp 222, Carobbi 193, Cavalca 239, Chaudron 193, Chayes 203, Chenevoy 207, Chudoba 201, Chukhrov 247, Church 225, Cisney 189, Clausen 252, Cole 233, Conybeare 228, Coombs 203, Coppens 224, Correns 208, Cotelo Neiva 211, Dake 224, Dallemagne 194, Danielsson 208, Delavault 210, De Ment 224, Denaeyer 209, Denysschen 222, Dreyer 202, Dyal 217, Earley 236, Eaton 191, Elgabaly 218, Ernst 198, Escard 219, Esquevin 220, Evans 224, 229, 230, Fahey 243–4, Fenner 204, Ferguson 228, Ferrari 239, Fersman 184, Fischer 227, Fleck 215, Fornaseri 241, Frechen 201, Foster 197, 243, Frondel 187 229, 230, Friedensburg 185, Fruer 236, Fumano' 250, Galloni 188, Garrels 202, Gentner 224, Ginzburg 189, Göksu 215, Gorfinkle 226, Grasselly 214, Green 212, Grigoriev 195, Hartshorne 181, Hayton 251, Hedlik 237, 241, Heinrich 213, Hellmers 209, Hellner 242, Hendricks 217, Hénin 190, 210, 220 Hildebrand 221, Hinds 194, Holland 225, Howland 202, Hummel 196, Hurlbut 230, Hurley 226, Hutchinson 245, Hutton 209, Hyde 191, Ito 232, 242, Jaffe 245, Jeffery 233, Kawano 202, Keevil 227, Keller 231, Kelley 211, Kendall 191, 196, Kerr 216, Kiefer 249, King 212, Kiriyama 241, Koblic 246, Koch 250, Kokkoros 240, Köppen 196, Koutek 210, Krishnamoorthy 217, Kristoffersen 191, Kulp 225, Kuno 204, Kunský 246, Kurylenko 252, Kutina 210, Lancman 252, Leitmeier 183, Lerner 252, Levin 201, Lindberg 187, Lokka 202, 226, Lombaard 205, McAndrew 186, McConnell 220, M'Ewen 220, Machatschki 240, McKelvey 227, McLachlan 205, Magéli 239, Mahadevan 206, Marble 231, Marel 216, Mason 188, Mathieu-Sicaud 190, Matthes 207, 216, Mazurak 217, Mehnert 213, Mélon 194, Mering 219, Mezsöi 214, Michel-Lévy 195, Millman 210, Milton 245, Minguzzi 249, Misra 204, Morgan 196, Morgante 214, Mori 240, Morimoto 235, Mould 220, Mrose 229, Muench 226, Muilenburg 231, Murdoch 243, Muthuswami 231, Myers 245, Nelson 227, Norrish 243, Novotný 199, Nuffield 244, O'Daniel 242, Orcel 210, Osborn 198, Overholt 245, Overstreet 217, Pabst 188, 237, Page 227, Pagliani 250, Pákozdy 250, Pauly 201, Peacock 186, Pecora 244, Pernoux 248, Perrin-Bonnet 219, Phoenix 244, Picard 191, Poldervaart 206, Pulfrey 206, Radhakrishna 215, 223, Radić 247, Ramdohr 187, Rankama 251, Reiche 208, Reitemeier 218, Robertson 234, Rodda 245, Roever 200, Rojas-Cruz 218, Rood 191, Rooksby 239, Rosenqvist 231, Sabatier 195, 248–9, Sadanaga 242, Saito 211, Sakamoto 211, Sakurai 241, Salmon 194, Sander 183, Sandréa 225, 252, Satava 222, Sathapathi 206, Schairer 198, Schaller 187, Schlossmacher 186, Schröder 192, Scüller 185, Schumann 182, 209, Scott 191, Seeliger 213, Sgrosso 214, Shainin 225, Sharma 203–4, Sharp 223, Sherwood 189, Shirozu 212, Silva 214, Smits 224, Sommerlatte 185, Spraggon 196, Srinivasan 232, Stringham 223, Strunz 189, Stuart 181, Swineford 221, Takéuchi 242–3, Taneda 200, Teichner 248, Terrey 194, Tertian 237, Tombs 239, Tunell 235, Tyndale-Biscoe 205, Ueda 240, Vachtl 207, Van Tassel 246, Vašíček 207, Vaux 245, Ventriglia 216, Vitaliano 188, Wadsley 192, Wallaeys 193, Warde 222, Warren 210, Wasserstein 235, Watanabé 242, Watt 193, Webb 210, Weeks 189, Weisz 233, White 224, Wiklander 218, Wilhelmi 237, Williams 233, Wood 233, Wright 182, Wyckoff 191, Yagoda 224, Yarzhemsky 247, Yeo 191, Yoder 197, Zemann 234–5.

Reprinted from The Geological Magazine 1951, Vol.88, No.3 pages 179-184.

Chalcedony and Flint

By H. G. MIDGLEY (Building Research Station) [1]

(PLATE IX)

ABSTRACT

The possibility of interaction between the alkalies in cement and flint and chalcedony has made it necessary to investigate the constitution of these minerals. It had always been thought that these minerals were a mixture of quartz and opal, but experiments have led to the belief that this is not true and that the minerals are composed of a quartz network with a large number of micropores.

INTRODUCTION

CHALCEDONY and flint have been studied by many workers in the past, usually in relation to their origin and occurrence. Little work has been done on their mineralogical properties, which are likely to prove of technological importance as it has been suggested that the alkalies present in cement may react with either mineral to form sodium silicate gel, and that as a result concrete made from these materials may disintegrate. Their constitution has been investigated at the Building Research Station and some of the results are reported in this paper.

It has usually been accepted that chalcedony and flint contain about 1 per cent of combined water, and that the two minerals are composed of an intimate mixture of quartz and opal. Donnay (1936) calculated that chalcedony consists of some 10 per cent opal and 90 per cent quartz. He determined these quantities by taking into account the water contents of chalcedony and opal and the difference in density between quartz and chalcedony. Using the refractive indices of quartz and opal, he calculated the refractive indices of a mixture of 10 per cent opal and 90 per cent quartz, and the results from these calculations agreed with the experimental results for natural chalcedony.

X-ray powder photographs of chalcedony and flint appeared to be identical with those of quartz, and it was assumed that the main opal band was hidden by the strong 4·26A line of quartz.

Investigations on a large number of specimens of chalcedony and flint have lead the author to doubt the validity of the quartz-opal admixture theory, and the results of these investigations are reported below.

OPTICAL PROPERTIES

The refractive indices of a number of specimens of chalcedony and flint were measured by the immersion method in sodium light with an accuracy of $\pm 0{\cdot}001$.

Chalcedony has α 1·534, γ 1·539, and flint α 1·537, γ 1·540.

[1] Published by permission of the Director of Building Research.

It will be seen that there is very little difference between the two minerals, but when the refractive indices of specimens were plotted against the water content, as determined by loss at 1,000° C., the difference was significant (Text-fig. 1). It was found that there was no continuous variation of refractive index with water content, but that those specimens with less than 1·0 per cent water had refractive indices α 1·534, γ 1·539, and with more than 1·0 per cent, α 1·537, γ 1·540. This suggests a means of dividing chalcedony and flint by mineralogical definition and not, as is more usual, by mode of occurrence, i.e. flint,

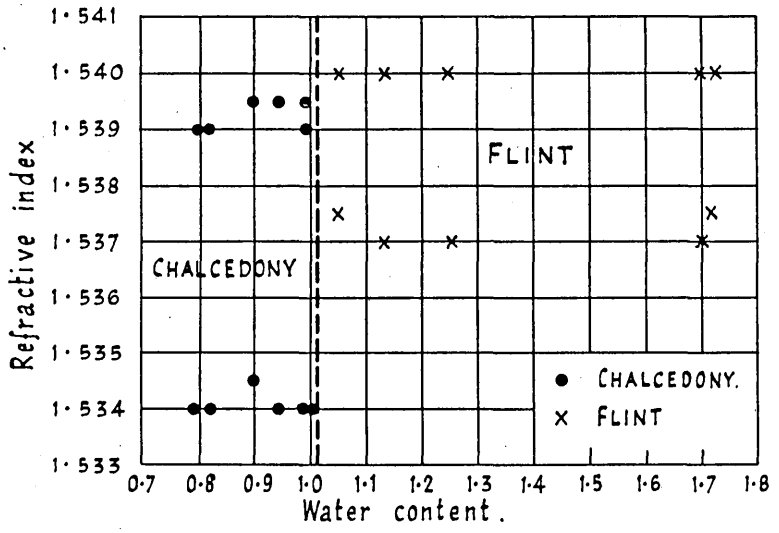

TEXT-FIG. 1

more than 1·0 per cent water, α 1·537, γ 1·540; chalcedony, less than 1·0 per cent water, α 1·534, γ 1·539.

X-RAY DIFFRACTION

Since Washburn and Navais (1922) first reported it, it has been known that chalcedony and flint gave X-ray powder diffraction photographs which appeared to be identical with those given by quartz (Plate IX, fig. 1 *a*, *b*, and *c*).

Samples of opal all give a broad band at about 4.2A. In certain opal specimens other lines may also be present; these can be indexed as due to cristobalite. The band, which is characteristic of opal, is very near the 4·26A strong line of quartz, and so it was thought that if opal were present in flint or chalcedony the band might have been obscured,

although it should have been possible to detect it by means of the relative intensity compared with other quartz lines.

X-ray diffraction photographs of the critical region around 4·2A were taken on an experimental semi-focusing camera constructed by my colleague, Dr. E. Aruja (to whom I am indebted for these photographs).

Photographs obtained from mixtures of opal and quartz and from opal, chalcedony, and flint are shown in Plate IX, fig. 2.

The band due to opal can be seen clearly at one side of the strong

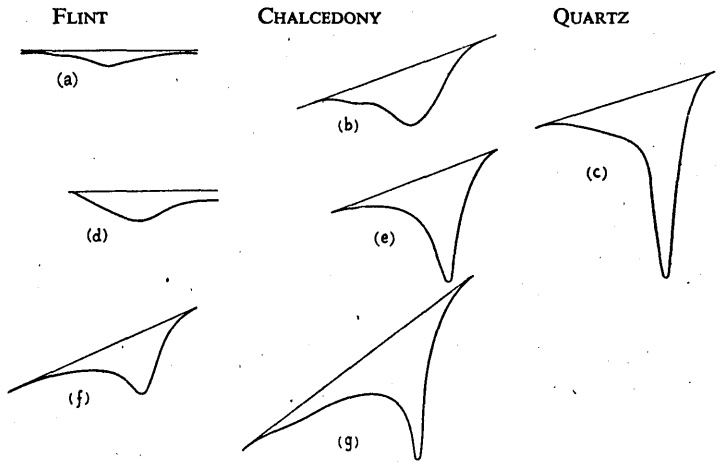

TEXT-FIG. 2

quartz line and in the 10 per cent opal 90 per cent quartz mixture it is still easily seen. No corresponding line can be seen in the spectra of chalcedony and flint and a microphotometer has failed to detect any trace of it.

From the X-ray evidence it would appear that chalcedony and flint are not composed of a mixture of quartz and opal, but consist almost entirely of quartz. From the broadening of the quartz lines it may also be concluded that the quartz crystallites in flint and chalcedony are very small.

DIFFERENTIAL THERMAL ANALYSIS

Differential thermal analysis curves were carried out on samples of chalcedony, flint, and quartz of equal weight. The results in the region of the α-β quartz inversion at 573° C. are given in Text-fig. 2 *a*, *b*, *c*. If, as Berklehamer (1944) suggests, the area under the break is proportional to the quantity of quartz present, then the quantity of quartz in flint is about 12 per cent and in chalcedony 65 per cent, or if we take

the height of the break, as suggested by Grimshaw, Westerman, and Roberts (1948), then the quantity of quartz in flint is 10 per cent and in chalcedony 35 per cent. These results are very different from those obtained by Donnay (1) by calculations from water content, density and refractive indices. Differential thermal analysis curves were also obtained on samples of chalcedony and flint which had been heated at 1,000° C. for sixteen hours (Text-fig. 2 *d*, *e*) and fifty-six hours (Text-fig. 2 *f*, *g*). All the water should have been removed by this treatment. Once again the α–β quartz inversions are not equal to that given by an equivalent mass of quartz, but the size of the break has increased with heating.

At first sight the differential thermal analysis results appear to contradict the X-ray evidence that the major constituent of flint and chalcedony is quartz. The explanation probably lies in the minute size of the crystallites in which the quartz occurs. Mample (1940) has made a theoretical study of the effect of particle size on a reaction spreading from nuclei and shows that for comparatively large particles there is no induction period and the reaction proceeds at a fast rate (proportional to the fourth power of time) ; for very small particles he suggests the law :—

$$l_n (1 - \alpha) = k(t - t_o) + \text{const.}$$

where α is the fraction transformed, k is a constant for the reaction, t elapsed time, and t_o an induction period.

The effect of an induction period varying with particle size and a general slowing up of inversion would be to spread out the thermal analysis break and reduce its height ; in the extreme case it would be almost impossible to say where the break begins or ends, and the measurement of area would be impracticable. The increase in size of the break, with time of treatment at 1,000° C., would then be attributed to crystal growth.

Surface Area

The surface area of specimens of chalcedony and flint was determined by the nitrogen adsorbtion method of Brunaur, Emmett, and Teller (1945). The surface measured is that available to the nitrogen molecule, and is generally considered to include internal structures and defects. Coarse fractions, 52–100 B.S. Sieve, were used, so that the external surface would be negligible in relation to the internal surfaces. The results are given in Table 1.

Table 1

Mineral.	*Surface Area, sq. cm./gm.*
Chalcedony . .	4,300
Flint . . .	2,200
Quartz . . .	0
Opal . . .	400,000

The internal surface area of chalcedony and flint could be due to two different causes : (*a*) to small micro-pores in the structure, or (*b*) to the opal content in a quartz-opal mixture. If the surface area is to be accounted for by the presence of opal then the quantity needed is, for chalcedony 1·0 per cent and for flint 0·5 per cent. The results once again are not in agreement with those calculated from water content or optical properties.

Thus it would appear more reasonable to suppose that the surface area of chalcedony and flint is due to a large number of micro-pores. It is of some interest to make a rough estimate of the size of the pores. The water content of chalcedony is about 0·8 per cent, and if it be assumed that the specific volume of this adsorbed water is the same as that for free water, then the volume of pores is about 0·8 c.c. for 100 gm. of chalcedony. The specific surface per unit volume of pore space is therefore 430,000 ÷ 0·8, or 537,500 sq. cm. per c.c. If the pores are cylindrical their specific surface per unit volume = $2/r$, whence r (radius of the pore) is about 1×10^{-6} cm. Similarly for flint r is about 14×10^{-6} cm. The existence of pores of approximately this size has been reported by Folk and Weaver (1950) in an electron microscope study of chert.

Conclusions

The main point to be decided is whether chalcedony and flint contain opal. The X-ray evidence proves conclusively that the quantity of opal, if it is present, must be considerably less than 10 per cent. On the other hand, to account for the accepted values of density and refractive index, more than 10 per cent of opal would be required. Specific surface measurements point to the existence of pores varying from 0·02 to 0·28 microns in diameter, and pores of 0·10 microns diameter have been detected by electron microscopy ; opal itself has such a high internal surface that it cannot be postulated that the specific surface of flint and chalcedony is due to admixed opal.

The presence of the large number of small micropores, filled with either water or air, or a mixture, would account for the apparent lowering of the refractive indices of chalcedony and flints, since in the micro size structures, where the individual discontinuities are of a size approximating to the wavelength of light, they will interfere and so reduce the apparent refractive index.

The only evidence which appears to contradict the theory that flint and chalcedony are composed of a microporous mass of silica is that obtained from differential thermal analysis ; these results are, however, satisfactorily accounted for by the small size of the quartz crystallites.

REFERENCES

BERKLEHAMER, L. H., 1944, Differential Thermal Analysis of quartz. *Bureau of Mines, U.S.A., Report* 3763.

BRUNAUER, S., 1945. *The Adsorption of Gases and Vapours.* Princeton.

DONNAY, J. D. H., 1936. Le birefringence de forme dans la chalcedonie. *Ann. Soc. Geol. Belge.*, lix, B289.

FOLK, R. L., and WEAVER, C. E., 1950. Surface Features of Chert as studied by the Electron Microscope. *Abs. of 31st Ann. Meeting, Min. Soc. Amer.*, 10.

GRIMSHAW, R. W., WESTERMAN, A., and ROBERTS, A. L., 1948. Thermal Effects accompanying the Inversion of Silica. *Trans. Brit. Cer. Soc.*, xliii, 1.

MAMPEL, K. L., 1940. Time v. amount of reaction formulas for heterogeneous reactions at the phase boundaries of solids. *Zeit. Phys. Chem.*, clxxxvii, 43.

WASHBURN, E. W., and NAVAIS, L., 1922. Relation of chalcedony to other forms of silica. *Proc. Nat. Acad. Sci.*, viii, 1.

EXPLANATION OF PLATE IX

FIG. 1.—*a*, quartz; *b*, chalcedony; *c*, flint; *d*, opal.

FIG. 2.—*a*, opal; *b*, 50 opal, 50 quartz; *c*, 10 opal, 90 quartz; *d*, chalcedony; *e*, flint.

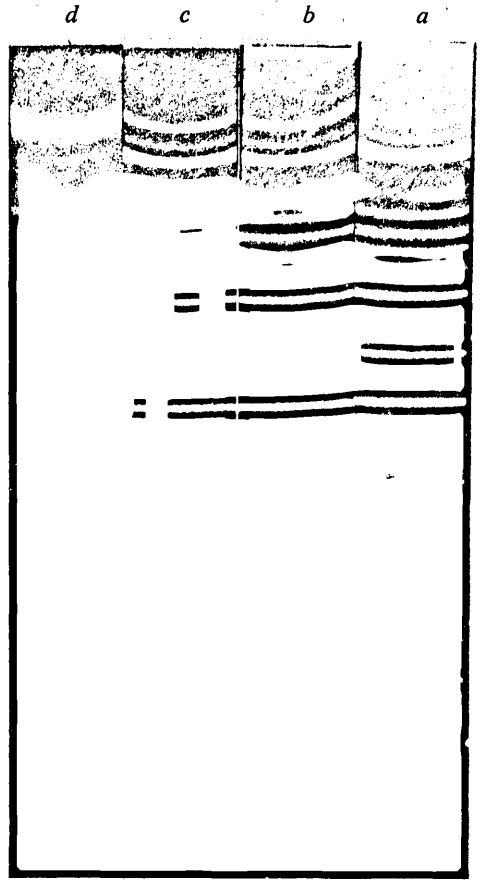

FIG. 1.

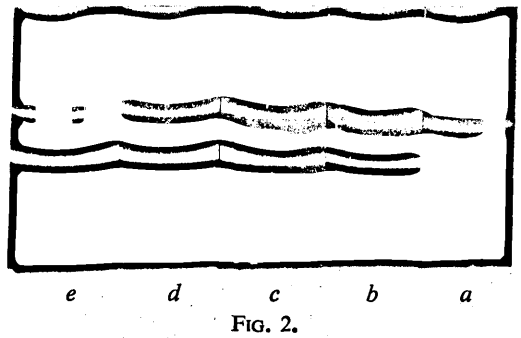

FIG. 2.

X-RAY POWDER DIFFRACTION PHOTOGRAPHS OF CHALCEDONY, FLINT, ETC.

Reprinted from "Silicates Industriels" 1951, 16(7), 211-7.

Association Belge pour favoriser l'Etude des Verres et des Composés Siliceux.
Journées internationales consacrées à l'étude et la mise en œuvre des laitiers.

THE MINERALOGY OF BLASTFURNACE SLAG(*)

by R.W. NURSE, M.Sc., F.Inst.P. and H.G. MIDGLEY, Ph.D., M. Sc., F.G.S.
(Building Research Station)

SUMMARY

Air-cooled slags from twenty one ironworks have been examined petrologically and chemically analysed. Normal petrological examination by thin sections, of which 90 were prepared, sufficed in most cases, but occasionally polished surfaces were used, and details of etching methods are given. Tables of the optical properties and compositions of the phases likely to occur in slags are given, and the phase assemblages found are compared with those calculated from a knowledge of the system CaO - MgO - Al^2O^3 - SiO^2. It is shown that under the conditions of cooling normally employed chemical equilibrium is not always maintained.

Minerals likely to cause disintegration under certain circumstances are calcium orthosilicate and calcium sulphide. Free magnesia is not a probable constituent of slags even when a dolomite burden is employed.

INTRODUCTION

About 8.000.000 tons of blastfurnace slag are produced annually in Great Britain, and of this amount 51 per cent. is disposed of in the form of air-cooled slag for use as roadstone. Relatively small, although important, amounts are used as concrete aggregate formed slag for lightweight concrete or for cement manufacture.

While the study of the iron-smelting process demands a knowledge of the constitution of liquid slags, a subject on which much work has been done in recent years, from the point of view of disposal it is important to know the constitution of the solidified slag, cooled under various conditions. The object of such studies will be to determine the conditions under which unstable or otherwise deleterious minerals may occur, and the effect of the mineralogical constitution on texture, friability, etc For example Parker and Ryder (1) have investigated the « dusting » or « falling » of slags and have shown that it is due to the inversion of β 2 CaO . SiO^2 to γ 2 CaO . SiO^2.

As in comparable studies on Portland cement, succes is likely to be achieved by a combination of the study of constitution diagrams, such as the system CaO - MgO - SiO^2 - Al^2O^3 discussed in the present work, and the use of microscopical and X-ray methods of examining the slag itself.

(*) Crown Copyright Reserved.

The present paper is confined to studies on air-colled slag and deals with the mineralogy of the blastfurnace slags comprising the collection made at the Building Research Station over the period 1932 to the present day. Slags from twenty one ironworks have been examined, comprising a collection of 90 thin sections.

METHODS USED

Microscopic examinations by transmitted light of thin sections prepared in the manner used in studying rocks was sufficient for the determination of the minerals present in most cases. Occasionally when exact refractive indices were desirable powdered specimens were used, and on rare occasions polished and etched surfaces were employed. Transmitted light technique is described by Rigby (2), Winchell (3), Larsen and Berman (4) and Rogers and Kerr (5); work on reflected light has been discussed by Short (6), Parker and Nurse (7). Parker and Ryder (1) and Snow (8), the particular methods used in the present study are described later.

MINERALS PRESENT IN BLASTFURNACE SLAG

In the present work on blastfurnace slag the following minerals have been identified : calcium sulphide, melilite, α and β calcium metasilicate, monticellite, α', β and γ calcium orthosilicate, merwinite, forsterite, diopside, anorthite, rankinite and spinel. The optical properties, mineral names and chemical composition of these are given in Table I. The properties of calcium aluminate are also given as it may occur even in slags of relatively low Al^2O^3 content, although it has not been observed by the present authors.

Calcium Sulphide CaS : This mineral (oldhamite) (9) occurs in nearly every sample of slag examined, either as euhedral crystals of cubic or

TABLE I — MINERALS OCCURRING IN BLASTFURNACE SLAGS

MINERAL NAME	CHEMICAL FORMULA	CRYSTAL SYSTEM	REFRACTIVE INDICES α	β	γ	*Birefringence*	OPTICAL CHARACTER — Sign	2V	*Habit*	*Twinning*	*Cleavage*	*Elongation*	*Extinction Angle*
Gehlenite	$2\,CaO\,.\,Al_2O_3\,.\,SiO_2$	Tetragonal	1,669	—	1,658	0,011	Uni	—	Tabular	—	001	+ve	—
Akermanite	$2\,CaO\,.\,MgO\,.\,2\,SiO_2$	Tetragonal	1,633	—	1,639	0,006	Uni	+	Tabular	—	001	—ve	—
Pseudowollastonite	α $CaO\,.\,SiO_2$	Monoclinic	1,648	—	1,614	0,034	Biax	+	Needles	Simple	—	—ve	Small
Wollastonite	β $CaO\,.\,SiO_2$	Triclinic	1,634	1,63	1,620	0,014	Biax	—	Tabular	—	—	± ve	—
Bredigite	α' $2\,CaO\,.\,SiO_2$	Orthorhombic	1,710	—	1,725	0,015	Biax	+	Spherical	Multiple	—	—	—
Larnite	β $2\,CaO\,.\,SiO_2$	Monoclinic	1,715	1,720	1,737	0,023	Biax	+	010 tablets or spherical	100	100	—	X: c 13 . 14°
Dicalcium Silicate	γ $2\,CaO\,.\,SiO_2$	Orthorhombic	1,64	—	1,66	0,02	Biax	—	Fibrous	—	010(?)	+ve	—
Forsterite	$2\,MgO\,.\,SiO_2$	Orthorhombic	1,635	1,651	1,670	0,035	Biax	+	Tabular	031 Rare	010 001	± ve	—
Merwinite	$3\,CaO\,.\,MgO\,.\,2\,SiO_2$	Monoclinic	1,706	1,711	1,724	0,018	Biax	+	—	Complex	010	—ve	X: c 36°
Rankinite	$3\,CaO\,.\,2\,SiO_2$	Orthorhombic	1,641	1,645	1,650	0,009	Biax	+	—	—	poor 010	+ve	Symmetrical
Monticellite	$CaO\,.\,MgO\,.\,SiO_2$	Orthorhombic	1,639	1,646	1,653	0,014	Biax	—	—	—	poor 010	+ve	—
Diopside	$CaO\,.\,MgO\,.\,2\,SiO_2$	Monoclinic	1,664	1,672	1,694	0,029	Biax	+	Prismatic	100 or 001	110	+ve	Z: c 38°
Spinel	$MgO\,.\,Al_2O_3$	Cubic	—	1,723	—	—			Cube or octahedra	—	—	—	—
Anorthite	$CaO\,.\,Al_2O_3\,.\,2\,SiO_2$	Monoclinic	1,576	1,584	1,588	0,012	Biax	—	—	—	—	—	—
Calcium Aluminate	$CaO\,.\,Al_2O_3$	Monoclinic (?)	1,643	—	1,663	0,020	Biax	—	Tabular	—	—	—	—

octahedral shape or as small dendritic crystals of high refractive index, usually of a pale green colour in thin section. It may, be distinguished from MnS by measuring the reflectance.

Fig. 1.

Melilite : The melilites are an isomorphous series of solid solutions with a general formula of : $(CaNaK)^2\,(MgFe''Fe''Al)\,(SiAl)^2O^7$, Midgley (10). The principal members are akermanite $Ca^2\,Mg\,Si^2O^7$ and gehlenite $Ca^2\,Al\,Si\,AlO^7$. Melilite usually occurs as colourless euhedral crystals and in most blastfurnace slags it is the predominant mineral. The habit is usually lath-like or tabular, elongated in the direction of the a axis, with a marked 001 cleavage (fig. 1). The refractive indices vary with composition from gehlenite ε 1,699 ω 1,658, uniaxial negative to akermanite ε 1,633 ω 1,639, uniaxial positive. The melilite crystals are often zoned with a gehlenite rich core and an akermanite rich rim, between these an isotropic band may be seen representing the composition where the optic sign changes from negative to positive (fig. 2). The melilite crystals may show a phenomenon known as « peg structure » where small crystals, usually oldhamite, are included in the melilite host crystal, and are frequently arranged in an hour-glass structure.

Fig. 2.

Calcium metasilicate $CaO\,.\,SiO^2$: Two types of calcium metasilicate have been identified in blastfurnace slags, they are the α and β forms of $CaO\,.\,SiO^2$, known respectively as pseudowollastonite and wollastonite. The former is stable at high temperatures

and metastable at low temperatures, the latter is only stable at low temperatures, the inversion temperature being 1125 ± 10°C (11), Peacock (12) has described a third form parawollastonite, but this has not been identified in slags. Pseudowollastonite is a common constituent of blastfurnace slags, while wollastonite is rare; this rarity is presumably caused by the known sluggishness of the inversion of pseudowollastonite to wollastonite, once the high temperature modification has been formed (13).

α **CaO . SiO² pseudowollastonite,** occurs as small needle crystals, frequently twinned, the twin pairs having difference in extinction direction of about 5°. It is monoclinic with X : a 2°, α=1,610, β 1,611, γ 1,651, γ — α 0,041, biaxial positive, 2V 9°, positive elongation.

β **CaO . SiO² wollastonite,** occurs as large with a distinct 100 cleavage, usually elongated in the b direction. It is triclinic with b = Y, X : c 32°, α 1,620, β=1,63, γ=1,634, γ — α 0,014, biaxial negative, 2V 39°. Since the crystals are elongated in the direction b = Y lath-like sections may be either positively or negatively elongated.

Wollastonite is known to take FeO . SiO² into solid solution (14) and such crystals occur in slags as small needles, usually slightly brown in colour, and may be pleochroic. This type of wollastonite has been described by Tilley (15) as iron-wollastonite.

2 MgO . SiO² forsterite, is an olivine and occurs as subhedral crystals, usually slightly rounded, showing no cleavage or sign of decomposition. The crystals are orthorhombic and elongated in the c direction; α 1,635, β 1,651, γ 1,670, γ — α 0,035, biaxial positive, 2V 88°. When fayalite, 2 FeO . SiO², is present in solid solution the crystals are subhedral and have a slightly smaller 2V, indicating a small replacement of Mg by Fe.

CaO . MgO . SiO² monticellite, has an olivine structure, but in blastfurnace slags it does not appear to form solid solutions with forsterite, but occurs as a separate phase. The crystals are subhedral with symmetrical or straight extinction, orthorhombic, α 1,639, β 1,646, γ 1,653; γ — α 0,014, biaxial positive or negative, 2V 90°.

3 CaO . 2 SiO² rankinite, occurs as euhedral crystals of square cross-section with α 1,641, β 1,645, γ 1,650, γ — α 0,009, biaxial positive, 2V 85°. In most sections of the mineral in blastfurnace slags the extinction is symmetrical, the 110 faces being predominant.

Pyroxenes are minerals of the general formula $(RR')^2 Si^2O^6$. The common variety in blastfurnace slags is diopside, CaO . MgO . 2 SiO², the other variety is probably an iron subsituted diopside.

CaO . MgO . 2 SiO² diopside, occurs in slags as very small needles usually in the interstitial material. The crystals are longated in the c direction wth Z : c 38°; α 1,664, β 1,672, γ 6,94, γ — α 0,029; biaxial positive, 2V 59°, positive elongation.

Ferriferous diopside has much the same properties as diopside, but is very faintly brown when viewed by ordinary light in thin section and has a higher refractive index.

Dicalcium Silicate : The orthosilicate of calcium, 2 CaO . SiO², occurs in four modifications designated α, α', β and γ. The α' form is known as bredigite (16) and β as larnite (17). Of the four forms α has not been found in blastfurnace slags, the α' form, bredigite, is very rare; while both the β, larnite, and γ forms are very common in blastfurnace slags. It is this mineral, which when inverting to the γ form expands and so causes the « falling » of slags as described in Parker and Ryder (1). The high temperature forms, in particular, can take into solid solution other minerals and it is in this way that these higher temperature forms may be stabilised.

α' **2 CaO . SiO², bredigite,** occurs very rarely in slags. It forms lath shaped irregular crystals with low birefringence; some crystals may show polysynthetic twinning. The mineral is orthorhombic, α 1,710, γ 1,725, γ — α 0,015, biaxial positive, 2V 30°.

β **2 CaO . SiO² larnite,** is a common mineral in some blastfurnace slags, it occurs as either small rounded grains or as 010 tablets. The mineral is monoclinic with α 1,714, β 1,720, γ 1,737, γ — α 0,023 biaxial positive, 2V 70° (large). It is almost always twinned on 100 and in good sections extinction angles up to 14° may be found.

γ **2 CaO . SiO²,** is common in blastfurnace slags; it is formed usually by inversion from the higher α' or β modifications. Owing to its formation by inversion it is usually fibrous in nature, but the old crystal outlines of the higher forms may be seen in thin sections. It is orthorhombic, α 1,64, γ 1,66, γ — α 0,02, biaxial negative, 2V 66°.

CaO . Al^2O^3 . 2 SiO², Anorthite, is one of the end members of the plagioclase solid solution series. It is triclinic, α 1,575, β 1,583, γ 1,588, γ — α 0,013, biaxial negative 2V 77°.

MgO . Al^2O^3, Spinel, occurs as euhedral crystals, either cubes or octahedra. It is cubic, isotropic n 1,723 (fig. 3).

Fig. 3.

POLISHED SPECIMENS

In some special cases polished specimens of slag were prepared by the method described by Parker and Ryder (1). The technique is particularly useful in distinguishing between merwinite, larnite and bredigite, and for convenience the details are repeated below. When the surface had been polished it was etched as follows : the etch reagent was poured into a small watch glass and the specimen rapidly immersed, polished surface down, care being taken to avoid trapping air bublles on the surface.

The watch glass was gently rocked during the etching period. The specimen was removed and rinsed, in alcohol if the etch reagent was made up in alcohol, otherwise in water. Many etch reactions depend on he formation of a thin film on the surface of the crystal, which produces interference colours. Care is therefore necessary in drying so that the film may not be scratched. The best method was to dab gently on lens cleaning tissue or a soft cloth. Where the etch acts by the removal of a surface film, the surface is not harmed by gently wiping. A method sometimes used was to expose the surface to HF vapour. The specimen was placed face down on a crucible of lead or platinum half filled with the acid. When using high magnifications, trouble may be caused by the objective misting over. This can be avoided by a final drying of the specimen with a jet of warm air.

The etching of a polished specimen of slag proved very useful in distinguishing whether $2\,CaO.SiO^2$ is present (1). A ¼ per cent. solution by volume of nitric acid in alcohol will etch $2\,CaO.SiO^2$ in slag, the specimen being immersed in the reagent for 3 seconds, then washed in alcohol. This reagent also etches CaS and $3\,CaO.MgO.2\,SiO^2$ (merwinite). An etching reagent which is specific for $2\,CaO.SiO^2$ in slag is a 10 per cent. solution of $MgSO^4$. The specimen is immersed in this solution, previously heated to 50°C, for one minute, washed in water and dried by gently wiping with a soft cloth. The $\beta\,2\,CaO.SiO^2$ crystals usually show parallel or cross hatched striations (fig. 4), while the $\alpha'\,2\,CaO.SiO^2$ has a pitted appearance.

Fig. 4.

TEXTURE OF SLAG

The texture of slag depends on its chemical composition and on the rate of cooling. Highly siliceous slags readily form glasses if quickly cooled and at the other end of the scale some hematite iron slags are so basic that it is impossible to produce a glass even by high pressure granulation methods. Those ironworks which dispose of their slag in the air-cooled condition have usually been able to devise a cooling method for their particular composition which gives them a product of close-grained crystalline texture, easily broken down to the gradings desired, but resistant to further crushing and abrasion. In the coated macadam industry the tar-retaining properties of the surface are important.

In the ball method the slag is cooled in 5-12 ton ladles, cooling is slow and euhedral crystals of melilite may in some cases grow to 2 mm × 1 mm in size. All the phases present are well crystallised and present no difficulty in identification.

Slags tipped onto a bank are in general not so well crystallised; the rate of cooling is controlled to some extent by the method of tipping, and melilite crystals may be found up to 0,5 × 0,1 mm in size. « Honeycombed » pieces are more frequent, and if an old bank is being excavated, products of weathering such as sulphates, free sulphur, calcium hydroxide or calcium carbonate may be found in the pores and forming a coating over the slag pieces.

In the pit method the rate of cooling is controlled by the size of the pit and the schedule of filling. The pits are designed so tha the contents of a single ladle forms a layer which may be from 1 ½" to 6" thick according to the slag composition. If the pits are filled almost continuously, the lower layers are subjected to a constant annealing process as subsequent layers are built up.

It should be noted that the annealing process just described, and also the general practice of carrying molten slag for some distance before disposal are both processes which would tend to complicate the calculation of compound contents from phase equilibrium data by introducing the possibility of independent crystallisation of liquid formed after the deposition of a primary phase. It will be shown later that this process does in fact occur.

NUMBER OF RECOGNISABLE PHASES

The number of phases present will depend on the cooling conditions and on the number of components (in the thermodynamic sense) comprising the slag. Even in the most well-crystallised slag no more than six phases have been identified, and four or five is more usual. Calcium sulphide is found in every slag, and melilite almost invariably is the main constituent. Owing to their complete mutual solubility gehlenite and akermanite are nearly always found as a single melilite phase, although in some cases zoning is so marked tha the two minerals can be said to occur separately; in a few cases secondary crystallisation of melilite may be observed and this is always akermanite-rich as compared with the gehlenite-rich primary melilite.

PHASE ASSEMBLAGES

The phase assemblages found are given in Table IV.

PHASE EQUILIBRIA

The oxides CaO, MgO, Al^2O^3, SiO^2, together with sulphide sulphur, make up the major part of the analysis of normal blastfurnace slags. Since the sulphur content is invariably crystallised out as calcium sulphide, the sulphur and the necessary calcium for its combination as CaS can be ignored, and the rest of the analysis can then be recast so as to fall within the quaternary system $CaO - MgO - Al^2O^3 - SiO^2$.

TABLE II — PRODUCTS OF FINAL CRYSTALLISATION IN PART OF SYSTEM CaO - MgO - Al^2O^3 - SiO^2

C^2AS	C^2MS^2	C^2S	—	C^3S^2	—	—	—	—	—	—	—	—
C^2AS	C^2MS^2	C^2S	—	—	C^3MS^2	—	—	—	—	—	—	—
C^2AS	C^2MS^2	—	—	—	C^3MS^2	MA	—	—	—	—	—	—
C^2AS	C^2MS^2	—	—	—	—	MA	—	—	CAS^2	—	—	—
C^2AS	C^2MS^2	—	CS	—	—	—	—	—	CAS^2	—	—	—
C^2AS	C^2MS^2	—	CS	C^3S^2	—	—	—	—	—	—	—	—
—	C^2MS^2	—	CS	—	—	—	CMS^2	—	CAS^2	—	—	—
—	C^2MS^2	—	—	—	—	—	CMS^2	—	CAS^2	M^2S	—	—
—	C^2MS^2	—	—	—	—	MA	—	—	CAS^2	M^2S	—	—
—	C^2MS^2	—	—	—	—	MA	—	CMS	—	M^2S	—	—
—	C^2MS^2	—	—	—	C^3MS^2	MA	—	CMS	—	—	—	—
—	—	—	—	—	C^3MS^2	MA	—	CMS	—	—	—	MgO
—	—	—	—	—	—	—	CMS^2	—	CAS^2	M^2S	MS	—

KEY :

C^2AS 2 CaO . Al^2O^3 . SiO^2, gehlenite } melilite.
C^2MS^2 2 CaO . MgO . 2 SiO^2, akermanite }
C^2S 2 CaO . SiO^2, dicalcium silicate.
C^3S^2 3 CaO . 2 SiO^2, rankinite.
CS CaO . SiO^2, wollastonite or pseudowollastonite.
C^3MS^2 3 CaO . MgO . 2 SiO^2, merwinite.
MA MgO . Al^2O^3, spinel.
CMS^2 CaO . MgO . 2 SiO^2, diopside.
CMS CaO . MgO . SiO^2, monticellite.
CAS^2 CaO . Al^2O^3 . 2 SiO^2, anorthite.
M^2S 2 MgO . SiO^2, forsterite.
MS MgO . SiO^2, enstatite.
MgO periclase.

TABLE III — CHEMICAL ANALYSES OF SLAGS
by F.J. McConnell and L.J. Larner

SLAG	No.	CaO	BaO	MnO	S	SiO^2	TiO^2	Al^2O^3	MgO	FeO
Flaenavon	90b	43,17	nd	0,72	1,24	32,91	0,35	15,18	1,77	1,73
Cleveland	101b	33,53	nd	nd	1,05	23,10	0,45	23,12	8,60	1,15
Cargo Fleet	106	41,04	nd	1,32	1,53	32,19	0,91	15,28	4,14	1,19
Stanton	75c	45,22	nd	0,13	1,85	28,48	0,31	20,44	1,94	0,17
Kettering	62h	44,76	nd	0,07	2,32	27,68	0,25	20,72	3,70	0,06
Sheepbridge	77b	43,10	nd	0,51	1,21	30,09	0,48	16,43	2,21	0,21
Kettering	62a	41,45	nd	0,04	2,36	29,68	0,30	21,57	4,33	0,64
Kettering	62b	41,45	nd	0,06	2,70	29,63	0,28	21,65	4,25	0,59
Kettering	62c	42,00	0,15	0,05	2,52	29,18	0,30	21,80	3,53	0,56
Kettering	62d	41,68	0,13	0,09	2,51	28,93	0,32	21,85	3,87	0,65
Kettering	62f	39,65	nd	0,16	2,47	30,41	nd	21,00	3,36	1,76
Appleby	67b	42,84	nd	nd	1,27	31.38	nd	13,66	4,84	nd
Appleby	67c	43,04	nd	nd	1,57	31,64	nd	13,32	5,37	nd
New Cransley...	84a	40,26	0,11	0,11	1,97	31,44	0,42	20,73	4,25	0,65
New Cransley...	84b	39,96	nd	nd	2,07	28,25	0,44	17,74	4,16	0,84
Park Gate	86a	39,42	0,93	1,68	1,72	28,86	0,64	14,97	8,05	1,08
Irlam	88b	44,20	nd	1,00	1,45	28,05	0,58	16,88	6,35	0,54
Irlam	88c	44,77	nd	0,86	1,51	28,20	0,60	15,88	6,48	0,52
Irlam	88d	45,33	nd	0,90	1,22	28,38	0,60	16,19	5,61	0,42
Fords, Dagenham	1945	42,00	nd	0,87	1,36	37,40	nd	15,92	3,72	0.14
Fords, Dagenham	1947	47,50	nd	0,39	1,42	36,00	nd	12,60	3,21	0,12
Appleby	64d	44,42	nd	1,09	2,24	29,19	0,50	14 23	3,16	0,32
Appleby	64e	43,20	nd	1,46	nd	29,22	nd	15,65	5,50	nd
Iscor, South Africa	206	29,37	nd	nd	1,26	34,91	0,31	13,57	19,60	0,57
Pease and Partners	203	38,70	nd	nd	2,06	29,93	0,15	9,60	16,18	0,63
Gjiers Mills	204	36,78	nd	nd	1,47	33,79	0,31	12,19	14,10	0,23
Broken Hill (N.S. Wales) ...	256	33,16	0,22	4,13	0,74	33,39	1,54	23,22	1,72	0,36
Broken Hill (N.S. Wales) ...	257	34,64	0,13	3,67	0,61	35,48	1,28	18,92	2,28	0,59
Islip	70a	40,82	nd	nd	2,35	29,52	0,40	22,17	3,80	0,62
Islip	70b	42,43	nd	nd	2,53	29,00	0,37	21,59	3,37	0,66
Islip	70c	42,60	nd	nd	1,78	27,07	0,22	19,48	3,08	0,42
Ebbw Vale	91a	41,42	nd	nd	1,34	31,61	0,69	17,54	4,64	0,98
Acklam	97a	39,96	0,33	1,12	1,62	29,85	0,58	16,28	7,86	0,83
Corby	69a	30,58	nd	nd	1,37	33,85	nd	21,19	5,41	2,83

nd = not estimated.

It has been assumed that BaO and MnO can be included with CaO, TiO^2 with SiO^2, and FeO with MgO. Other types of replacement are certainly possible, for instance Ti for Al and Fe for Ca; the error involved is in any case not very great.

Previous attempts have been made to delineate some or all of the 4-phase tetrahedra within the system CaO - MgO - Al^2O^3 - SiO^2, notably those of McCaffery (19), Jänecke (20) and Berezhnoi (21). All these authors have also made some attempt at

identifying the nature of the invariant points in the system and have delineated some of the primary phase volumes. In the absence of adequate experimental data these hypothetical constructions can be very misleading. However, although many of the combinations postulated by McCaffery and his coworkers can be shown not to occur, credit is due to these authors for indicating the value of phase data in the study of slags in a pioneer work which clearly showed the complexity of the problem. Parker's (22) assemblages for low magnesia slags are confirmed in the present works, in which the 4-phase tetrahedra have been worked out anew on the basis of published work, both phase studies and mineralogical observations, and on the basis of unpublished phase data within the quaternary obtained by a number of works at the Building Research Station (23). The principal facts not available to the previous investigators are : (a) the existence of merwinite ($3\,CaO\,.\,MgO\,.\,2\,SiO^2$) as a primary phase in the system $CaO - MgO - SiO^2$, and the non-existence of the compound $5\,CaO\,.\,2\,MgO\,.\,6\,SiO^2$; (b) the existence of a quaternary compound (18) near the composition of calcium aluminate; (c) the occurrence of sapphirine $4\,MgO\,.\,5\,Al^2O^3\,.\,2\,SiO^2$ in the system $MgO - Al^2O^3 - SiO^2$ (24); (d) the true composition of the phases in the system $CaO - Al^2O^3$ i.e. $12\,CaO\,.\,7\,Al^2O^3$ instead of $5\,CaO\,.\,3\,Al^2O^3$ and $CaO\,.\,2\,Al^2O^3$ instead of $3\,CaO\,.\,5\,Al^2O^3$; (e) the non existence of « madisonite » $2\,CaO\,.\,2\,MgO\,.\,Al^2O^3\,.\,3\,SiO^2$; (f) the importance and size of the spinel field within the quaternary system was also underestimated.

Details of the solid-phase equilibria in the system $CaO - MgO - Al^2O^3 - SiO^2$ will be published in more detail elsewhere. A number of points remain obscure, for instance, Foster does not clearly delineate the solid phase relations of sapphirine, and it is possible that a $\beta - Al^2O^3$ phase of approximate composition $CaO\,.\,6\,Al^2O^3$ may exist (25, 26). Even when these last two phases are ignored, the larger system is divided into 38 tetrahedra, of which 20 may be involved in the crystallisation of blastfurnace slags.. Of these the 13 most frequently occuring are tabulated in Table II, those containing gehlenite and akermanite being given first owing to their greater importance.

Analyses of 34 blastfurnace slag samples are given in Table III; in most cases the analysis was carried out on the sample examined mineralogically. However, since a slide is made from a single piece, sampling errors are naturally large, and agreement between observed and calculated composition cannot be expected in every case. Actually the agreement, as shown in Table IV is remarkably good, and in cases of disagreement an explanation can be given, except for one sample.

Very small changes in chemical composition can often lead to a radical change in the nature of the phase assemblage formed on cooling. These conditions occur when the apex of a composition tetrahedron terminates on one of the bounding ternary systems. Such a tetrahedron for instance is the four-phase space $C^2AS - CAS^2 - MA - C^2MS^2$(*), which terminates on the plane $CaO - MgO - SiO^2$; as a consequence, for slags low in Al^2O^3 a very small change in either CaO, MgO or SiO^2 will bring the slag composition out of thos tetrahedon into one of the neighbouring ones.

The agreement between observed and calculated composition would only be perfect for slags fully crystallised under equilibrium conditions. However. cases of frozen equilibrium and independent crystallisation of the liquid phase occur. A notable instance is the group of slags having $3\,CaO\,.\,2\,SiO^2$ as a possible constituent. Owing to the incongruent melting of $3\,CaO\,.\,2\,SiO^2$ to give $2\,CaO\,.\,SiO^2$ and liquid, the $2\,CaO\,.\,SiO^2$ primary phase volume pentrates both the tetrahedra involved. It frequently follows that this group of slags crystallises $2\,CaO\,.\,SiO^2$ as an early phase, which redissolves with difficulty on further cooling.

The zoning of the melilite has already been mentioned; the conditions under which such zoning occurs have been described by Bowen (27). It is a necessary consequence that whenever zoning is observed the slag is not in equilibrium, and since the central portion of the massive melilite crystals is gehlenite-rich, the composition of the remaining melt after melilite crystallisation is complete must lie in the region of the quaternary diagram reached by extending the straight line from gehlenite (or a point on the join gehlenite-akermanite) through the original composition point. As an example, slags 101b and 69a both fall in the composition tetrahedron $C^2AS - C^2MS^2 - MA - CAS^2$. However the primary gehlenite forms large zoned crystals such that the remaining melt might fall within either of the tetrahedra $C^2MS^2 - MA - CAS^2 - M^2S$ or $C^2MS^2 - CAS^2 - CMS^2 - CS$. In the event of independent crystallisation of this liquid, any of the new phases CMS^2, M^2S or CS might be found. In fact CMS^2 solid solutions (pyroxenes) are found in both slags.

It is therefore clear that deductions concerning the constitution of blastfurnace slag arrived at by a study of the phase equilibrium diagrams must always be checked by direct mineralogical observation. This was already recognised by Parker and Ryder (1) in their studies on falling slags, and as a consequence a microscopic examination is included in the British Standard for Air-Cooled Blastfurnace Slag for Concrete Aggregate (War Emergency, B.S. 1057: 1942).

CONCLUSIONS

Slags derived from a burden employing limestone flux normally crystallise with melilite or dicalcium silicate as a primary phase. If completely crystallised under equilibrium conditions such slags would yield the phase assemblages given in the first part of Table II. Slags are however rarely equilibrium products, glass frequently being present and independent cystallisation of residual liquids taking place. Anorthite, being one of the last phases to crystallise, is rarely found in blastfurnace slags.

In slags derived from a dolomitic burden the melilite phase may be pure akermanite; the magnesium-containing minerals merwinite, monticellite or forsterite may be found in these slags, but not periclase.

(*) See key, Table II.

TABLE IV

SLAG	No.	C_2AS	C_2MS_2	CS	C_2S	CMS	C_3MS_2	M_2S	CMS_2	C_3S_2	MA	CAS_2	Notes
Blaenavon	90b	XO	XO	X	ZO	—	—	—	—	X	—	—	—
Cleveland	101b	XO	XO	—	—	—	—	—	ZO	—	XO	XO	—
Cargo Fleet	106a	XO	XO	XO	—	—	—	—	—	XO	—	—	—
Stanton	75c	XO	XO	XO	ZO	—	—	—	—	X	—	—	—
Kettering	62h	XO	XO	ZO	XO	—	—	—	—	XO	—	—	—
Sheepbridge	77b	XO	XO	XO	ZO	—	—	—	—	X	—	—	—
Kettering	62a	XO	XO	XO	—	—	—	—	—	—	—	X	—
Kettering	62b	XO	XO	XO	—	—	—	—	—	—	—	X	—
Kettering	62c	XO	XO	XO	—	—	—	—	—	—	—	X	—
Kettering	62d	XO	XO	XO	—	—	—	—	—	—	—	X	—
Kettering	62f	XO	XO	XO	—	—	—	—	—	O	—	X	(i)
Appleby	67b	XO	XO	—	XO	—	—	—	—	X?O	—	—	—
Appleby	67c	XO	XO	—	XO	—	—	—	—	XO	—	—	—
New Cransley...	1a	XO	XO	XO	O	—	—	—	—	O	—	X	(i)
New Cransley...	84b	XO	XO	XO	O	—	O	—	—	X	—	—	(ii)
Park Gate	86a	XO	XO	—	—	—	XO	—	—	—	X	—	—
Irlam	88b	XO	XO	—	—	—	XO	—	—	—	X	—	—
Irlam	88c	XO	XO	—	—	—	XO	—	—	—	X	—	—
Irlam	88d	XO	XO	—	XO	—	XO	—	—	—	—	—	—
Fords, Dagenham (*) ...	1945	XO	XO	XO	—	—	—	—	—	O	—	X	(i)
Fords, Dagenham (*) ...	1947	XO	XO	ZO	XO	—	—	—	—	XO	—	—	—
Appleby	64a	XO	XO	—	XO	—	—	—	—	X	—	—	—
Appleby	64c	XO	XO	—	XO	—	—	—	—	X	—	—	—
Iscor, South Africa	206	—	XO	—	—	—	—	XO	—	—	XO	X	—
Pease and Partners	203	—	XO	—	—	XO	XO	—	—	—	XO	—	—
Gjiers Mills	204	XO	XO	—	—	O	XO	—	—	—	XO	—	—
Broken Hill (N.S. Wales) ...	256	XO	XO	X	—	—	—	—	—	—	—	X	(iii)
Broken Hill (N.S. Wales) ...	257	XO	XO	X	—	—	—	—	—	—	—	X	(iii)
Islip	70a	XO	XO	—	—	—	—	—	—	—	—	—	(iii)
Islip	70b	XO	XO	XO	—	—	—	—	—	—	—	X	—
Islip	70c	XO	XO	—	XO	—	—	—	—	X	—	—	—
Ebbw Vale	91a	XO	XO	XO	—	—	—	—	—	X	—	—	—
Acklam	97a	XO	XO	—	—	—	XO	—	—	—	X	—	—
Corby (*)	69c	XO	XO	—	—	—	—	—	ZO	—	X	X	—

KEY :

O = Phase determined by mineralogical examination.
X = Phase determined by calculation from chemical analysis, complete equilibrium.
Z = Phases observed would be formed if liquid crystallised independently of the primary phase.

NOTES :

(*) Mineralogical observations made on different grade of sample from that used for chemical analysis.
(i) Content of CAS_2 small, observed result could be due to slight error in sampling or analysis.
(ii) Unexplained discrepancy.
(iii) Glassy slags.

Although the potential phase composition may be forecast with high accuracy from a knowledge of the system $CaO - MgO - Al_2O_3 - SiO_2$, a mineralogical examination is necessary to establish the presence or absence of a phase with certainty.

The only minerals which are likely to cause disintegration when the air-cooled slag is used as roadstone or concrete aggregate are calcium orthosilicate and calcium sulphide or its products when weathered. The measures necessary to avoid trouble from these sources will be discussed elsewhere (28). The phase constitution study shows that magnesia is unlikely to form either as a primary phase or devitrification product in granulated slags which may be used for cement manufacture.

ACKNOWLEDGMENTS

This paper is published with permission of the Director of Building Research and was carried out as part of the programme of research of the Building Research Board.

REFERENCES

1. PARKER, T.W., and RYDER, J.F., *Jour. Iron & Steel Inst., 146*, 2, 21 P-61 P, 1942.
2. RIGBY, G.R., *Mineralogy of Ceramic Materials*, Stoke, 1948.
3. WINCHELL, H.N., *Elements of Optical Mineralogy*, New York, 1937.
4. LARSEN, E.S., and BERMAN, H., *The microscopic determination of the non-opaque minerals*, Washington, 1934.
5. ROGERS, A.F., and KERR, P.F., *Optical Mineralogy*, New York, 1942.
6. SHORT, N.M., *U.S. Geol. Survey Bull.*, 914, 1940.
7. PARKER, T.W. and NURSE, R.W., *J.S.C.I., 58*, 255, 1939.
8. SNOW, R.B., *Amer. Inst. of Min. & Met. Eng. Tech. Pub.*, 2167, 1947.
9. VOGT, J.H.L., *Die Schlacke*, Dresden, 1912.
10. MIDGLEY, H.G., *Thesis*, Ph.D. London University, 1949.
11. OSBORN, E.F., and SCHAIRER, J.F., *Amer. Jour. Sci., 239*, 721, 1941.
12. PEACOCK, M.A., *Amer. Jour. Sci., 30*, 495, 1935.
13. LEA, F.M., and NURSE, R.W., *Diss. of Faraday Soc.*, n° 5, 1949.
14. SUNDIUS, N., *Amer. Min.*, 16, 411, 1931.
15. TILLEY, C.E., *Amer. Min., 33*, 736, 1948.
16. TILLEY, C.E., *Min. Mag., 28*, 255, 1948.
17. TILLEY, C.E., *Min. Mag., 22*, 77, 1929.
18. PARKER, T.W., *Private Communication.*
19. McCAFFERY, R.S., OESTERLE, J.F., and SCHAPIRO, L., *Amer. Inst. Min. & Met. Eng. Tech. Pub.*, 383, 1928.
20. JAENECKE, E., *Miner. und Phase., Fordsch. t. Min., 14*, 98, 1933.
21. BEREZHNOI, A.S., *Zhurnal. Prikladnoi. Khimii., 21*, (7), 717, 1948.
22. PARKER, T.W., *Chemistry & Industry, 60*, (5), 59, 1941.
23. NURSE, R.W., STUTTERHEIM, N., POMEROY, A.M., THEOKRITOFF, S., unpublished data, 1948, 1949. 1950.
24. FOSTER, W.R., *Jour. Amer. Cer. Soc., 33*, 373, 1950.
25. FILONENKO, N.E., *C.R. Acad. Sci.*, URSS. *48*, 430, 1945.
26. SUORI KATO and TOSHUJOSHI YAMAUCHI, *J. Japan Ceramic Assoc., 51*, 465, 1943.
27. BOWEN, N.L., *Amer. Jour. Sci., 35*, 1913.
28. PARKER, T.W., *Paper to be read at Inst. of Eng. and Shipbuilders of Scotland*, 1950.

RESUME DE LA DISCUSSION

M. KOZAKEVITCH. — L'auteur a-t-il étudié l'influence des conditions de solidification de ces différents échantillons ?

M. NURSE. — Ces essais n'ont pas été entreprise au laboratoire. Tous les échantillons étaient des types de scories industrielles utilisées comme matériaux de construction et ont été seulement examinés au point de vue de leur cristallisation.

DS 98319/1/1061 300 10/51 CL

6

MIDGLEY (H·G)
D.Sc. 1967

Reprinted from *Acta Crystallographica*, Vol. 4, Part 6, November 1951

PRINTED IN GREAT BRITAIN

Acta Cryst. (1951). 4, 565

A quick method of determining the density of liquid mixtures.

By H. G. MIDGLEY, *Building Research Station, Garston, Watford, Herts, England*

(*Received* 15 *August* 1951)

Crystallographers frequently determine the density of crystals by flotation in heavy liquid mixtures. The density of the liquid has then to be found, usually by means of a density bottle. At least 5 cm.^{3} of liquid are required, and the determination takes some time.

A more rapid method, which needs as little as 0·1 cm.^{3} of liquid, involves measuring the refractive index on a suitable refractometer. Both the refractive index and density of liquid mixtures are approximately proportional to the quantity of each component, so that calibration curves of refractive index against density can be drawn up. The temperature coefficients of refractive index and density approximately compensate each other so that only one curve is necessary for normal use.

A suitable mixture for many crystals is methylene iodide and benzene; the refractive index/density values for such mixes are given in Table 1. Using a curve prepared from this table, the density of any mixture of methylene iodide and benzene may be obtained in less than a minute by using a direct-reading refractometer such as the Abbé.

Table 1. *Refractive index and density of methylene iodide–benzene mixtures*

Refractive index at 20° C.	Density at 20° C. (g. cm.$^{-3}$)
1·740	3·316
1·717	3·008
1·700	2·958
1·678	2·759
1·665	2·651
1·643	2·431
1·625	2·236
1·609	2·072
1·588	1·886
1·574	1·728
1·555	1·537
1·538	1·332
1·519	1·109
1·501	0·877

6

DISCUSSION

H. G. MIDGLEY

MELILITE FROM HIGH-ALUMINA CEMENT

One of the minor constituents of high-alumina cement is a melilite, usually referred to as gehlenite. In one sample of cement clinker, that described in the paper by Dr. Parker as U.S. and Example No. 2, the melilite occurred in sufficient quantity to attempt a mineral separation. The clinker contained about 25 per cent of melilite, but the crystals were not of very good shape and on crushing many of the grains consisted of more than one phase, so that to obtain a pure separation a very large quantity of material was needed to give a reasonable yield.

The method of separation was as follows: the raw clinker was crushed, retaining the fraction of 52-100 B.S. sieve size; this sample was hydrated in a very large excess of water, the whole being shaken for seven days. The hydration affected the calcium aluminates and some of the iron-bearing phases, the hydrates were removed by washing with dilute sodium hydroxide, the residue being washed with alcohol and dried. Control of the separation was maintained by frequent microscopic examination of the material at all stages. The residue after hydration and washing consisted of the melilite and part of the ferrites. The melilite is non-magnetic so a further concentration was made using a Hallimond electro-magnetic separator. To obtain the final complete separation the non-magnetic concentrate was centrifuged with heavy liquids of suitable density. Using nearly all the available material, about 50 g, only 0·2 g of pure melilite was obtained. This sample was analyzed and the result is given in Table 1.

TABLE 1: Analysis of melilite from high-alumina cement (analysis by *Larner*)

SiO_2	17·1	Al_2O_3	38·5
FeO	1·7	CaO	39·5
Fe_2O_3	0·6	MgO	0·5
TiO_2	1·7	loss on ign.	nil

The atomic ratios, referred to seven oxygen atoms, give as the formula:

$$Ca_{2\cdot00}(Mg_{0\cdot003}Fe''_{0\cdot07}Fe'''_{0\cdot002}Al_{0\cdot095})_{1\cdot025}(Al_{1\cdot17}Si_{0\cdot83})_2O_7$$

This formula is in agreement with the general formula proposed by Warren[1] for melilites

$$(CaNaK)_2(MgFe''Fe'''Al)\,(SiAl)_2O_7$$

However, in the case of the melilite from high-alumina cement there is an unusual feature in that the $(SiAl)_2O_7$ radical contains more Al than Si, which means that some mineral containing more Al than gehlenite must be present in solid solution. It can be calculated that this compound is CA_2.

REFERENCE

1. WARREN, B. E. *Zeitschrift für Kristallographie.* 1930. Vol. 74. p. 131.

Midgley[40] has partially overcome this difficulty by concentrating the C_2S fraction of clinker by a process of differential hydration of the clinker minerals. By this means he has shown that only lines corresponding to β are found in X-ray patterns of concentrates from the clinker collection at the Building Research Station.

In one case Midgley was able to carry the concentration process further and to obtain an essentially homogeneous sample of C_2S large enough for chemical and physical examination. The preparation gave a β pattern and the analysis is given in Table 8.

TABLE 8: Analysis of C_2S separated from Bassett clinker. Analysis by *L. J. Larner*

CaO	57·76
MgO	0·62
SiO_2	32·76
Fe_2O_3	0·64
TiO_2	0·14
Mn_2O_3	0·03
Na_2O	0·01 max.
K_2O	0·14 max.
Al_2O_3	4·62
Loss on ignition	3·45

Unfortunately the clinker was of an unusual type, being produced by the Bassett process. Also some surface coating was visible under the microscope and this taken with the high figure for Al_2O_3 and combined water suggests that alumina gel is present, formed by complete hydrolysis of the calcium aluminates of the clinker. All the sample was expended in analysis, so further treatment to remove gel could not be attempted. It is hoped however that further development of the separation process will make it possible to obtain reliable analyses of the clinker phase. Leaving the question of combined Al_2O_3 open, then the content of possible stabilizers of the β form in the present example is remarkably small. Since metallic iron was present in the clinker the iron quoted as Fe_2O_3 was probably present in divalent condition; sulphide was definitely present and probably also SO_3; the latter

will be included in the loss on ignition. It is possible therefore that the stabilizers in this special case were CaS and K_2SO_4.

It has been shown by Swayze,[1] Yamauchi[2] and Malquori and Cirilli[3] that a solid solution series exists between dicalcium ferrite and a composition near to $6CaO.2Al_2O_3.Fe_2O_3$. X-ray powder spacings of some compositions in this series have been given by Malquori and Cirilli.[3] X-ray powder examination of compositions in this series have also been made by the author at the Building Research Station, the results are slightly different from those of Professor Malquori and Professor Cirilli, but agree with the results of Hansen and Brownmiller.[4] As Professor Malquori and Professor Cirilli have shown, the lattice dimensions change with composition and this then gives a method of estimating the composition of the ferrite phase in commercial clinkers. In X-ray powder photographs of untreated clinker specimens usually only one line of the ferrite phase can be determined (Midgley),[5] i.e. the 200 reflection at approximately 2·63Å, the strongest line of the ferrite pattern. This spacing varies very little with composition, so another reflection must be used, such as the 202, which varies from 1·944Å in $2CaO.Fe_2O_3$ to 1·911Å in $6CaO.2Al_2O_3.Fe_2O_3$. This reflection is then suitable as an indicator line to determine the composition of the ferrite phase. A graph showing composition of phase plotted against the *d* value of the 202 spacing is given in Figure 1.

The 202 reflection cannot be detected in a powder photograph of the untreated clinker but by taking a sized (52–100 B.S. sieve) sample of the clinker and passing it through an electromagnetic separator the ferrite phase was concentrated in the magnetic fraction sufficiently for the 202 reflection to be resolved.

DISCUSSION

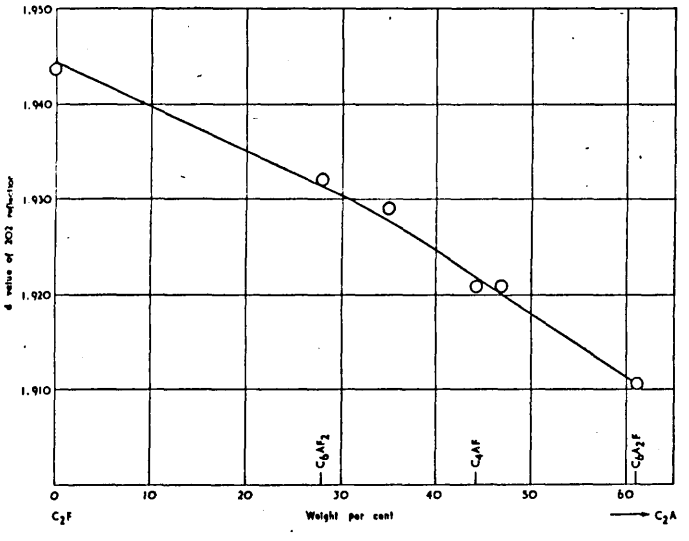

Figure 1.

A number of cement clinkers in the Building Research Station collection were subjected to this treatment and the results of this examination are given in Table 1.

On examination of the photographs of the cement clinkers it was found, in some cases, that the 202 indicator line could be measured with accuracy (to $\pm 0{\cdot}004$Å), this being equivalent to ± 4 per cent in determination of composition. In many other cases, however, the reflection was broad; this broadening could be ascribed to the small crystal size, but other reflections in the pattern such as 200 were of normal width, so another explanation must be sought. It seems very probable that this line broadening is due to crystal zoning, caused by non-equilibrium whilst cooling. The phenomenon of zoning in solid solutions is very common and has been discussed by Bowen.[6] The zones would represent compositions on either side of the bulk composition, so that the X-ray diffraction pattern would show this by broad lines. A microphotometer trace of the broad lines shows a flat area, the limits of which can be estimated reproducibly by visual examination of the original photograph. This visual examination was used in compiling the data for Table 1.

In clinker samples No. A7, A8, A33, the broad line extended beyond a d value of 1·911Å, this is probably due to interference by the 1·905Å line of C_3A. In compiling the table it has been assumed that in these cases the solid solution of maximum C_2A content is present.

In one clinker, A141, the broad band is resolved into two distinct peaks—at 1·911 and 1·927Å, corresponding to two separate generations of ferrite phases of compositions C_2A:C_2F, 35:65 and C_2A:C_2F, 62:28 respectively.

Of the samples examined, two have a composition of C_4AF, two C_6AF_2, four between C_6AF_2 and C_4AF, and four samples show zoning with a composition range.

TABLE 1.

Cement No.	202 spacing Å	Composition by weight (per cent.)	
		C_2A	C_2F
A9	1·922	44	56
Ferrari	1·921	44	56
A35	1·935	25	75
A113	1·932	24	76
A20	1·929	34	66
A40	1·928	34	66
A39	1·928	34	66
A37	1·929	34	66
A141	1·927 ⟷ 1·911	35–62	65–38
A10	1·928 ⟷ 1·911	35–62	65–38
A36	1·935 ⟷ 1·911	26–62	74–38
A143	1·927 ⟷ 1·911	35–62	65–38
A7	1·920 ⟶	46–62	54–38
A5	1·919 ⟶	47–62	53–38
A33	1·931 ⟶	29–62	71–38

TABLE 2: Chemical analyses of cement clinkers (analyses by *F. J. McConnell, L. J. Larner* and *W. J. Grindle*)

	A9	A10	A20	A35	A36	A37	A39	A40	A143
SiO_2 ..	20·10	21.00	21·65	20·43	20·26	22·63	20·22	20·72	23·78
CaO ..	65·60	65·45	66·10	65·08	64·28	64·90	66·91	66·94	64·90
Al_2O_3 ..	6·14	5·69	6·00	6·71	6·45	4·97	6·77	5·94	5·14
Fe_2O_3 ..	4·19	4·25	2·55	2·34	2·95	2·48	3·07	3·07	2·88
FeO ..	0·17	0·07	Nil	Nil	Nil	Nil	Nil	Nil	Nil
TiO_2 ..	0·28	0·28	0·25	0·35	0·30	0·23	0·25	0·27	0·35
MgO ..	1·19	1·20	2·27	1·32	0·89	1·98	0·92	1·15	1·17
Na_2O } ..	0·6	0·85	0·17	0·16	0·28	0·18	0·36	0·33	0·13
K_2O } ..			0·16	0·78	0·60	0·60	0·47	0·76	0·76
SO_3 ..	1·08	0·84	0·05	1·74	n.e.	1·38	0·21	0·25	n.e.
Loss on Ign.	1·11	0·78	n.e.	n.e.	2·02	n.e.	n.e.	n.e.	n.e.

n.e. = not estimated.

REFERENCES

1. SWAYZE, M. A. *American Journal of Science.* 1946. Vol. 244. p. 65.
2. YAMAUCHI, T. *Journal of the Japanese Ceramic Society.* 1937. Vol. 45. p. 279. 1938. Vol. 46. p. 66.

3. MALQUORI, G. and CIRILLI, V. *Third International Symposium on the Chemistry of Cement.* London. 1952.
4. HANSEN, W. C. and BROWNMILLER, L. T. *American Journal of Science.* 1928. Vol. 15. p. 225.
5. MIDGLEY, H. G. *Journal of Applied Physics.* 1952, Vol. 3, p. 279.
6. BOWEN, N. L. *American Journal of Science.* 1913. Vol. 35. p. 583.

Reprinted from The Journal of the Iron and Steel Institute
June 1953, Vol. 174, pp-121-131

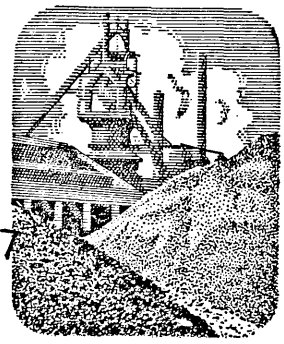

Studies on the Melilite Solid Solutions

By R. W. Nurse, M.Sc., F.Inst.P., and H. G. Midgley, M.Sc., Ph.D., F.G.S.

SYNOPSIS

Melilite is the major constituent of crystalline blast-furnace slag; the melilite series of minerals is also found in cement clinkers and in some natural rocks. From a consideration of the structure and chemical composition of melilites, the following general formula may be postulated: $(CaNaK)_2$ (Mg, Fe″Fe‴Al) $(SiAl)_2O_7$. This suggests the following end members: åkermanite, $Ca_2MgSi_2O_7$; gehlenite, $Ca_2Al_2SiO_7$; iron-åkermanite. $Ca_2Fe''Si_2O_7$; iron-gehlenite, $Ca_2Fe'''SiAlO_7$; sodium-melilite, $NaCaAlSi_2O_7$; potassium-melilite, $KCaAlSi_2O_7$. Of these, the first five have been prepared artificially from pure oxides and the following systems have been investigated: (i) $Ca_2MgSi_2O_7$-$Ca_2Fe'''SiAlO_7$; (ii) $Ca_2Al_2SiO_7$-$Ca_2Fe'''SiAlO_7$; (iii) $NaCaAlSi_2O_7$-$Ca_2MgSi_2O_7$; (iv) $NaCaAlSi_2O_7$-$Ca_2Al_2SiO_7$; (v) $KCaAlSi_2O_7$-$Ca_2Al_2SiO_7$, and (vi) $Ca_2MgSi_2O_7$-$Ca_2Al_2SiO_7$-$Ca_2Fe'''SiAlO_7$.

Phase equilibrium and refractive indices diagrams have been constructed. The results show that these melilites form complete solid solutions with each other. It has also been found experimentally that diopside and calcium orthosilicate enter into solid solution, to a very limited extent, with melilites. 752

Introduction

THE melilites are tetragonal silicates or alumino-silicates forming an extensive series of solid solutions that cover a wide range of chemical composition. The group was first named by Bellevue;[1] early workers suggested the formula $3CaO.Al_2O_3.SiO_2$ for naturally occurring gehlenite, but Shepherd and Rankin[2] showed, by means of synthetic preparations, that the composition is $2CaO.Al_2O_3.SiO_2$. Later, Ferguson and Buddington[3] delineated the phase diagram for the most important solid-solution series, gehlenite ($2CaO.Al_2O_3.SiO_2$)-åkermanite ($2CaO.MgO.2SiO_2$).

Melilites are of technological importance because they form the major constituent of crystalline blast-furnace slag; they are also found in high-alumina cement, and they may be formed during slag attack on basic refractories. They are found in nature, where they occur in the zone of contact of metamorphosed limestones, and in basic igneous rocks with a high CaO content.

Natural melilites contain appreciable quantities of alkalis and iron, and various workers have suggested solid-solution series to account for this. Berman[4] suggested the general formula: $(Ca + Na)_{20-x}Mg_y Al_2Si_{2g-y-z}O_{70}$, where $x = 0$–3, $y = 0$–10 and $z = 0$–20.

Warren[5] determined the atomic structure by X-ray analysis and gave as the general formula: $(Ca,Na)_2 (Mg,Al)(Si,Al)_2O_7$.

The substitution of Al for Si in the Si_2O_7 radical is only possible to the extent that a trivalent element such as Al or Fe‴ occurs in the second bracket. With this proviso, it is possible to extend the formula to take into account most of the minor constituents important in slag technology, as follows: $(Ca,Na,K)_2$ $(Mg,Fe''Fe''',Al)(Si,Al)_2O_7$.

The present work deals with the end members

$Ca_2Al_2SiO_7$	–gehlenite
$Ca_2MgSi_2O_7$	–åkermanite
$Ca_2Fe''Si_2O_7$	–iron-åkermanite
$Ca_2Fe'''SiAlO_7$	–iron-gehlenite
$NaCaAlSi_2O_7$	–sodium-melilite
$KCaAlSi_2O_7$	–potassium-melilite

and with the following systems between them:

gehlenite–åkermanite
gehlenite–iron-gehlenite
iron-gehlenite–åkermanite
gehlenite–åkermanite–iron-gehlenite
gehlenite–sodium-melilite
gehlenite–potassium-melilite
åkermanite–sodium-melilite.

During the description and discussion, it will be convenient to write the formulae of the various components in different ways. The ionic formula (*e.g.*, $Ca_2Al_2SiO_7$ for gehlenite) brings out clearly the structural relationship of the various melilites. On the other hand, the ' oxide formula ' (*e.g.*, $2CaO.Al_2O_3.SiO_2$) enables the composition to be located readily in phase diagrams. Table I gives the mineral names and the various methods of writing the formulae.

EXPERIMENTAL METHODS

Synthetic preparations were made up from silica, alumina, ferric oxide, magnesium carbonate, sodium carbonate, potassium carbonate, and calcium carbonate of high purity. Analyses of these materials are given in Table II. The methods of preparation were as described by Nurse.[6] For the determination of melting points and solidus points, the quenching technique was used, employing special furnaces as described by Nurse and Welch.[7] Refractive indices were determined by the immersion method, using sodium light, and X-ray spacings were determined

Manuscript received 11th December, 1952.
Mr. Nurse is a Senior Principal Scientific Officer at the Building Research Station, Garston, Herts Dr. Midgley is a Senior Scientific Officer.

Table I

KEY TO COMPOUNDS

Åkermanite	$Ca_2MgSi_2O_7$	$2CaO.MgO.2SiO_2$	Calcium-orthosilicate	Ca_2SiO_4	$2CaO.SiO_2$
Gehlenite	$Ca_2Al_2SiO_7$	$2CaO.Al_2O_3.SiO_2$			
Iron-åkermanite	$Ca_2Fe'''Si_2O_7$	$2CaO.FeO.2SiO_2$	Diopside	$CaMgSi_2O_6$	$CaO.MgO.2SiO_2$
Iron-gehlenite	$Ca_2Fe'''SiAlO_7$	$4CaO.Fe_2O_3.Al_2O_3.2SiO_2$	Pseudo-wollastonite	$CaSiO_3$	$CaO.SiO_2$
Sodium-melilite	$NaCaAlSi_2O_7$	$Na_2O.2CaOAl_2O_3.4SiO_2$			
Potassium-melilite	$KCaAlSi_2O_7$	$K_2O.2CaO.Al_2O_3.4SiO_2$	Wollastonite	$CaSiO_3$	$CaO.SiO_2$
			Nepheline	$NaAlSiO_4$	$Na_2O.Al_2O_32SiO_2$

Table II

ANALYSES OF MATERIALS USED

	SiO_2, %	Al_2O_3, %	MgO, %	Fe_2O_3, %	CaO, %	Na_2O, %	K_2O, %	SO_3, %
SiO_2	99·72	0·102	0·035	0·039	0·004	0·017	nil	0·014
Al_2O_3	n.e.	99·26	n.e.	0·03	0·04	0·19	0·04	0·08
$CaCO_3$	n.e.	0·03	0·01	0·01	56·08	n.e.	n.e.	0·01
Na_2CO_3	nil	0·003	n.e.	nil	0·01	73·3	nil	0·01
K_2CO_3	0·01	0·01	0·003	0·001	0·004	1·78	87·08	n.e.
Fe_2O_3	0·15	0·01	0·02	99·29	nil	0·07	nil	trace
MgO*	0·25	0·04	99·25	0·046	0·07	n.e.	n.e.	0·36

* Ignited at 1200° C. just before weighing n.e. = Not estimated

Table III

VALUES OF INTERPLANAR SPACINGS OF MELILITE END MEMBERS

Gehlenite[9] $CuK_\alpha\lambda = 1·542$	Åkermanite[9] $CuK_\alpha\lambda = 1·542$	Iron-gehlenite $CuK_\alpha\lambda = 1·542$	Sodium-melilite $CuK_\alpha\lambda = 1·542$	Iron-åkermanite[11] $FeK_\alpha\lambda = 1·9373$
VVW 4·232	VW 4·222	VW 4·083	VVW 4·17	
WM 3·708	W 3·717	W 3·649	VVW 3·80	
VVW 3·439				
WM 3·063	VW 3·508	VVW 3·414	S 3·21	
S 2·846	M 3·088	W 3·035	S 2·98	S 2·874
VVW 2·719	S 2·874	S 2·821	S 2·81	
VVW 2·534	VVW 2·505	VVW 2·705	VW 2·548	
	M 2·480			
M 2·432	W 2·426	VVW 2·517	W 2·392	S 2·499
M 2·407	WM 2·386	M 2·398	W 2·319	
M 2·396	WM 2·318	M 2·291	W 2·267	
M 2·297	W 2·283	VVW 2·181	M 2·069	
M 2·287	VVW 2·223	WM 2·026	VW 2·014	
VW 2·193	VVW 2·111	VW 1·847	S 1·965	M 2·199
VVW 2·116	M 2·039	VW 1·812	VW 1·908	M 2·036
WM 2·040	VW 1·996	VW 1·754	VVW 1·862	
VW 1·966	WM 1·961	VW 1·723	VW 1·831	
WM 1·922	WM 1·902	S 1·629	VW 1·788	M 1·762
W 1·865	VW 1·859	VVW 1·510	S 1·736	
W 1·854	WM 1·849	VW 1·433	WM 1·700	W 1·699
WM 1·813	WM 1·779	MS 1·374	WM 1·677	
S 1·755	MS 1·763	VVW 1·318	MS 1·603	
S 1·752	W 1·734	W 1·248	M 1·584	
W 1·720	VVW 1·670	W 1·182	WM 1·492	
VVW 1·707	VVW 1·655		WM 1·462	
W 1·632	W 1·643		WM 1·421	
W 1·628	W 1·599		VVW 1·395	
VW 1·613	VW 1·537		S 1·374	
VVW 1·547	VW 1·515		S 1·361	
M 1·516	WM 1·508		VVW 1·334	
VW 1·474	VW 1·487		M 1·304	
VVW 1·445	W 1·470		M 1·269	
W 1·435	VVW 1·456			
VW 1·423	WM 1·436			
VVW 1·410	WM 1·431			
VW 1·387	W 1·407			
M 1·374	VVW 1·398			
W 1·359	W 1·386			
	M 1·385			

S = strong WM = weak medium VW = very weak
MS = medium strong W = weak VVW = very very weak
M = medium

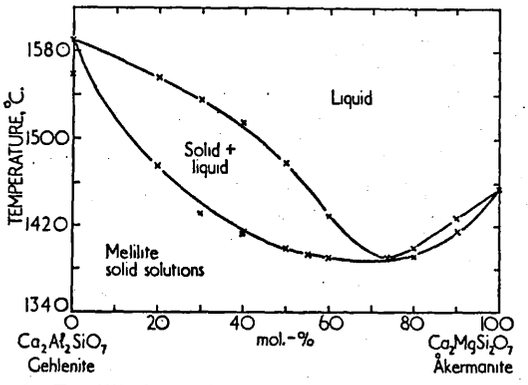

Fig. 1—Equilibrium diagram for system gehlenite–åkermanite (after Osborn and Schairer[8])

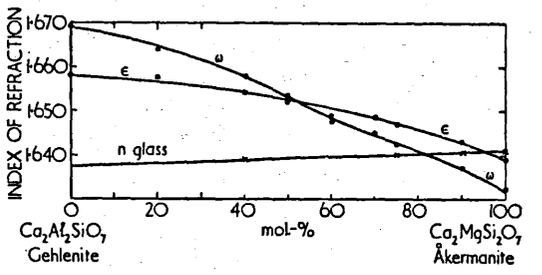

Fig. 2—Refractive indices in system gehlenite–åkermanite (after Ferguson and Buddington[3])

using a 9-cm. powder camera with filtered CuK_α radiation. Any unusual procedures or techniques necessary for special systems will be described when dealing with those systems.

PROPERTIES OF THE END MEMBERS

Gehlenite ($Ca_2Al_2SiO_7$)

Synthetic gehlenite melts at 1590° C.[8] It crystallizes in short-prisms with distinct basal cleavage. It is uni-axial negative, with refractive indices $\varepsilon = 1{\cdot}658$, $\omega = 1{\cdot}669$, and it has a unit cell of $c = 5{\cdot}067$Å., $a = 7{\cdot}690$Å. Powder X-ray spacings[9] for this and the following end members are given in Table III.

Åkermanite ($Ca_2MgSi_2O_7$)

Synthetic åkermanite melts at 1454° C.[8] It is uni-axial positive, with refractive indices $\varepsilon = 1{\cdot}639$, $\omega = 1{\cdot}632$, and it has a unit cell of $c = 5{\cdot}010$Å., $a = 7{\cdot}843$Å.

Osborn and Schairer[8] and Bowen, Schairer, and Posnjak[10] have suggested that åkermanite decomposes at intermediate temperatures. The evidence for this is that åkermanite glass, when devitrified at 1375° C., gave only åkermanite, whereas, at 1050° C., Ca_2SiO_4 was also formed. Moreover, large homogeneous åkermanite crystals grown from sodium tungstate yielded inclusions of the general appearance of diopside when they were annealed below 1325° C. Both these experiments have been repeated by the present authors, but only pure åkermanite was obtained, even after annealing for 48 hr. However,

Table IV

QUENCHING EXPERIMENTS IN THE SYSTEM GEHLENITE–IRON-GEHLENITE

Refractive Indices			Composition, mol.-%		Temperature, ° C.			
n Glass	ε	ω	Gehlenite	Iron-gehlenite	All Crystalline	Crystalline + Glass	Glass + Crystalline	All Glass
1·639	1·658	1·669	100	0	...	...	...	1590
1·651	1·664	1·673	90	10	1565	1570	1585	1590
1·657	1·670	1·681	80	20	1500	1505	1575	1580
1·678	1·684	1·693	60	40	1430	1435	1545	1550
1·698	1·691	1·698	50	50	1390	1395	1525	1530
1·705	1·696	1·704	40	60	1355	1360	1510	1515
1·730	1·711	1·715	20	80	1305	1310	1415	1420
1·770	1·723	1·726	0	100	...	...	...	1285

Table V

QUENCHING EXPERIMENTS IN THE SYSTEM ÅKERMANITE–IRON-GEHLENITE

Refractive Indices			Composition, mol.-%		Temperature, ° C.			
n Glass	ε	ω	Åkermanite	Iron-gehlenite	All Crystalline	Crystalline + Glass	Glass + Crystalline	All Glass
1·641	1·639	1·632	100	0	...	...	...	1454
1·655	1·650	1·645	90	10	1410	1415	1430	1435
1·665	1·657	1·654	80	20	1375	1380	1395	1402
1·685	1·661	1·660	65	35	1340	1345	1345	1350
1·690	1·674	1·675	60	40	1330	1335	1340	1345
1·699	1·684	1·686	50	50	1315	1320	1335	1340
	1·693	1·695	40	60	1305	1310	1335	1340
1·740			25	75	1290	1300	1335	1340
1·750	1·716	1·720	10	90	...	...	1315	1320
1·770	1·723	1·726	0	100	...	...	...	1285

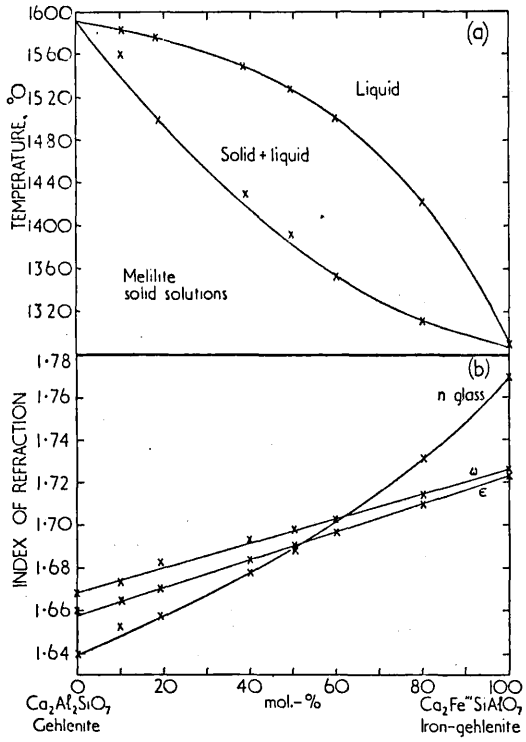

Fig. 3—System gehlenite–iron-gehlenite: (*a*) Equilibrium diagram; (*b*) change in refractive indices

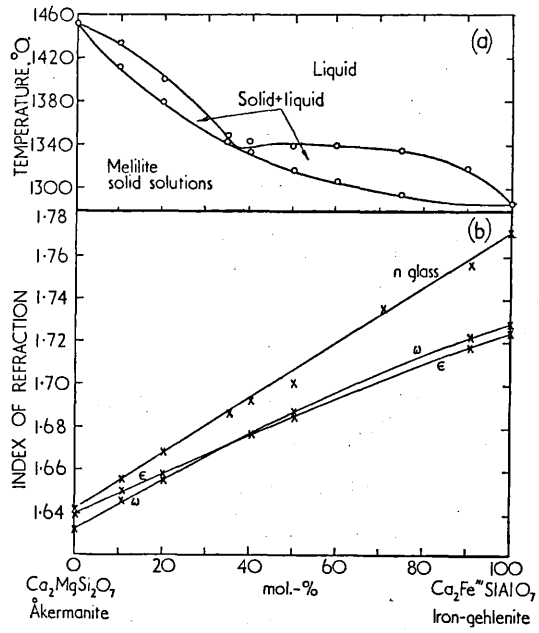

Fig. 4—System åkermanite–iron-gehlenite: (*a*) Equilibrium diagram; (*b*) change in refractive indices

mixtures of åkermanite with 0·2% Ca_2SiO_4 or 0·2% $CaMgSi_2O_6$ gave a single melilite phase at 1350–1375° C., but on annealing at 1200° C. they developed a 'peg structure' of the second phase.

It therefore seems that pure åkermanite is stable at intermediate temperatures, but that slightly impure material may appear to decompose because of exsolution of the impurity dissolved at higher temperatures. It is interesting to note that most melilites in slags or rocks produced by the cooling of liquids exhibit 'peg structure,' but not in those that are produced by reaction in the solid state, such as contact-metamorphosed limestones (*e.g.*, Carlingford).

Iron-åkermanite ($Ca_2Fe''Si_2O_7$)

Iron-åkermanite is stable only below 775° C.[10] It does not therefore occur in contact with liquid in the ternary system CaO–FeO–SiO_2, the liquidus temperatures being too high. Above 775° C. it decomposes into wollastonite, $CaSiO_3$, and lime-iron olivine, $CaFeSiO_4$. It has been prepared by devitrifying glass of its own composition below 775° C., and is uni-axial negative, with refractive indices $\varepsilon = 1{\cdot}673$, $\omega = 1{\cdot}690$. No systems containing ferrous iron have been studied in the present investigation, because this work is

Table VI

QUENCHING EXPERIMENTS IN SYSTEM GEHLENITE–ÅKERMANITE–IRON-GEHLENITE

Refractive Indices			Composition, mol.-%			Temperature, ° C.			
n Glass	ε	ω	Gehlenite	Åkermanite	Iron-gehlenite	All Crystalline	Crystalline + Glass	Glass + Crystalline	Glass
1·710	1·692	1·699	20	20	60	1330	1335	1415	1420
1·685	1·682	1·688	30	30	40	1335	1340	1445	1450
1·656	1·666	1·672	60	20	20	1420	1425	1520	1525
1·685	1·665	1·666	20	60	20	1345	1350	1370	1375
1·658	1·660	1·659	10	70	20	1345	1350	1355	1360
1·651	1·660	1·665	60	30	10	1415	1420	1500	1505
1·642	1·655	1·654	25	65	10	1355	...	...	1360
1·655	1·654	1·652	20	70	10	1350	1355	1355	1360
1·655	1·655	1·653	45	50	5	1380	1385	1435	1440
1·655	1·650		30	65	5	1370	1375	1385	1390
1·657	1·653	1·650	25	70	5	1360	1365	1365	1370
			10	50	40	1335	1340	1350	1355
			10	40	50	1315	1320	1375	1380
			30	20	50	1335	1340	1465	1470
			40	20	40	1355	1360	1475	1480
			40	40	20	1365	1370	1460	1465
			30	40	30	1355	1360	1435	1440

proceeding at the Geophysical Laboratory, Washington.

Iron-gehlenite ($Ca_2Fe'''SiAlO_7$)

Iron-gehlenite has not previously been described. It melts at 1285° C.; it is tetragonal, uni-axial negative, with refractive indices $\varepsilon = 1{\cdot}723$, $\omega = 1{\cdot}726$. It has a probable unit cell of $c = 4{\cdot}855$Å., $a = 7{\cdot}54$Å.

Sodium-melilite ($NaCaAlSi_2O_7$)

Sodium-melilite is also a new compound. It is stable only below 1080° ± 10° C. It can be made in the pure state by devitrifying glass of its own composition below this temperature. At 1080° ± 10° C. it decomposes to give wollastonite, $CaSiO_3$, and nepheline, $NaAlSiO_4$. It is tetragonal, uni-axial negative, with refractive indices $\varepsilon = 1{\cdot}575$, $\omega = 1{\cdot}580$. The unit cell is probably $c = 4{\cdot}809$Å., $a = 8{\cdot}511$Å.

Potassium-melilite ($KCaAlSi_2O_7$)

This composition yields a mixture of wollastonite, $CaSiO_3$, and kaliophilite at all temperatures below

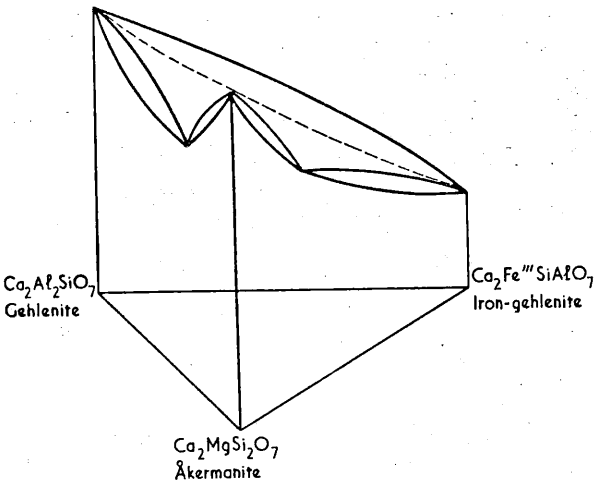

Fig. 6—Ternary system gehlenite–iron-gehlenite–åkermanite

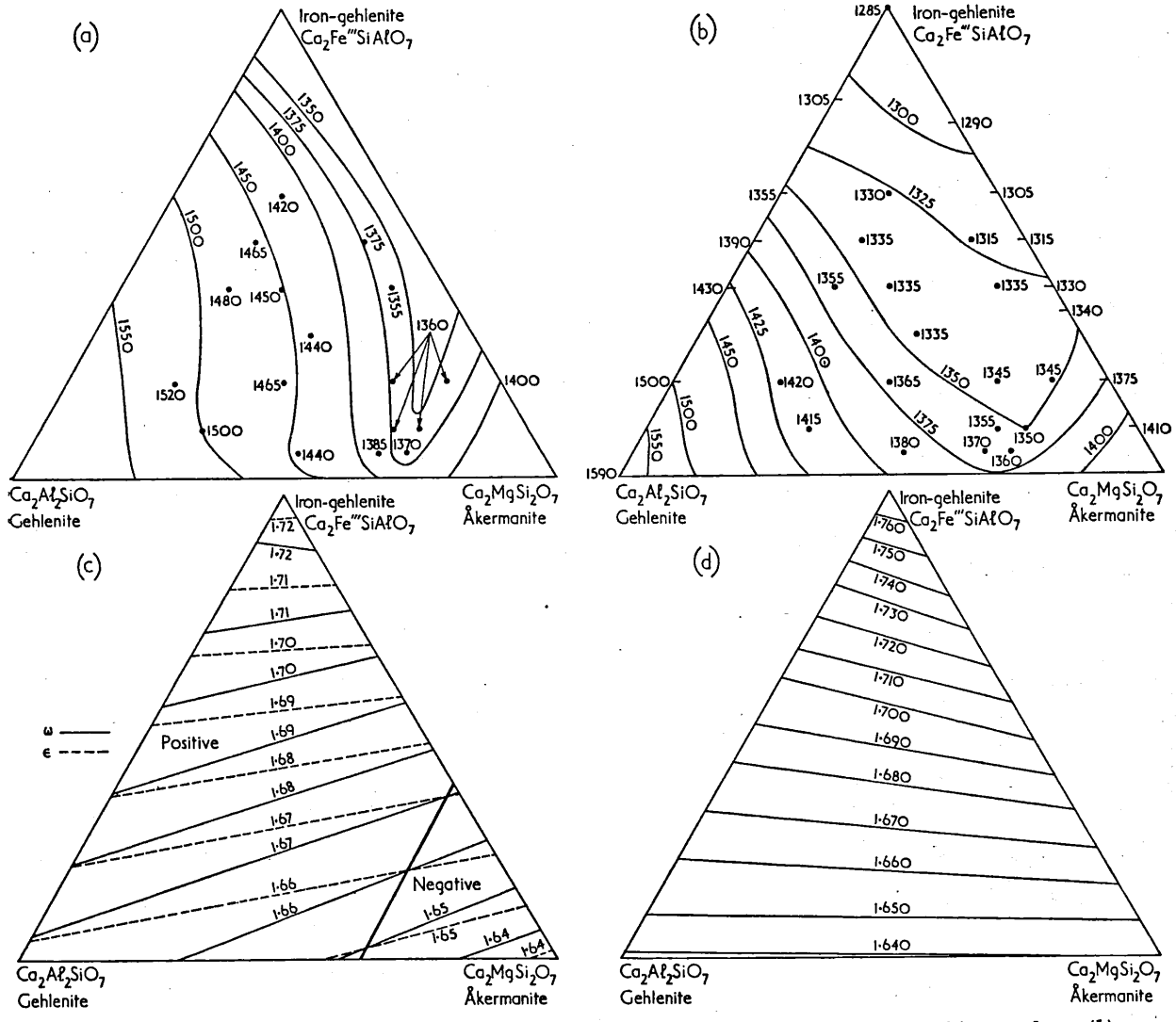

Fig. 5—Ternary system gehlenite–åkermanite–iron-gehlenite: (*a*) Isothermus of liquidus surface; (*b*) isothermus of solidus surface; (*c*) change in refractive indices; (*d*) isofracts of glasses in system

the solidus. It is to be presumed that the large K ion cannot be accommodated in the melilite structure to the extent indicated by the formula $CaKAlSi_2O_7$. That it can enter to some extent is shown by the fact that up to 20% of the hypothetical molecule will form a solid solution with gehlenite (*see* p. 130).

BINARY SYSTEMS OF THE TERNARY SYSTEM GEHLENITE–ÅKERMANITE–IRON-GEHLENITE

System Gehlenite–Åkermanite

The system $Ca_2Al_2SiO_7$–$Ca_2MgSi_2O_7$, as originally reported,[3] has been slightly revised by Osborn and Schairer.[8] The corrected diagram is reproduced as Fig. 1. Refractive indices are plotted in Fig. 2.

System Gehlenite–Iron-gehlenite

The equilibrium diagram for this system (Fig. 3*a*) has been constructed from the data given in Table IV, which also includes the refractive indices of the various mixes. A continuous series of solid solutions is formed without a singular point. Figure 3*b* is the refractive indices diagram.

System Åkermanite–Iron-gehlenite

The experimental data in Table V were used to construct the equilibrium diagram (Fig. 4*a*) that represents a solid-solution series with a singular point, as in the system åkermanite–gehlenite. Refractive indices are plotted in Fig. 4*b*. In this system the solidus curve was difficult to determine owing to the ease with which melts were supercooled. The supercooled glasses devitrified readily and produced quench growths. It was therefore necessary to determine this curve from completely crystalline preparations, observing the temperature at which liquid first formed.

THE TERNARY SYSTEM GEHLENITE–ÅKERMANITE–IRON-GEHLENITE

The bounding binary systems having been established, the ternary system was delineated; the addi-

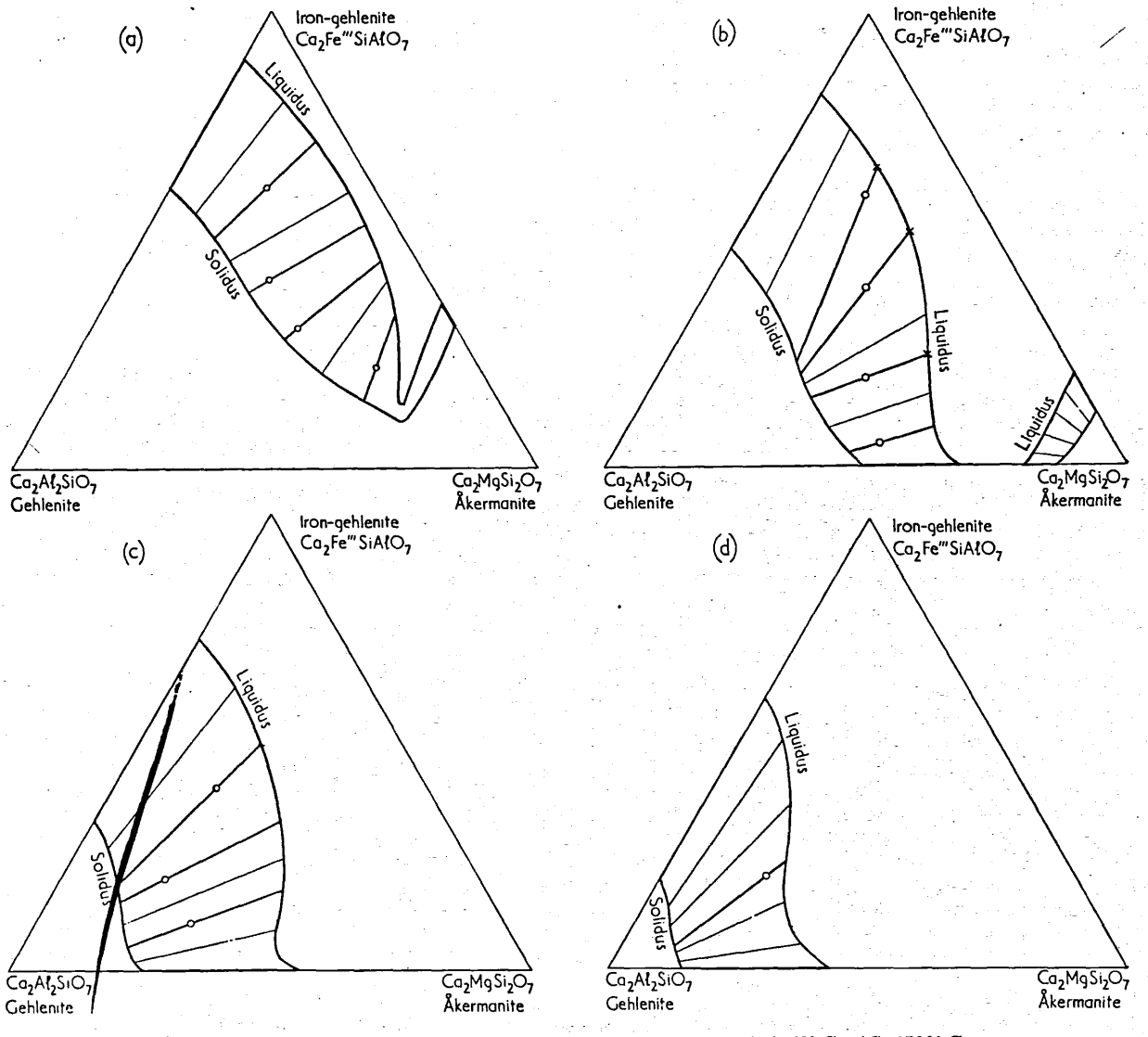

Fig. 7—Isothermal plane at (*a*) 1350° C., (*b*) 1400° C., (*c*) 1450° C., (*d*) 1500° C.

Table VII

REFRACTIVE INDICES AND COMPOSITION OF PHASES PRODUCED AT VARIOUS TEMPERATURES

Refractive Indices			Composition of Liquid, mol.-%			Composition of Crystals, mol.-%		
Temperature, °C.	*n* Glass	*n* Crystalline	Åkermanite	Gehlenite	Iron-Gehlenite	Åkermanite	Gehlenite	Iron-Gehlenite
1520	1·660	...	20	60	20	...	...	...
1500	1·665	1·668	22	54	24	11	95	4
1480	1·670	1·670	26	46	28	11	78	10
1460	1·675	1·674	34	36	30	11	75	14
1450	1·770	1·674	39	35	26	12	72	16
1440	1·660	1·675	46	35	19	14	66	20
1420	...	1·672	...	...	...	20	60	20

tional data are given in Table VI. A complete series of solid solutions was formed. Figure 5*a* represents the projection of the liquidus surface on to the composition triangle, temperatures being represented by contours. Figure 5*b* is a similar projection of the solidus surface. In Fig. 5*c* the refractive index surface is projected for the two refractive indices of the crystalline phase, and in Fig. 5*d* the isofracts are those of the corresponding glasses. Figure 6 is a perspective drawing of the solid model, showing the solidus and liquidus when temperature is plotted vertically on the composition triangle as base. The valley separating åkermanite-like from gehlenite-like solid solutions approximately coincides with the isotropic melilite compositions.

Crystallization paths in ternary systems have been discussed theoretically by Marsh[12] and by Hall and Insley.[13] To facilitate the estimation of paths for any composition, isothermal sections in Figs. 7*a–d* have been prepared. In these diagrams, the boundary curves have a high degree of accuracy, being obtained from Figs. 5*a* and *b*, but the tie lines have been drawn by using as a basis a very limited number of compositions for which paths have been completely determined. The method employed is as follows. If a mix of composition x is allowed to cool to T_1 just below its liquidus temperature, crystals will appear, and, if this mix is quenched, the liquid will give a glass of refractive index G_1 and the crystals will have indices of n_1 and n'_1. The composition of the liquid is given by the intersection of the glass isofract G_1

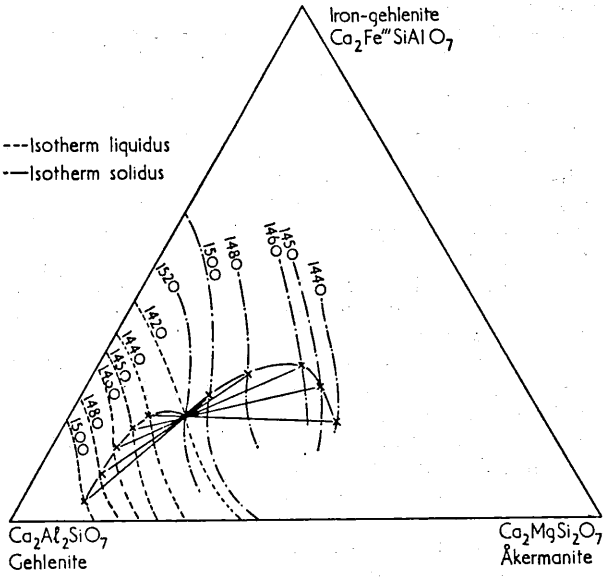

Fig. 8—Crystallization path in system iron-gehlenite–gehlenite–åkermanite

Table VIII

QUENCHING EXPERIMENTS IN SYSTEM GEHLENITE–SODIUM-MELILITE

Composition, mol.-%		Temp., °C.	Phases Present*
Gehlenite	Sodium-melilite		
100	0	1590	glass
100	0	1585	melilite
90	10	1580	glass + trace melilite
90	10	1585	glass
75	25	1535	glass
75	25	1530	glass + melilite
75	25	1340	melilite + trace glass
75	25	1335	melilite
60	40	1490	glass
60	40	1485	glass + trace melilite
60	40	1265	melilite + trace glass
60	40	1260	melilite
50	50	1445	glass
50	50	1440	glass + trace melilite
50	50	1235	melilite + trace glass
50	50	1230	melilite
40	60	1410	glass
40	60	1405	glass + trace melilite
40	60	1205	melilite + trace glass
40	60	1200	melilite
25	75	1340	glass
25	75	1335	glass + trace melilite
25	75	1170	glass + mel + pwol
25	75	1160	melilite + pwol + neph
10	90	1240	glass
10	90	1235	glass + trace melilite
10	90	1185	glass + melilite
10	90	1170	mel + pwol + glass
10	90	1165	mel + pwol + neph
0	100	1210	glass
0	100	1205	glass + pwol
0	100	1185	glass + pwol
0	100	1180	glass + pwol + mel
0	100	1170	glass + pwol + mel
0	100	1165	glass + pwol + mel
0	100	1160	mel + pwol + neph
0	100	1090	mel + pwol + neph
0	100	1080	melilite

* pwol = pseudo-wollastonite, neph = nepheline, mel = melilite

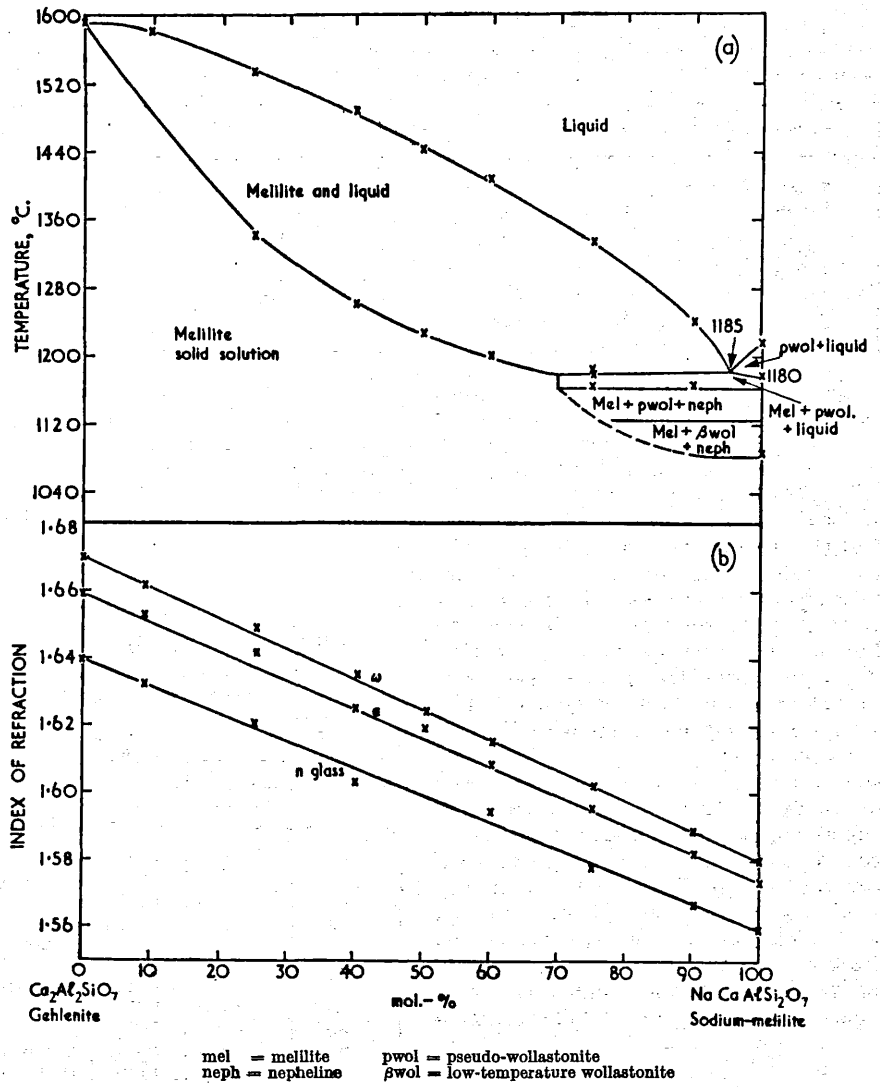

Fig. 9—System gehlenite–sodium-melilite: (*a*) Equilibrium diagram; (*b*) change in refractive indices

and the liquidus isotherm T_1; the composition of the crystalline phase is given by the intersection of the isofracts n_2 and n'_2 (crystalline phase) with the solidus isotherm T_2. This then gives the solid phase in equilibrium with the liquid. The process is repeated at T_2 and T_3, etc., until T_n is reached, this being the solidus temperature of the mix x. There is thus produced a series of points representing the change in composition of the solid phase on cooling, and also the change in composition of the liquid. As an example, Table VII gives the results obtained for a mix of composition 60% gehlenite–20% åkermanite–20% iron-gehlenite (molecular percentages), and the derived crystallization path is plotted in Fig. 8.

SODIUM-BEARING MELILITES

System Gehlenite–Sodium-melilite

Sodium-melilite, $NaCaAlSi_2O_7$, lies in the quaternary system Na_2O–CaO–Al_2O_3–SiO_2 between wollastonite, $CaSiO_3$, and nepheline, $NaAlSiO_4$. This system has been investigated by Foster,[14] who failed to detect a melilite phase, although he suspected its presence; he showed a true binary system between the components, although his experimental data show three phases to have been present at times. Since sodium-melilite decomposes without melting, it is best prepared by annealing glass of the appropriate composition, for one month, at about 900° C. Such a preparation gives an X-ray powder pattern of melilite type, but it is not very suitable for optical study. An equimolecular mixture of wollastonite and nepheline held at 900° C. for two months showed, on X-ray analysis, a mixture of nepheline, wollastonite, and sodium-melilite. This indicates that sodium-melilite can be formed as a stable phase by reaction between wollastonite and nepheline if it is reacted below the decomposition temperature of sodium-melilite, *i.e.*, 1080° ± 10° C. A mixture of 60 mol.-% of wollastonite and 40 mol.-% of nepheline, when cooled slowly from the molten state, gave better crystals of sodium-melilite, which could be used for optical study. This also afforded confirmatory evidence that the $CaSiO_3$–

$NaAlSiO_4$ join is interrupted at the sodium-melilite composition ($NaCaAlSi_2O_7$), as only $CaSiO_3$ and $NaCaAlSi_2O_7$ were present in the completely crystalline mass. Quenches at intermediate temperatures suggested that the system $CaSiO_3$–$NaAlSiO_4$ is in fact quaternary, but the crystallization paths were extremely complicated and the experimental evidence serves only to establish $CaSiO_3$–$NaCaAlSi_2O_7$ as an Alkemade join.

The pseudo-binary system gehlenite–sodium-melilite was established by means of data given in Table VIII, and is shown in Fig. 9*a*. It is truly binary over most of the composition range, the decomposition of sodium-melilite intervening over only a short range. Refractive indices are shown in Fig. 9*b*.

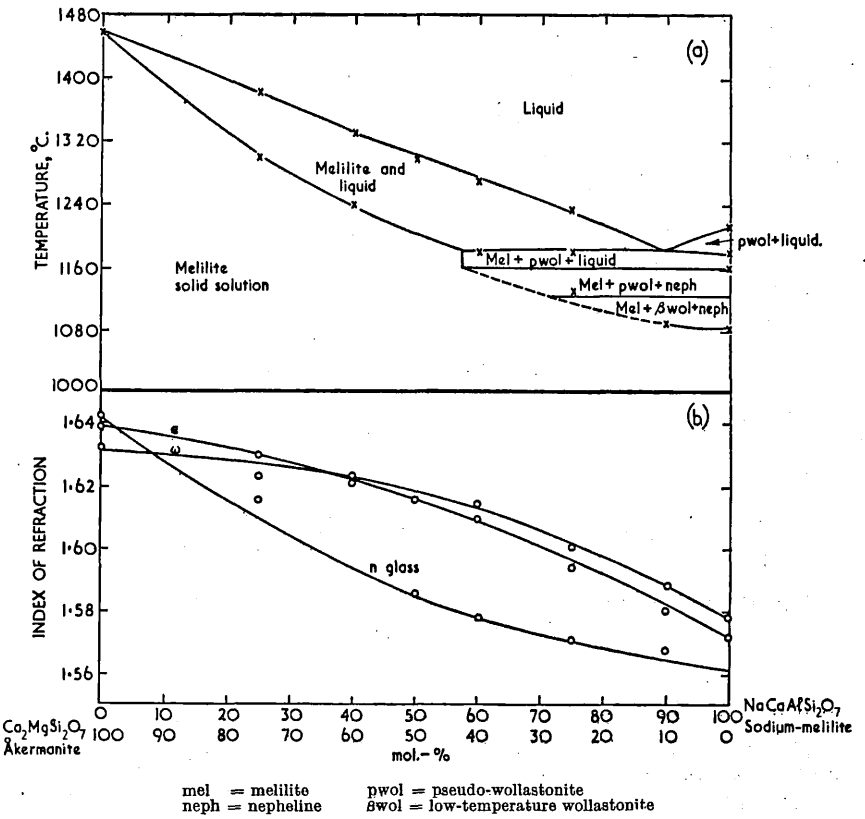

mel = melilite pwol = pseudo-wollastonite
neph = nepheline βwol = low-temperature wollastonite

Fig. 10—System åkermanite–sodium-melilite: (*a*) Equilibrium diagram; (*b*) changes in refractive indices

System Åkermanite–Sodium-melilite

This system is again only pseudo-binary, because of the decomposition of sodium-melilite. It lies in the plane åkermanite–nepheline–wollastonite, which forms part of the quinary system CaO–MgO–Al_2O_3–Na_2O–SiO_2. The equilibrium diagram, established by the data in Table IX, is given in Fig. 10*a*, and the refractive indices are shown in Fig. 10*b*. Here again, there is a change of optical sign, and an isotropic melilite is produced at a composition approximating to 35% sodium-melilite.

Discussion on Sodium-bearing Melilites

A number of authors have suggested mechanisms

Table IX

QUENCHING EXPERIMENTS IN SYSTEM ÅKERMANITE–SODIUM-MELILITE

Composition, mol.-%		Temp., °C.	Phases Present*	Composition, mol.-%		Temp., °C.	Phases Present*
Åkermanite	Sodium-melilite			Åkermanite	Sodium-melilite		
100	0	1455	glass	25	75	1240	glass
100	0	1450	glass + trace melilite	25	75	1230	glass + melilite
75	25	1380	glass	25	75	1185	melilite + glass
75	25	1375	glass + trace melilite	25	75	1170	mel + pwol + glass
75	25	1300	melilite + glass	25	75	1140	mel + pwol + neph
75	25	1295	melilite	25	75	1130	melilite
60	40	1330	glass	10	90	1180	glass
60	40	1325	glass + trace melilite	10	90	1120	mel + pwol + neph
60	40	1245	melilite + glass	10	90	1090	melilite
60	40	1240	melilite	0	100	1210	glass
50	50	1300	glass	0	100	1205	glass + pwol
50	50	1290	glass + melilite	0	100	1185	glass + pwol
40	60	1270	glass	0	100	1180	glass + pwol + mel
40	60	1265	glass + melilite	0	100	1170	glass + pwol + mel
40	60	1200	melilite + glass	0	100	1165	glass + pwol + mel
40	60	1185	melilite + glass	0	100	1160	mel + pwol + neph
40	60	1180	mel + pwol + glass	0	100	1090	mel + pwol + neph
				0	100	1080	melilite

* pwol = pseudo-wollastonite, neph = nepheline, mel = melilite

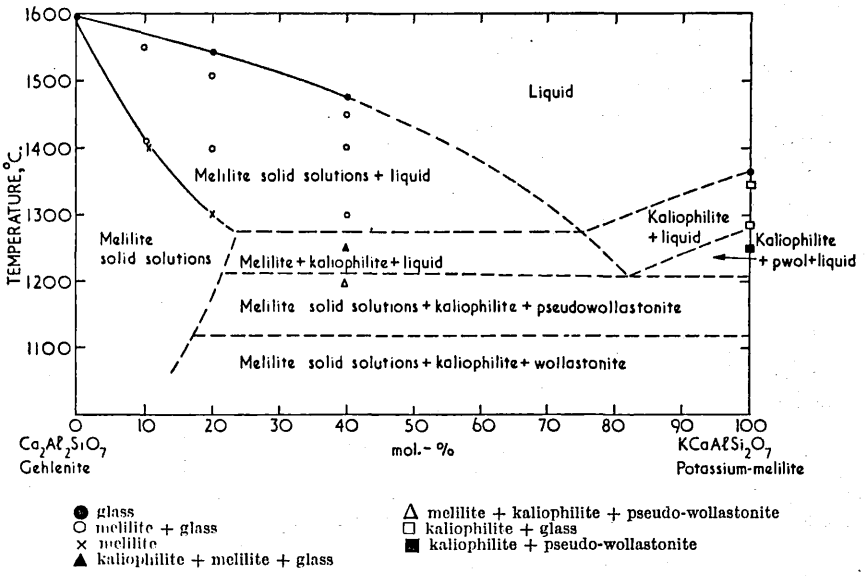

Fig. 11—Pseudo-binary system gehlenite–potassium-melilite in system gehlenite–wollastonite–kaliophilite

to account for the presence of sodium in melilites derived from alkaline rocks. Smalley[15] suggested that nepheline could enter into solid solution with gehlenite, and he also put forward the reaction series:

$$2NaAlSiO_4 + Ca_2Al(SiAl)O_7 \rightarrow CaSiO_3 + 2NaAlO_2 + CaAl_2Si_2O_8$$

$$NaAlSiO_4 + CaSiO_3 \rightarrow NaCaAlSi_2O_7.$$

Assuming that the two melilites would enter into solid solution, this means that nepheline would react with gehlenite to form a sodium-bearing melilite and sodium aluminate. The latter, however, has never been reported as a rock-forming mineral. Goldsmith[16] suggested that a sodium silicate, $Na_2Si_3O_7$, goes into solid solution with gehlenite, but not with åkermanite. He states that sodium-melilite, if it existed, would be a mixture of gehlenite and sodium silicate.

If interstitial substitution is excluded as being unlikely with substances of such structural complexity as those under discussion, the extensive and, in most cases, complete solid solution now reported can only be explained on the basis that the end members are—if not identical—very similar in structural type. The present work, in demonstrating the existence of a sodium-melilite, gives a much more satisfactory interpretation of the rôle played by sodium in the melilite series. It is also shown that, unless the eutectic temperature is very low, melilites rich in the sodium member are not likely to form in contact with liquid, but are much more likely to occur in rocks as a result of solid-state reaction. Goldsmith's[16] observation that the refractive index of gehlenite varied when it crystallized out in the presence of Na_2O and SiO_2, but that åkermanite was unaffected under similar circumstances, is readily explained by the fact that Al ions are necessary to establish neutrality of charge when Na is introduced into the melilite structure. In the latter case, therefore, no sodium-melilite could form.

Table X

QUENCHING EXPERIMENTS IN SYSTEM POTASSIUM-MELILITE–GEHLENITE

Refractive Indices			Composition, mol.-%		Temperature, °C.	Phases*
n Glass	ϵ	ω	Gehlenite	Potassium-melilite		
1·639	1·658	1·669	100	0	1590	glass
			90	10	1550	mel + glass
...	1·657	1·663	90	10	1410	mel + glass
			90	10	1400	mel
			80	20	1540	glass
1·616	1·653	1·658	80	20	1510	mel + glass
			80	20	1400	mel + glass
			80	20	1300	mel
			60	40	1480	glass
			60	40	1450	glass + mel
1·600		mix	60	40	1400	glass + mel
			60	40	1300	glass + mel
			60	40	1250	mel + kaliophilite + glass
			60	40	1200	mel + kaliophilite + wol
			0	100	1360	glass
			0	100	1350	glass + kaliophilite
			0	100	1290	glass + kaliophilite
			0	100	1250	kaliophilite + wol

* wol = wollastonite, mel = melilite

POTASSIUM-BEARING MELILITES

System Potassium-melilite–Gehlenite

Potassium-melilite, if it existed, would lie in the quaternary system $CaO–K_2O–Al_2O_3–SiO_2$, but it has proved to be impossible to synthesize it. The presence of K_2O in natural melilites is, however, attributed to a partial solid solution of a potassium-bearing melilite, as it is possible for some potassium substitution to take place in the melilite structure before it becomes unstable.

The pseudo-binary system gehlenite–potassium-melilite has been partially investigated. The results of quenching experiments are given in Table X, and these results are plotted as an equilibrium diagram in Fig. 11. The results show that the pseudo-binary system is part of the ternary system gehlenite–pseudo-wollastonite–kaliophilite and that a solid solution of potassium-melilite in gehlenite exists to about 20%.

Acknowledgments

The authors wish to acknowledge the help given by Mr. F. J. McConnell, Mr. L. J. Larner, and Mr. W. G. Grindle, of the Building Research Station, for the determination of the analyses quoted in Table II.

This paper is published with permission of the Director of Building Research and was carried out as part of the programme of work of the Building Research Board. Some of the work formed Parts I and III of a thesis by one of the authors (H.G.M.) for the London University Degree of Doctor of Philosophy.

References

1. F. BELLEVUE: *Journal de Physique*, 1800, vol. 51, p. 456.
2. E. S. SHEPHERD and G. A. RANKIN: *Indust. Eng. Chem.*, 1911, vol. 3, p. 211.
3. J. B. FERGUSON and A. F. BUDDINGTON: *American Journal of Science*, 1920, vol. 50, pp. 131–140.
4. H. BERMAN: *American Mineralogist*, 1929, vol. 14, pp. 389–407.
5. B. E. WARREN: *Zeitschrift für Kristallographie*, 1930, vol. 74, pp. 131–138.
6. R. W. NURSE: *Chem. Ind.*, 1950, Apr., pp. 263–267.
7. R. W. NURSE and J. H. WELCH: *J. Sci. Instruments*, 1950, vol. 27, pp. 97–99.
8. E. F. OSBORN and J. F. SCHAIRER: *American Journal of Science*, 1941, vol. 239, pp. 715–763.
9. K. W. ANDREWS: *Mineralogical Mag.*, 1948, vol. 28, pp. 374–379.
10. N. L. BOWEN. J. F. SCHAIRER, and E. POSNJAK: *American Journal of Science*, 1933, vol. 26, pp. 194–284.
11. A. MUAN and E. F. OSBORN: *Yearbook Amer. Iron Steel Inst.*, 1951, pp. 325–360.
12. J. S. MARSH: "Principles of Phase Diagrams": 1935, New York, McGraw-Hill Book Co., Ltd.
13. F. P HALL and H. INSLEY: "Phase Diagrams for Ceramists": 1947, Ohio, The American Ceramic Society.
14. W. R. FOSTER: *Journal of Geology*, 1942, vol. 50, pp. 152–173.
15. R. G. SMALLEY: *Journal of Geology*, 1947, vol. 55, pp. 27–37.
16. J. R. GOLDSMITH: *Ibid.*, pp. 381–404.

DS7690/1 1184 290 10/53CL

MIDGLEY (H.G.) II

Reprinted from Clay Minerals Bulletin, Vol. 3, No. 16. D. Sc. 1967

THERMAL REACTIONS OF SMECTITES

By H. G. MIDGLEY[1] and K. A. GROSS[2]

(1) Building Research Station, Watford.
(2) Defence Standards Laboratory, Victoria, Australia.

[Read 14th April, 1956.]

ABSTRACT

The thermal dehydration of a series of smectites has been investigated by X-ray methods. It has been found that the rate of collapse of the layers is governed by the type of exchangeable ion present.

The high temperature changes of a new saponite have been investigated. The saponite dehydrates to talc and then to enstatite, the 5·2Å fibre axis remaining constant throughout.

Part 1. Role of the Exchangeable Cation in the Hydration States of Smectites.

INTRODUCTION

A series of smectites, with different ions in the exchangeable position, has been examined by X-ray diffraction methods at temperatures up to 320°C. The work was suggested by a study which was being made of the thermal reactions of a fibrous saponite from Church Cove, Lizard, Cornwall, found by one of us, (H. G. M.). This sample will be described for the first time in this paper.

It is well known that when smectites are heated in the range 0-200°C they lose water reversibly, accompanied by a change in the basal spacing from 14 Å to 9·6 Å (Greene-Kelly (1953)). However, the intermediate condition was not examined. Experiments on smectites containing magnesium in the exchangeable position have shown that, on heating in the range up to 125°C, an intermediate phase is produced which has a basal spacing of about 11·5 Å; with further heating, values of about 10·5 Å at about 200°C and 9·9 Å at 320°C are obtained. When sodium is in the exchangeable position there is no discrete intermediate stage, the basal spacing decreases to 9·5 Å by at least 95°C, and remains at this value with further heating. With calcium as the exchangeable ion there is a nearly continuous reduction of basal spacing until it reaches 9·5 Å at about 200°C.

The difference in the amount of water absorbed appears to bear a relation to the cation present in the exchangeable position and this is discussed by Mackenzie (1950) and Hendricks *et al.* (1940). It seems likely that the stages in the dehydration of smectites represent differently bonded water.

II

Experimental Procedure

A small furnace was made which could be mounted on the "Unicam" single-crystal goniometer. The specimen in the form of a fibre, flake, or powder in a capillary tube could be placed at the centre of the furnace and the diffraction pattern was recorded on a flat-plate cassette. With CuKα radiation and a specimen-to-film distance of 6·0 cm the first and second orders of the basal spacings could be recorded. During heating the sample was exposed to the normal laboratory atmosphere, no attempt being made to control the humidity. The temperatures were recorded with a Pt-PtRh thermocouple placed close to the specimen. The accuracy of this measurement was about ± 5°C.

Material. The following samples were used in the experiments. 1, saponite, Church Cove; 2, calcium-saturated saponite; 3, sodium-saturated saponite; 4, magnesium-saturated bentonite, Wyoming; 5, calcium-saturated bentonite, Wyoming; 6, sodium-saturated bentonite, Wyoming; 7, magnesium-saturated bentonite, Cheta.

The saponite has not been described before, so a description is given below. The other samples were prepared to have the requisite exchangeable cation, by shaking with the appropriate metal salt solution. The Cheta bentonite was a sample kindly provided by J. A. White of the Illinois Geological Survey.

Saponite. The material occurs as a vein invading Kennack gneiss at Church Cove, Lizard, Cornwall. It is fibrous, green to pale green, soft H=2, soapy to the touch, and has refractive indices α 1·520, γ 1·535 $\pm$ 0·005, γ:z 11°, positive elongation, the fibres giving an interference figure, biaxial positive, 2V small. A chemical analysis (by L. J. Larner) gave SiO_2 42·92, FeO 0·43, Fe_2O_3 1·57, Al_2O_3 5·99, CaO 0·80, MgO 26·71 MnO 0·03, Loss at 1000°C 21·81, Loss at 110°C 13·72. This chemical analysis is equivalent to a formula:—

$$[Mg_{5\cdot82}Al_{0\cdot1}Fe^{2+}_{0\cdot1}]_6\,[Si_{6\cdot76}Al_{1\cdot04}Fe^{3+}_{0\cdot2}]_8\,O_{20}(OH)_4\,10H_2O$$
$$\downarrow$$
$$Ca_{0\cdot1}\,Mg_{0\cdot48}$$

Chemical tests have shown that magnesium and a trace of calcium are the exchangeable ions. This analysis is typical of a magnesium smectite.

Powder X-ray diffraction patterns of the mineral and of a sample saturated with glycerol were taken on a 10 cm diameter camera with CuKα radiation. The spacings are given in Table 1. The occurrence of a long spacing at 14 Å which, when the sample was saturated

TABLE 1—X-ray Powder Data of Saponites

Church Cove		Church Cove†		Milford (Cahoon 1954)		Transvaal (Schmidt 1953)		Lizard† (Midgley 1951)	
d	*I*	*d*	*I*	*d*	*I*	*d*	*I*	*d*	*I*
14·2	10	17·5	10	16·1	10	14·65	vs	18·8	10
7·4	1	8·93	6	13·0	?			9·1	5
4·96	4	5·93	3	4·94	2	4·87	m	6·05	1
4·57	5	4·53	7	4·51	8	4·56	s	4·45	5
3·67	8	3·55	6	3·70	4	3·63	m	3·605	5
2·99	1	2·97	5	3·21	1	2·94	s		
		2·70	1	2·89	4	2·627	m	3·00	4
2·58	2	2·60	7*	2·58	5	2·554 }	s	2·605	6
2·42	2	2·53	6*			2·487 }			
2·30	2	2·21	1	2·26	1			2·48	3
2·22	2	2·13	1					2·26	2
2·09	3	2·07	1	2·06	1	2·081	w	2·00	1
		1·97	2						
1·84	3	1·84	2						
1·73	2	1·74	4	1·72	3	1·731	w	1·733	4
1·71	2	1·69	2			1·689	w		
1·53	9	1·53	8	1·52	9	1·530	s	1·533	7
1·46	2								
1·32	4	1·32	5	1·31	5	1·321	w	1·318	4
1·28	2	1·27	1	1·26	1	1·271	w	1·268	2
1·05	2			1·05	1				
1·00	2			0·99	3				
0·89	2			0·88	4				

Measurements of *d* in Å, *I*=intensity, *=diffuse, †=glycerol stabilised, s=strong, m=moderate, w=weak, v=very.

with glycerol, expanded to 17 Å, confirms the identity of the mineral as a smectite.

The sample of saponite from the Lizard is strongly fibrous and a fibre X-ray photograph taken in an X-ray goniometer shows strong preferred orientation (Fig. 1 a). The photograph shows the repeat distance along the fibre axis to be 5·2 Å, and the cell dimensions to be 5·2, 9·2 and 14·7 Å.

Three samples of saponite have recently been described in the literature, by Schmidt (1953) from the Krugersdorp District, Transvaal, by Cahoon (1954) from Milford, Utah, and by Midgley (1951) from the Lizard. The diffraction patterns are given for comparison in Table 1. The chemical compositions (Table 2) do not differ appreciably except for the exchangeable ions; the samples from Church Cove and from the Transvaal have predominantly magnesium as the exchangeable ion, the mineral from Church Cove having more than that from the Transvaal. The analysis quoted for the sample from Milford did not specify the exchangeable ion, but calculations from

the chemical analysis show that it is probably calcium. The refractive indices vary considerably but, as the minerals are strongly fibrous, the estimation of refractive index is liable to considerable error.

The X-ray patterns of the various saponites are similar except for the differences in the 00*l* spacings. In the two samples stabilised with glycerol the second order basal spacings are very much stronger than in the unstabilised samples, for example the specimen from Church Cove shows an increase in intensity from 1 to 6. The samples from Milford and Transvaal do not show the second order spacing, but in the unstabilised specimens it might be too faint to be recorded. Schmidt and Heystek (1953) in their discussion of the saponite from the Lizard say that it is impure and has the X-ray diffraction peaks of talc. It is probable that they mistook the second order 9·1 Å spacing for the strong line of talc.

Heating Experiments on Smectites. The results of the experiments on heated samples of smectites in the high temperature X-ray camera are collected together in Figs. 1 and 2. These results show the relationship between the basal spacing and the temperature; they fall into three groups. (a) Magnesium-saturated, (b) Calcium-saturated, (c) Sodium-saturated.

Those samples with magnesium ions in the exchangeable position show that, with dehydration by heating, the basal spacing decreases

TABLE 2—Molecular Composition of Saponites

Church Cove			Milford, Utah (Cahoon 1954)	Transvaal (Schmidt 1953)
	Mg	2·90	2·85	2·99
	Al	0·05 } 3·00	0·04 } 2·90	} 3·00
	Fe^{2+}	0·05	0·01	0·01
	Si	3·39	3·70 } 4·00	3·63 } 4·00
	Al	0·52 } 4·00	0·30	0·37
	Fe^{3+}	0·10		
	O	10	10	10
	OH	2	2	2
	nH_2O	5	—	—
exchangeable	Ca	0·05	0·08*	
	Mg	0·24		0·18
refractive	α	1·520	1·511	1·486-1·493
indices	γ	1·535 ± ·005	1·514	

* Calculated by authors from analysis given in Cahoon (1954).

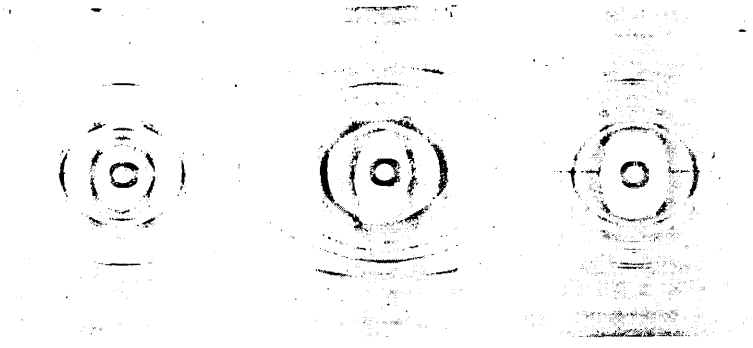

FIG. 1—X-ray photographs of saponite heated to various temperatures. A—saponite, B—saponite heated to 550°C (9·7 Å lattice), C—saponite heated to 950°C (enstatite) (fibre axes horizontal).

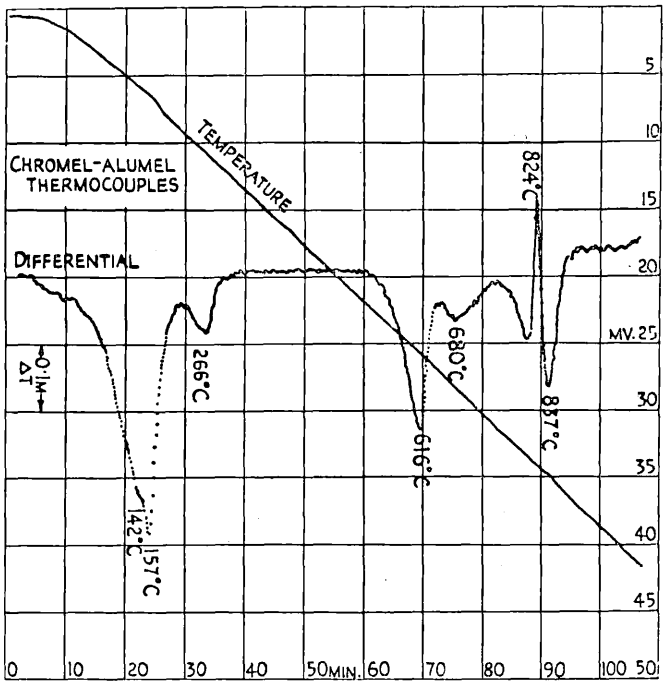

FIG. 2—Differential thermogram of saponite from Church Cove.

from about 15 Å at room temperature to a value of between 11 and 12 Å at temperatures between 80° and 150°C, then to about 10·5 Å at about 200°C and to about 10·0 Å by 320°C (Fig. 2 a). The sodium-impregnated specimens do not show the 11-12 Å intermediate stage, the basal spacing is reduced to 9·5 Å by at least 95°C and remains at that value with further heating (Fig. 2 c). In the specimens containing calcium, the basal spacing reduces in value fairly regularly from 15—9·5 Å between room temperature and 200°C. Whilst there is no sharp arrest with values of 11-12 Å, there are, with saponite at least, several points of inflection that show some correspondence with the magnesium-saturated samples (Fig. 2 b).

The lattice spacing is comparable with talc and it is likely that on dehydrating, the talc lattice is produced. With the magnesium-saturated samples the value of 9·7 Å for the basal spacing must also be related to the talc structure, the layer not being held so strongly as in talc.

The samples when examined were very prone to rehydration. Exposure to the normal moist laboratory atmosphere caused the 9·7 Å talc-like structure to rehydrate to give the montmorillonite structure. For example, if a sample which originally had a basal spacing of 13·5 Å was heated to 140°C to give a basal spacing of 9·7 Å, rehydration in moist air for 2½ hours gave a value of 11·7 Å and after 3 days 12·2 Å.

It is known that in the fully hydrated state, where the basal spacing is more than 14 Å, more than one layer of water occurs. It is suggested from the above evidence that one layer of water is more strongly held than the other in those smectites that have a divalent ion in the exchangeable position. It is thought that when magnesium is the cation, some of the water is held much more strongly than the rest; experimental evidence for this is the formation of a lattice with a *c* spacing of 11·7 Å which is stable for about 150°C. This stage is probably equivalent to the talc lattice with a single water layer between. When sodium is the exchange cation this bound water is not held so strongly, and so is removed by heating and there is no intermediate stage.

The intermediate behaviour of calcium cannot be explained readily but is, perhaps, due to the ionic radius of divalent calcium being rather larger than that of magnesium. However, it is also notable that, with one exception, the basal spacing (00*l* reflection) is always a sharp well-defined ring, indicating that the various intermediate values are discrete states rather than statistical means of the 14,

11·5 and 9·7 Å values. This is not consistent with the concept of a strongly bound planar mono-molecular layer of water molecules between talc layers in the 11·5 Å state, but does seem to agree with the results of MacKenzie's theoretical reasoning. The exception is the sodium-saturated compound which gives a broad ring when fully hydrated.

Differential thermal analysis carried out on samples of smectites saturated with megnesium show a double peak at about 150°C. The original sample of magnesium-saturated saponite showed such a double peak at 150°C, but when saturated with Ca^{2+} the peak was single. A sample of bentonite when calcium saturated gave only a single peak on the d.t.a. but, when magnesium-saturated, gave a double peak at 150°C. It should be noted, however, that a number of examples of d.t.a. curves given in the literature show double peaks and in many of these the exchangeable ion is stated to be calcium but, in all cases cited, the exchangeable ion is calculated from the bulk analysis and has not been determined independently. From the analyses given there is always sufficient magnesium present for this to be the exchangeable ion. Further work on a number of samples where the exchangeable ion is known, is needed to clear up this discrepancy.

Part II. High-temperature Decomposition of Saponite

Introduction

The fibrous saponite from the Lizard, described earlier in this paper, when mounted with the fibre axis vertical gave a preferred orientation photograph (Fig. 1 a) very suitable for examining the thermal decomposition. By taking photographs of material either after air quenching from the required temperature or in a high-temperature X-ray camera the process of break-down of structure can be traced.

Experimental

A d.t.a. was carried out on a sample of saponite, in an apparatus having ceramic crucibles with chambers $7 \times 10 \times 12$ mm, and chromel-alumel thermocouples. The temperature was measured in the sample and a heating rate of 10°C/min ± 0·2°C was used. For the saponite thermogram 0·807 g of sample was used undiluted, the reference material being kaolinite fired to 1050°C. The trace is reproduced unretouched as Fig. 2. Peaks occur at 142, 157, 266, 616, 680 and 837°C.

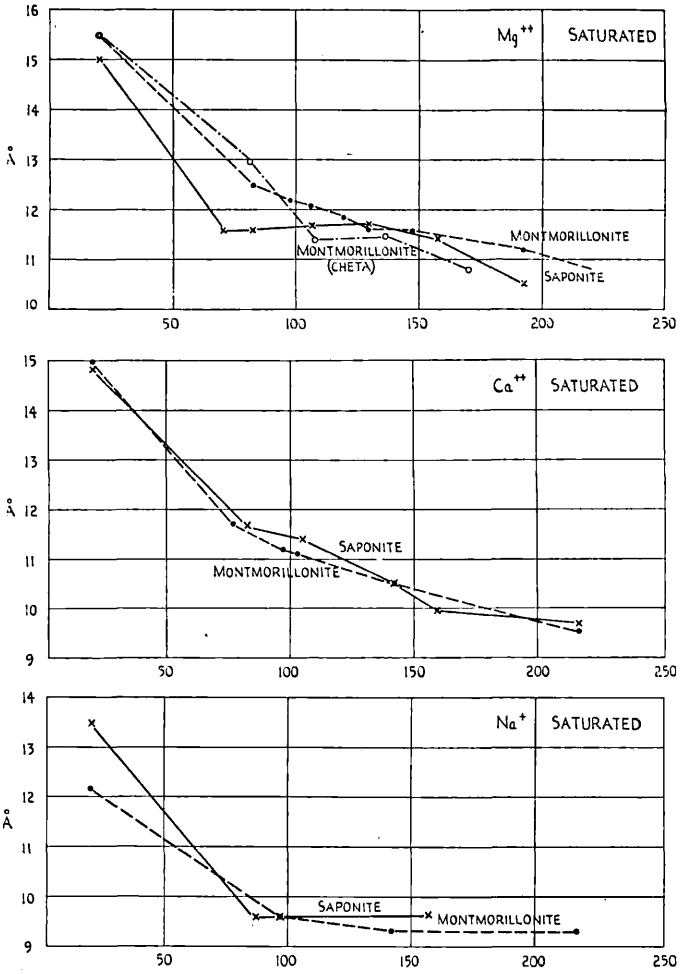

FIG. 3—Dehydration effects on basal spacings of various montmorillonites. (Co-ordinates in °C.).

A weight-loss curve was also carried out with the following results:—

T°C	Wt. Loss (%)	Wt. Loss Cumulative (%)
100	5·15	5·15
180	0·75	5·90
240	0·94	6·84
550	0·94	7·78
610	1·79	9·57
740	1·68	11·25
890	2·81	14·06

Temperature peaks on the d.t.a. thermogram represent some change in the mineral, and so X-ray examinations between these temperatures were considered to be most profitable. Samples of saponite were heated at 180°, 300°, 500°, 550°, 600°, 650°, 750° and 900°C in an electric muffle furnace, air quenched, then placed in a desiccator until required for the X-ray examination. A suitable fibre was selected by splitting the sample, and glued to a glass fibre with shellac. This was mounted in a 6 cm diameter camera, and the diffraction pattern photographed with CuKα radiation.

The samples heated at 180° and 300°C gave diffraction patterns identical with those obtained at room temperature. The picture consisted of a series of basal reflections showing most marked preferred-orientation maxima about the zero layer line, together with Debye-Scherrer rings, with maxima at the layer line positions, corresponding to a cell dimension of 5·2 Å. These rings showed the typical diffuse outer edge of a two-dimensional lattice. The spacing value of the 00*l* basal reflection was 14·2 Å.

The diffraction pattern of the sample heated to 500°C showed a new set of basal spacings corresponding to a unit cell length of 9·7 Å superimposed on the residual pattern of the 14 Å unit cell. A further series of heating experiments was carried out at closer intervals near to 500°C. At 470°C, samples showed no sign of the formation of the 9·7 Å dehydrated stage, even after 24 hours heating; those heated at 550°C showed no reaction after 1 hour, but after 5 hours the reaction was complete and only the 9·7 Å phase was found. At intermediate times composite patterns of the 14 and 9·7 Å phases were obtained. In samples heated to 600, 650 and 750°C the 00*l*-spacing was further reduced to 9·5 Å. At no stage up to 750°C does there appear to be any significant change in the two-dimensional *hk* reflections, either in position or intensity.

Some care is needed in interpreting these results since the rate of rehydration in moist air can be very rapid. From the results of the experiments carried out in the high-temperature camera it is known that up to 320°C the variable 00*l*-spacing can be reduced to 9·9 Å, and this spacing will, if the specimen is left in contact with the normal atmosphere, rehydrate and expand to 15 Å. The sample heated to 550°C for more than 5 hours only showed a spacing of 9·7 Å. It did not rehydrate rapidly; after 24 hours in water it did expand and give the 15 Å lattice spacing. Also a specimen left in contact with the normal atmosphere for 1 year showed on examination the 15 Å lattice. Samples heated to 650°C, however, give only a spacing of

9·5 Å, and these samples will not rehydrate; for example, after soaking in water for 4 months the pattern was unchanged. A comparison of the powder data given by the heated samples is given in Table 3.

TABLE 3—X-ray diffraction data of heated saponites.

Saponite		Saponite heated to 500°C and left in moist air		Saponite heated to 600°C		Talc (Brindley 1951)	
d	*I*	*d*	*I*	*d*	*I*	*d*	*I*
14·2	vs	14·2	vs				
		9·74	vs	9·52	vs	9·4	8
7·4	vw						
4·96	m	4·92	w	4·72	vw		
4·57	m	4·63	s	4·57	s	4·69	4
3·67	ms	3·97	mwb			3·88	lb
2·99	vw	3·55	w			3·37	3
		3·22	s	3·14	vs	3·11	10
						2·70	1
2·58	w	2·63	m	2·60	ms	2·59	2
		2·53	m	2·48	ms	2·47	5
2·42	w						
2·30	w	2·33	w	2·27	wb	2·32	1
2·22	w					2·20	3
2·09	mw	1·92	m			2·09	2
1·84	mw			1·88	m	1·86	3
1·73	w	1·73	mb	1·70	mwb	1·725	2
1·71	w						
						1·67	4
						1·652	1
						1·632	1
1·53	s	1·54	s	1·56	w	1·55	3
				1·52	s	1·52	4
						1·501	2
1·46	w					1·461	1
						1·446	½
						1·390	3b
1·32	m	1·33	m	1·34	w	1·330	2
						1·315	2
1·28	w	1·28	w	1·30	mw	1·291	3

Measurements of *d* in Å, s=strong, m=moderate, w=weak, b= broad, v=very.

From the preferred-orientation fibre X-ray photographs it is possible to deduce two unit cells: 5·2×9·2×14·7 Å, and 5·2×9·2×9·5Å, both with a fibre axis of 5·2 Å (Fig. 1 b.). The first unit cell is that of a smectite and the second probably that of talc, (5·26×9·1×18·81 Å) (Bragg 1937). There may also be an intermediate stage with a unit cell of 5·2×9·2×9.9-9·7 Å.

Both Cahoon (1954) and Schmidt and Heystek (1953) carried out static heating experiments on samples of saponite: Cahoon does not give any precise details of his experiments but notes that on rehydration the 00*l* spacings will vary with water content. Schmidt and Heystek however noted a further effect: when they heated their sample of saponite from Travancore to 450°C and then allowed it to rehydrate, the diagram produced did not fully agree with the original sample in that three lines 4·87, 3·63 and 2·94 Å did not return. In the experiments reported in this paper, when the partly dehydrated stage is rehydrated either by contact with moist air or in water, the lines, 4·81, 3·63 and 2·94 Å (or their equivalents) are always present and do not disappear.

If the sample is further heated the 9·5 Å (talc) lattice breaks down and it is possible, at temperatures between 750°C and 950°C, to arrest the decomposition by air quenching; the X-ray diffraction pattern given by these consists only of faint broad bands at low angles, indicating that an ordered diffraction pattern is absent and the specimen exists in a disordered state.

Finally, samples heated to above 950°C showed the formation of a completely new lattice. To investigate the formation of this, a fibre was mounted vertically in a single crystal goniometer and the diffraction pattern obtained. The sample was removed, heated to 950°C, air quenched, and the fibre was mounted as before and the new diffraction pattern obtained (Fig. 1 c). The saponite pattern was the normal preferred-orientation one, while that given by the new lattice also showed preferred orientation.

In the latter case, maxima were observed about the zero layer and could be indexed as 0*k*0 and *hk*0; maxima were visible to give the layer lines, this distance being equivalent to a lattice spacing of 5·2 Å, (the fibre axis). It was possible to index the pattern approximately on a cell of $5{\cdot}2 \times 18{\cdot}8 \times 8{,}8$ Å, in very close agreement with the unit cell of enstatite, $MgSiO_3$, $5{\cdot}2 \times 18{\cdot}2 \times 8{\cdot}86$ Å. The interesting fact from the X-ray photographs is that the diffraction pattern shows preferred orientation and the fibre axis is still 5·2 Å.

The enstatite lattice can be produced from the saponite or talc layer lattices by splitting the layers into chains and rearranging alternate chains. The habit of the original saponite, which is strongly fibrous, is reflected in this splitting of the layers, for as the original layer is trioctahedral there should be nothing to choose between three directions, mutually 120° to each other; in fact however that direction which retains the 5·2 Å fibre axis vertical is always preferred.

The chemical reaction accompanying the decomposition of talc to enstatite yields an excess of SiO_2. This appears as amorphous silica, as shown by a broad band at about 4·2 Å on the photographs.

Finally some attempt must be made to relate the peaks found in the thermogram of saponite to the lattice changes:

	Value of c spacing	Peak T°C
Reversible Range	15 Å decreasing to	35
	11·5 Å	142
		152
	10·5 Å	266
	9·7 Å	616
	9·7 Å	680
		824
	Enstatite	

Acknowledgment. This paper is published by permission of the Director of Building Research. The work was carried out, during the attachment of one of us (K. A. G.) to the Building Research Station, as part of the programme of the Building Research Board.

References

Bragg, W. L. 1937. Atomic Structure of Minerals, New York.

Brindley, G. W. 1951. X-ray Identification and Crystal Structures of Clay Minerals, p. 311.

Cahoon, H. P. 1954. *Amer. Min.*, **39**, 222.

Greene-Kelly, R. 1953. *Clay Min. Bull.*, **2** (9), 52.

Hendricks, S. B., Nelson, R. A. and Alexander L. T. 1940. *J. Phys. Chem.*, **62**, 1457.

Mackenzie, R. C. 1950. *Clay Min. Bull.*, **4**, 145.

Midgley, H. G. 1951. *Miner. Mag.*, **29**, 526.

Schmidt, E. R. and Heystek, H. 1953. *Miner. Mag.*, **30**, 201.

Reprinted from Magazine of Concrete Research 1957 9 (25) March, 17-24.

BUILDING RESEARCH STATION
DEPARTMENT OF SCIENTIFIC AND INDUSTRIAL RESEARCH

A compilation of X-ray powder diffraction data of cement minerals*

by H. G. Midgley, M.Sc., Ph.D., F.G.S.

SUMMARY

X-ray powder diffraction methods are being used increasingly for the identification of minerals in cement. Since the last compilation was made a considerable amount of work has been done and this new compilation includes the most recent data.

Introduction

X-ray powder diffraction methods are being used increasingly for the identification of minerals in cement, and so this compilation of data should be useful. Some of the existing published data do not include spacings with *d* values greater than about 8Å and with simple powder cameras now recording to about 25Å it has become necessary to measure and record the long spacings.

High-resolution cameras make the presenting of standard data difficult since in this type of camera many lines characteristic of the lower symmetry minerals are resolved into doublets or even multiplets. In this compilation the data presented are those that can be resolved with simple cylindrical-type cameras recording to about 25Å. Some lines that are known to be split by focussing-type cameras have been marked.

Notes on the identification of the minerals present in Portland cement clinkers

These notes refer to the visual identification of photographs. It must be emphasized here that the best results will be obtained only if special care is taken with the preparation of specimens and accurate centring in the cameras. At the Building Research Station it has been found possible to use cellulose acetate capillaries 0·2 mm in diameter for the mounting of specimens and with these the resulting lines are quite sharp.

In Portland cement the predominant mineral is tricalcium silicate, which gives a very strong pattern and dominates the diffraction pattern. It can occur in more than one polymorphic modification; the two types to be distinguished are pure $3CaO.SiO_2$ and alite (a solid solution of Al_2O_3 and MgO in $3CaO.SiO_2$). Simons, according to Jeffery[1], has shown that alite has single lines at 1·761 and 1·485 Å while pure $3CaO.SiO_2$ has doublets (or multiplets if focussing cameras are used). By examination of the lines at 1·761 and 1·485 Å the polymorphic state may be determined.

The second most important mineral in Portland cement is $2CaO.SiO_2$ occurring in four polymorphic modifications designated α, α′, β, and γ. The modification most likely to be met is β (larnite) although if the cement has 'dusted' on storage the γ form may occur. The identification of $2CaO.SiO_2$ in mixtures is difficult since the strong lines of $2CaO.SiO_2$ almost coincide with those of alite or $3CaO.SiO_2$; the identification therefore depends on weak lines. The most useful lines are the pair at 2·448, 2·403 Å; one of these (2·448) almost coincides with the weak $3CaO.SiO_2$ line at 2·449 Å, but the line 2·403 Å is clear except for a weak line of $3CaO.Al_2O_3$ at 2·39 Å. Since $3CaO.Al_2O_3$ is usually present in small quantities this weak line does not show in a cement clinker film.

Using a high-resolution Guinier camera Yannaquis has examined a sample of $2CaO.SiO_2$ obtained from Portland cement by hand picking under the microscope[2]. The pattern, essentially that given in the present paper, differed from that of a pure β-$2CaO.SiO_2$ examined using the same camera; the pattern of the pure β-$2CaO.SiO_2$ was more complex, some lines that were single in the cement mineral being resolved into complex lines in the synthetic preparation.

The ferrite phase is a solid-solution series of composi-

tion $2CaO.Fe_2O_3$ to $6CaO.2Al_2O_3$. X-ray powder diffraction data of the solid-solution series show that there is a change in the lattice spacing with composition; a determination of the necessary lattice constants therefore gives the composition of the ferrite phase. The strongest line (200) occurs at about 2·62 but is very near to the 2·60 Å line of $3CaO.SiO_2$; if a very sharp line can be obtained, this line can be used to determine the composition, the value of the reflection varying from 2·67 Å in $2CaO.Fe_2O_3$ to 2·62 Å in $6CaO.2Al_2O_3.Fe_2O_3$. A graph relating these spacing values with chemical composition is given in Figure 1. If very sharp lines clear of other lines cannot be obtained, a magnetic fraction of ground cement clinker should be selected (this can be done by drawing a bar magnet through the powder and using the material adhering to it). A powder X-ray pattern of this fraction should show more lines due to the ferrite phase, and lines with higher Bragg angles can be used. A suitable spacing is the 202 reflection at 1·91–1·94 Å. This also has a continuous change in spacing with composition and a reference graph is also given in Figure 1.

Tricalcium aluminate phase can usually be detected by its strongest line at 2·69 Å; in fact this is frequently the only line due to this compound seen.

Other possible phases that can be detected are CaO, by its line at 1·390, and MgO, by its line at 2·106 Å. The 1·390 Å line of CaO is one of the weaker lines of the compound, the strongest line at 2·405 coinciding with a line of β-$2CaO.SiO_2$. If, however, there is more than about 5% of CaO present, the 1·390 line becomes very strong and its enhanced intensity relative to its neighbour reveals the presence of CaO.

The minimum quantities of the various phases detectable by X-rays are given by Bogue[3] as

$3CaO.SiO_2$	8%
$2CaO.SiO_2$	15%
$3CaO.Al_2O_3$	6%
$4CaO.Al_2O_3.Fe_2O_3$	15%
MgO	2·5%
CaO	2·5%

At the Building Research Station, using only simple powder techniques, the following figures were obtained for minimum quantities detectable.

$3CaO.SiO_2$	5%
$2CaO.SiO_2$	15%
$3CaO.Al_2O_3$	3%
Ferrite phase	5%
CaO	2%
MgO	1·5%

The results are generally similar and show how difficult the detection of the $2CaO.SiO_2$ phase can be. The detection of the tricalcium aluminate is easier; this is useful when assessing the sulphate resistance of a cement.

Identification of minerals in high alumina cements

The identification of the constituents of high alumina cement is simpler than for Portland cements since the main hydraulic phases $CaO.Al_2O_3$ and $6CaO.4Al_2O_3.FeO.SiO_2$ give very distinct X-ray powder patterns and so are easy to identify. The other phases likely to be present are melilite, calcium alumino-ferrites, and possibly glass. The ferrite composition can be determined as in Portland cement by measuring either the 200 or 202 reflection and using the graph in Figure 1. The melilite composition can also be determined by measuring the strong line at about 2·3 Å and referring to the data given by Nurse and Midgley[4].

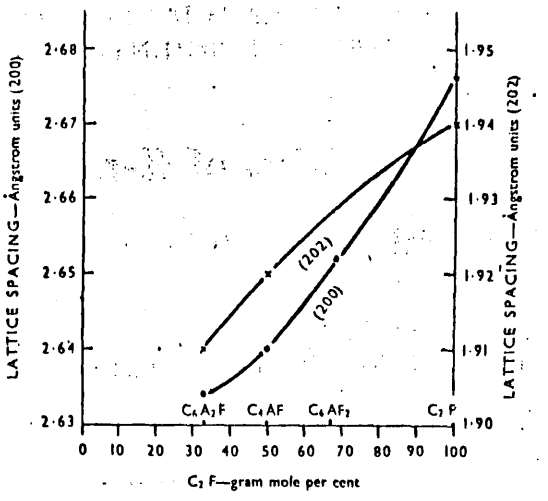

Figure 1: Graph relating spacing values with chemical composition.

Identification of cement minerals in set Portland cement

The identification of the minerals present in a set Portland cement is very much more difficult and if only simple techniques are available a full analysis is impossible. There is still a considerable difference of opinion as to whether calcium silicate hydrate (I) [CSH(I)] or afwillite is the main cementing agent in set Portland cement.

A simple powder X-ray diagram for set Portland cement will show a predominance of unhydrated material, with perhaps the strong lines of $Ca(OH)_2$ and ettringite and some of the lines due to hydrated calcium aluminate hydrates; these lines will be very few and faint against the strong pattern of $3CaO.SiO_2$.

The need is to concentrate the hydrates by removal of unhydrated material, and this can be accomplished by gravity separation. The cement is ground to pass 300 B.S. sieve size and then centrifuged in a bromoform-benzene mixture of specific gravity 2·90; the fraction that floats contains the hydrates, and by powder X-ray analysis of this fraction the hydrate minerals should be detected. The technique is that proposed by H. F. W. Taylor[5].

An alternative method of separation is that described

by Nurse and Taylor[6], in which the fine fraction of the set cement (less than ½ micron) is obtained from a lightly crushed cement by a combination of elutriation and super-centrifuging in anhydrous alcohol.

Identification of minerals in set high alumina cement

It is easier to identify the minerals present in set high alumina cement than those in set Portland cement. The hydrated calcium aluminates produced are more crystalline than the hydrated calcium silicates of set Portland cement and therefore give better X-ray diffraction patterns. In set high alumina cement stored under normal temperature conditions in Great Britain, the main cementing agent is $CaO.Al_2O_3.10H_2O$, which may be readily identified by the long spacing of 14 Å. Another possible hydrate is $2CaO.Al_2O_3.8H_2O$, with a long spacing of 10·7 Å. If the high alumina cement has been stored under warm wet conditions the cement will have undergone conversion and the phases likely to be present are cubic $3CaO.Al_2O_3.6H_2O$ and gibbsite, γ-$Al_2O_3.3H_2O$.

ACKNOWLEDGEMENTS

The author acknowledges the considerable help given by E. Aruja, D. Rosaman, and Miss P. M. Green during the preparation of this compilation, which is published with the permission of the Director of Building Research.

REFERENCES

1. JEFFREY, J. W. The tricalcium silicate phase. *Proceedings of the third international symposium on the chemistry of cement. London*, 1952. London, Cement and Concrete Association, 1954. pp. 30, 32, 34.
2. YANNAQUIS, N. Etude aux rayons X des silicates du clinker. *Revue des Matériaux de Construction et de Travaux Publics (Edition C)*. No. 480. September 1955. pp. 213–228.
3. BOGUE, R. H. *The chemistry of Portland cement*. 2nd edition. New York, The Rheinhold Publishing Corporation, 1955. pp. xviii, 793.
4. NURSE, R. W. and MIDGLEY, H. G. Studies on the melilite solid solutions. *Journal of the Iron and Steel Institute*. Vol. 174. June 1953. pp. 121–131.
5. TAYLOR, H. F. W. *Studies on the hydration of Portland cement*. XXVIIe Congrès International de Chimie Industrielle, Brussels, September 1954. p. 168.
6. NURSE, R. W. and TAYLOR, H. F. W. Contribution to discussion on the reactions and thermochemistry of cement hydration at ordinary temperature. *Proceedings of the third international symposium on the chemistry of cement, London*, 1952. London, Cement and Concrete Association, 1954. pp. 311–318.
7. SWANSON, H. E., GILFRICH, N. T. and COOK, M. I. *Standard X-ray diffraction powder patterns*. United States National Bureau of Standards. Circular No. 539. 26th September 1956. pp. 62.
8. *Cumulative, alphabetical and grouped numerical index of X-ray diffraction data*. Philadelphia, American Society for Testing Materials. Card No. 3163. 1955.
9. NURSE, R. W. The dicalcium silicate phase. *Proceedings of the third international symposium on the chemistry of cement, London*, 1952. London, Cement and Concrete Association, 1954. p. 60.
10. HELLER, L. *The structures of calcium aluminate and dicalcium silicate β hydrate*. Thesis presented to the University of London for the degree of Ph.D. 1951. pp. 96.
11. PARKER, T. W., RYDER, J. F. and MIDGLEY, C. M. Private communication. 1952.
12. HELLER, L. and TAYLOR, H. F. W. *Crystallographic data for the calcium silicates*. London, H.M.S.O. 1956. pp. vi, 79.
13. YANNAQUIS, N. X-ray studies of some calcium aluminates. *Proceedings of the third international symposium on the chemistry of cement, London*, 1952. London, Cement and Concrete Association, 1954. pp. 111–117.
14. ROOKSBY, H. P. Oxides and Hydroxides of aluminium and iron. *X-ray identification and crystal structures of clay minerals*. London, The Mineralogical Society, 1951. pp. 244–265.

Contributions discussing the above paper should be in the hands of the Editor not later than 31st July 1957.

continued overleaf

POWDER X-RAY DATA ON CEMENT MINERALS

GENERAL NOTES

The values of *I* represent relative intensity.

The *d* values for the spacings are given in Ångstrom units (Å); the intensities are on an arbitrary numerical scale, 10 being the strongest and 1 the weakest. Where it is known that doublets would be shown by using a camera of very high resolving power (such as the Guinier camera) the lines are marked with an asterisk. The three strongest lines are underlined. The symbol *B* indicates a broad line. A dagger indicates new data by the author. Owing to considerations of space, the data at large angles have been omitted in some cases.

CaO[7]

d	*I*
2·778	8
2·405	10
1·701	9
1·451	6
1·390	3
1·203	1
1·1036	1
1·0755	4
0·9819	4
0·9258	1
0·8504	1
0·8131	3
0·8018	3

MgO[7]

d	*I*
2·431	1
2·106	10
1·489	9
1·270	1
1·216	2
1·0533	1
0·9665	1
0·9419	2
0·8600	2
0·8109	1

$Ca(OH)_2$[7]

d	*I*
4·90	7
3·112	2
2·628	10
2·447	1
1·927	4
1·796	4
1·687	2
1·634	1
1·557	1
1·484	2
1·449	2
1·314	1
1·228	1
1·211	1
1·1762	1
1·1432	2
1·1275	1
1·0599	2
1·0366	1
1·0143	2

Brucite $Mg(OH)_2$[8]

d	*I*
4·76	8
2·37	10
1·79	8
1·57	7
1·49	6
1·37	6
1·31	6
1·18	5
1·09	2
1·03	4
1·00	6
0·95	4
0·94	6
0·91	4

$3CaO.SiO_2$[1]

d	*I*
5·901	4*
3·862	3*
3·510	2
3·346	2
3·227	1
3·022	8*
2·957	6*
2·891	3
2·818	1
2·776	10*
2·730	8
2·670	1
2·602	10
2·549	1
2·449	3*
2·326	6
2·304	5
2·277	2*
2·234	1
2·185	10*
2·159	1
2·125	3*
2·083	4*
2·045	2
2·011	1
1·979	6*B*
1·940	7
1·926	6
1·900	2*B*
1·863	1
1·825	6*B*
1·797	3
1·771	9(1)*
1·752	8(1)*
1·642	2
1·632	8
1·623	6
1·543	6

Alite[1]

d	*I*
3·861	3
3·517	1
3·334	2
3·144	2
3·022	8
2·959	6
2·880	2
2·804	1
2·764	10
2·739	9
2·682	3
2·592	9
2·436	3
2·313	6
2·178	9
2·172	6
2·089	1
2·060	1
2·028	1
1·973	5
1·928	6
1·831	5
1·819	5
1·799	2
1·761	9(1)
1·689	2
1·64	2
1·623	8
1·537	6
1·522	2
1·485	9(1)

Pure $3CaO.SiO_2$ can be distinguished from alite since at (1) it gives doublets instead of single lines.

Nagelschmidtite α-$2CaO.SiO_2$[9]

d	*I*
8·60	2
7·04	2
4·79	2
3·882	8
3·800	2
3·496	2
3·456	8
3·329	6
3·143	6
2·963	6
2·888	6
2·829	10
2·684	10
2·570	2
2·501	2
2·297	2
2·209	8
2·121	2
2·088	2
2·044	2
1·966	4
1·946	8
1·897	2
1·850	6
1·831	6
1·799	2
1·772	2
1·740	8
1·702	2
1·657	2
1·641	2
1·615	2
1·579	2
1·576	2
1·547	6
1·525	8
1·516	2
1·488	8

Bredigite α'-$2CaO.SiO_2$[9]		β-$2CaO.SiO_2$†		γ-$2CaO.SiO_2$[9]		$3CaO.Al_2O_3$†		$4CaO.Al_2O_3.Fe_2O_3$†		$6CaO.2Al_2O_3.Fe_2O_3$†		$2CaO.Fe_2O_3$†	
d	*I*	*d*	*I*	*d*	*I*	*d*	*I*	*d*	*I*	*d*	*I*	*d*	*I*
3·811	2	4·92	1	5·625	4	4·08	2	7·24	5	7·17	5	7·36	4
3·484	2	4·65	1	4·320	4	3·34	1	3·63	3	4·87	2	5·23	1
3·216	2	3·79	3	4·047	2	2·70	10	3·39	1	3·62	4	3·88	2
3·031	2	3·38	1	3·794	4*	2·39	2	2·77	8	3·37	1	3·68	4
2·889	2	3·34	1	3·354	2	2·258	1	2·67	7	2·99	1	3·05	2
2·730	10	3·09	1	3·002	10*	2·200	5	2·63	10	2·76	8	2·78	7
2·663	10	3·04	2	2·881	2	2·039	4	2·57	2	2·69	1	2·71	6
2·595	2	2·874	2*	2·728	10*	1·984	1	2·43	1	2·65	8	2·67	10
2·489	2	2·778	10*	2·525	2	1·951	1	2·20	3	2·62	10	2·60	2
2·413	2	2·740	10*	2·508	2	1·907	9	2·15	3	2·56	4	2·35	1
2·341	2	2·714	1	2·460	2	1·826	1	2·04	6	2·44	1	2·22	1
2·291	2	2·607	10	2·320	2	1·556	8	1·92	8	2·41	1	2·18	3
2·259	8	2·544	3	2·243	2	1·346	5	1·86	2	2·19	6	2·07	5
2·170	2	2·448	4*	2·186	2*	1·206	5	1·81	4	2·14	6	1·94	7
2·111	2	2·403	4	2·024	2	1·106	2	1·73	2	2·04	7	1·90	1
2·067	6	2·279	3	1·963	2	1·023	5	1·57	4	1·91	8	1·88	2
2·008	4	2·189	6*	1·928	8			1·53	4	1·85	3	1·84	4
1·923	8	2·163	4	1·878	2			1·51	1	1·81	6	1·74	3
1·895	2	2·128	1	1·800	6			1·50	2	1·79	1	1·66	1
1·837	4	2·088	1*	1·751	6			1·45	1	1·72	4	1·62	2
1·790	2	2·044	2	1·685	8			1·42	1	1·66	1	1·59	4
1·751	2	2·019	1	1·669	2*			1·39	2	1·60	2	1·55	4
1·725	2	1·982	7	1·632	6			1·33	1	1·57	6	1·54	1
1·686	2	1·911	1	1·539	2			1·32	2	1·56	1	1·52	2
1·665	2	1·892	4	1·524	2					1·53	7	1·48	1
1·646	2	1·844	1	1·498	2					1·51	2	1·46	1
1·621	2	1·806	2	1·469	2					1·50	3	1·43	1
1·574	6	1·787	2	1·457	2					1·45	2	1·38	1
1·554	6	1·763	1	1·443	2*					1·41	2	1·36	1
1·528	2	1·706	3	1·414	2					1·38	3	1·34	4
1·470	2	1·632	7	1·401	2*					1·35	3		
1·424	4	1·606	4	1·374	2					1·34	1		
1·392	2	1·587	2	1·352	2*					1·33	2		
1·380	2	1·573	2	1·268	2					1·32	4		
1·362	6	1·55	1*B*										
1·333	6	1·523	4										
1·294	4	1·483	3										
1·258	2	1·448	1										
		1·427	1										

$CaO.Al_2O_3$[10]		$6CaO.4Al_2O_3.MgO.SiO_2$[11]		$12CaO.7Al_2O_3$†		$CaO.2Al_2O_3$†		Calcium silicate hydrate (I) $CSH(B)$[12]		Calcium silicate hydrate (II) C_2SH_2[12]	
d	*I*	*d*	*I*	*d*	*I*	*d*	*I*	*d*	*I*	*d*	*I*
5·54	6	5·40	1	4·89	10	6·20	3	9·14	10	9·8	9
4·66	9	4·90	3	4·24	2	4·44	7	3·06	10	4·9	2
4·04	7	4·60	2	3·795	5	3·59	4	2·81	8	3·07	10
3·71	8	4·11	5	3·20	5	3·49	10	1·83	8	2·85	5
3·41	3	3·70	8	2·999	7	3·21	3	1·67	4	2·80	9
3·29	7	3·01	7	2·680	10	3·08	5	1·53	2	2·40	4
3·19	7	2·97	1	2·553	4	2·87	4	1·40	4	2·20	1
3·06	1*B*	2·87	10	2·445	8	2·74	4	1·17	1	2·10	1
2·98 / 2·95	10	2·76	10	2·347	3	2·70	4	1·11	2	2·00	6
2·90	5	2·69	3	2·186	7	2·59	9	1·07	1	1·83	9
2·85	8	2·60	1	2·056	2	2·53	3			1·72	1
2·75	5	2·53	1	1·944	7	2·43	4			1·62	1
2·53 / 2·50	10	2·44	5	1·898	1	2·40	1			1·56	5
2·43	4	2·37	6	1·894	2	2·32	3			1·40	4
2·42 / 2·39	10	2·34	6	1·762	2	2·21	1			1·225	3
2·33	8	2·21	2	1·729	4	2·17	3			1·165	3
2·29	7	2·18	2	1·694	2	2·06	1			1·1	1
2·26	7	2·11	4	1·662	7	2·05	5			1·045	2
2·20 / 2·19	9	2·03	6	1·646	1	2·00	3			1·025	1
2·16	4	1·92	6	1·630	4	1·96	2			1·000	1
2·13	8	1·89	1	1·601	7	1·93	1				
2·10	7	1·84	2	1·559	1	1·90	3				
2·08	1*B*	1·79	7	1·522	3	1·87	3				
2·01	8	1·76	8	1·497	2	1·80	5				
2·00	4	1·72	4	1·475	3	1·76	5				
1·956	7	1·66	4	1·393	6	1·68	4				
1·921	10	1·63	5	1·357	1	1·62	3				
1·909	8	1·55	4	1·339	3	1·55	1				
1·852	4	1·52	5	1·322	1	1·53	5				
1·830	8	1·48	6	1·307	4	1·51	2				
1·802	2	1·45	1	1·292	2	1·48	2				
1·780	2			1·277	2	1·45	1				
1·740	7			1·263	3	1·42	1				
1·721	6			1·235	2	1·40	1				
1·696	6			1·210	2	1·37	5				
				1·198	1	1·35	2				
				1·186	1	1·33	4				
				1·174	2	1·31	1				
						1·29	2				

These are the data for the poorly crystalline material. The long spacing can vary considerably and may also be undetected.

Afwillite[12]		$2CaO.SiO_2$ α-hydrate $C_2SH(A)$[12]		Hillebrandite (synthetic) $C_2SH(B)$[12]		$CaO.Al_2O_3.10H_2O$†		$2CaO.Al_2O_3.8H_2O$†		$3CaO.Al_2O_3.6H_2O$[13]	
d	*I*	*d*	*I*	*d*	*I*	*d*	*I*	*d*	*I*	*d*	*I*
6·45	8	5·35	3	12·0?	1	14·3	10	10·7	10	5·14	9
5·74	8	4·63	1	8·1	3	7·16	10	5·36	8	4·453	4
5·08	5	4·22	9	5·7	3	5·39	4	4·25	1	3·366	5
4·73	8	3·90	8	4·74	9	4·75	4	4·10	1	3·149	5
4·15	5	3·54	8	4·03	4	4·52	3	3·94	1	2·816	8
3·91	5	3·27	10	3·51	6	4·16	3	3·80	2	2·571	2
3·75	5	3·04	3	3·32	6	3·93	1	3·58	6	2·300	10
3·28	5	2·87	8	3·00	7	3·72	5	2·86	7	2·226	1
3·19	10	2·80	8	2·90	10	3·56	7	2·78	2	2·043	9
3·05	5	2·77	3	2·80	2	3·26	6	2·68	6	1·991	1
2·84	10	2·71	3	2·75	8	3·10	5	2·54	7	1·817	1
2·74	10	2·69	2	2·67	4	2·88	6	2·49	2	1·683	5
2·67	5	2·65	6	2·62	4	2·69	5	2·45	1	1·599	2
2·59	5	2·60	8	2·44	3	2·55	7	2·39	6	1·574	1
2·44	4	2·56	3	2·36	7	2·47	5	2·24	3	1·484	1
2·35	6	2·52	6	2·23	9	2·36	6	2·15	1	1·408	8
2·31	5	2·47	1	2·05	6	2·26	6	2·10	5	1·366	1
2·21	5	2·41	9	1·95	6	2·18	6	2·03	1	1·342	2
2·145	8	2·31	2	1·93	6	2·11	4	1·97	3		
2·064	4	2·27	2	1·85	6	2·06	4	1·94	1		
2·017	4	2·24	3	1·80	9	1·94	5	1·84	3		
1·989	6	2·18	5	1·75	5	1·87	1	1·79	1		
1·949	8	2·16	3	1·71	2	1·83	3	1·73	1		
1·924	5	2·10	2	1·68	1	1·79	4	1·67	6		
1·862	6	2·08	3	1·66	1	1·75	1	1·65	4		
1·805	8	2·06	4	1·62	2	1·71	3	1·59	4		
1·776	8	2·03	3	1·56	2	1·64	5	1·51	2		
1·724	4	2·02	3	1·53	3	1·60	6	1·44	3		
1·704	6	1·982	5	1·52	2	1·56	1	1·42	1		
1·683	6	1·956	3	1·46	4	1·52	2	1·37	2		
1·630	6	1·926	5	1·44	2	1·47	3	1·09	3		
1·604	8	1·890	3	1·41	2	1·40	2	1·06	1		
1·589	6	1·872	4	1·35	1	1·38	4				
1·563	4	1·842	2	1·33	1	1·27	1				
1·507	5	1·820	5	1·32	2	1·24	2				
1·413	4	1·788	8	1·17	4	1·18	2				
1·382	4	1·737	4	1·11	2	1·07	2				
1·380	4	1·712	4	1·09	2						
1·369	4	1·687	1								

$4CaO.Al_2O_3.13H_2O$†			Ettringite† $3CaO.Al_2O_3.3CaSO_4.32H_2O$			$3CaO.Al_2O_3.CaSO_4.13H_2O$†			Gibbsite[11]		
d	I		d	I		d	I		d	I	
8·05	10		9·8	10		8·92	10		4·83	10	
4·50	1		5·7	8		4·88	1		4·337	6	
4·05	2		4·9	6		4·72	1		3·303	3	
3·90	5		4·67	7		4·46	6		3·165	2	
3·63	1		4·34	2		3·99	6		3·086	1	
2·86	9		3·87	8		3·65	1		2·451	5	
2·69	6		3·60	3		2·87	7		2·374	5	
2·54	3		3·45	6		2·73	4		2·278	1	
2·45	6		3·26	4		2·60	1		2·236	2	
2·36	3		3·02	3		2·45	6		2·157	3	
2·23	4		2·79	9		2·41	5		2·039	4	
2·17	1		2·67	3		2·35	1		1·936	3	
2·04	2		2·57	8		2·33	2		1·909	3	
1·97	3		2·43	3		2·25	2		1·797	4	
1·93	2		2·36	1		2·19	2		1·743	4	
1·86	3		2·20	8		2·06	4		1·677	4	
1·74	2		2·14	6		1·99	2		1·643	1	
1·66	8		2·06	3		1·90	1		1·630	1	
			1·94	3		1·87	1		1·582	2	
			1·89	2		1·82	4		1·569	1	
			1·84	4		1·66	5		1·548	1	
			1·80	1		1·63	4		1·524	1	
			1·75	4		1·58	1		1·503	1	
			1·70	4		1·55	1		1·475	1	
			1·66	6		1·54	1		1·452	4	
			1·62	2		1·44	2		1·433	2	
			1·57	4		1·42	1		1·405	3	
			1·54	2		1·39	2		1·394	2	
			1·50	4		1·37	1		1·375	1	
			1·45	3		1·35	1		1·356	3	
			1·34	3							
			1·30	3							

0584635/1. R59. 150. 11/57 XL.

MIDGLEY (H.G.) D.Sc. 1967 13

Reprinted from the Magazine of Concrete Research 1958, 10 (28) March · Pages 13-16.

BUILDING RESEARCH STATION
DEPARTMENT OF SCIENTIFIC AND INDUSTRIAL RESEARCH

The composition of the ferrite phase in Portland cement*

by H. G. Midgley, M.Sc., Ph.D., F.G.S.

SUMMARY

A study of the composition of the ferrite phase present in commercial Portland cements has been made using powder X-ray diffraction techniques. From the results of an examination of thirty-one different samples, the most frequently occurring composition lies between $4CaO.Al_2O_3.Fe_2O_3$ and $6CaO.Al_2O_3.2Fe_2O_3$.

Introduction

The ferrite phase of Portland cement was first described by Törnebohm[1] in 1897 as dark orange-yellow grains with high birefringence and named "celite" Hansen, Brownmiller and Bogue,[2] when investigating the system $CaO-Al_2O_3-Fe_2O_3$ identified celite as a phase with a composition of $4CaO.Al_2O_3.Fe_2O_3$ to which the name Brownmillerite was later given. These authors also determined that there was a solid solution between the $4CaO.Al_2O_3.Fe_2O_3$ composition and $2CaO.Fe_2O_3$. Subsequently Yamauchi[3] and independently Swayze[4] showed that this solid solution extended to a composition near to $6CaO.2Al_2O_3.Fe_2O_3$. Malquori and Cirilli[5] in a further investigation of the system $2CaO.Fe_2O_3$–$6CaO.2Al_2O_3.Fe_2O_3$ by X-ray and magnetic susceptibility measurements showed that the system could be represented as a complete solid solution, all compositions being formed by isomorphous replacement in the basic $2CaO.Fe_2O_3$ structure. Swayze[4], however, gave evidence from heating experiments on synthetic mixtures in the system that $4CaO.Al_2O_3.Fe_2O_3$ was a compound or a special point in the solid solution. In the discussion to the papers on the ferrite phase during the Third International Symposium on the Chemistry of Cement in 1952, Midgley[6] suggested a method to determine the composition of the ferrite phase in commercial Portland cement. This depended upon the determination of one of the axial parameters from a measurement of the powder X-ray diffraction pattern. The highly magnetic fraction was used and the 202 reflection at about 1·94 Å was used as an "indicator line". His contribution suggested that a mechanical magnetic separator should be used, but subsequent work has shown that just as effective a separation can be made by passing a bar magnet through the cement powder and using the magnetic fraction. Since this work, Midgley has suggested[7] that, with better resolution in the X-ray diffraction pattern, the 200 reflection at about 2·63 Å can be used. This reflection can be seen in most clinkers without magnetic concentration.

Experimental

All the data available at the Building Research Station have been gathered together for this paper, the composition of the ferrite phase being determined by measurement of either the 200 or the 202 reflection and read off from Figure 1. In the majority of cases, the X-ray diffraction pattern was recorded on film in an 18 cm diameter camera with cobalt K alpha radiation, using an iron foil as a filter, and the 202 reflection was measured; in the remainder, a camera of 10 cm diameter was used with cobalt K alpha radiation, an iron filter and an aluminium foil, and both the 200 and 202 reflections were read. It has been found that the 202 reflection can be measured with an accuracy of ±0·004 Å, this being equivalent to ±4% in determination of composition. In many cases, however, this reflection is broad; this broadening could be ascribed to small crystal size, but other reflections in the pattern are of normal width, so another explanation must be sought. It seems very probable that this line broadening is due to crystal zoning, caused by non-equilibrium whilst cooling. The phenomenon of zoning in solid solutions is very common and the inner and

13

TABLE 1: **Chemical analyses (per cent by weight) and composition of ferrite phase of Portland cements.** (Chemical

Cement No. Weight (%)	A9	A10	A20	A35	A36	A37	A39	A40	A143	AF	A141	A7	A5	A33
SiO_2	20·10	21·06	21·65	20·43	20·26	22·63	20·22	20·72	23·78	20·06	21·97	22·82	19·26	20·72
CaO	65·60	65·45	66·10	65·08	64·28	64·90	66·91	66·94	64·90	64·74	65·06	65·70	65·75	62·92
Al_2O_3	6·14	5·69	6·00	6·71	6·45	4·97	6·77	5·94	5·14	4·71	5·58	6·15	7·89	6·54
Fe_2O_3	4·19	4·25	2·55	2·34	2·95	2·48	3·07	3·07	2·88	6·02	2·73	2·11	3·37	2·14
MgO	1·19	1·20	2·27	1·32	0·89	1·98	0·92	1·15	1·17	1·70	1·43	1·15	0·96	2·90
TiO_2	0·28	0·28	0·25	0·35	0·30	0·23	0·25	0·27	0·35	0·28	0·29	0·37	0·26	0·24
Na_2O	0·60	0·85	0·17	0·16	0·28	0·18	0·36	0·33	0·13	0·16	0·14	0·23	1·20	0·30
K_2O			0·16	0·78	0·60	0·60	0·47	0·76	0·76	0·66	0·15	0·92		1·05
SO_3	1·08	0·84	0·05	1·74	n.e.	1·38	0·21	0·25	n.e.	0·47	0·06	0·49	0·84	2·28
Mn_2O_3	n.e.	n.e.	n.e.	n.e.	n.e.	n.e.	n.e.	n.e.	n.e.	MnO 0·08	MnO 0·08	n.e.	n.e.	n.e.
Loss	1·11	0·78	n.e.	n.e.	2·02	n.e.	n.e.	n.e.	n.e.	0·89	1·61	0·76	0·44	n.e.
										FeO 0·17	FeO 0·07		FeO 0·52	
										P_2O_5 0·10				
TOTAL	100·46	100·41	99·20	98·91	98·03	98·75	99·18	99·43	99·11	100·05	100·27	100·70	100·47	97·93
$\frac{Al_2O_3}{Fe_2O_3}$	1·46	1·34	2·36	2·87	2·18	2·00	2·20	1·93	1·78	0·78	2·04	2·92	2·34	3·06
C_2F (%)	56	$\frac{65}{39}$ (52)	66	$\frac{71}{39}$ (55)	$\frac{74}{39}$ (57)	66	66	66	$\frac{65}{39}$ (52)	56	$\frac{65}{39}$ (52)	$\frac{54}{39}$ (47)	$\frac{54}{39}$ (47)	$\frac{71}{39}$ (55)
C_3S	60·0	59·5	60·7	56·3	60·0	51·2	68·4	70·0	45·0	65·5	56·5	48·4	61·1	45·0
C_2S	12·5	15·5	15·5	15·5	12·7	26·2	6·5	6·8	34·5	8·0	20·3	29·0	9·1	23·5
C_4AF	12·8	12·7	7·8	7·1	9·0	7·5	9·3	9·2	8·8	18·4	8·2	6·5	10·2	6·6
C_3A	9·2	8·0	11·6	13·8	12·1	9·0	12·8	9·9	8·8	2·5	10·2	12·6	15·4	13·7

NOTES: n.e. = not estimated. Cements with prefix A are clinker samples, those without are ground cement with added gypsum.
The following show zoning: A10, A35, A36, A143, A141, A7, A5, A33, and 485. In these samples the two numbers respresent estimated limits of solid solution; the number in the bracket is the average composition.
In sample A141, the band showing zoning is resolvable into two distinct peaks at 1·911 and 1·927 A, corresponding to compositions of C_2F 65 and C_2F 28.

outer zones would represent compositions on either side of the bulk composition, so that the X-ray diffraction pattern would show this by broad lines. A microphotometer trace of such broad lines shows a flat area, the limits of which can be estimated reproducibly by visual examination of the original photograph, as has been done in compiling the data for Table 1. From the experience gained in the experiments reported here it is felt that the greatest accuracy and reproducibility can be obtained by using the magnetic fraction and measuring the 202 reflection.

For this investigation the composition of the ferrite phase has been determined, by the methods given above, for 31 different Portland cements; some specimens were clinker and some were ground cements. The results of this examination are given in Table 1, together with the chemical analyses and potential compound calculation. The average composition of the ferrite phase, expressed as a percentage of the composition C_2F in the series C_2F–C_2A range from 40 to 75, whilst ten samples show a range of composition.

To obtain some idea of the distribution of the composition of the ferrite phase in commercial Portland cements, a frequency histogram has been constructed (Figure 2). In this, the composition of the ferrite phase has been assigned to one of five broad groups, having mean compositions as below:

$6CaO.2Al_2O_3.Fe_2O_3$
$10CaO.3Al_2O_3.2Fe_2O_3$
$4CaO.Al_2O_3.Fe_2O_3$
$5CaO.Al_2O_3.Fe_2O_3$
$6CaO.Al_2O_3.2Fe_2O_3$

and the frequency of occurrence has been determined as a percentage of the whole. From this it can be seen in Figure 2 that the majority of Portland cements have ferrite phases with a composition somewhere between $4CaO.Al_2O_3.Fe_2O_3$ and $6CaO.Al_2O_3.2Fe_2O_3$.

So far it has not been possible to determine what

analyses by F. J. McConnell, L. J. Larner and R. S. Gillett.)

423	461	484	485	503	507	492	512	515	517	519	520	516	500	539	540
20·34	22·51	25·08	21·83	20·44	22·14	22·55	21·58	21·57	20·09	22·02	22·21	22·21	21·62	20·74	22·46
63·97	67·00	61·82	65·36	63·51	63·66	63·95	64·48	62·45	63·45	63·83	63·89	67·87	65·70	62·76	61·37
5·79	7·29	4·60	5·21	5·98	5·01	4·97	5·50	5·54	5·45	5·08	4·92	4·05	4·66	4·18	4·40
3·03	2·56	2·07	2·31	2·75	1·99	2·26	2·26	2·72	2·49	2·15	2·01	0·47	2·08	6·17	6·35
1·29	2·58	1·69	1·70	1·35	1·15	1·20	1·11	1·09	3·84	1·10	1·20	0·46	1·09	0·95	0·88
0·30	0·42	0·25	0·26	0·29	0·32	0·32	0·38	0·32	0·34	0·29	0·32	0·06	0·34	0·28	0·30
0·31	0·23	0·19	0·22	0·16	0·17	0·14	0·06	0·12	0·24	0·12	0·14	0·10	0·15	0·20	0·21
0·81	0·92	0·77	0·56	0·84	0·61	0·48	0·94	0·93	0·45	0·63	0·49	0·14	0·50	0·69	0·73
2·49	2·83	2·57	1·47	2·80	2·36	2·22	1·99	1·95	1·65	2·21	2·37	2·04	1·41	2·33	2·06
0·06	0·50	0·05	0·06	0·07	0·12	0·09	0·06	0·07	0·05	0·10	0·10	0·04	0·11	0·05	0·08
1·43	3·03	1·29	1·34	2·10	2·81	3·15	1·90	3·32	2·26	2·53	2·47	2·46	2·64	1·85	1·22
	Sulphide 0·25														
100·00	100·00	100·34	100·32	100·29	100·34	100·30	100·26	100·08	100·32	100·06	100·02	99·85	100·30	100·20	100·06
1·90	2·85	2·22	2·26	2·18	2·52	2·20	2·44	2·04	2·19	2·35	2·45	8·60	2·25	0·68	0·70
71	42	40	$\frac{71}{42}$ (55)	66	66	65	66	66	66	75	75	75	66	62	62
55·7	41·0	20·0	57·5	51·2	47·8	46·5	52·7	43·8	60·7	49·2	45·8	73·8	64·8	56·2	34·5
16·3	33·6	58·5	19·2	20·0	27·8	29·5	22·1	28·8	11·8	26·0	29·1	8·0	13·2	17·0	38·3
9·3	7·8	6·2	7·0	8·4	6·0	6·8	6·8	8·3	7·6	6·5	6·2	1·4	6·2	18·8	19·3
10·2	15·0	8·7	10·0	11·3	9·9	9·4	10·7	10·1	10·4	9·8	9·6	10·0	8·9	0·7	0·9

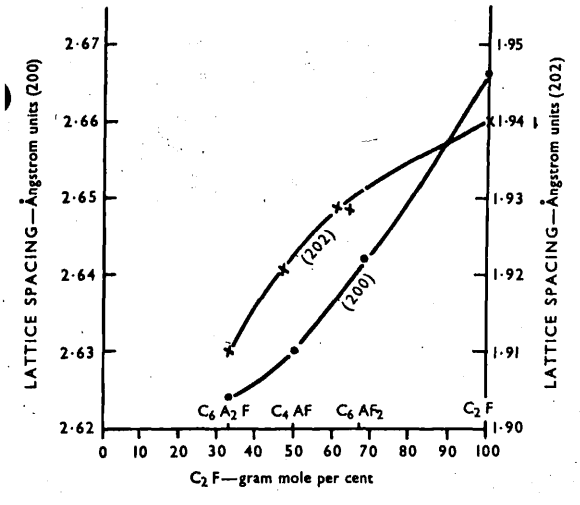

Figure 1

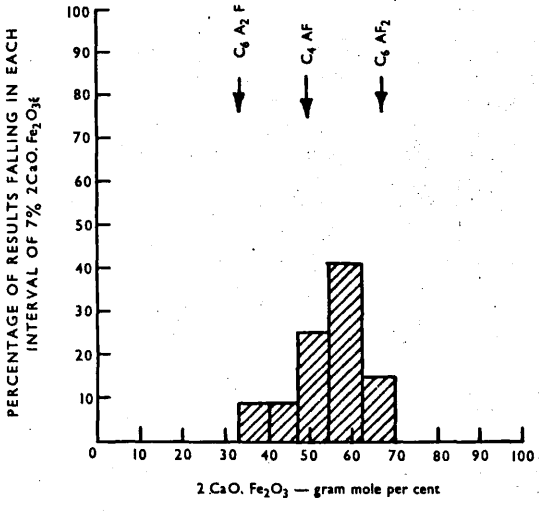

Figure 2

governs the composition of the ferrite phase, for there is no correlation between the ferrite composition and the ratio of Al_2O_3 to Fe_2O_3.

Conclusion

From a study of the composition of the ferrite phase in Portland cement, as determined by an X-ray diffraction method, it is found that the most frequently occurring composition lies between $4CaO.Al_2O_3.Fe_2O_3$ and $6CaO.Al_2O_3.2Fe_2O_3$.

ACKNOWLEDGEMENTS

This paper is published by permission of the Director of Building Research; the work formed part of the programme of the Building Research Board. The author would like to thank his colleagues Mr D. Rosaman and Mr J. J. Smith for help with the experimental work.

REFERENCES

1. TÖRNEBOHM, A. E. *Tonindustrie Zeitung*. 1897. p. 1148.
2. HANSEN, W. C., BROWNMILLER, L. T. and BOGUE, R. H. *Journal of the American Ceramics Society*. Vol. 50. 1928. p. 396.
3. YAMAUCHI, T. A study on the celite part. Parts III, IV and V. *The Journal of the Japanese Ceramic Association*. Vol. 45. 1937. No. 533. pp. 433–366. No. 537. pp. 614–631. No. 540. pp. 880–896.
4. SWAYZE, M. A. A report on studies of (1) the ternary system $CaO-C_3A_3-C_2F$; (2) the quaternary system $CaO-C_3A_3-C_2F-C_2S$; (3) the quaternary system as modified by 5% magnesia. *American Journal of Science*. Vol. 244. January 1946. pp. 1–30. February 1946. pp. 65–94.
5. MALQUORI, G. L. and CIRILLI, V. The ferrite phase. *Proceedings of the Third International Symposium on the Chemistry of Cement, London 1952*. London, Cement and Concrete Association, 1954. pp. 120–136.
6. MIDGLEY, H. G. Contribution to discussion on Paper 5. The ferrite phase. *Proceedings of the Third International Symposium on the Chemistry of Cement, London 1952*. London, Cement and Concrete Association, 1954. pp. 140–143.
7. MIDGLEY, H. G. A compilation of X-ray powder diffraction data of cement minerals. *Magazine of Concrete Research*. Vol. 9, No. 25. March 1957. pp. 17–19.

Contributions discussing the above paper should be in the hands of the Editor not later than 30th September 1958.

14

MIDGLEY (H.G.) D.Sc.

[Reprinted from the *Mineralogical Magazine*, London, June 1958, Vol. XXXI, No. 241, p. 883.]

1967

SHORT COMMUNICATIONS

A further occurrence of phosgenite.

In a recent note Kingsbury[1] described two new localities for phosgenite in the United Kingdom. This mineral has some interest in building since it may be a corrosion product of lead materials in contact with chloride solutions. Opportunity was taken to establish the standard data when a sample found by Mr. G. W. Mack in an ancient lead pot deep in Wookey Hole was presented for study in 1948. The mineral occurs as flattened plates about $1 \times 1 \times 0{\cdot}3$ cm. maximum, colourless and for the most part clear. Chemical analysis by R. S. Gillett gave: PbO 81·2, Cl 12·6, CO_2 8·0 %, equivalent to $Pb_2(CO_3)Cl_2$. The crystals have refractive index about 2·15, uniaxial positive; crystallographically the most prominent face is *c* {001}; other forms identified include *u* {120}, *x* {111}, *m* {110}, *b* {010}, and *o* {021}. The material has the high specific gravity of 6·15. An X-ray powder diffraction pattern using filtered Co-$K\alpha$ radiation gave the following results:

d.	*I.*	*d.*	*I.*	*d.*	*I.*	*d.*	*I.*
5·71 Å.	w	2·40 Å.	vvw	1·800 Å.	m	1·402 Å.	vvw
4·40	s	2·28	vw	1·757	mw	1·393	vvw
4·04	ms	2·21	m	1·672	mw	1·364	w
3·61	vs	2·03	vw	1·636	vvw	1·352	w
3·50	vvw	1·97	mw	1·588	vvw	1·327	w
3·09	vvw	1·94	vvw	1·508	vw	1·294	mw
2·99	vw	1·91	mw	1·495	vvw	1·285	vvw
2·86	vvw	1·887	mw	1·469	mw	1·277	vvw
2·79	vvs	1·841	vvw	1·445	mw	1·267	vw
2·56	vs	1·820	vvw	1·426	m		

If the unit cell proposed by Oftedal[2] is taken as a guide, the data above give unit-cell dimensions *a* 8·112 Å., *c* 8·814 Å., $c/a = 1{\cdot}086$.

The formation of phosgenite under similar conditions has been reported by Lacroix from Maldia, Tunis,[3] where an ancient metallic object was immersed in sea-water, and also from Bourbonne-les-Bains, France,[4] where a lead pipe was exposed to a hot spring.

Building Research Station,
Watford, Herts.

H. G. Midgley

[1] A. W. G. Kingsbury, Min. Mag., 1957, vol. 31, p. 500.
[2] I. Oftedal, Norsk Geol. Tidsskr., 1945, vol. 24, p. 79.
[3] A. Lacroix, Compt. Rend. Acad. Sci. Paris, 1910, vol. 151, p. 276.
[4] A. Lacroix, Min. France, 1909, vol. 3, p. 779.

BUILDING RESEARCH STATION
DEPARTMENT OF SCIENTIFIC AND INDUSTRIAL RESEARCH

The staining of concrete by pyrite*

by H. G. Midgley, M.Sc., Ph.D., F.G.S.

SUMMARY

Concretes and mortars made with some Thames river gravels have, in recent years, been suffering from brown staining. This has been traced to the mineral pyrite, FeS_2; not all specimens of the mineral are reactive and it is possible to distinguish between the two types, reactive and unreactive by a simple test: on immersion of the suspect pebble or grain in lime water, the reactive forms will produce a brown precipitate within a few minutes while the unreactive form is stable.

It appears that the reactivity is associated with the "defect" structure of the mineral, the unreactive forms being "stabilized" by ions of some metal impurity.

Introduction

It has been noticed for some years now that concrete and mortars made from some Thames river gravels and sands are prone to unsightly dark brown staining (Figures 1 and 2). This staining has been traced to a reactive form of the mineral pyrite, FeS_2. The brown product has been identified as goethite, an iron hydroxide, and it is thought that this is formed by the reaction of iron sulphide with water and atmospheric oxygen to form ferrous sulphate which subsequently decomposes readily in air to form the hydroxide. At this stage the sulphate ions react with the calcium aluminates in the cement to form the mineral ettringite (calcium sulphoaluminate hydrate). Experiments have shown that these reactions take place readily only in the presence of lime water, and also that only certain varieties of the mineral pyrite are reactive. Small pats of cement with the mineral embedded at the surface have been used to determine the possible reactivity. Figure 3 shows two pyrite samples which have not reacted after two years' exposure; Figure 4 shows a reactive form after only three months.

All the samples, both reactive and unreactive, when examined by X-ray powder diffraction methods give a typical pyrite pattern without any special features. In physical appearance the specimens tested range from well crystallized cubes through massive and fibrous varieties to granular varieties, but there appears to be no relation between physical appearance and reactivity.

Chemical properties

A full chemical analysis has been made of two samples, a reactive one (HR) from Thames river gravel and an unreactive one (A) from Spain. Analyses are given in Table 1.

TABLE 1: **Chemical analysis of pyrite** (*L. J. Larner*).

	HR Thames river gravel	A Spain
Loss at 110°C	2·58	0·34
Total S as S	36·55	48·45
SiO_2	19·65	0·20
Al_2O_3	1·82	0·29
TiO_2	0·16	0·05
CaO	0·32	0·53
MgO	0·23	0·19
Fe	33·38	43·95
Cu	0·04	1·12
As	0·01	0·23
Sb	nil	0·20
Sn	nil	0·20
Zn	trace	1·45
Mn	trace	0·03
Ni	0·06	0·02
Co	0·02	0·01
Pb	trace	0·21
Fe/S (mol)	0·525	0·519
	$FeS_{1·915}$	$FeS_{1·930}$
Total metals/S (mol)	0·526	0·550
	(Fe+Me) $S_{1·916}$	(Fe+Me) $S_{1·815}$

Figure 1

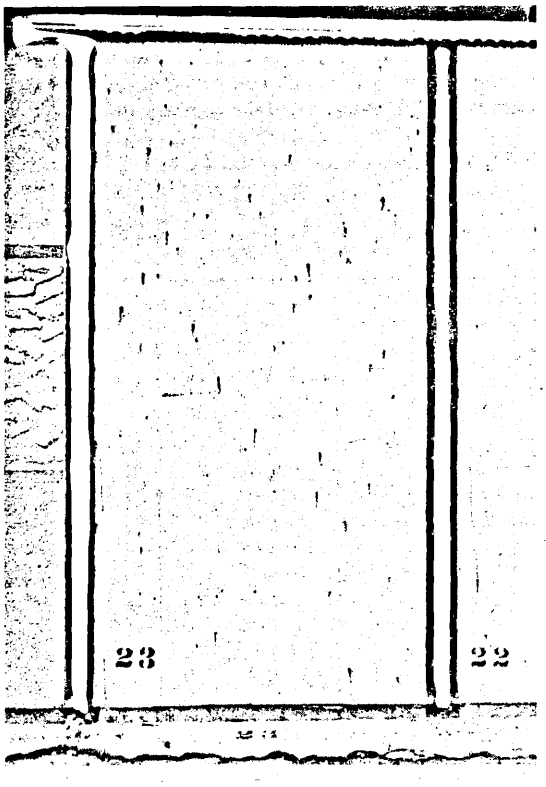

Figure 2 (It has been estimated that only one grain in two million produced this.)

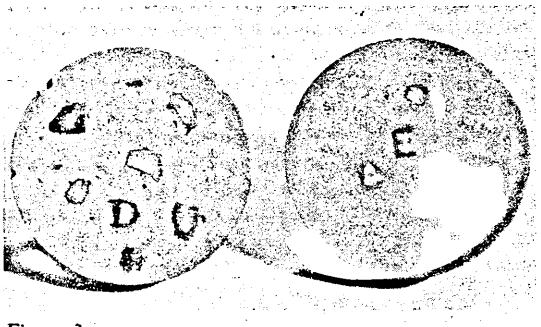

Figure 3

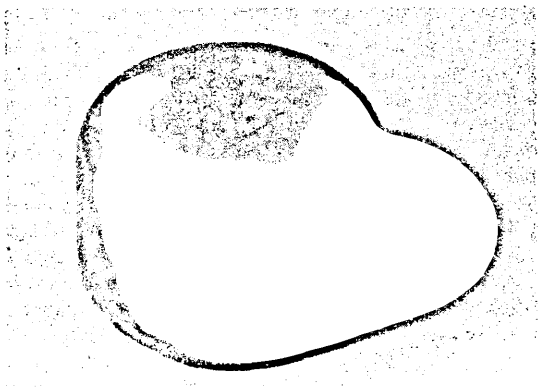

Figure 4

TABLE 2: **Details of the samples.**

Mark	Source	Description
A	Pyrite, Spain. Sample obtained through chemical suppliers	Massive, dull brassy colour
292	Pyrite, Spain	Crystalline specimen; aggregate of crystals, mostly showing cube faces, brassy colour
389	Pyrite, Spain	Massive, no crystal faces, brassy colour
679	Pyrite, from slate, Ballachulish.	Crystalline and massive specimens, cube faces show on crystalline specimens, brassy colour
701	Pyrite from clay borehole, 31 ft down, east of Dobsweir, Hodston, Surrey	Finely granular pyrites, occurring as botryoidal growths, dull brown in colour
562	Pyrite, Anglesey	Small crystalline grains, bright brass colour
574	Pyrite, Snowdon, North Wales	Divided, granular
293	Radiating pyrite, Kent	Radiating pyrite, bright brass colour
558	Pyrite, Ham river gravel. Sample obtained from concrete coping (Figure 2)	Dull black colour
HRL	Pyrite, Thames river gravel	Amorphous, light grey colour
HRD	Pyrite, Thames river gravel	Amorphous, black colour
HRF	Pyrite, Thames river gravel	As HRD, but occurring in flakes

TABLE 3: **Spectrographic examination of pyrite samples (*S. R. Bowden*).**

Mark	Reactivity		Ni	Co	Zn	Cu	Pb	Sn	As	Sb
	Pat test	Lime water								
A	—	—	—	—	xx	xx	x	xx	x	x
292	—	—	—	—	xx	xx	x	xx	xx	—
389	—	—	x	—	xx	xx	—	x	—	—
679	—	—	x	x	—	x	x	—	—	—
701	—	—	xx	x	—	—	—	—	x	—
562	—	—	—	x	—	x	x	x	x	—
574	—	—	—	—	—	x	xx	—	—	x
293	+	+	xx	—	—	—	—	—	—	—
558	+	+	xx	—	—	—	—	—	—	—
HRL	+	+	xx	x	—	—	—	—	—	—
HRD	+	+	xx	x	—	—	—	—	—	—
HRF	+	+	xx	x	x	—	—	—	—	—

+ = positive reaction. — = negative reaction. xx = present. x = present in smaller quantity.

Two differences between the reactive (HR) and the unreactive pyrite (A) can be seen from the chemical analysis; the unreactive sample has a greater sulphur deficiency than the reactive, 0·185 against 0·084 mol, but this is solely due to the presence in it of a considerable number (0·054 mol) of metal cations; if we only consider the iron/sulphur ratio it is the reactive sample which has the greater sulphur deficiency: 0·085 against 0·070 mol.

Spectrographic analyses were therefore made of a number of samples (Table 2) all of which had been tested for soundness by a pat test.

Those that had not reacted at the end of one month were still unreactive after three years. The results of part of the analysis are given in Table 3.

The results of the spectrographic examination suggest that the lack of reactivity of the pyrite is associated with the presence of a number of metal cations and the re-

active varieties appear to be deficient in these extra metal cations. Pyrite is known to have a " defect " structure and rarely possesses the exact 2:1 ratio of sulphur to iron shown by the ideal formula; it seems likely that the presence of extra metal cations in some way stabilizes the structure against attack by lime water.

The fact that the decomposition of the pyrite takes place only in lime water suggests a very rapid test for reactivity. If the aggregate appears to contain dark pebbles or grains that might be pyrite the reactivity may be determined rapidly by placing the suspect pebble in a saturated solution of lime. A blue-green gelatinous precipitate of ferrous sulphate should be formed within 5 min. and this rapidly changes to brown ferric hydroxide on exposure to air and light. This reaction should be complete within 30 min. If no brown gelatinous precipitate is found when a suspect pebble is placed in saturated lime water there is no likelihood of any reaction taking place in concrete or mortar if the pebble is used as an aggregate.

It has been suggested that aggregate that is unsalable because of the presence of reactive pyrite can be reclaimed for use by washing with lime water. No experience of this treatment in practice is available.

ACKNOWLEDGEMENT

This work formed part of the programme of the Building Research Board and is published by permission of the Director of Building Research.

Contributions discussing the above paper should be in the hands of the Editor not later than 30th November 1958.

Reprinted from the Magazine of Concrete Research 1958, 10 (29) August 75-78

MIDGLEY (H.G.) 16

Reprinted from *Clay Minerals Bulletin*, 1959, Vol. 4, No. 22. D. Sc.

A SEPIOLITE FROM MULLION, CORNWALL 1967.

By H. G. MIDGLEY
Building Research Station, Garston, Watford, Herts.

[Read 15th April, 1959]

ABSTRACT

Sepiolites are rare minerals in Great Britain, there being hitherto only two recorded occurrences. The identity of the present sample has been established by means of X-ray diffraction, differential thermal analysis, thermogravimetry, chemical analysis, and infra-red absorption analysis, and some speculations on its genesis are offered.

INTRODUCTION

Sepiolites are rare minerals in Great Britain, the first recorded occurrence being from Kynance Cove, Cornwall (Caillère and Hénin, 1949) and the second from the Keuper Marl of the Midlands (Keeling, 1956). The new occurrence of sepiolite now described is in a locality not far from the first at Kynance Cove, but the material differs from that of Kynance in general appearance and in its mode of occurrence. It was found as a thin vein about 7 mm thick, cutting the massive serpentine rock on the south-east side of the harbour at Mullion; no associated calcite was seen.

DESCRIPTION OF THE MINERAL

The sample is markedly fibrous, the outside is hard and of a buff colour. The vein when broken open shows a mixture of felted fibres and granules; on keeping in the laboratory atmosphere the sample becomes remarkably hard. In thin section the mineral is seen to be a mixture of two types of material: the first is fibrous with a high birefringence and a moderate refractive index (n=1·51-1·52), the fibres having straight extinction and positive elongation; the second is interstitial and appears to be microcrystalline or amorphous. Some of the fibres surround the isotropic material to form grains of approximately 0·02 mm diameter.

A chemical analysis* of the bulk material gave: SiO_2 50·06, Fe_2O_3 3·49, TiO_2 0·16, Al_2O_3 1·27, CaO 0·04, MgO 22·24, Mn_2O_3 0·06, Na_2O 0·08, K_2O 0·10, H_2O (−110°C) 12·02, H_2O (+110°C) 10·40, total 99·92. This analysis is equivalent to $2MgO.3SiO_2.2H_2O$, the usually accepted formula for sepiolite, and is very close to that given for Bou Azzer sepiolite by Caillère (1952).

*Analyst, L. J. Larner.

16

An X-ray powder diffraction examination was made using both filtered CuKα and CoKα radiation with a camera of 10 cm radius; the data are given in Table 1. These are typical for sepiolite and compare with those given by Keeling (1956) and by the A.S.T.M. X-ray Powder Data File, card No. 2-0032; they do not, however, agree with the results of Longchambon quoted by Caillère (1951). The main difference is the absence of a strong reflection at 4.28 Å in the data of Longchambon. As there appeared to be two types of material in the Mullion sepiolite, an attempt was made to identify the extra line with the isotropic phase, but subsequent examination of other sepiolites using the same X-ray diffraction cameras always showed the line at about 4·28 Å. Two of these sepiolites were of the sedimentary type, one a meerschaum from Kenya, East Africa,

TABLE 1—X-ray powder diffraction data for sepiolite.

d(Å)	I	d(Å)	I	d(Å)	I	d(Å)	I
12·1	vvs	3·35	m	2·26	m	1·519	mv
7·45	w	3·17	m	2·13	vvw	1·505	vvw
6·74	vvw	3·03	vw	2·06	w	1·465	vw
5·02	vw	2·82	vw	1·95	vvw	1·411	w
4·54	m	2·70	vw	1·87	vw	1·307	vvw
4·28	ms	2·57	s	1·69	w	1·295	m
3·74	m	2·44	m	1·587	w	etc.	
3·55	vw	2·40	vw	1·546	mw		

and the other from Salinelles, Gard, France. It seems likely that the line at 4·28 Å is not due to an impurity, and that the pattern quoted by Caillère (1951) is incorrect. In the data for the Mullion sepiolite there is an extra line at 3·03 Å, which may be due to a small amount of calcite impurity.

A differential thermal curve was obtained for 0·2 g of the sample diluted with 0·4 g of α-Al_2O_3 (corundum) in a ceramic crucible, using α-Al_2O_3 as the reference material; the temperatures were measured with chromel-alumel thermocouples and the heating rate was 10°C/min. This curve (Fig. 1) shows two endotherms, one at 122°C and a second at approximately 815°C; superimposed on the latter is a sharp exotherm with a peak temperature of 837°C. To discover the significance of the peaks, samples of the sepiolite were heated in a thermostatically controlled oven and furnace, at 180°C for five days, and at 1000°C for five and for twenty-four hours. The sample heated at 180°C showed no change, the X-ray diffraction

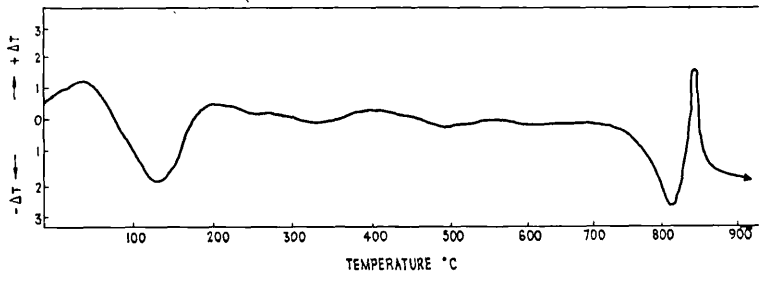

FIG. 1—Differential thermal curve for sepiolite from Mullion, Cornwall.

pattern being identical with the unheated material, indicating that the first endotherm is due to the removal of water not essential to the structure. The shape of the endotherm is typical of loosely-held water which may be regarded as zeolitic in nature. The second endotherm at 815°C is due to dehydroxylation; superimposed on this is the exotherm at 837°C which is caused by the chemical heat of formation of anhydrous silicates. X-ray diffraction of the samples heated at 1000°C indicates the presence of enstatite, $MgSiO_3$, and a trace of cristobalite.

A thermogravimetric analysis was made on a 155 mg sample of the sepiolite, using a recording thermobalance with a sensitivity of 0·1 mg; the sample was heated from room temperature to 1000°C in 3 hours, at approximately 5·5°C/min. The thermogram (Fig. 2)

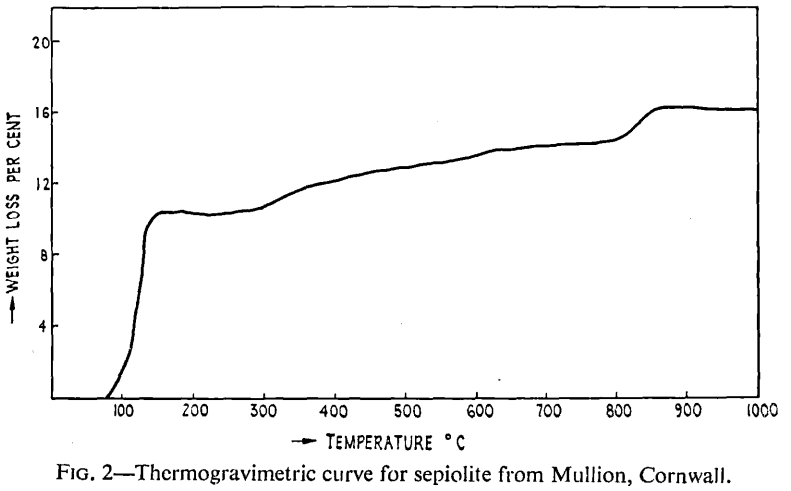

FIG. 2—Thermogravimetric curve for sepiolite from Mullion, Cornwall.

is similar to those published by Caillère and Hénin (1957), resembling most the curve for the compact material from Ampandrandava. There is some discrepancy between the results obtained by dynamic thermogravimetry and by static loss on ignition (quoted in the analysis). This is probably mainly due to the drying out of the sample on storage in the laboratory, since the static weighing was made soon after collecting the sample, while the thermogram was made some six years later.

On the thermobalance there is a rapid loss in weight of 10·4 per cent. between 80°C and 140°C, followed by a less steep loss of 3·1 per cent. between 250°C and 600°C; at 600°C there is an inflection and a further loss in weight of 1·1 per cent. between that temperature and

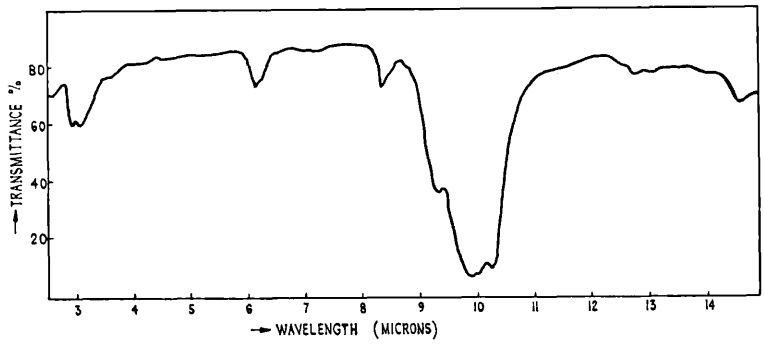

FIG. 3—Infra-red absorption spectrum of sepiolite from Mullion, Cornwall.

800°C, where there is a change in the rate of loss; finally 1·5 per cent. is lost between 800°C and 900°C.

An infra-red absorption spectrogram of the Mullion sepiolite is shown in Fig. 3. The sample for the analysis was made by milling about 5 mg in iso-propyl alcohol in a vibrating ball mill of the type described by Ford, Wilkinson, and Price (1954); when it had been milled for about 15 minutes a drop of the suspension was removed by pipette and spread on a sodium chloride plate, the iso-propyl alcohol was allowed to evaporate, and the plate was ready for the spectrometer. The sample used weighed 2 mg on a disc of 25 mm diameter, or 0·004 mg/mm^2. The method of deposition from iso-propyl alcohol was preferred to the KBr disc method, since sepiolite contains both free water and hydroxyl groups, and experience has shown that there may be some reaction with the hygroscopic KBr.

Sepiolite being of a fibrous nature, there is no great likelihood of the deposited sample showing much preferred orientation.

The absorption spectrum was obtained on a double-beam Perkin-Elmer Infracord spectrometer, the record being between 2·5 and 15μ. The spectrum shows peaks at about 2·9, 3·1, 6·1, 6·25, 8·35, 9·33, 9·9, and 10·3μ, and there are also minor peaks at 12·7 and 14·5μ. There is a general resemblance with the spectrum for sepiolite published by Launer (1952); however, there is some disagreement in the absorption peak values for the Si—O vibrations in the 9—12μ region. The peaks at 6·1 and 6·25μ are not very sharp, and may only represent the spreading out of the peak at 6·2μ due to the broad H—O—H angle deformation vibrations. This peak can be assigned to the "free water," and is probably associated with the zeolitic water mentioned earlier. The double peak at 2·9 and 3·1μ is due to H—O stretching, and may be influenced by sorbed water. Illites and montmorillonites also show this double peak, but, unlike sepiolite, the peaks are of unequal size; kaolinites and micas have only a single peak in this region.

Origin of Sepiolite

There must be some speculation as to the origin of the sepiolite from Mullion. Caillère (1951) notes that sepiolite may occur as an alteration product of serpentine, although it is usually described as being formed under lacustrine conditions of high basicity (Millot, 1949). At Mullion the sepiolite is associated with serpentine rock; the serpentine may be represented as $6MgO.4SiO_2.4H_2O$, while sepiolite is $2MgO.3SiO_2.2H_2O$. This indicates that the sepiolite was formed either by the removal of magnesia or by the addition of silica. If magnesia had been removed, it is likely that some trace of it would be found in the area either as dolomite or as magnesite. There are numerous calcite veins in the area, and chemical tests on a large number have failed to show any significant amount of magnesium; it is therefore unlikely that the sepiolite was formed by the removal of magnesium. This leads to the conclusion that the sepiolite owes its origin to the addition of silica, which in the Lizard area is readily available, for in many of the areas, Mullion and Kynance Cove included, an acid igneous rock has invaded the serpentine. Reaction with the siliceous emanations from this material presumably led to the formation of the sepiolite. The invading acid "magma," Kennack gneiss, was not seen in the Mullion sepiolite locality, but a saponite was formed by reaction between serpentine rock and in-

vading Kennack gneiss at Church Cove (Midgley and Gross, 1956); by analogy, it seems likely that the Mullion sepiolite originated under similar conditions.

Acknowledgment.—The work described has been carried out as part of the research programme of the Building Research Board of the Department of Scientific and Industrial Research, and this paper is published by permission of the Director of Building Research.

References

Caillère, S., 1951. X-ray identification and crystal structure of clay minerals (G. W. Brindley, editor). Mineralogical Society, London. Chapter 8, p. 224.

Caillère, S., 1952. *Bull. Soc. franc. Minér.*, **75**, 305.

Caillère, S., and Hénin, S., 1949. *Nature, Lond.*, **163**, 962.

Caillère, S., and Hénin, S., 1957. The Differential Thermal Investigation of Clays (R. C. Mackenzie, editor). Mineralogical Society, London. Chapter 9, p. 231.

Ford, M. A., Wilkinson, G. R., and Price, W. C., 1954. Molecular Spectroscopy (G. Sell, editor). Inst. Petroleum, London, p. 82.

Keeling, P. S., 1956. *Miner. Mag.*, **31**, 328.

Launer, P. J., 1952. *Amer. Min.*, **37**, 764.

Midgley, H. G., and Gross, K. A., 1956. *Clay Min. Bull.*, **3**, 79.

Millot, G., 1949. *Géol. appl.*, **2**, Nos. 2-3-4.

MIDGLEY (H.G.) '4

Reprinted from *Clay Minerals Bulletin*, Vol. 4, No. 23, 1960. D.Sc. 1967

THE MINERALOGY OF SOME COMMERCIAL VERMICULITES

By H. G. MIDGLEY and C. M. MIDGLEY
Building Research Station, Garston, Watford, Herts.

[Read 3rd November, 1958]

ABSTRACT

A number of different commercial vermiculites have been examined and it has been found that the exfoliable minerals can be divided into three main groups; those which give a 26 Å spacing on an X-ray diffraction pattern, those which give a 14 Å spacing, and those which give various spacings and are partially dehydrated. All are mixed-layer minerals of one type or another, but all have some vermiculite layers in their constitution. The expansibility of these minerals is not linked with their structural types, but there is an indication that the largest expansion is associated with the occurrence of hydrobiotite and the lowest expansion with the occurrence of true vermiculite.

INTRODUCTION

'Vermiculites' are used extensively in the building industry for insulating material and as a lightweight aggregate for concrete. The material may be imported in the unexfoliated state and exfoliated near where it is needed. This is a considerable assistance in transport, which constitutes a major part of the cost of a building material.

A number of samples of commercial vermiculite have from time to time been submitted to the Building Research Station for examination, and the opportunity has been taken of making a mineralogical examination.

EXPERIMENTAL

Differential thermal analysis, X-ray flake and powder diffraction analysis, and expansibility measurements have been carried out on the samples.

Differential thermal analysis was performed in ceramic crucibles with chromel-alumel thermocouples, the temperature being measured in the sample; the heating rate was 10 ± 1°C/min. and between 0·7 g and 1·0 g of sample was used.

The X-ray diffraction patterns were recorded on films, using cylindrical cameras of 10 cm diameter; the radiations used were filtered CuKα and CoKα. The samples used in the cameras were either flakes or powder. The flakes were cut from the mineral and

'7

gave strongly oriented photographs, only the basal spacing being recorded. For the powder samples, the mineral was ground to pass a 100-mesh B.S. sieve and then introduced into a 0·2 mm cellulose acetate capillary; these gave non-oriented photographs, the basal reflections being supplemented by general reflections.

The expansibility was measured by the change in the apparent density. A known volume was weighed, exfoliated by heating in an electric muffle furnace at 750°C for about ten minutes, and the apparent volume again measured by tipping the loose fragments into a measuring cylinder without compaction. In some instances the volume was also measured by the volume of sand it displaced.

Classification

It was found convenient to divide the commercial vermiculites on the basis of the X-ray flake diagram into three groups—the 26 Å, the 14 Å, and the mixed. In the 26 Å group the flake X-ray diagram, but not always the powder diagram, showed a strong reflection at about 26 Å; the second group gave a strong 14 Å reflection but none at 26 Å, the mixed group showed various reflections and some indications of being partially dehydrated.

26Å Group. Five samples, for which complete X-ray data are given in Table 1, fall into this class. As there are some differences between the samples it was possible to subdivide the group into two—namely, samples C and F, and samples O, E and N. Samples C and F showed in the flake photograph that there was ordering of the basal reflections, the *d* values being reasonably integral and all the reflections being present. The effect of heating a flake of C to 520°C is shown in Table 2; a similar result was obtained with Sample F.

This result is indicative of a mixture of a mica-type layer structure and a dehydrated or partially dehydrated vermiculite. It is therefore suggested that samples C and F are regular 1:1 mixed-layer vermiculite-mica minerals, equivalent to the hydrobiotite of Gruner (1934).

The other three samples of the 26 Å group, O, N and E, gave data similar to those quoted in Table 3 for sample O. From this Table it can be seen that the flake pattern is very similar to that of sample C, but in contrast to C the powder data for sample O are different from those given by a flake, showing a strong reflection at 15 Å as well as at 12·5 Å; the former expands to 24 Å on glycerol treatment. This is typical of a true vermiculite, and it is suggested that

TABLE 1—X-ray flake diffraction data for the 26 Å group.

C*		O*		F*		E*		N*		Indices
d(Å)	I	*d*(Å)	I	*d*(Å)	I	*d*(Å)	I	*d*(Å)	I	
25·5	vs	26·2	vw	24·3	w	24·1	vw	23·8	w	001
12·4	vs	12·1	ms	12·9	vs	12·3	vs	12·5	ms	002
8·2	w			8·1	ms	8·05	vw	7·9	vvw	003
6·15	vvw							6·5	vvw	004
4·92	ms	4·88	s	4·86	s	4·88	vs	4·84	vs	005
4·11	vw									006
3·53	vs	3·47	vs	3·49	vs	3·50	vs	3·51	vs	007
3·09	vs	3·07	m	3·01	m	3·02	ms	3·03	w	008
		2·71	m	2·73	m	2·74	ms	2·74	w	009

*Sample designation.

TABLE 2—X-ray diffraction data for sample C.

Normal flake		Heated to 520 C	
d(Å)	I	*d*(Å)	I
25·5	vs	13·5	w
12·4	vs	12·15	w
8·2	w	9·85	vs
6·15	vvw		
4·92	ms	4·88	vw
4·11	vw	4·54	vvw
3·53	vs	4·06	vw
3·09	vs	3·27	m

the second sub-group is a mixture of hydrobiotite and vermiculite. The mixture occurs within each individual flake but there is no ordered repeating of the layers. Such minerals could represent stages in the interlayer hydration of the basic mica layer structure.

The differential thermal curves of the 26 Å group of commercial vermiculites are reproduced in Fig. 1; they do not show so clearly the division into the two sub-groups. All the curves show large endothermic peaks at about 157°C together with smaller ones at about 270°C, and all show peaks of varying height at about 550°C and 600°C. There is some difference between samples C and F (hydrobiotites) and samples O, N and E (hydrobiotite-vermiculite mixtures), in that the hydrobiotites have the smaller peaks at 820°C. However, the size of this peak is probably influenced by the type of exchangeable ion present and is not characteristic of the structural type (Barshad, 1948; Ernst, Havens and Wilson, 1958). It has been shown by Ernst, Havens and Wilson (1958) that the smallest peak in this region is obtained when K^+ is the exchangeable ion. The samples in the first sub-group contain more mica layers than those in

TABLE 3—X-ray diffraction data for sample O.

Flake		Powder		Glycerol-treated		Heated to 520°C	
d(Å)	I	*d*(Å)	I	*d*(Å)	I	*d*(Å)	I
26·2	vw	15	vs	24	s b		
12·1	m	12·5	s	12·5	s	10·15	vs
4·88	s	4·5	ms	4·9	s	4·96	mw
3·47	vs	3·4	m	3·5	s	3·37	m
3·07	mw	2·75	w	3·02	w		
2·71	mw	2·6	m				

TABLE 4—X-ray flake diffraction data for the 14 Å group.

Indices	AB*		M*		AA*		R*		P409*		P136*	
	d(Å)	I	*d*(Å)	I	*d*(Å)	I	*d*(Å)	I	*d*(Å)	I	*d*(Å)	I
002	14·3	vs	14·4	vs	14·4	vs	14·2	s	14·4	vs	14·3	s
004	7·1	mw	7·2	mw	7·13	mw	7·15	w	7·15	mw	7·15	mw
006	4·74	s	4·78	ms	4·78	m	4·78	s	4·79	s	4·80	s
008	3·56	vs	3·58	s	3·58	vs	3·59	vs	3·59	vs	3·58	vs
00,10	2·85	vs	2·87	vs	2·875	vs	2·87	vs	2·88	vs	2·87	s
00,12	2·38	vw	2·39	vvw	2·40	vvw	2·38	w	2·40	vvw		
00,14	2·04	m	2·05	vvw	2·05	vw			2·06	vw		

*Sample designation.

the second, which is quite consistent with this interpretation since they will have a greater proportion of interlayer K^+.

14 Å Group. The samples in the 14 Å group all give similar X-ray flake diffraction photographs (Table 4), and all except M, are of a similar nature. They will be discussed as one group with reference to sample AB, for which X-ray diffraction data on treatment with glycerol and on heating to 520°C are given in Table 5.

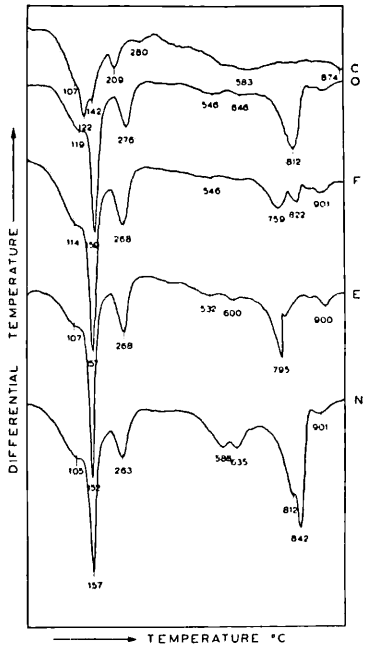

FIG. 1—Differential thermal curves for commercial vermiculites of the 26 Å group.

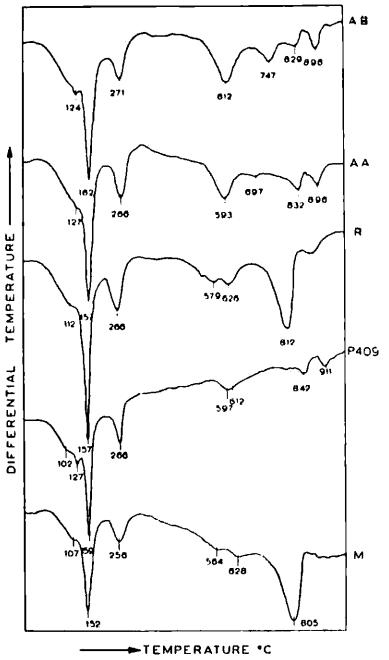

FIG. 2—Differential thermal curves for commercial vermiculites of the 14 Å group.

The results are what would be expected from a true vermiculite, but could also be produced from a vermiculite-chlorite mixed-layer mineral. Walker and Cole (1957) have shown that these two types can be distinguished by their differential thermal curves; the pure vermiculite does not have an endothermic peak at about 600°C, while chlorite-vermiculite mixtures do. From the curves in Fig. 2 it can be seen that samples AB, AA, R and P409 have a peak at about

TABLE 5—X-ray diffraction data for sample AB.

Flake		Glycerol-treated		Heated to 520°C	
d(Å)	I	*d*(Å)	I	*d*(Å)	I
14·3	vs	14·4	vs	9·15	s
7·1	w	7·1	m		
4·74	s	4·79	m	4·61	w
3·56	vs	3·59	vs		
2·85	vs	2·87	s	2·98	m
2·38	vw				
2·04	m				

600°C, sample R having the smallest and sample AA the largest; this indicates that sample R is the nearest to a pure vermiculite found in this investigation. No curve can be given for sample P136 as insufficient material was available.

The mineralogy of sample M is, however, more complicated than that of any of the samples so far discussed; X-ray diffraction data are given in Table 6.

From the flake data it would appear that the sample is similar to the vermiculite or chlorite-vermiculite minerals, but the powder data show an additional spacing at 12·5 Å, which when glycerol-treated expands to 30 Å and 15 Å, the 14 Å spacing remaining unaffected. When a sample is heated to 520°C spacings at 12·7 Å and 10·2 Å are produced in the diffraction pattern, and it is suggested that under these conditions the 14 Å spacing is reduced to 10 Å, while the 12 Å spacing is unaffected. From this it is concluded that the lattice that gives the 14 Å spacing, which is unaffected by glycerol and which is reduced to 10 Å on heating, is of the vermiculite type; while the lattice that gives a 12·5 Å spacing which

TABLE 6—X-ray diffraction data for sample M.

Flake		Powder	Glycerol-treated	Heated to 520°C
d(Å)	I	*d*(Å)	*d*(Å)	*d*(Å)
14·4	vs	14	30	12·7
7·2	mw	12·5	15	10·2
4 78	ms	7·5	14	
3·58	s	4·5	7·0	4·98
2·87	vs	3·55	4·7	
2·39	vvw	2·85	3·55	3·36
2·05			2·85	

TABLE 7—X-ray diffraction data for the mixed group.

A*		B*		AD*		AC*	
d(Å)	I	*d*(Å)	I	*d*(Å)	I	*d*(Å)	I
		15·4	w	25·5	vw	27	vw
9·875	s	9·95	s	15·6	vw	10·5	mw
4·98	mw	4·98	mw	11·0	m	9·4	vw
4·58	vw	4·16	mw	9·2	mw	5·54	vs
4·12	vw	3·33	vs	4·96	mw	4·98	s
3·31	vs			4·15	w	4·11	w
				3·41	vs	3·41	s
				3·24	s	3·25	s

*Sample designation.

expands to 15 Å and 30 Å on glycerol treatment and which is not affected by heat, is thought to be a mixed-layer mineral of montmorillonite and mica.

This makes sample M a mixture of vermiculite and a mixed-layer montmorillonite-mica.

Mixed group. The X-ray diffraction data for the mixed group are given in Table 7. All have spacings at about 10 Å and it is therefore suggested that they are partially dehydrated. None of the specimens were exfoliated when received, but as neither their origin nor their previous history was known, no further discussion of their mineralogy is possible.

EXPANSIBILITY

All the commercial vermiculites reported in this paper expanded and exfoliated, and their volume expansion is given in Table 8.

These data indicate that the minerals with the highest expansibility are C, O, F, E, N, AC, AD and M; all of these except M contain a lattice which gives a 26 Å spacing and are probably hydrobiotites; M is a mixed-layer mineral. Those which gave the lowest expansion

TABLE 8—Volume expansion of some commercial vermiculites.

26 Å group		14 Å group		Mixed group	
Sample	Expansion	Sample	Expansion	Sample	Expansion
C	6·0	M	6·1	A	2·0
O	7·0	AA	3·5	B	2·0
F	6·9	AB	5·5	AC	9·0
E	6·0	R	5·8	AD	6·3
N	7·0	P409	3·4		

were the vermiculite-chlorite mixed-layer minerals and the two mixed group specimens A and B which had probably already been heated.

Conclusions

Of 16 commercial vermiculites examined, which show expansibility ranging from ×2 to ×9, none were true vermiculites; six were mixed-layer vermiculite-chlorite minerals, two were hydrobiotite (mixed-layer vermiculite-mica), three were mixed-layer vermiculite-hydrobiotite minerals, one a mixture of vermiculite and a mixed-layer montmorillonite-mica mineral; four showed signs of dehydration—of these two were probably hydrobiotite, one was a mixed-layer mineral, and one (A) was of unknown structure.

The greatest expansibility is found in those minerals with a hydrobiotite layer structure, the minerals with vermiculite-chlorite layers having the lowest expansion.

Acknowledgment.—This paper describes work that forms part of the programme of the Building Research Board, and is published by permission of the Director of Building Research.

References

Barshad, I., 1948. *Amer. Min.*, **33**, 655.

Ernst, W. S., Havens, I. F., and Wilson, H. H., 1958. *J. Amer. ceram. Soc.*, **41**, 238.

Gruner, J. W., 1934. *Amer. Min.*, **19**, 557.

Walker, G. F., and Cole, W. F., 1957. The Differential Thermal Investigation of Clays (R. C. Mackenzie, editor). Mineralogical Society, London, Chapter 7, p. 191.

REPRINTED FROM *MAGAZINE OF CONCRETE RESEARCH*. VOL. 12, No. 34. MARCH 1960. pp. 19–26.

Hydrothermal reactions in the lime-rich part of the system $CaO\text{-}SiO_2\text{-}H_2O$*

by H. G. Midgley, M.Sc., Ph.D., F.G.S.† and S. K. Chopra, M.Sc.‡

BUILDING RESEARCH STATION: DEPARTMENT OF SCIENTIFIC AND INDUSTRIAL RESEARCH

SUMMARY

The mineralogy of autoclaved products from various forms of calcium silicate and from lime and silica has been investigated. The results are as follows. With a CaO/SiO_2 ratio of 1, the product is always well crystallized tobermorite. With a CaO/SiO_2 ratio of 2, the product varies: starting with lime and silica, dicalcium silicate alpha-hydrate is the first product; this eventually changes into dicalcium silicate beta-hydrate, the stable phase; starting with calcium silicate hydrate I and lime, the first product comprises Flint's CSH(A) and dicalcium silicate alpha-hydrate, and it seems likely that the Flint's CSH(A) will eventually convert to dicalcium silicate alpha-hydrate and the dicalcium silicate alpha-hydrate to dicalcium silicate beta-hydrate; if one starts with β-$2CaO.SiO_2$, the product in the first place is dicalcium silicate gamma-hydrate; in the length of processing used in the experiments reported in this paper, no other phase was found, but it is considered that dicalcium silicate gamma-hydrate is only metastable.

With a CaO/SiO_2 ratio of 3, again the products vary with the starting minerals: with mixes of lime and silica and with mixes of $2CaO.SiO_2$ and lime, the first product is dicalcium silicate alpha-hydrate which is eventually converted to the beta-hydrate; with mixes of calcium silicate hydrate (I) and lime, the product is always Flint's CSH(A) with or without some dicalcium silicate alpha-hydrate; with $3CaO.SiO_2$ as the starting material, the product is always $3CaO.SiO_2.1\frac{1}{2}H_2O$.

It is clear from this work that the form of the starting material has a considerable influence on the nature of the metastable phases produced, and also that, in this part of the system $CaO\text{-}SiO_2\text{-}H_2O$, even prolonged processing up to 90 days is insufficient to produce true equilibrium phases.

Introduction

Although the hydrothermal reactions in general in the system $CaO\text{-}SiO_2\text{-}H_2O$ have been the subject of many investigations in the past[1], of late considerable interest has been shown in the lime-rich part of the system[2-5] because of its usefulness in understanding the hydration of cement compounds[6] and its technical importance in the manufacture of autoclaved products.

Recent work by Kalousek and his co-workers[2] has shown how the type of silica, conditions of mixing, temperature and time of processing, etc., influence the synthesis of dicalcium silicate alpha-, beta- and gamma-hydrates, and that no definite conditions could be established for the preparation of dicalcium silicate beta-hydrate. The latter observation is significant in view of the fact that Peppler[3] and Assarson[4] have reported the formation of only one type of dicalcium silicate hydrate, hillebrandite (dicalcium silicate beta-hydrate), which is thought by these authors to be the only stable phase. Buckle, Gard and Taylor[5] in their investigations of the hydration of anhydrous $3CaO.SiO_2$ have found that the only phase produced is $3CaO.SiO_2.1\frac{1}{2}H_2O$.

In view of the different products found by previous authors resulting from the hydration of $3CaO.SiO_2$ and β-$2CaO.SiO_2$[7] under hydrothermal conditions, it seems necessary to examine the influence of the starting materials on the products formed at 150 and 180°C, and the present paper describes the results of a study in this direction.

†Building Research Station, D.S.I.R.

‡Central Building Research Institute, Roorkee, U.P., India.

TABLE 1: **Chemical analysis of raw materials (by F. J. McConnell, L. J. Larner and R. S. Gillett).**

Material	Constituents (%)												
	SiO_2	Fe_2O_3	Al_2O_3	CaO	MgO	MnO	Na_2O	K_2O	SO_3	P_2O_5	Cl	Loss at 110°C	Loss at 1,000°C
Calcium carbonate	0·01	0·01	—	55·96	0·05	nil	0·01	0·01	0·01	0·005	nil	0·06	43·88
Silica gel	97·18	0·02	0·02	—	—	—	nil	nil	nil	nil	nil	1·10	1·34
Calcium silicate hydrate I	38·12	0·04	0·16	34·24	—	—	0·21	0·01	—	—	—	—	26·76

Experimental details

The starting materials were either pure oxides, anhydrous calcium silicates, or calcium silicate hydrate I. The pure samples of silica and lime used were respectively a highly amorphous silica gel with no free alkalis present, and calcium oxide made by igniting a pure sample of calcium carbonate at 1,000°C for 4–5 hours (Table 1). The calcium silicate hydrate I was prepared by double decomposition or by shaking silica gel with lime solution.[8] Double decomposition of calcium nitrate with sodium silicate was preferred because of the relative ease and rapidity of preparation. After a few trials had been made, the following procedure was adopted: 1·80 g of pure silica gel was dissolved in NaOH solution (2·4 g in 100 ml water); to this was added 250 ml of $Ca(NO_3)_2$ solution containing 14·76 g $Ca(NO_3)_2$; a thick precipitate formed and was filtered through a Buchner funnel, and then washed with 4 l. of lime solution, followed by 50% acetone, 100% acetone and finally dry ether. The sample of hydrate was dried to a constant weight without exposing it to the atmosphere. Relevant data are given in Table 1. The anhydrous calcium silicates used were pure tricalcium silicate and beta dicalcium silicate made by heating together appropriate mixes of oxides.[9]

The hydrothermal reactions were carried out in steel bombs[10] with silver liners, or in stainless steel bombs, of 8 ml capacity, placed in an electrically heated oven thermostatically controlled to ±2°C. The methods of preparing and processing mixes were as described by Heller and Taylor[10]: the dry powder was mixed by shaking, then a small quantity of water was added to form a paste, which was placed in the bomb, where more water was added to cover the paste. The processed solids were washed first with acetone and then with ether and afterwards dried to a constant weight over fused calcium chloride.

The temperatures of processing in this study, 150 and 180°C, were chosen because these are commonly employed in the manufacture of autoclaved products. The periods of processing were selected on the basis of previously reported findings in the literature and modified in the light of the results from the present study.

The phases present in the reaction products were identified with the help of powder X-ray diffraction analysis using a 10 cm powder camera with cobalt K alpha radiation and by differential thermal analysis. The thermograms were obtained on an apparatus which heated a sample of about 0·7 g in a ceramic crucible at 10°C/min from room temperature to 1,000°C; the temperature, measured in the sample, and the differential temperature between the sample and an inert material heated at the same rate, were measured with chromel-alumel thermocouples. The resulting thermograms represent a plot of time against difference in temperature between a decomposing sample and a sample which is inert; thus, for example, the heat needed to drive off the bound water will be represented by a valley, or endothermic peak, on the thermogram whilst, conversely, the heat given off by the heat of reaction of a chemical change will be represented by an upward peak, or exothermic peak.

The hydrated phases encountered during this investigation were tobermorite, Flint's CSH(A), dicalcium silicate alpha-, beta- and gamma-hydrates and tricalcium silicate hydrate. The X-ray powder diffraction data obtained for these compounds agree well with the data given by Heller and Taylor[11] and Midgley[12].

The differential thermograms for some of the calcium silicate hydrates are given in Figure 1. The peak at 490°C in the curve for CSH(A) is due to $Ca(OH)_2$ known to be present as impurity. An exothermic peak occurs at 825°C in both tobermorite and Flint's CSH(A) and so cannot be used for diagnostic purposes. Dicalcium silicate gamma-hydrate has only one minor endothermic peak at just below 700°C. Dicalcium silicate alpha- and beta-hydrates give good endothermic peaks at 500 and 600°C respectively. Tricalcium silicate hydrate has one prominent peak at about 565°C.

Results and discussion

REACTIONS AT 150°C

Starting materials: lime and silica

The crystalline solid phases formed as a result of the hydrothermal reactions between lime and silica are reported in Table 2.

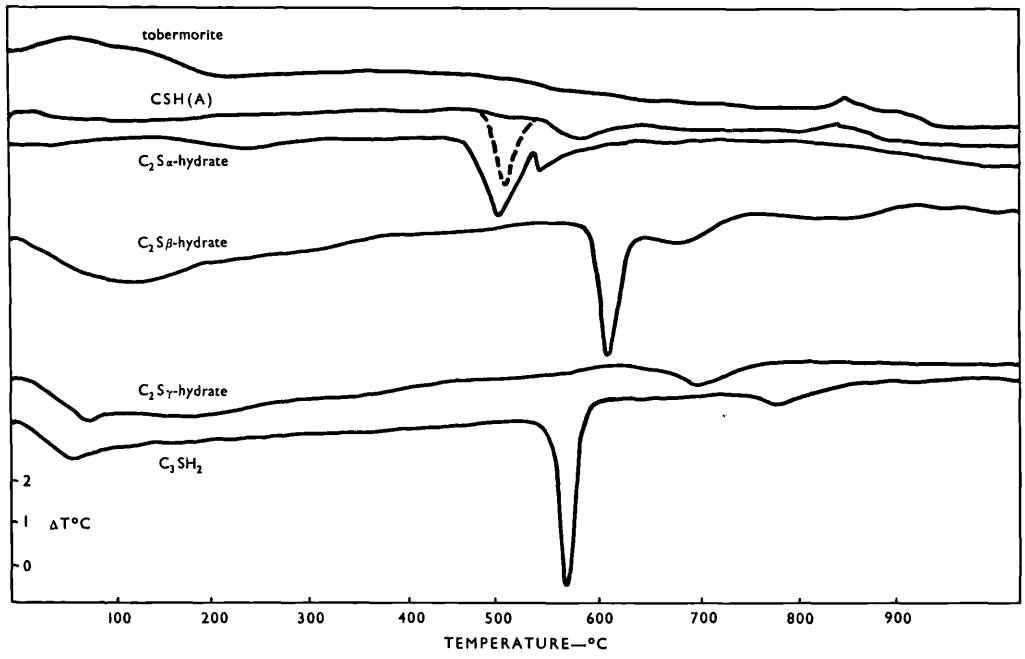

Figure 1: Differential thermograms of various calcium silicate hydrates. (Each sample 0·1 g, diluted with 0·4 g αAl_2O_3 heated in ceramic crucible at 10°C/min.)

These results show that dicalcium silicate alpha-hydrate is the predominant phase present in all the preparations with molar ratios ranging from 2·0 to 3·5, irrespective of the period of processing. When the CaO/SiO_2 ratio was 2 and the period of autoclaving 14 or 30 days, pure dicalcium silicate alpha-hydrate was produced. With longer periods of autoclaving, the dicalcium silicate alpha-hydrate was found to be contaminated with dicalcium silicate beta-hydrate. Mixes with a CaO/SiO_2 ratio of 2·5, processed for 14 days, contained almost pure dicalcium silicate alpha-hydrate and a small amount of unreacted calcium hydroxide, showing that the amount of lime was slightly more than is required for the formation of dicalcium silicate alpha-hydrate. More dicalcium silicate beta-hydrate was formed as the processing period increased. Tricalcium silicate hydrate was not found in any of the mixes with a CaO/SiO_2 ratio of 3·5, irrespective of the time of processing. Table 3 gives the X-ray data for representative preparations of this series at 150°C. The diffraction data for dicalcium silicate alpha-hydrate (columns 1 and 2) agree very well with the data published earlier[12]. When a mix with a CaO/SiO_2 ratio of 2 was processed for 60 days, the X-ray data revealed the appearance of a line at 2·92 Å with medium intensity, and a change in the intensities of the lines at 2·80 and 2·35 Å, indicating that a small quantity of dicalcium silicate beta-hydrate was also present.

Thermograms of a series of mixes with a CaO/SiO_2 ratio of 2 autoclaved at 150°C are given in Figure 2. The curve for the mix autoclaved for 14 days shows endothermic peaks at 471 and 513°C and an exothermic peak at 834°C; the second endothermic cannot be considered as being due to $Ca(OH)_2$ since the peak temperature is higher in relation to the peak area for pure $Ca(OH)_2$ and no unreacted $Ca(OH)_2$ was found by chemical methods. The thermogram of the mix autoclaved for 30 days shows the first endothermic peak resolved into two, at 452 and 466°C; that at 452°C may be due to a small amount of $Ca(OH)_2$, but the temperature is rather lower than would normally be expected. The third thermogram shows only a peak at 460°C due to the dicalcium silicate alpha-hydrate.

TABLE 2: **Hydrothermal reactions of mixes of lime and silica gel autoclaved for various periods at 150°C.**

Preparation No.	Initial molar ratio CaO/SiO_2	Time of processing (days)	Phases identified*
SKC 44	2·0	14	α
SKC 40		30	α
SKC 57		60	α + β (little)
SKC 45	2·5	14	α + CH (little)
SKC 36		30	α + β (trace) + CH (little)
SKC 33		60	α + β (trace) + CH (little)
SKC 46	3·0	14	α + CH (moderate)
SKC 37		30	α + β (little) + CH (moderate)
SKC 34		60	α + β (little) + CH (moderate)
SKC 47	3·5	14	α + CH (moderate)
SKC 38		30	α + β (little) + CH (moderate)
SKC 35		60	α + β (little) + CH (moderate)

*α = dicalcium silicate alpha-hydrate, β = dicalcium silicate beta-hydrate, CH = $Ca(OH)_2$.

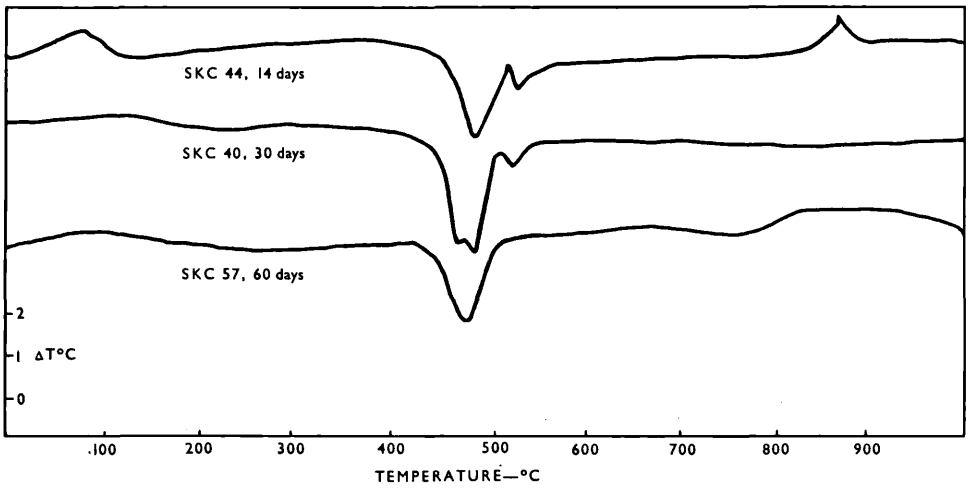

Figure 2: Differential thermograms of lime-silica mixes (CaO/SiO_2 = 2) autoclaved at 150°C. (Each sample 0·1 g, diluted with 0·4 g αAl_2O_3, heated in ceramic crucible at 10°C/min.)

Starting materials: calcium silicate hydrate I and lime

The crystalline solid phases produced by hydrothermal reactions between calcium silicate hydrate I and lime at 150°C are given in Table 4.

The phases produced at the lower lime-silica ratios (gyrolite and phase Z[4] of Assarsson at CaO/SiO_2 = 0·61 and tobermorite, afwillite and Flint's CSH(A)[11] at CaO/SiO_2 = 1·42) are those which would be expected from the results of earlier workers. At the higher CaO/SiO_2 ratios, the main phase is dicalcium silicate alpha-hydrate, but it should be noted that an additional phase is that known as Flint's CSH(A). These latter results should be compared with those where the starting materials were lime and silica (Tables 2 and 4).

Starting material: $3CaO.SiO_2$

Only one experiment on autoclaving $3CaO.SiO_2$ at 150°C has been carried out. The results show that at 30 days the products are $3CaO.SiO_2.1\frac{1}{2}H_2O$, dicalcium silicate alpha-hydrate and $Ca(OH)_2$.

REACTIONS AT 180°C

Starting materials: lime and silica

The crystalline phases formed as a result of hydrothermal reaction between lime and silica gel are given in Table 5. These results show that when the period of processing is 14 days, it is dicalcium silicate alpha-hydrate which is formed, irrespective of the CaO/SiO_2 ratio; from this it follows that the reactions at 180°C are no different from those at 150°C up to 14 days of processing. After that period, dicalcium silicate alpha-hydrate begins to change into the beta-hydrate. In the case of a mix with a CaO/SiO_2 ratio of 2, it took 90 days of processing for the complete change to the beta-hydrate. When the phases present after 30 and 60 days of processing are compared with those formed at 150°C, it is seen that dicalcium silicate beta-hydrate is the predominant phase and not the alpha-hydrate. After long periods of autoclaving (90 days), the residual dicalcium silicate alpha-hydrate is present only in traces. As at 150°C, in none of the mixes was tricalcium silicate hydrate identified.

The relevant X-ray data are given in Table 6 and clearly show how the dicalcium silicate alpha-hydrate pattern changed during processing until at 90 days a pure dicalcium silicate beta-hydrate pattern is obtained. For the sake of comparison, X-ray data for a natural sample of hillebrandite are given in the last column.

The differential thermograms for the mixes with CaO/SiO_2 ratio = 2, processed at 180°C, are given in Figure 3. The first curve, SKC 54, is of dicalcium silicate alpha-hydrate and the last curve, SKC 20, is of a mixture of dicalcium silicate alpha- and beta-hydrates. The peak at about 500°C is due to the alpha-hydrate and that at 550°C to the beta-hydrate. The rate of production of the beta form from the alpha can be seen clearly.

Starting materials: calcium silicate hydrate I and lime

The crystalline phases produced when mixes of calcium silicate hydrate I and lime were autoclaved at 180°C are given in Table 7.

The mineralogy of the products formed by the hydrothermal treatment of CSH(I) and lime mixes may be summarized as follows: when the CaO/SiO_2

TABLE 3: **X-ray powder diffraction data for some of the mixes of lime and silica after autoclaving for various periods at 150°C.**

$CaO/SiO_2 = 2$ 14 days		$CaO/SiO_2 = 2$ 30 days		$CaO/SiO_2 = 2$ 60 days		$CaO/SiO_2 = 2{\cdot}5$ 30 days	
d(Å)	I/I_o*	d(Å)	I/I_o	d(Å)	I/I_o	d(Å)	I/I_o
5·33	vvw	5·32	vvw	5·32	vvw	5·32	vvw
4·910	vvw					4·90	vvw
4·64	vvw	4·62	vvw				
4·22	s	4·22	s	4·22	s	4·22	s
3·92	m	3·92	m	3·92	m	3·90	ms
3·53	m	3·53	m	3·53	m	3·53	s
3·27	vs	3·27	vs	3·27	vs	3·26	vs
		3·105	vvw			3·11	vvw
3·045	vs	3·01	vvw			3·03	vvw
				2·95	m	2·94	s
2·87	m	2·87	m	2·875	m	2·87	ms
2·80	m	2·80	m	2·80	m	2·81	m
						2·76	vw
2·70	vvw	2·70	vvw	2·70	w	2·74	vw
2·66	w	2·66	w	2·65	w	2·66	vw
2·60	ms	2·60	ms	2·60	ms	2·61	ms
2·57	w	2·57	w	2·56	vw	2·57	m
2·53	w	2·53	w	2·53	w	2·53	vvw
2·497	vvw	2·497	vvw	2·495	vvw		
2·469	vvw	2·469	vvw	2·46	vvw		
2·41	s	2·41	s	2·41	s	2·41	s
2·34	vvw	2·34	vvw	2·35	w†	2·32	vw
2·31	vw	2·31	vw				
2·24	vw	2·24	vw	2·23	vw	2·23	vvw
2·16	vw	2·16	vw	2·15	vw		
2·106	vw	2·106	vw	2·10	vvw	2·10	vw
2·082	vw	2·082	vw	2·06	vvw	2·07	vw
2·059	w	2·059	w			2·05	w
2·029	vw	2·029	vw	2·025	vw		
1·984	vvw	1·984	vvw				
1·956	vw	1·956	vw	1·95	vvw	1·96	mw
1·927	w	1·927	w	1·925	vw	1·925	mw
1·892	vw	1·892	vw	1·89	vw		
1·87	vvw	1·87	vvw			1·87	w
1·846	vw	1·846	vw	1·83	vw	1·83	w
						1·815	w
1·788	s	1·788	s	1·788	s	1·785	m
1·735	w	1·735	w	1·735	vvw		
1·711	w	1·711	w	1·705	vvw		
1·693	vvw	1·693	vvw				

*The intensity scale used throughout the X-ray data is an arbitrary one :

vvs = very, very strong
vs = very strong
s = strong
ms = moderately strong
m = medium
w = weak
vw = very weak
vvw = very, very weak

†Fuzzy

TABLE 4: **Hydrothermal reactions of mixes of calcium silicate hydrate I and lime autoclaved for 30 days at 150°C.**

Preparation No.	Raw materials*	Initial molar ratio CaO/SiO_2	Phases identified†
SKC 14	2 mol. CSH(I) +1 mol. SiO_2	0·61	gyrolite, phase Z[4]
SKC 15	1 mol. CSH(I)	0·92	tobermorite
SKC 16	1 mol. CSH(I) +½ mol. CaO	1·42	tobermorite, afwillite, CSH(A)
SKC 17	1 mol. CSH(I) +1 mol. CaO	1·92	C_2S alpha-hydrate, calcium hydroxide, CSH(A)
SKC 18	1 mol. CSH(I) +2 mol. CaO	2·92	C_2S alpha-hydrate, calcium hydroxide, CSH(A)

*CSH(I) = calcium silicate hydrate I.
†C_2S = dicalcium silicate.

TABLE 5: **Hydrothermal reactions of mixes of lime and silica gel autoclaved for various periods at 180°C.**

Preparation No.	Initial molar ratio CaO/SiO_2	Time of processing (days)	Phases identified*
SKC 54	2·0	14	α
SKC 39		30	α + β (moderate)
SKC 24		60	α + β (moderate) + CH (?)
SKC 20		90	β + α (trace)
SKC 48	2·5	14	α + CH (little)
SKC 29		30	β + α (little) + CH (little)
SKC 25		60	β + α (little) + CH (little)
SKC 21		90	β + α (trace)
SKC 55	3·0	14	α + CH (moderate)
SKC 30		30	β + α (little) + CH (moderate)
SKC 26A		60	β + α (little) + CH (moderate)
SKC 22		90	β + α (trace) + CH (moderate)
SKC 49	3·5	14	α + CH (moderate)
SKC 31		30	β + α (little) + CH (moderate)
SKC 27A		60	α + CH (moderate)
SKC 23		90	β + α (trace) + CH (moderate)

*α = dicalcium silicate alpha-hydrate; β = dicalcium silicate beta-hydrate; CH = calcium hydroxide.

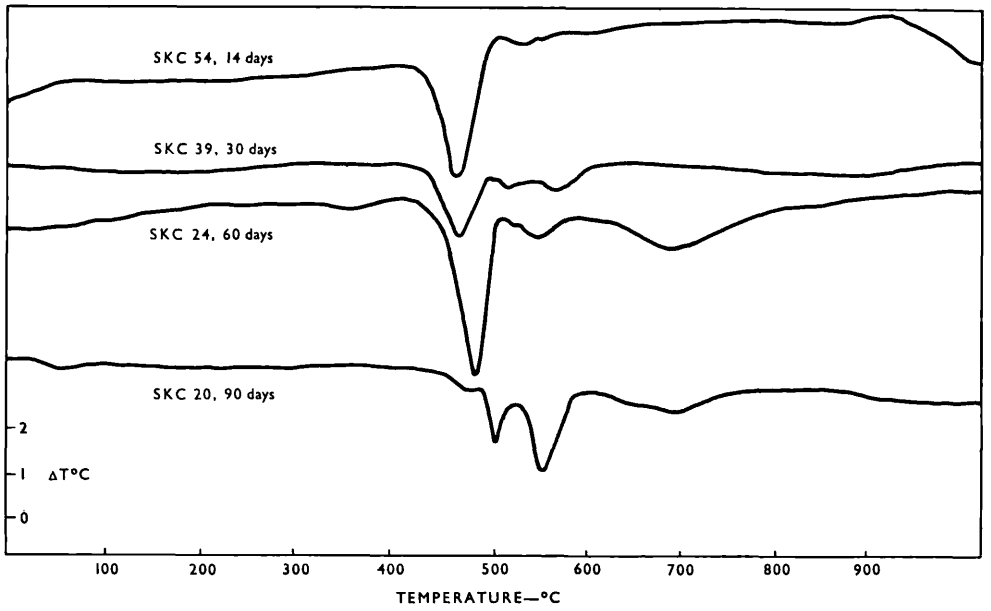

Figure 3: Differential thermograms of lime-silica mixes ($CaO/SiO_2 = 2$) autoclaved at 180°C. (Each sample 0·1 g, diluted with 0·4 g αAl_2O_3, heated in ceramic crucible at 10°C/min.)

ratio is 1, the product is tobermorite; when the CaO/SiO_2 ratio is 2 or greater, the product is firstly Flint's CSH(A) and then dicalcium silicate alpha-hydrate.

Starting material: $3CaO.SiO_2$

The phases produced when pure $3CaO.SiO_2$ was autoclaved at 180°C are given in Table 8.

The relevant X-ray powder data are given in Table 9; the agreement with the data for $3CaO.SiO_2.1\frac{1}{2}H_2O$ given by Buckle, Gard and Taylor[5] is good.

It can be seen from these results that, with pure tricalcium silicate as the starting material, even after autoclaving for 90 days at 180°C, the product is $3CaO.SiO_2.1\frac{1}{2}H_2O$.

Starting materials: beta dicalcium silicate and lime

The crystalline phases produced by hydrothermal treatment of beta dicalcium silicate and lime mixes at 180°C are given in Table 10.

The relevant X-ray powder data are given in Table 11; it will be noted that autoclaving pure beta dicalcium silicate gives dicalcium silicate gamma-hydrate, whilst autoclaving with added lime produces the alpha-hydrate.

Conclusions

The mineralogy of the products of autoclaving various forms of calcium silicate and lime and of silica and lime may be summarized in the following way.

(1) With a CaO/SiO_2 ratio of 1, the product is always well crystallized tobermorite (Tables 4 and 7, and Heller and Taylor[10]).

(2) With a CaO/SiO_2 ratio of 2, the product varies. Starting with lime and silica, the product is dicalcium silicate alpha-hydrate, which will eventually convert to the stable form dicalcium silicate beta-hydrate; starting with calcium silicate hydrate I and lime, the first product is a mixture of Flint's CSH(A) and dicalcium silicate alpha-hydrate, and it seems likely that the CSH(A) will eventually convert to dicalcium silicate alpha-hydrate and the alpha- to the beta-hydrate. When the starting material is $2CaO.SiO_2$, the product is dicalcium silicate gamma-hydrate; in the length of time of the experiments reported here no other phase has been formed.

(3) With a CaO/SiO_2 ratio of 3, the final products vary according to the starting materials. With mixes of lime and silica, the first product is dicalcium silicate alpha-hydrate, which is converted to beta-hydrate; with mixes of ß-$2CaO.SiO_2$ and lime, the product is dicalcium silicate alpha-hydrate; with mixes of calcium silicate hydrate I and lime, the product is Flint's CSH(A) and dicalcium silicate alpha-hydrate; with $3CaO.SiO_2$ as the starting material, the product is always $3CaO.SiO_2.1\frac{1}{2}H_2O$.

It is clear from this work that the form of the starting material has a considerable influence on the nature of the metastable phases produced and also that, in this part of the system $CaO\text{-}SiO_2\text{-}H_2O$, even prolonged processing up to 90 days is insufficient to produce true equilibrium phases.

ACKNOWLEDGEMENTS

The authors would like to thank their colleagues Mr D. Rosaman, Mr J. J. Smith and Dr E. Aruja for

TABLE 6: **X-ray powder diffraction data for some of the mixes of lime and silica autoclaved at 180°C.**

$CaO/SiO_2 = 2$ 14 days, 180°C		$CaO/SiO_2 = 2$ 30 days, 180°C		$CaO/SiO_2 = 2$ 90 days, 180°C		Hillebrandite*	
d(Å)	I/I_o	*d*(Å)	I/I_o	*d*(Å)	I/I_o	*d*(Å)	I/I_o
		8·50	w	8·232	vw	8·245	vw
		6·75	vvw	6·86	vvw	6·712	vvw
		5·90	vw	5·89	vw	6·079	vvw
5·33	w	5·30	w			5·93	vw
		4·96	vvw			4·96	vvw
		4·76	w	4·79	ms	4·80	vs
4·62	w						
4·22	vs	4·22	s			4·303	vvw
				4·18	vvw		
3·89	ms	3·90	mw	3·887	vvw	4·078	w
3·54	ms	3·52	m	3·54	vvw	3·558	w
						3·411	vvw
				3·36	m	3·36	ms
						3·29	vvw
3·27	vs	3·27	vs	3·26	w	3·24	vvw
3·095	vw						
3·01	vw	3·025	w	3·048	mw	3·04	ms
						3·037	ms
						2·96	mw
		2·94	vs	2·94	vvs	2·94	vvs
2·87	s	2·87	ms				
2·80	s	2·80	ms			2·836	w
				2·82	w		
						2·784	w
		2·765	vvw	2·765	vw	2·761	vw
						2·723	s
2·695	vw	2·695	w	2·68	vw	2·696	vw
2·65	m	2·65	mw	2·664	vw	2·649	vw
						2·629	vw
2·60	ms	2·595	m			2·609	vvw
						2·581	vvw
2·56	w	2·565	w				
2·55	vvw						
2·495	vvw	2·525	vvw				
				2·508	vvw	2·478	vw
2·46	vvw	2·46	vvw				
2·41	vs	2·41	s			2·396	m
				2·38	m	2·83	ms
2·30	vw	2·30	ms			2·273	ms
				2·25	m	2·25	ms
2·23	w	2·23	m			2·22	w
						2·19	vvw
2·16	w	2·15	w	2·157	vvw	2·16	vvw
						2·139	vvw
2·10	vw	2·10	vw			2·119	vvw
						2·094	vvw
2·07	w	2·075	w	2·068	w	2·070	ms
2·05	mw	2·055	w			2·055	vvw
2·025	w	2·025	w	2·025	w	2·03	vvw
						2·00	vvw
1·98	vw			1·952	w	1·974	ms
1·95	vw	1·95	vw			1·939	w
1·925	m	1·92	mw			1·929	vvw
						1·919	vvw
1·885	w	1·885	w			1·880	w
1·84	vw	1·845	vw	1·873	vw	1·865	vvw
		1·82	mw	1·82	ms	1·824	s
1·785	s	1·785	s				
				1·757	vw	1·760	vw
1·73	w						

*New data, present paper.

TABLE 7: **Hydrothermal reactions of mixes of calcium silicate hydrate I and lime autoclaved for various periods at 180°C.**

Preparation No.	Initial molar ratio CaO/SiO_2	Autoclaving period (days)	Phases identified*
SKC 10	0·92	14	tobermorite
SKC 11	1·92	14	Flint's CSH(A) + CH
SKC 12	2·92	14	Flint's CSH(A) + CH
SKC 63	2·92	30	Flint's CSH(A) + CH
SKC 64	2·92	90	Flint's CSH(A) + α + CH

*α = dicalcium silicate alpha-hydrate; CH = calcium hydroxide.

TABLE 8: **Hydrothermal reactions of pure tricalcium silicate autoclaved for various periods at 180°C.**

Preparation No.	Initial molar ratio CaO/SiO_2	Time of processing (days)	Phases identified
SKC 60		14	$3CaO.SiO_2.1\frac{1}{2}H_2O$
SKC 61	3·0	30	$3CaO.SiO_2.1\frac{1}{2}H_2O$
SKC 62		90	$3CaO.SiO_2.1\frac{1}{2}H_2O$

TABLE 9: **X-ray powder diffraction data for pure tricalcium silicate autoclaved at 180°C, with data given by Buckle. Gard and Taylor[5] for tricalcium silicate hydrate.**

Period of autoclaving				$3CaO.SiO_2.1\frac{1}{2}H_2O$[5]	
30 days		90 days			
d(Å)	I/I_o	*d*(Å)	I/I_o	*d*(Å)	I/I_o
8·7	vs	8·7	vs	8·6	vs
5·01	w	5·0	m	5·01	ms
4·25	w			4·24	w
3·41	w	3·42	w	3·78	m
3·27	s	3·27	s	3·28	s
2·90	s	2·99	s	3·03	s
3·60	s	2·93	s	2·89	s
2·82	s	2·81	s	2·82	s
2·47	m	2·46	ms	2·49	w
2·42	w	2·40	w	2·44	ms
		2·27	w		
2·17	w	2·16	w	2·16	mw
2·08	m	2·07	m	2·08	s
2·03	w	2·02	w		
1·99	w	1·98	w	1·986	m
1·870	m	1·867	m	1·870	s

TABLE 10: **Hydrothermal reactions of mixes of beta dicalcium silicate and lime autoclaved for various periods at 180°C.**

Preparation	Initial molar ratio CaO/SiO_2	Period of treatment (days)	Phases identified*
SKC 65	2·0	14	γ
SKC 66		30	γ
SKC 67	3·0	14	α + CH
SKC 68		30	α + CH

*γ = dicalcium silicate gamma-hydrate; α = dicalcium silicate alpha-hydrate; CH = $Ca(OH)_2$.

TABLE 11: **X-ray powder diffraction data for mixes of beta dicalcium silicate and lime autoclaved for 14 days at 180°C.**

$CaO/SiO_2 = 2$		$CaO/SiO_2 = 3$	
d(Å)	I/I_o	*d*(Å)	I/I_o
3·80	w	5·30	mw
3·62	w	4·89	m
3·55	w	4·60	vw
3·34	w	4·26	m
3·18	w	3·90	mw
3·02	vs	3·52	mw
2·91	w	3·24	vs
2·83	m	3·10	vw
2·76	w	3·02	vw
2·68	m	2·87	m
2·56	w	2·80	m
2·53	m	2·77	vw
2·47	m	2·70	w
2·33	w	2·65	mw
2·27	w	2·62	mw
2·22	w	2·60	mw
2·15	w	2·56	vw
1·91	m	2·52	m
1·89	m	2·46	vw
1·80	m	2·41	s
		2·30	vw
etc.		etc.	

their help during this investigation, which was carried out at the Building Research Station, Watford, where one of them (S.K.C.) was visiting as a British Council Fellow. The work formed part of the programme of the Building Research Board and is published by permission of the Director of Building Research.

REFERENCES

1. TAYLOR, H. F. W. and BESSEY, G. E. A review of hydrothermal reactions in the system $CaO-SiO_2-H_2O$. *Magazine of Concrete Research*. Vol. 2, No. 4. July 1950. pp. 15–26.
2. KALOUSEK, G. L., LOGINDICE, J. S. and DODSON, V. H. Studies on the lime-rich crystalline solid phases in the system lime-silica-water. *Journal of the American Ceramic Society*. Vol. 37, No. 1. January 1954. pp. 7–13.
3. PEPPLER, R. B. The system of lime, silica and water at 180°C. *Journal of Research of the National Bureau of Standards*. Vol. 54, No. 4. April 1955. pp. 205–211.
4. ASSARSSON, G. O. Hydrothermal reactions between calcium hydroxide and amorphous silica; the reactions between 180° and 220°. *Journal of Physical Chemistry*. Vol. 61. 1957. p. 473.
5. BUCKLE, E. R., GARD, J. A. and TAYLOR, H. F. W. Tricalcium silicate hydrate. *Journal of the Chemical Society*. April 1958. pp. 1351–1355.
6. THORVALDSON, T. Portland cement and hydrothermal reactions. *Proceedings of the Symposium on the Chemistry of Cements, 1938*. Stockholm, Ingeniörsvetenskapsakademien, 1939. pp. 246–267.
7. HELLER, L. and TAYLOR, H. F. W. Hydrated calcium silicates. Part IV, Hydrothermal reactions: lime/silica ratios 2:1 and 3:1. *Journal of the Chemical Society*. July 1952. pp. 2535–2541.
8. TAYLOR, H. F. W. Hydrated calcium silicate. Part I, compound formation at ordinary temperatures. *Journal of the Chemical Society*. December 1950. pp. 3682–3690.
9. NURSE, R. W. Technique of silicate chemistry at high temperatures. *Chemistry and Industry*. 8th April 1950. pp. 263–267.
10. HELLER, L. and TAYLOR, H. F. W. Hydrated calcium silicates. Part II, hydrothermal reactions: lime/silica ratio 1:1. *Journal of the Chemical Society*. September 1951. pp. 2397–2401.
11. HELLER, L. and TAYLOR, H. F. W. *Crystallographic data for the calcium silicates*. 1st edition. London, H.M.S.O., 1956. pp. vi, 79.
12. MIDGLEY, H. G. A compilation of X-ray powder diffraction data of cement materials. *Magazine of Concrete Research*. Vol. 9, No. 25. March 1957. pp. 17–24.

Contributions discussing the above paper should be in the hands of the Editor not later than 30th June 1960.

Printed by the Cement and Concrete Association
52 Grosvenor Gardens, London S.W.1

REPRINTED FROM *MAGAZINE OF CONCRETE RESEARCH*. VOL. 12, No. 35. JULY 1960. pp. 73–82.

Hydrothermal reactions between lime and aggregate fines*

by H. G. Midgley, M.Sc., Ph D., F.G.S † and S. K. Chopra, M.Sc.‡

BUILDING RESEARCH STATION: DEPARTMENT OF SCIENTIFIC AND INDUSTRIAL RESEARCH

SUMMARY

Hydrothermal reactions between lime and aggregate such as pulverized fuel ash, expanded colliery shale, ground quartz, granulated and foamed blastfurnace slag have been studied. The compressive strength and mineralogy have been determined for various mixtures of lime and aggregate fines autoclaved at 160 lb/in² for 2, 6, 16 and 48 hours. The cementitious minerals identified were: tobermorite (calcium silicate hydrate) and a hydrogarnet when the aggregate was pulverized fuel ash or shale; tobermorite and zonotlite when it was quartz; and poorly crystalline tobermorite (tobermorite gel), dicalcium silicate alpha-hydrate and a hydrogarnet when the aggregate was slag glass.

When dicalcium silicate alpha-hydrate was the predominant phase, the strength of the blocks was lower than when tobermorite was the main phase.

Introduction

Although a great deal is known about the hydration of cement during high-pressure steam curing of concrete[1-3], comparatively little is known of the products formed by the interaction of lime (either added as such or set free by the setting of cement) and siliceous aggregate fines, although it is known that such reactions influence the quality of the autoclaved products[4]. Such a study is also of interest in the manufacture of aerated concrete and sand-lime bricks.

The experiments reported in this paper have been concerned with the autoclaving of varying proportions of lime and fine aggregates, determining the compressive strength of the products and attempting to correlate this with the mineralogical nature of the hydrated phases.

Experimental procedures

Five different aggregates were selected: unprocessed pulverized fuel ash, expanded colliery shale, ground quartz sand, granulated slag and foamed slag. The chemical and mineralogical analyses of these aggregates and the lime used are presented as Table 1. Representative samples of the aggregate, with the exception of the quartz, were ground to pass a B.S. No. 200 sieve, enough material being prepared at one time for the whole investigation. The ground quartz sand aggregate was treated differently, only 47% being ground to pass the B.S. No. 200 sieve. Four different dry mixes of hydrated lime and of each of the aggregate fines were prepared, in the proportions 10:90, 20:80, 30:70, 40:60 by weight of lime to aggregate. To distinguish each mix the lime:aggregate ratio will be used; for example, a mix consisting of 30% by weight of lime to 70% by weight of aggregate will be described as mix 30:70.

Cylindrical specimens of 1·5 in. diameter by 2 in. in height were moulded at a pressure of 2 tons/in² after the requisite amount of moulding moisture had been added. The amount of water was determined by trial as the largest quantity which did not cause cracking of the specimen after autoclaving. For all the mixes except quartz it was 12% by weight of total solids; for the quartz mixes it varied, being 5% for mixes 10:90 and 20:80 and 6% for mixes 30:70 and 40:60. Specimens were processed for 2, 6, 16 and 48 h in an autoclave at a steam pressure of 160 lb/in², these periods being chosen so that a study of the rate of reaction between lime and the aggregate could be made. At the conclusion of each autoclaving period, the specimens were removed and placed in a desiccator to cool and

†Building Research Station, D.S.I.R.

‡Building Research Institute, Roorkee, U.P., India.

TABLE 1: **Chemical analysis of constituents** ***(by L. J. Larner and R. S. Gillett)***

Sample	Particulars	Constituents (%)									Mineralogical composition (by X-rays)
		SiO_2	Fe_2O_3	TiO_2	Al_2O_3	CaO.	Na_2O	K_2O	Loss at 1,000°C	SO_3	
Pulverized fuel ash	Croydon	42·90	7·90	1·20	26·70	4·10	1·20	2·92	10·12	—	carbon, glass, mullite, quartz
Sintered colliery shale		53·30	9·20	0·97	25·10	0·75	0·45	4·40	4·54	—	carbon, glass, mullite, quartz
Quartz	Pure quartz sand	98·40	—	—	—	trace	trace	trace	0·48	—	quartz
Granulated blastfurnace slag	B 319	33·75	0·51 (as FeO)	0·50	15·84	41·50	—	—	—	0·02	glass, gehlenite
Foamed blastfurnace slag	Staveley	32·30	0·80	0·58	19·40	39·70	0·42	1·28	41·54	—	glass, gehlenite
Hydrated lime	Buxton	0·46	0·70	0·01	0·19	73·52	0·03	0·01	25·02	—	calcium hydroxide

were retained under dry CO_2-free conditions until they were needed for further examination.

Examination of the autoclaved specimens

The cylindrical specimens were tested for compressive strength, the crushed material being saved for mineralogical examination. It was quartered down to obtain a representative sample of about 5 g, which was ground to pass a B.S. No. 100 sieve. The free lime of this sample was determined by the modified Franke method[5], and the minerals present were identified by differential thermal analysis (d.t.a.) and X-ray powder diffraction analysis. The thermograms were obtained on an apparatus which heated a sample of about 0·7 g in a ceramic crucible at 10°C/min from room temperature to 1,000°C; the temperature in the sample, and the differential temperature between the sample and an inert material heated at the same rate, were measured with chromel-alumel thermocouples. The X-ray powder diffraction patterns were obtained by photographic means on a Debye-Scheerer camera of 10 cm diameter. In all the experiments reported here, cobalt K alpha radiation was used.

Results of mineralogical examination

MIXES OF LIME AND PULVERIZED FUEL ASH OR COLLIERY SHALE

The series using pulverized fuel ash and that using colliery shale are discussed together for, as can be seen from the chemical and mineralogical analysis given in Table 1, they are almost identical in constitution, and the results obtained on autoclaving were similar.

The amounts of free lime present in the various autoclaved mixes as determined by differential thermal analysis or by chemical means show that practically all the lime in mixes 10:90 and 20:80 had reacted with the fines in 6 h, and in mixes 30:70 and 40:60 in 16 h. By comparing the amounts of free lime present after autoclaving for 16 h with those in specimens autoclaved for 48 h it may be inferred that the reaction of lime with aggregate fines is complete within 16 h.

The principal phase found by X-ray diffraction in the autoclaved mixes was tobermorite. The measurements given in Table 2 are for one mix autoclaved for one period only; the results for the rest of the series are in general similar, with one important exception, a variation in the intensity of the 002 basal reflexion at about 11·3 Å. This line varies in intensity from strong in mixes with high lime content and long steam treatment to completely absent in mixes with low lime content autoclaved for short periods. In the latter mixes, the tobermorite gives only the following reflections on the powder X-ray pattern (in Å): 3·07 vs, 2·80 s, 2·4 w, 2·1 w and 1·83 s. Such a pattern is very similar to that quoted by McConnell[6] for plombierite, but it would appear that, in the present work, further crystallization produces a tobermorite with an 11 Å basal spacing, whereas McConnell's plombierite is the gel form of a 14 Å tobermorite. The poorly crystallized tobermorite will therefore be referred to as tobermorite gel. It has not been possible so far to

TABLE 2: **X-ray powder diffraction data for one mix and one autoclaving period typical of the mixes of lime and fuel ash and lime and colliery shale.**

Tobermorite (synthetic)			30% lime, 70 p.f.a. 16 at 160 lb/in²		
d(Å)	I/I_o*	Indices	*d*(Å)	I/I_o	Identification†
11·45	s	002	11·34	s	T
5·495	ms		5·433	ms	T + F
			5·052	m	H
			4·24	vvw	F
3·52	w				
			3·428	mw	F
3·313	vvw		3·355	w	F
3·085	vvs	220	3·080	vvs	T
2·978	vs	222	2·983	mw	T
2·810	s	400			
			2·761	m	H
			2·704	vvw	F
			2·644	vvw	H
2·522	vw		2·535	vvw	F + H
2·426	vw		2·432	vw	H
2·293	mw		2·296	vw	F
2·256	vw		2·253	vvw	H
			2·209	w	T
2·145	mw		2·126	vw	F + H
2·077	w		2·095	vvw	T
2·011	mw		2·003	vvw	H + T
1·840	vs	040	1·846	mw	T
			1·825	vw	H
1·737	vvw		1·709	vvw	H + F
1·673	s	620			
			1·647	vw	H

*The intensity scale used throughout the X-ray data is an arbitrary one:

vvs = very, very strong
vs = very strong
s = strong
ms = moderately strong
m = medium
w = weak
vw = very weak
vvw = very, very weak

†T = tobermorite
H = hydrogarnet
F = unreacted pulverized fuel ash

determine the CaO/SiO_2 ratio of this tobermorite.

From these results it may be inferred that an increase in the lime-aggregate ratio or the autoclaving period, or both, materially assists in the development of the crystallographic perfection of the tobermorite.

If the spacings and intensities of the various reflections produced by the tobermorite found in the autoclaved preparations are compared with the corresponding values given by a tobermorite synthesized from pure materials (Table 3, column 1), it will be noted from Table 4 that, in the tobermorite from autoclaved mixes, the relative intensity of the 222 spacing at about 2·98 Å is reduced and the 400 spacing at about 2·81 Å is absent. In the data for autoclaved mixes,

TABLE 3: **X-ray powder diffraction data for pure calcium silicate hydrates.**

Tobermorite[8]	Xonotlite[8]	CSH (A)[8]	Fibrous lime-silica hydrate[13]	C-S α-hydrate
11 s			11 vvw	
	8·5 vw			
			7·2–7·4 w-m	
	7·05 mw			
		6·13 vw		
5·6 ms			5·4 vw-w	5·35 w
		4·52 w		4·63 vvw
	4·27 mw	4·24 w		4·22 vs
	3·96 vw*			
				3·90 s
		3·80 vw		
	3·65 ms			
3·55 vvw		3·58 w		3·54 s
3·28 m	3·23 ms	3·21 m		3·27 vvs
3·07 vvs	3·07 vs		3·02–3·05 s	3·04 w
		3·01 vs		
2·97 s				
				2·87 s
2·80 s	2·83 m	2,78 m		2·80 s
	2·71 mw		2·76–2·78 w	2·77 w
	2·65 vw*			2·71 w
				2·69 vw
2·52 vw	2·51 mw	2·50 m		2·65 m
				2·60 s
				2·56 w
2·48 vw				2·52 m
				2·47 vvw
	2·34 w			2·41 vs
				2·31 vw
2·28 ms	2·25 w	2·23 s		2·27 vw
				2·24 w
2·15 m		2·116 vw		2·18 m
				2·16 w
				2·10 vw
2·07 m	2·04 s			2·08 w
		2·013 w		2·06 mw
				2·03 w
2·00 m				2·02 w
	1·95 s			1·982 m
1·93 vvw		1·893 s		1·956 w
				1·926 m
		1·868 vw		1·890 w
				1·872 mw
1·83 vs	1·84 mw		1·82–1·827 m	1·842 vw
		1·808 vw		1·820 m
1·76 vvw	1·756 w			1·788 s
1·71 vvw	1·710 mw	1·772 m		
				1·662 mw
1·67 s	1·687 vw	1·632 vw	1·659–1·672 vvw	1·654 m

*Lines vary in intensity.

there is also a line of medium-strong intensity at 2·76 Å which, together with some other extra, weaker lines, suggests the presence of a cubic phase of the hydrogarnet series, unit cell a_o = 12·37 Å which, from the data given by Carlson[9] suggests an approximate composition of $3\,CaO.Al_2O_3.SiO_2.4H_2O$.

Thermograms of 40:60 mixes typical of the lime and

TABLE 4: **X-ray powder diffraction data for mixes of lime and quartz autoclaved at 160 lb/in².**

30% lime, 70% quartz 16 h	40% lime, 60% quartz			
	2 h	6 h	16 h	48 h
	5·38 vvw T		5·56 vvw T	
	4·90 ms CH	4·90 ms CH		
	4·675 vw			
4·26 vvw Q	4·26 vvw Q	4·26 vvw Q		4·20 w Q
	4·14 vvw			
	4·03 vvw			
	3·86 vvw A	3·83 vvw A	3·84 vvw A	3·88 vvw A
3·68 vw X	3·66 w X	3·66 vw	3·66 vvw X	3·66 vvw X
3·55 vw T		3·52 vvw	3·54 vvw A, T	3·54 vvw A, T
3·34 vvs Q	3·34 vvs Q	3·34 vvs Q	3·34 vvs Q	3·34 vvs Q
	3·25 vvw A, T	3·25 vw A, T	3·25 vw A, T	3·26 vvw A, T
	3·11 vw CH	3·112 vvw CH		3·06 vvw X
3·07 w T	3·02 vw	3·025 mw	3·03 mw A, T	3·01 mw A, T
2·96 vvw T				
	2·88 vw T		2·88 vvw T	
2·81 vw T				2·83 vvw X
2·72 vw X	2·70 vvw X		2·71 vw X	2·71 vw X
	2·628 vvs CH	2·628 m CH		
				2·57 vw
				2·54 vvw A, X
	2·515 vvw T			
			2·475 vvw T	
2·458 vvw Q	2·458 vvw A	2·458 vvw Q	2·458 vvw Q	2·458 vvw Q
	2·447 w CH	2·447 vvw CH	2·415 vvw	2·41 vvw
	2·40 vvw	2·41 vvw		
2·282 vvw Q, T	2·282 vvw Q, T	2·282 vvw Q, T	2·282 vvw Q, T	2·282 vvw Q, X, T
2·237 vvw Q	2·237 vvw Q, A	2·237 vvw Q, A	2·237 vvw Q, A	2·237 vvw Q, A
2·128 vvw Q, T	2·128 vvw Q, A	2·128 vvw Q, A	2·128 vvw Q, A	2·128 vvw Q, A
		2·08 vvw T	2·09 vvw T	2·09 vvw T
2·06 vvw T		2·05 vvw X	2·055 vvw X	2·05 vvw X
2·01 vvw T	1·99 vvw		1·980 vvw Q	1·98 vvw Q
1·980 vvw Q	1·980 vvw Q	1·980 vvw Q		
1·93 vvw X, T	1·927 w CH	1·927 vvw CH	1·91 vw	
		1·87 vvw A	1·87 vw A	1·88 vvw A
1·83 vvw T, X	1·84 vvw T, X	1·83 vvw T, X	1·83 vvw X, T	1·83 vvw X, T
1·817 vvw Q	1·817 vvw Q	1·817 vvw Q	1·817 vvw	1·817 vvw Q, A
	1·796 w CH	1·796 vvw CH		
				1·70 vvw X
	1·681 vw CH	1·687 w CH		
1·672 vvw T, Q	1·672 vvw T	1·672 vvw Q, T	1·672 vvw Q, T	1·672 vvw Q, A, T
	1·65 vvw			

Q = quartz. CH = calcium hydroxide. X = xonotlite. T = tobermorite. A = Flint's CSH(A)[10].

fuel ash series are given in Figure 1; it was necessary to carry out the differential thermal analysis in an inert atmosphere (nitrogen) to suppress the exothermic peak due to the oxidation of carbon, and to allow the endothermic peak due to the decomposition of the $Ca(OH)_2$ to be recorded. The most prominent peak is the endothermic one at above 100°C, which is thought to be due to the dehydration of the poorly crystalline tobermorite gel mineral. It has been shown that this peak is not due to free water, for, by adding 25% of water to the sample, separate peaks were produced at 114 and 127°C.

The correlation of the d.t.a. and X-ray data presents some difficulty for, whilst the endothermic peak at just above 100°C appears to be characteristic of the poorly crystalline tobermorite gel, i.e. the tobermorite with no 002 spacing, it will be noted that the 11 Å basal spacing is present in the 40:60 mix autoclaved for 48 h, whilst the thermogram still shows a large endothermic peak at 125°C. However, the size of this peak is about the same as in the same mix after autoclaving for only 6 h and it is suggested that during the longer steam treatment new tobermorite is being formed in the gel state while already existing gel is crystallizing, so that there is still apparently about the same quantity of poorly crystallized tobermorite gel and an increase in the amount of 11 Å tobermorite.

In these mixes, therefore, tobermorite gel is found in low lime mixes autoclaved for short periods; as the lime/silica ratio is increased or the autoclaving time is

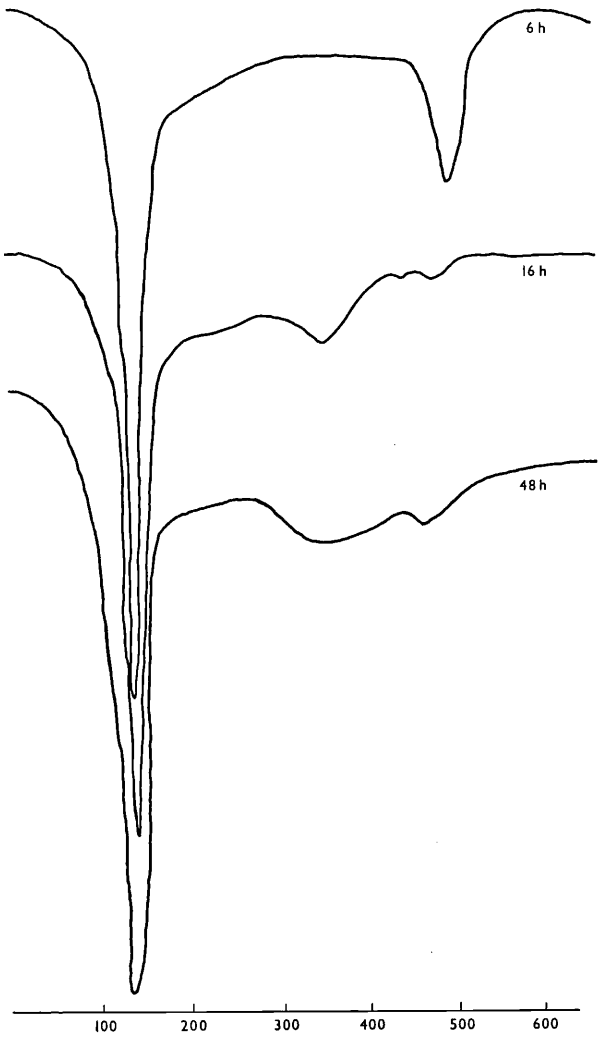

Figure 1: Thermograms for mixes containing 40% lime and 60% pulverized fuel ash autoclaved for various periods.

extended, the gel crystallizes and some hydrogarnet is also formed.

MIXES OF LIME AND QUARTZ SAND

Some experiments on the lime-quartz system have been included in this series so that a comparison may be made with other aggregates used, although some previous work[10] has already been reported. Free lime, as determined either by d.t.a. or by chemical methods, indicates that all the lime has reacted in mixes 10:90 and 20:80 after 2 h, and in mix 30:70 after 6 h, but that in mix 40:60 even after 48 h 1·37% free lime remained.

All the X-ray diffraction photographs of lime-quartz autoclaved mixes showed the presence of free unreacted quartz, and some also showed the presence of calcium hydroxide. A characteristic series of results is given in Table 4, with the conclusions based on the data.

Mixes 10:90 and 20:80 autoclaved for 2 h only showed two lines characteristic of calcium silicate hydrate I[7], 3·07 and 1·835 Å, while after autoclaving for longer periods (6, 16 and 48 h) more lines were recorded.

3·67 Å	vvw*		(*intensities refer to the
3·075	?		strongest line of quartz,
2·96	vvw	fuzzy	3·34 Å)
2·795	vvw	fuzzy	
1·835	vvw		

On the basis of these results, tobermorite poorly crystallized in the *c* direction is thought to be one of the phases produced; on the basis of one line at 3·67 Å, it is thought that xonotlite may also be present.

The X-ray diffraction patterns of the 30:70 mixes contain many more lines and the presence of both xonotlite and tobermorite is established (see Table 4, column 1). The examination of mix 40:60 autoclaved for 2, 6, 16 and 48 h (Table 4) suggests the formation of Flint's CSH(A)[8] and xonotlite. This mix, after being autoclaved for 48 h, contained 24·8% soluble silica as determined by the buffered acetic acid method and, on this basis, the CaO/SiO_2 ratio in the hydrated material is calculated as 1·29.

Representative differential thermograms of lime and ground quartz autoclaved mixes are given in Figures 2 and 3. The almost complete absence of the $Ca(OH)_2$ endothermic peak at 500°C for a mix containing 30% lime shows that the reaction is almost complete after autoclaving for 16 h. The larger endothermic peaks at just above 100°C are due to the tobermorite gel phase and indicate that the amount found after treatment for 16 h is the maximum found in this type of mix. The large exothermic peak at 810°C is due to the formation of an anhydrous crystalline calcium silicate.

The thermograms in Figure 3 are for the 40:60 mix autoclaved for 2, 6, 16 and 48 h, and show the progressive reaction of lime, as can be deduced by the gradual disappearance of the peak at about 500°C. The endothermic peak at just above 100°C is due to the poorly crystalline tobermorite mineral; it shows an increase in amount from the 2 h period up to the 16 h period, and then falls with further autoclaving.

In the sample autoclaved for 2 h there is no exothermic peak, but in the sample autoclaved for 6 h a small peak occurs at 842°C, whilst in a sample autoclaved for 48 h this peak is much larger and is accompanied by a smaller one at 810°C. These exothermic peaks occurring at 810 and 842°C are due to the heat of formation of anhydrous calcium silicate phases. The lower peak at 810°C has been shown experimentally to be due to the formation of wollastonite (beta monocalcium silicate) and the higher one at 842°C to be due to the formation of beta dicalcium silicate; when both peaks occur, both anhydrous phases are produced.

While Kalousek[3] considered the exothermic peak in the region of 800–850°C to be characteristic of calcium silicate hydrate I, Nurse[11] was doubtful if this was so. The results reported in this paper and some unpublished data by the present authors seem

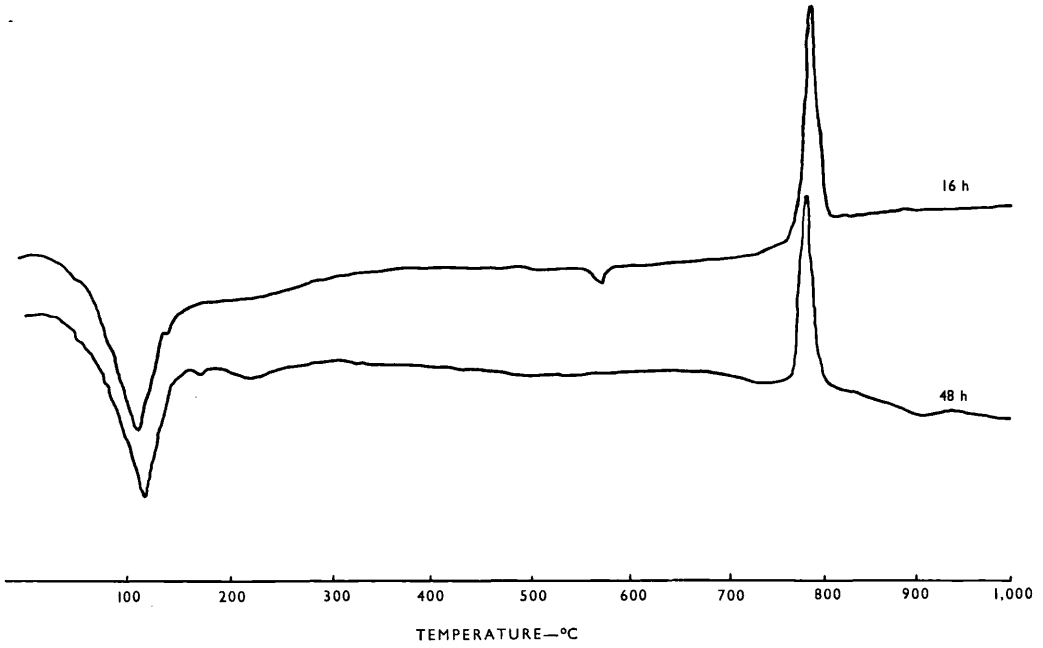

Figure 2: Thermograms for mixes containing 30% lime and 70% quartz autoclaved for various periods.

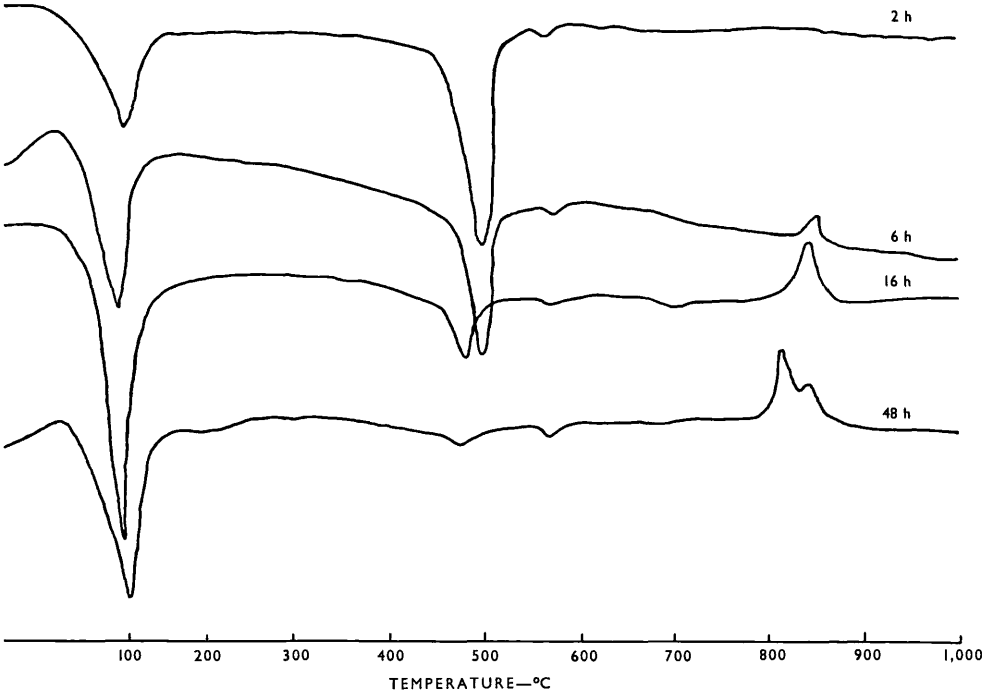

Figure 3: Thermograms for mixes containing 40% lime and 60% quartz autoclaved for various periods.

to confirm the view that the presence or absence of calcium silicate hydrate I cannot be established by means of exothermic peaks in the region of 800–850°C.

From these results it can be concluded that for mixes of low lime/quartz ratio the hydrated phases are tobermorite gel and xonotlite, whilst for the higher ratios the phases are xonotlite, tobermorite gel and Flint's CSH(A).

MIXES OF LIME AND SLAG

The two types of slag, foamed and granulated, are discussed together, for it appears that they behave in a similar mannèr.

The determination of free lime in the mixes showed that, except in the case of mix 10:90 autoclaved for at least 6 h, free lime was always present, the quantity increasing as the percentage of lime in the original

TABLE 5: **X-ray powder diffraction data for some of the mixes of lime and slag.**

100% slag 16 h at 160 lb/in²			C88 5% lime, 95% slag 16 h at 160 lb/in²			C23 10% lime, 90% slag 6 h at 160 lb/in²			C80 10% lime, 90% slag 48 h at 160 lb/in²			C35 40% lime, 60% slag 2 h at 160 lb/in²		
d(Å)	I/I_o	Identification	*d*(Å)	I/I_o	Identification	*d*(Å)	I/I_o	Identification	*d*(Å)	I/I_o	Identification	*d*(Å)	I/I_o	Identification
			5·44	m	T,α									
			4·98	ms	H	4·96	vw	CH	4·98	mw	H, CH	4·34	vvw	H
			4·33	m	H				4·22	vvw		4·20	vw	α
												3·90	w	α
			3·565	vvw	α	3·68	vw	α				3·68	w	α
			3·27	m	α	3·25	m	α	3·25	s	α	3·50	vvw	α
3·04		T	3·05	vs	T	3·04	vs	T	3·04	vs	T	3·25	s	α
2·71	m	H	2·72	vvs	H	2·72	vs	H	2·72	vs	H	3·07	s	T
			2·59	vw	H	2·62	w	CH	2·58	vvw	H	2·74	s	H
			2·48	ms	H	2·49	w	H	2·49	w	H	2·62	vvs	CH
2·29	m		2·29	ms	H+slag	2·41	vvw	α	2·395	mw	α	2·51	mw	H
			2·22	s	H	2·22	m	H	2·22	m	H	2·40	ms	α
			2·03	mw	H	2·03	w	H				2·23	m	H
1·97	m	H	1·97		H	1·97	m	H	1·97	ms	H	2·15	vvw	α
			1·92	w	H	1·92	w	H	1·925	w	H	1·99	vvw	H
			1·83	w	T	1·835	vw	T	1·83	vvw	T			
1·75	m		1·75	s	H+slag	1·745	vw	H+slag	1·78	vvw	H+slag	1·785	w	H+slag
			1·72	vvw	H									
			1·68	m	H, T	1·685	m	H, T	1·68	m	H, T	1·70	w	H, T
1·62	m	H	1·62	s	H	1·625	m	H	1·62	m	H	1·64	m	H
slag + a hydrogarnet + tobermorite			slag + a hydrogarnet $3\,CaO.Al_2O_3.SiO_2.2H_2O$ + tobermorite + dicalcium silicate alpha-hydrate			slag + a smaller amount of hydrogarnet than C88 + tobermorite + dicalcium silicate alpha-hydrate + trace of $Ca(OH)_2$			slag + hydrogarnet as C23 + tobermorite + dicalcium silicate alpha-hydrate			slag + a smaller amount of hydrogarnet than C23 + tobermorite + dicalcium silicate alpha-hydrate + a lot of $Ca(OH)_2$		

T = tobermorite. CH = calcium hydroxide. H = hydrogarnet phase. α = dicalcium silicate alpha-hydrate.

mix increased; the maximum quantity of lime the slag could take into combination was about 10%. In view of this, extra mixes with only 0·5, 1, 2·5 and 5% added lime were also partially investigated.

X-ray powder diffraction data for some of the mixes are given in Table 5, from which it can be seen that for slag alone the hydrate phases are poorly crystalline tobermorite gel and hydrogarnet; when 5% lime is added, more tobermorite is formed for the same processing time and the hydrogarnet phase is also present in greater quantity; a trace of dicalcium silicate alpha-hydrate is also formed. It is possible to estimate the composition of the hydrogarnet from its unit cell, a_o = 12·13 Å; viz. $3\,CaO.Al_2O_3.2\,SiO_2.H_2O$, plazolite[9-12]. An increase in either autoclaving time or lime concentration increases the quantity of dicalcium silicate alpha-hydrate at the expense of the tobermorite phase. Unreacted $Ca(OH)_2$ was present in 20:80, 30:70 and 40:60 mixes irrespective of autoclaving period.

Differential thermal analysis was carried out on some samples of the lime and slag, and a representative series showing the change with increase in lime concentration is given in Figure 4.

In the first curve, representing slag alone autoclaved for 16 h, there is only one peak, an endotherm at just over 100°C, ascribed to poorly crystalline tobermorite gel; with 5% of added lime, this peak increases; with 10% of lime, the tobermorite peak decreases again but a second endotherm appears at just below 500°C, which is thought to be due to dicalcium silicate alpha-hydrate. With the further addition of lime, the peak due to dicalcium silicate alpha-hydrate increases.

It can be seen that slag glass of the composition used here will harden in the autoclave without the addition of lime, poorly crystalline tobermorite being formed. When up to between 5 and 10% of lime is added, tobermorite is formed; if a larger percentage of lime is added, dicalcium silicate alpha-hydrate is produced at the expense of tobermorite.

The CaO/SiO_2 ratio of the slag alone is 1·3, whilst with 10 and 20% added it lime rises to 1·7 and 2·1

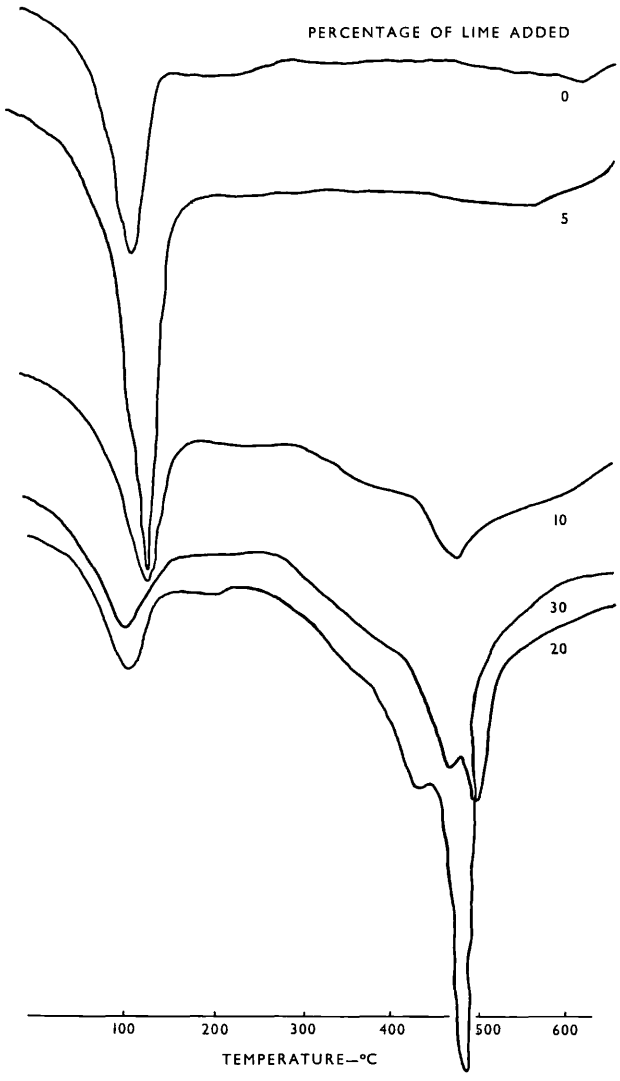

Figure 4: Thermograms for mixes autoclaved for 16 h and containing slag and various percentages of added lime.

respectively. It appears that the limiting CaO/SiO_2 ratio for the formation of dicalcium silicate alpha-hydrate is about 1·6.

Compressive strength

The compressive strength of the cylinders was tested after they had cooled on removal from the autoclave, one cylinder only being tested for each mix and condition of curing.

The results are given in Tables 6 and 7. The difference in strength between specimens made from different aggregates may be due in part to the differing degrees of compaction, as shown by the average bulk densities which were found to be 101 lb/ft³ for pulverized fuel ash, 112 lb/ft³ for expanded colliery shale, 114 lb/ft³ for ground quartz, 115 lb/ft³ for granulated slag and 116 lb/ft³ for foamed slag. The quartz sand mixes also differ from the others in having some coarser material present. However, whilst the comparison of strength between mixes using different aggregates may be misleading[3], the comparison of the mixes of differing lime ratios and times of processing for any one of the aggregates is justified.

TABLE 6: **Compressive strength of mixes of lime and aggregate fines autoclaved at 160 lb/in².**

Aggregate	Mix proportions		Compressive strength (lb/in²)			
	Lime	Fines	2 h	6 h	16 h	48 h
Pulverized fuel ash	10	90	2,069	2,755	2,434	3,177
	20	80	3,079	4,637	4,370	5,296
	30	70	3,165	5,690	6,391	6,183
	40	60	3,256	6,294	4,578	5,003
Expanded colliery shale	10	90	4,234	6,330	6,208	7,170
	20	80	6,549	8,290	9,591	11,261
	30	70	4,675	6,610	11,479	11,413
	40	60	4,744	5,170	5,759	7,426
Quartz sand	10	90	6,247	6,500	4,638	4,504
	20	80	10,174	12,180	9,310	12,048
	30	70	10,854	10,820	14,391	12,901
	40	60	8,168	8,279	8,521	5,107
Staveley slag	10	90	4,224	5,465	3,043	—
	20	80	2,723	2,630	1,869	—
	30	70	—	2,662	2,069	—
	40	60	2,641	2,841	1,461	—

TABLE 7: **Compressive strength of cylinder in lb/in², slag B319.**

Added lime (%)	Slag content (%)	Period of curing (h)			
		2	6	16	48
0	100	—	177	3,780	—
0·5	99·5	—	2,460	—	—
1	99	—	3,410	—	—
2·5	97·5	—	—	6,650	—
5	95	—	5,272	8,589	—
10	90	4,114	4,017	4,639	6,910
20	80	2,337	3,652	3,628	3,342
30	70	1,887	2,811	3,600	3,165
40	60	1,546	2,114	2,434	2,921

As regards development of compressive strength, the aggregates fall into two distinct classes, the siliceous group (ash, shale, sand) and the two slags.

In the siliceous group the maximum strength is developed in 30:70 mixes after 16 h autoclaving. Mixes of lower lime content gain strength with longer autoclaving time, although the sand mixes behave rather erratically. At lime contents greater than the optimum, the maximum strength is generally reached after shorter autoclaving periods.

In the first series of tests, with slag aggregates, a maximum strength value was not attained, and further tests were made using smaller additions of lime. The optimum lime addition was found to be 5% and the best time of treatment again 16 h (Figure 5). Mixes

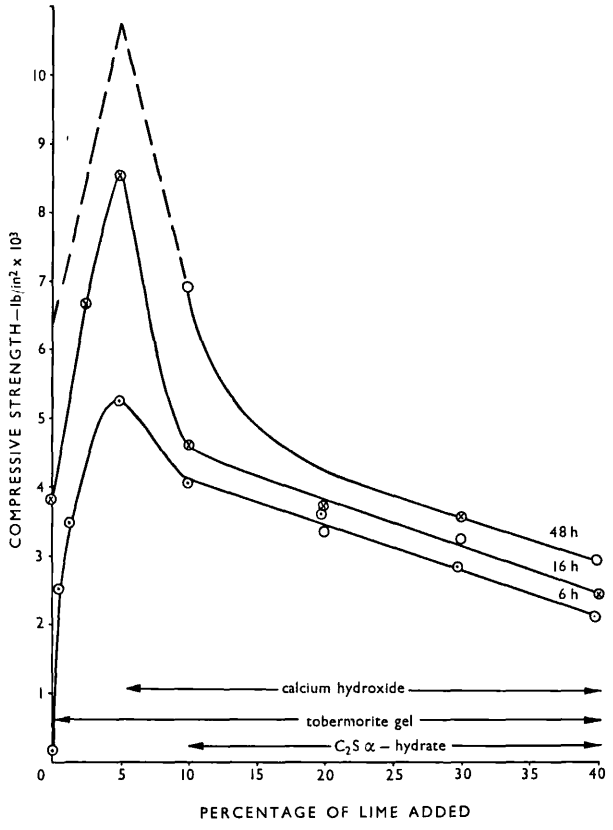

Figure 5: Relation between compressive strength and percentage of lime added for various periods of autoclaving.

with lower lime contents were slow to gain strength, whilst longer autoclaving time again appears in general to be detrimental to mixes richer in lime than the optimum.

Conclusions

In all the mixes the development of strength is associated with the reaction of lime with silica to form tobermorite, the degree of crystallinity increasing with lime/silica ratio and processing time. When the aggregate contains alumina (fly ash, sintered shale, slag), a hydrogarnet is also formed. Quartz mixes, which under the conditions of the experiment always contained an excess of quartz as large particles, formed xonotlite as well as tobermorite. At high CaO contents and long processing times, Flint's CSH(A) was also formed; in these mixes the strength had fallen considerably below the maximum which, in the case of the 30:70 mix, was obtained after it had been processed for 16 h.

Slag differs from the other aggregates in already containing CaO, the CaO/SiO_2 ratio being 1·3; for the 5% added CaO, the best strength would be obtained with a CaO/SiO_2 ratio of 1·5. In the 30:70 mix giving the best strength with ash or shale, the CaO/SiO_2 ratio would be about 1·0. The fall in strength with greater quantities of added lime and longer processing times is associated with $Ca(OH)_2$ and the formation of dicalcium silicate alpha-hydrate.

These observations are tentative and the experiments described suggest the need for further work. It appears, however, that the mineralogical examination of reaction products can give a useful guide to the best conditions for processing cement or lime products in the autoclave. Work is also in progress on the hydration of Portland cement and the hydrothermal reaction of lime and silica in various forms at both lower temperatures and pressures. The work is part of a larger programme being undertaken on the relation of strength to the type of mineral produced by both hydrothermal and normal temperature hydration.

ACKNOWLEDGEMENTS

The authors acknowledge the help of Mr D. Rosaman and Mr J. J. Smith with the practical work. This work was undertaken as part of the programme of the Building Research Board and is published by permission of the Director of Building Research.

REFERENCES

1. HANSEN, W. C. Chemical reactions in high-pressure steam curing of Portland cement products. *Journal of the American Concrete Institute.* Vol. 24, No. 9. May 1953. pp. 841–855.
2. KALOUSEK, G. L. The reactions of cement hydration at elevated temperatures. *Proceedings of the Third International Symposium on the Chemistry of Cement, London, 1952.* London, Cement and Concrete Association, 1954. pp. 334–355.
3. KALOUSEK, G. L. Studies on the cementitious phases of autoclaved concrete products made of different raw materials. *Journal of the American Concrete Institute.* Vol. 25, No. 5. January 1954. pp. 365–378.
4. ACI COMMITTEE 716. High-pressure steam curing. *Journal of the American Concrete Institute.* Vol. 15, No. 5. April 1944. pp. 409–414.
5. PRESSLAR, E. E., BRUNAUER, S. and KANTRO, D. L. Investigations of the Franke method of determining free calcium hydroxide. *Analytical Chemistry.* Vol. 28, No. 5. May 1956. pp. 896–911. Reprint by Portland Cement Association, May 1956. Bulletin No. 62.
6. MCCONNELL, J. D. C. The hydrated calcium silicates riversideite, tobermorite and plombierite. *Mineralogical Magazine.* Vol. 30, No. 224. 1954. pp. 293–305.
7. NURSE, R. W. and TAYLOR, H. F. W. The reactions and thermochemistry of cement hydration at ordinary temperatures. Discussion. *Third International Symposium on the Chemistry of Cement, London 1952.* London, Cement and Concrete Association, 1954. pp. 311–318.
8. HELLER, L. and TAYLOR, H. F. W. *Crystallographic data for the calcium silicates.* 1st edition. London, H.M.S.O., 1956. pp. vi, 79.
9. CARLSON, E. T. Hydrogarnet formation in the system lime-alumina-silica-water. *Journal of Research of the National Bureau of Standards.* Vol. 56, No. 6. 1956. pp. 327–335.
10. TAYLOR, H. F. W. and BESSEY, G. E. A review of hydrothermal reactions in the system $CaO\text{-}SiO_2\text{-}H_2O$. *Magazine of Concrete Research.* Vol. 2, No. 4. July 1950. pp. 15–26.

11. NURSE, R. W. The reactions of cement hydration at elevated temperatures. Discussion. *Proceedings of the Third International Symposium on the Chemistry of Cement, London 1952*. London, Cement and Concrete Association, 1954. p. 356.
12. FLINT, E. P., MCMURDIE, H. F. and WELLS, L. S. Hydrothermal and X-ray studies of the garnet-hydrogarnet series and the relationship of the series to hydration product of Portland cement. *Journal of Research of the National Bureau of Standards*. Vol. 26. 1941. pp. 13–33.
13. KALOUSEK, G. L. Tobermorite and related phases in the system CaO-SiO_2-H_2O. *Journal of the American Concrete Institute*. Vol. 26, No. 10. June 1955. pp. 989–1011.

Contributions discussing the above paper should be in the hands of the Editor not later than 30th September 1960.

Printed by the Cement and Concrete Association
52 Grosvenor Gardens, London S.W.1

MIDGLEY (H.G.) 20

Reprinted from *Clay Minerals Bulletin*, Vol. 4, No. 25, 1961. D.Sc. 1967.

A MINERALOGICAL EXAMINATION OF SUSPENDED SOLIDS FROM NINE ENGLISH RIVERS

By R. F. PACKHAM
The Water Research Association, Redhill, Surrey
D. ROSAMAN and H. G. MIDGLEY
Building Research Station, Garston, Watford, Herts.

[Read 12th April, 1960]

ABSTRACT

X-ray powder diffraction data were used to determine the mineralogical composition of the fine suspended material present in nine English rivers. The mineralogy of these solids is discussed in relation to the geological formations through which the rivers flow.

INTRODUCTION

The task of collecting, purifying and distributing water to the community is normally undertaken by a multitude of independent Water Authorities which must collect their water from the most convenient and economical sources available. Purification of river water for domestic supply is, therefore, of considerable importance, and in investigating a process for this it became necessary to determine the nature of the suspended mineral matter accumulated during the water's passage downstream. Nine rivers were selected for this study (Table 1 and Fig. 1) and were so chosen that water flowing over a wide variety of geological formations (Table 2) could be examined. The sampling points were, with one exception, at or near the intake of a Water Authority.

TABLE 1—Location of sampling sites.

River	Water Authority	Place of sampling
Hull	Kingston-on-Hull Corp. Water Dept.	Hempholme, Yorks
Mole	—	Leatherhead, Surrey
Kennet	Reading Corp. Water Dept.	Fobney, Oxon
Severn	Coventry Corp. Water Dept.	Upton-on-Severn, Glos.
Ouse	Bucks Water Board	Foscott, Bucks
Nar	Wisbech and District Water Board	Marham, Norfolk
Itchen	Southampton Corp. Water Dept.	Eastleigh, Hants
Avon	S. Devon Water Board	Avon Dam, Devon
Chelmer	Chelmsford Borough Corp. Water Dept.	Chelmsford, Essex

20

EXPERIMENTAL

At each sampling point a small centrifugal pump was employed to pass a flow of about 2 gallons per hour through a continuous centrifuge. At this flow the turbidity of the effluent from the centrifuge was always less than 1 p.p.m., indicating almost complete removal of suspended matter. In order to obtain a sufficient quantity of sample

FIG. 1—Map showing positions from which river-water samples were taken.

for this investigation and for other work, it was necessary to continue the centrifuging process for approximately one month. The amount of suspended matter deposited in the bowl of the centrifuge by the end of this period varied with the character of the river water. 90 g of sample was obtained from the River Severn, but with the Avon almost exactly the same volume of water yielded only 4·5 g.

On arrival at the laboratory the samples were in the form of 'fluffy' powders contaminated with organic material, particularly those from River Hull and River Mole, which had an especially putrid smell.

X-ray examination of the samples as received yielded no informa-

tion on the clay-mineral content since all were heavily contaminated with quartz and some contained large amounts of calcite.

To separate the clay-mineral fractions, each sample was treated with cold 0·2N hydrochloric acid to remove carbonates, the acid liquor being decanted after spinning in a small centrifuge. The organic material was destroyed by shaking with successive additions of 20 vol. hydrogen peroxide and warming on a hot plate until evolution of oxygen had ceased. The liquid was decanted after centrifuging, the residue dispersed in distilled water and the fine

TABLE 2—Geological formations traversed by rivers and mineralogy of suspended solids.

River	Geology	Mineralogy
Hull	Chalk, Recent	Much quartz and calcite, some kaolinite, little montmorillonite.
Mole	Wealden, Lower Greensand, Upper Greensand and Gault, Chalk	Much quartz, some kaolinite, little illite, little chalybite? The 0·2 N/HCl extract gave strong reactions for Fe^{2+} and Fe^{3+}
Kennet	Chalk, Oligocene and Eocene, Recent	Much calcite and quartz, some kaolinite, little montmorillonite, little illite?
Severn	Silurian, Bunter Sandstone, Coal Measures, Cambrian, Keuper Marl and Sandstone	Much quartz, some illite, some chlorite.
Ouse	Oolite, Recent	Much quartz and calcite, some illite, little kaolinite?
Nar	Chalk, Upper Greensand and Gault (just)	Much calcite and quartz, little illite, (diffuse band on X-ray film at about 4·27 Å moving to about 2·78 Å on glycerol treatment)?
Itchen	Chalk, Oligocene and Eocene	Much quartz and calcite, some montmorillonite, little kaolinite. Coarse fraction contains white mica and glauconite.
Avon	Granite, Devonian	Much quartz, some kaolinite, little illite?
Chelmer	Oligocene and Eocene	Much fine quartz, some calcite, some illite, little kaolinite, little montmorillonite?

sand allowed to settle. The clay suspension was decanted and the solid was recovered by centrifuging to small volume and allowing to dry in air at room temperature.

X-ray powder diffraction photographs of the clay-mineral fraction

of each sample were taken, before and after glycerol treatment, using a 10 cm diameter camera and CoKα radiation.

Conclusions

From the mineralogical data in Table 2 it can be seen that the fine material from river water consists essentially of fine quartz together with smaller amounts of calcite and clay minerals. Quartz occurs whatever the geological formation, and calcite occurs, as would be expected, when the rivers drain large tracts of limestone, *e.g.*, chalk and oolite. The clay minerals are derived from the clay and slate beds. Some observations can be made on the occurrence of mineral types in relation to the geological formation: illites occur in all ages, kaolinite in the Mesozoic and Tertiary and also in the Devon granite, montmorillonite in the Tertiary and Quaternary, and chlorite in the Palaeozoic.

21

MIDGLEY (H.G.) D.Sc. 1967.

ON THE OCCURRENCE OF SIDEROTIL IN THAMES RIVER GRAVEL

BY

H. G. MIDGLEY

(with chemical analysis by L. J. LARNER)

Reprinted from American Mineralogist, 47: (1962)
Pages 404-409

21

THE AMERICAN MINERALOGIST, VOL. 47, MARCH-APRIL, 1962

ON THE OCCURRENCE OF SIDEROTIL IN THAMES RIVER GRAVEL

H. G. MIDGLEY
(with chemical analysis by L. J. LARNER)
Building Research Station, Garston, Watford, Herts, England.

Thames river gravels consist mainly of flint, but commonly pyrite occurs as an accessory constituent (Midgley, 1958). One sample of such a gravel from Chertsey, Surrey, left to weather at the Building Research Station was found to contain a high proportion of pyrite pebbles, which were covered with a white crystalline powder. This powder under the microscope consisted of very small equant grains with a refractive index of about 1.535. A powder x-ray diffraction pattern obtained on a 10 cm diameter cylindrical camera with filtered cobalt K_α radiation suggested by reference to the A.S.T.M. index (1960) that the mineral was $FeSO_4 \cdot 5H_2O$ (Table 1, ii, iv).

An electron microscopic examination of the mineral showed it was composed of aggregates of small tabular crystals of about 0.05×0.15 micron (Fig. 2), or aggregates of crystals, 0.1×0.01 micron, in which the crystals were commonly arranged to give a "boat-shaped" outline (Fig. 3).

TABLE 1

(i) Siderotil Chertsey		(ii) Siderotil Chertsey		(iii) Synthetic $FeSO_4.4H_2O$ (Kossenberg and Cooke, 1961)		(iv) Synthetic $FeSO_4.4H_2O$ (A.S.T.M., 1960)		(v) Rozenite (=siderotil) (Kubisz, 1961)	
*d*Å	I	*d*Å	I	*d*Å	I	*d*Å	I	*d*Å	I
6.89	27	6.85	7	6.60	19	6.9	38	6.893	5
5.69	4			5.72	6				
5.51	85	5.46	9	5.31	67	5.5	100	5.483	9
		5.15[2]	1					5.179	1
4.77	34	4.75	2	4.73	43			4.762	3
4.50	100	4.48	10	4.37	100	4.49	100	4.498	10
3.98	47	3.97	8	3.90	72	3.99	75	3.979	8
								3.840	1
3.62	9	3.60	2			3.60	3	3.682	2
3.43	40	3.40	8	3.35	56	3.40	50	3.410	8
3.30[1]	23	3.28[1]	3					3.295	2
3.235	30	3.22	7	3.20	45	3.24	50	3.239	7
2.994	24							2.993	7
2.970	22	2.97	6	2.93	72	2.97	75	2.973	8
2.915	7	2.91	1					2.899	1
2.775	6	2.767	2			2.75	20	2.738	4
2.735	9			2.71	30				
2.584	24	2.573	6	2.56	48	2.58	38	2.579	7
2.481	14	2.465	2					2.478	1
2.3795	11	2.426	6	2.40	39	2.43	38	2.436	7
2.364	8	2.367	5	2.34	48			2.381	7
								2.327	7
2.295	4	2.253	4					2.293	1
2.271	20			2.24	44	2.27	38	2.272	6
2.247	6	2.24	1					2.247	1
								2.223	1
		2.181	1			2.18	3	2.188	1
		2.144	1					2.148	2
		2.113	1	2.10	39	2.11	8	2.116	1
		2.049	1			2.04	3	2.0577	1
1.973	12	1.967	4			1.97	38	1.9731	5
								1.9520	2
1.899	6	1.895	4	1.88	35	1.89	20	1.8999	3
								1.8757	2
								1.8627	2
1.802	5	1.815	1					1.8248	1
1.788	4	1.796	4	1.78	22	1.80	18	1.7975	5
		1.755	3			1.76	8	1.7592	3
1.729	5					1.72	10	1.7278	3
Diffractometer Cu K_α I peak height (I 4.50Å = 100)		Cylindrical camera 10 cm dia Co K_α I arbitrary		Camera Co K_α I photometer		Camera Mo K_α I calibrated strips		Data not given	

[1] Quartz.
[2] Melanterite.

The refractive index and appearance of the crystals indicated that the mineral resembled siderotil (Schrauf, 1892; Larsen, 1921; Palache *et al.*, 1951; Spencer, 1897). This mineral was first described by Schrauf (1892) on a sample from Idria, Italy as $FeSO_4 \cdot 5H_2O$. The authors of this note have not been able to see the original paper. Palache *et al.* (1951) quote an analysis by Schrauf as: FeO 30.0, SO_3 34.3, H_2O 34.0, on a sample of a few milligrams. They also suggest that the mineral may in fact be the tetrahydrate.

Kubisz (1960) described a new mineral, "rozenite" which is also $FeSO_4 \cdot 4H_2O$, but, as Fleischer (1961) pointed out in his evaluation of the paper, this mineral should be described as siderotil.

The sample from the Thames river gravel was sufficient in quantity for separation of the white crystals from the pyrite by means of heavy liquid flotation, about 2 gm of the white crystals being obtained.

A chemical analysis of the separated material gave (wt. per cent): SO_3 34.85, FeO 29.9, Fe_2O_3 absent or trace, other sulfur compounds absent or trace, water (Karl Fischer method) 30.5, matter insoluble in water (SiO_2) (*ca.*) 4.75. The analysis of the soluble portion gives the following ratios: FeO 1, SO_3 1.04, H_2O 4.06. This shows that siderotil is the ferrous sulfate tetrahydrate ($FeSO_4 \cdot 4H_2O$).

Kubisz (1960) gives: FeO 31.13, MgO 0.97, MnO 0.06, SO_3 36.29, H_2O 32.98, total 101.43; (FeO.MgO) 1., SO_3 0.99, H_2O 4.00, for what must be another example of siderotil.

A more careful *x*-ray examination of the separated siderotil from the Thames gravel was made using a counter diffractometer, set at 40 Kv., 20 ma., $\frac{1}{4}°$/min., $\frac{1}{2}°$ scatter slit, 0.1 receiving slit, rate 8, time const. 8. The result is given in Table 1, ii.

A comparison with the data for rozenite (siderotil) from "Staszie" mine (Kubisz, 1960), for synthetic $FeSO_4 \cdot 4H_2O$ (Kossenberg and Cooke, 1961), A.S.T.M. index (1960) and siderotil from Chertsey is given in Table 1. The data show the identity of siderotil and synthetic $FeSO_4 \cdot 4H_2O$, the only differences being in the weaker reflections, their presence or absence depending on the method of recording. The natural minerals may be contaminated by traces of melanterite ($FeSO_4 \cdot 7H_2O$) and quartz.

A D.T.A. record of siderotil from Chertsey gave endotherms at 74°, 114°, 555° and 700° C., and exotherms at 275° and 400° C. (Fig. 1). This is in agreement with the thermogram quoted by Kubisz (1960) as Fig. 1, with the addition of a low temperature endotherm at 74° C., due probably to adsorbed moisture and an exotherm at 275° C. due to the oxidation of a small trace of pyrite.

Single crystal electron diffraction patterns (Fig. 4) were obtained from the tablets (Fig. 2) on an A.E.I. E.M.6 electron microscope, and cali-

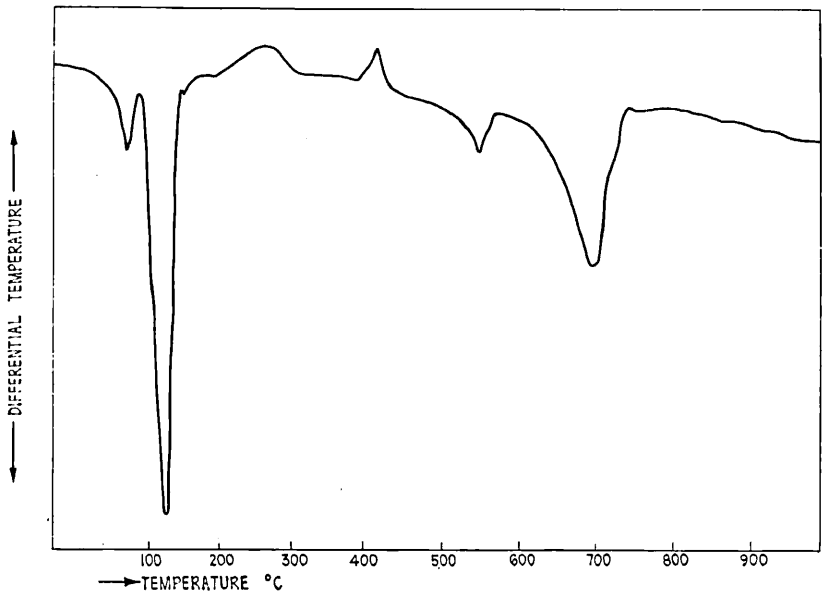

FIG. 1. Differential thermal analysis of siderotil from Thames River gravel.

brated with carbon and MgO, using an accelerating voltage of 100 Kv. These tablets were lying on the basal pinacoid and gave a diffraction pattern of the a.b. plane. From the diffraction pattern the parameters 7.0 and 11.75 Å were obtained.

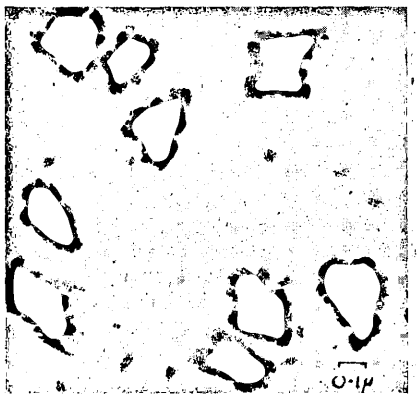

FIG. 2

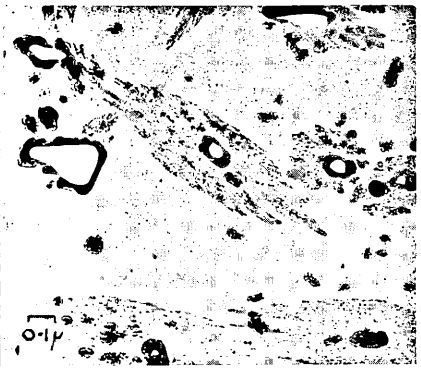

FIG. 3

FIG. 2. Electron micrograph of siderotil (001) tablet.
FIG. 3. Electron micrograph of siderotil ("boat-shaped" crystal) (010) plates.

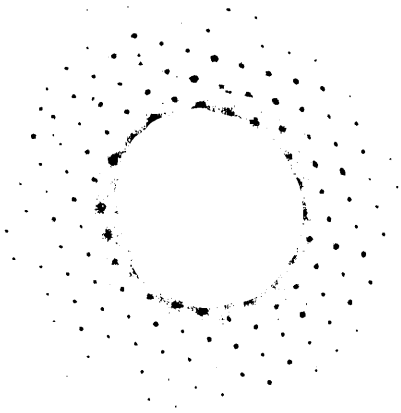

FIG. 4. Electron diffraction pattern of a *b* plane.

Single crystal electron diffraction patterns were also obtained from the "boat-shaped" crystal (Fig. 3); they were of poorer quality than those given by the a.b. plane, but they were indexed approximately, giving the parameters 11.8 and 10.2 Å, $\beta = 102°$. In these patterns there was strong pseudohalving of the 10.2 Å direction, alternative layer lines being extremely weak. From these data a unit cell of approximate dimension $a = 11.75$, $b = 7.0$, $c = 10.2$ Å, $\beta = 102°$ was obtained. It was then possible to index the more accurate powder *x*-ray diffraction data and the following unit cell was obtained:

$$a = 11.82, \quad b = 14.08, \quad c = 10.96 \text{ Å}, \quad \beta = 101.9°.$$

These data suggest that siderotil is isomorphous with the Ba $Ni(CN)_4 \cdot 4H_2O$ group of substances, the structure of which are given by Wyckoff (1960). Kubisz (1960) suggests that $FeSO_4 \cdot 4H_2O$ is isomorphous with ilosite, $(Mn, Zn, Fe)SO_4 \cdot 4H_2O$, and leonhardite $MgSO_4 \cdot 4H_2O$.

There is no indication from the conditions of weathering why siderotil ($FeSO_4 \cdot 4H_2O$) should be formed instead of the more usual melanterite ($FeSO \cdot 7H_2O$), the stable phase at room temperature. The siderotil stored in the laboratory atmosphere remained unchanged at the end of the year.

References to the occurrence of siderotil are rare; Ross (1940) referred to it in cavities in quicksilver ore from Contra Costa County, California, which he suggests "may be derived by dehydration from melanterite

($FeSO_4 \cdot 7H_2O$), one of the more widespread and more abundant sulphates." Schaller (1940) also refers to siderotil as associated with a phosphate-sulfate of aluminum from Utah. Kubisz (1960) described a new mineral, rozenite, $FeSO \cdot 4H_2O$, from "Staszie." Siderotil is a well-established mineral name and so has precedence.

REFERENCES

A.S.T.M., (1960), Index of Powder Diffraction Patterns. Card No. **0422.**

FLEISCHER, M., (1961), New Mineral Names, Rozenite. *Am. Mineral.*, **46,** 242–243.

KOSSENBERG, M. AND A. C. COOK, (1961), Weathering of sulphide minerals in coal: production of ferrous sulphate heptahydrate. *Mineral. Mag.*, **32,** 829–830.

KUBISZ, J., (1960), Rozenite—$FeSO_4 \cdot 4H_2O$—a new mineral. *Bull. Acad. Polonaise., Sci.*, **VIII** (2), 107–113.

LARSEN, E. S., (1921), The microscopic determination of non-opaque minerals, *U. S. Geol. Surv. Bull.*, **679.**

MIDGLEY, H. G., (1958), The staining of concrete by pyrite. *Mag. Concrete Res.*, **10,** 75–78.

PALACHE, C., H. BERMAN, AND C. FRONDEL, (1951), Dana's System of Mineralogy, Vol. II, John Wiley and Sons, N. Y., p. 491.

ROSS, C. P., (1940), Quicksilver deposits of the Mount Diablo district, Contra Costa County, California. *U. S. Geol. Surv. Bull.*, **922B,** 31–54.

SCHALLER, W. T., (1940), A probably new phosphate-sulphate of aluminum from Utah. *Am. Mineral.*, **25,** 213–214.

SCHRAUF, A., (1891), *Jahrb. k.k. geol. Reichsanst*, **XLI,** 380.

SPENCER, L. J., (1897), A list of New Mineral Names. *Min. Mag.*, **11,** 335.

WYCKOFF, R. W. C., (1960), Crystal Structure, Vol. **III.** ch. X.

Paper II–S2. X-Ray Diffraction Examination of Portland Cement Clinker*

(H.G.) MIDGLEY D.Sc. 1967.

H. G. Midgley, D. Rosaman, and K. E. Fletcher

Synopsis

Two methods of determining the mineral composition of portland cement clinker are discussed, both of which depend on X-ray diffraction analysis. The first is a modified method of compound calculation from the oxide chemical analysis, knowing the composition of the ferrite phase from an X-ray diffraction analysis. The second is compound analysis by direct X-ray powder diffraction using a counter spectrometer.

A comparison between the modified calculation, direct diffractometry and the more usual Bogue method shows that there is a better agreement between the first two than between the latter and either of the first two.

The greatest errors in the Bogue method appear in those cements with the lowest C_3A. In these cements the ferrite appears to be richest in C_2F which makes the Bogue estimate of C_3A too low. In these cases the direct diffractometry is not yet entirely satisfactory, owing to interference.

Résumé

Cet exposé présente la discussion de deux méthodes pour déterminer la composition minérale du clinker de ciment Portland; toutes deux dépendent de l'analyse à l'aide de la diffraction des rayons X. La première est une méthode modifiée du calcul des composés à partir de l'analyse chimique des oxydes lorsque la composition de la phase ferrite est connue grâce à une analyse à l'aide de la diffraction des rayons X. La seconde, qui utilise un spectromètre à compteur Geiger, est une analyse des composés par diffraction directe des rayons X par la méthode à poudre.

Une comparaison entre le calcul modifié, la diffractométrie directe et la méthode de Bogue plus habituelle, montre qu'il y a du meilleur accord entre les deux premières qu'entre cette dernière et l'une ou l'autre des deux premières.

Dans la méthode de Bogue les plus grandes erreurs se montrent avec les ciments de moindre teneur en C_3A. C'est dans ces ciments que le ferrite semble être le plus riche en C_2F, ce qui rend trop basse l'évaluation de Bogue. Dans ces cas-ci la diffractométrie directe n'est pas encore complètement satisfaisante à cause d'interférence.

Zusammenfassung

Zwei Methoden für die Bestimmung der Mineralzusammensetzung der Portlandzementklinker, die beide auf einer Analyse der Röntgenstrahlenbeugung beruhen, werden erörtert. Die erste Methode ist eine Spezialberechnungsmethode, die man anwenden kann, wenn man die chemische Oxydanalyse und die Zusammensetzung der Ferritphase von einem Röntgenstrahlenbeugungsdiagramm kennt. Die zweite Methode ist eine Verbindungsanalyse durch eine direkte Herstellung eines Röntgenpulverdiagramms, in der man ein Spektrometer mit Zähler benutzt.

Ein Vergleich zwischen der modifizierten Berechnung, der direkten Beugungsmessung und der gewöhnlich angewandten Bogue Methode zeigt, daß die ersten beiden Methoden besser miteinander übereinstimmen, als mit der Bogue Methode.

Die größten Fehler treten in der Bogue Methode bei Zementen mit kleinsten C_3A-Gehalten auf. In diesen Zementen ist der Ferrit augenscheinlich im C_2F angereichert, und das bringt hervor, daß die Bogue Abschätzung zu klein ausfällt. In diesen Fällen ist die direkte Beugungsmessung noch nicht ganz zufriedenstellend, da Interferenz auftritt.

Introduction

The normal Bogue [1][1] method of calculating the compound content of a cement assumes that there is complete combination between raw materials at maximum temperature in the kiln, and that the clinker formed is cooled slowly so that chemical equilibrium is maintained. The formulae for the Bogue system show the four constituents to be linear mathematical functions of the chemical analysis. As a result, if some property such as strength is to be related statistically to composition, it follows from the mathematics that an analysis in terms of the Bogue constitution is no more informative than one in terms of the simple oxide analysis but it gives a more enlightened picture of the function of chemical composition in cement technology.

As a result of the study of the quaternary system CaO-SiO_2-Al_2O_3-Fe_2O_3 by Lea and Parker [2] it became possible to correct the Bogue treatment for possible deviations from equilibrium which might result from rapid cooling or separate crystallisation of that part of the clinker which had been liquid at the burning temperature.

In drawing up formulae for calculating compound composition it is assumed that the minerals

*Fourth International Symposium on the Chemistry of Cement, Washington, D.C., 1960. Contribution from the Building Research Station, Department of Scientific and Industrial Research, Watford, England.

[1] Figures in brackets indicate the literature references at the end of this paper.

identified in cement clinker are exactly the same as those found in phase rule studies using pure chemicals. This leads to two sources of error. Firstly, in real cement there are present the so-called minor constituents such as alkalis, FeO, MnO, and SO_3; these alter the relationship between the main cement compounds and, by entering into solid solutions with them, alter their nature as well as the amount present. Secondly, even in pure mixtures the cement compounds dissolve in each other to some extent.

Examples of the first kind are given by Welch and Gutt [3]. The best known example of the second is shown by the fact that the iron compound is not necessarily C_4AF, but a member of a solid solution series of variable composition [4–7].

To overcome these difficulties, either the composition of the ferrite must be determined before calculation, or a direct method of estimating the cement minerals must be employed. The only suitable way available for either ferrite composition determination or direct compound determination is X-ray powder diffraction. Midgley [8, 9] has shown that the ferrite composition may be determined by reference to the parameters of the ferrite solid solutions; Von Euw [10] and Copeland et al., [11] have shown that X-ray diffraction methods may be used to determine the phase composition. When the ferrite composition is known the oxide chemical analysis may be used to calculate the phase composition in the modified Bogue method as follows. First the composition of the ferrite phase is determined from powder X-ray data; all the Fe_2O_3 in the chemical analysis is assigned to $2CaO{\cdot}Fe_2O_3$ with which the appropriate amount of CaO and Al_2O_3 are then combined to give the ferrite composition determined. The remaining Al_2O_3 is assigned to C_3A; then the remaining CaO and SiO_2 are combined in the normal Bogue manner to form $3CaO{\cdot}SiO_2$ and $2CaO{\cdot}SiO_2$.

This paper will present investigations by X-ray methods into the two important questions, determination of ferrite composition and direct measurement of phase composition by X-ray powder diffractometry.

Measurement of Ferrite Composition

It is usually accepted that the ferrite phase in portland cement lies in the solid solution range C_6AF_2-C_6A_2F. The determination of the composition of this phase is not possible by chemical analysis for it is impossible to separate the ferrite from the other cement phases. It is therefore necessary to use an indirect physical measurement as an indication of the composition. Three possible physical properties that might be used are refractive index, magnetic susceptibility and X-ray diffraction. Parker and Ryder [12] used the refractive index method to determine the composition of ferrites in high-alumina cement clinkers, but unpublished data of Midgley and Ryder [13] did not give reliable results for portland cement clinker. Magnetic susceptibility measurements have not been used on portland cement clinker, for although Malquori and Cirilli [6] showed that there was a direct relationship between ferrite composition and magnetic susceptibility, the measurement of susceptibility of a cement would not give a measure of composition without knowing how much of the constituent was present. In the case of portland cement clinker both composition and quantity are equally unknown. There remains the X-ray diffraction method. It was shown by Midgley [8] that the composition of the ferrite phase could be determined from the lattice parameters measured in the powder X-ray diffraction pattern.

Three methods of measuring these parameters have been suggested: firstly on a magnetically separated fraction [8, 9] by measuring the 202 reflection at 1.94 A; secondly on the normal cement clinker by measuring the 141 reflection at 2.63 A [11, 14]; or thirdly, on a chemically separated fraction [15].

Nothing more need be said about the first two methods but the third method due to Fratini and Turriziani has been further investigated and the results are given below.

Fratini and Turriziani described a reagent consisting of 25 cm^3 water, 65 cm^3 ammonia, and 10 g ammonium citrate which preferentially dissolves the silicates from portland cement, leaving a residue consisting mainly of C_3A and ferrite. They used the method in order to obtain better X-ray powder diffraction patterns of the ferrite phase than was possible from the original cement.

The treatment they describe consists of shaking 1 g of the sample of cement with 100 cm^3 of the reagent for 12 hr. The solution is decanted from the residue and the residue shaken with a further 100 cm^3 of reagent for a further 12 hr. The residue is filtered off on a sintered glass crucible, washed rapidly with ammonia and dried at 110 °C. Their residue varied between 34 and 38.7 percent.

Keil and Gille [16] have pointed out that the aluminates are more sensitive to attack than the aluminoferrites, while Fratini and Turriziani [15] indicate that the aluminoferrites become less sensitive to attack with increasing iron content. The latter authors found that brownmillerite, ground just to pass a 178 mesh sieve, dissolved up to a maximum of 6 percent in 12 hr and that the X-ray pattern of the residue was similar to that of the original sample.

Data for the solubility of three ferrites, C_6AF_2, C_4AF and C_6A_2F, have been redetermined and the results are given in figure 1. The rate of solubility for C_3A is even greater than for C_6A_2F. Despite this, the method does give a concentration of the ferrite and C_3A phases in portland cements. Fratini and Turriziani suggest that the ferrites in

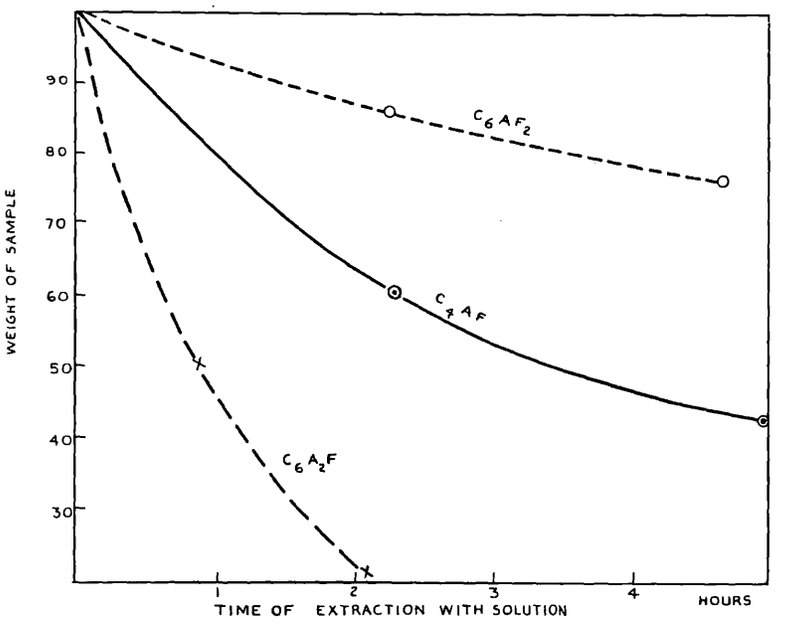

FIGURE 1. *Comparative rates of solution of ferrites (1g solid/100 cm³).*

TABLE 1. *Weight percent of C_2F in 15 clinkers, determined by three methods*

Clinker	Camera; magnetic fraction (1958)	Direct X-ray diffraction	X-ray diffraction after Fratini and Turriziani extraction	
	202 reflection	141 reflection	141 reflection	202 reflection [a]
A. 9	56	54	52	48
A. 10	65 39 (52)	56 47 (51)	60 54 (57)	50 42 (46)
A. 20	66	60 48 (54)	61 51 (56)	No distinct peak.
A. 35	71 39 (55)	57	58 53 (55)	50
A. 36	74 39 (57)	56 48 (52)	50	48
A. 37	66	63 47 (55)	56	46 35 (40)
A. 39	66	50	54 50 (52)	49 41 (45)
A. 40	66	63 52 (57)	56	46
A. 143	65 39 (52)	59 50 (55)	56 48 (52)	48 42 (45)
A. F	56	73 59 (66)	64	62
A. 141	65 39 (52)	62 50 (56)	63 55 (59)	45
A. 7	54 39 (47)	64 46 (55)	62 52 (57)	No distinct peak.
A. 5	54 39 (47)	62 54 (58)	54	48
A. 33	71 39 (55)	68 51 (59)	63 57 (60)	37 33 (35)
A. 113	----------	70 54 (62)	70 46 (58)	66 46 (56)

[a] The use of the 202 reflection is not very satisfactory for the diffractometric techniques of using KBr or Si as an internal standard. Both KBr and Si give peaks close to the ferrite 202 region; i.e., ferrites (46.6–47.5)° 2θ; KBr 45.60°2θ, 47.74°2θ; Si 47.30°2θ.

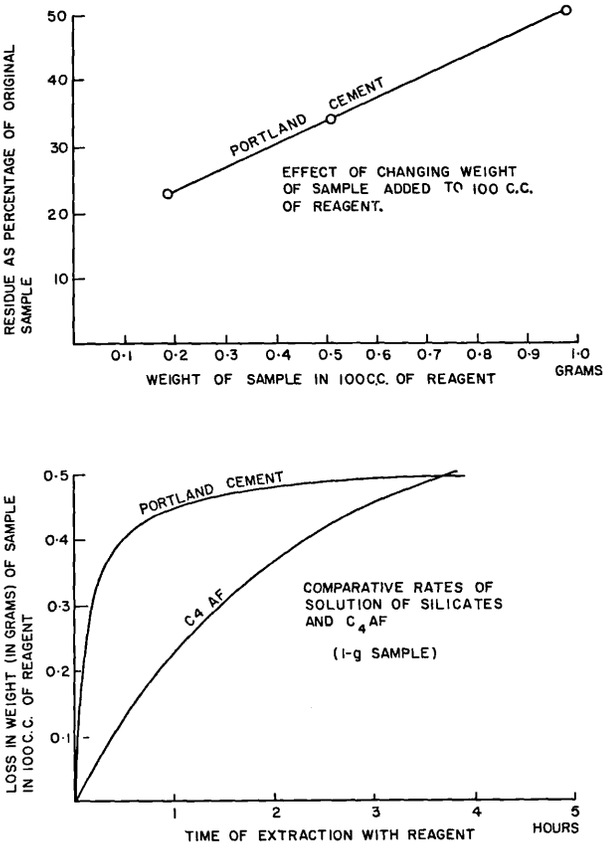

FIGURE 2. *Comparative rates of solution of silicates and C_4AF.*

portland cement are protected from attack by the silicate phases. We would suggest the much more rapid dissolution of the silicate phase can effectively deactivate the reagent before solution of the other phases has proceeded to any extent.

Further work on the chemical method has been carried out, and we have found that a single extraction carried on for about three hours can leave a residue of about 22 percent whose X-ray diffraction pattern indicates the complete removal of crystalline silicate phases. This is effected by reducing the initial concentration of the sample in 100 cm^3 of reagent to about 0.2 g (fig. 2).

The three methods outlined above have been tried on 15 of the cements originally investigated by Midgley [8] and the results are given in table 1. The experimental error in the composition is about ± 3 percent C_2F.

The results given by magnetic separation, by direct diffractometry, and those given by the 141 reflection after chemical separation agree reasonably, but the results given by measurement of the 141 and 202 reflection on the same sample disagree badly. This discrepancy may be due to solid solution with some other component such as MgO.

Direct Determination of Cement Composition by X-ray Diffractometry

The method used for the quantitative estimation of cement compounds is based on the fact that the integrated intensity of a reflection produced by X-ray powder diffraction is directly proportional to the amount of the substance producing it [17, 18].

In the method reported here the integrated intensity of the diffracted beam is recorded by a ratemeter using a Geiger-Müller tube. The different diffracted beams are recorded on a ratemeter recorder plotting intensity against 2θ; thus the integrated intensity can be measured as the area under the peak produced. The apparatus used is the commercial Dutch Philips Diffractometer. To obtain a reasonably small standard deviation of the integrated intensity the powder sample for the diffractometer must be ground to less than 5μ. Various methods are available to carry out the grinding; agate pestle and mortar, ball mills, or vibratory mills, but experience has shown that all these methods either take too long or require too large a sample. To overcome these difficulties a miniature vibratory rod mill (fig. 3) has been designed and built at the Building Research Station, which will grind 0.3 g of sample in isopropyl alcohol to less than 5μ in 2 hr.

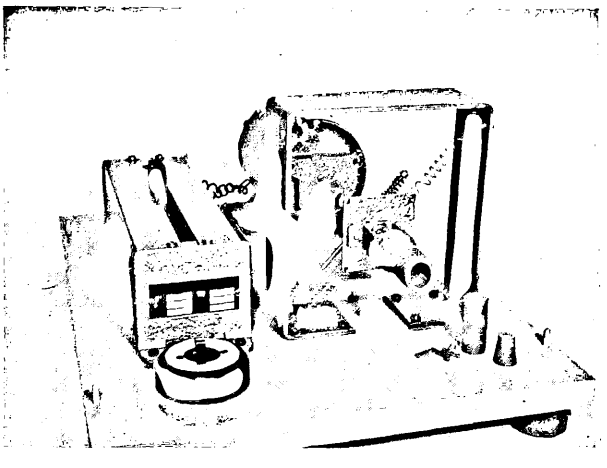

FIGURE 3. *Vibratory micro-rod mill.*

It is usual to compare all intensities with that produced by a fixed proportion of a suitable internal standard. This eliminates differences which might arise from sample to sample due to the method of preparation. It was found that a 12 to 1 weight ratio of sample to potassium bromide was satisfactory. In only one case has potassium bromide proved unsatisfactory as an internal standard, namely, for a cement containing calcium chloride. It is for such cases that silicon as an internal standard would be preferable. Silicon is much more difficult to grind than potassium bromide and if the sample is not equally ground, segregation may occur and there will be discrepancies in the diffraction intensities produced. The micro rod mill will adequately handle silicon mixes.

The samples were prepared by a loose packing method in a standard sample holder to avoid preferred orientation.

Mechanical mixtures of the four main cement minerals, alite, β-dicalcium silicate, tricalcium aluminate, and ferrite were made. After repeated diffractometer traces, the average integrated intensity of the compound (I_C) divided by the integrated intensity of the potassium bromide peak (I_{KBr}) was plotted against the percentage of the compound present; these were the calibration graphs.

In preparing the calibration graphs sixteen mixtures were used, eight containing alite, C_2S, C_3A, and C_4AF, four containing C_3A and C_3S, one containing alite, β-C_2S, and C_3A and three containing alite and C_3A. The standardization was complicated by the presence of C_3A in the alite used. In work on the ferrite phase it was found that, as a first approximation, the calibration for C_4AF could be used for ferrites of slightly different composition. The calibration was extended to the range C_6AF_2–C_6A_2F. The calibration constant for a composition within the range can be found by interpolation.

The peaks used for the particular compounds were as follows:

CuKα radiation,

Alite 29.4° 2θ=3.04 A
Alite 30.0° 2θ=2.98 A
β-C_2S 31.1° 2θ=2.87 A
C_3A 33.2° 2θ =2.699 A
C_4AF 33.5°—33.85° 2θ=2.67A.

The calibration graphs obtained were all straight line plots passing through the origin.

Any interference due to adjacent peaks was allowed for in the graphical interpretation of the resulting pattern. In interpreting the patterns produced by cements, frequent reference is made to the original standard patterns, and also to superimposed patterns of the four main cement compounds.

The peak due to C_2S at 31.1° 2θ is weak and we have attempted a different treatment for estimating C_2S. At 32.6° 2θ and 34.4° 2θ peaks occur which are due to C_2S and alite. The total intensity is the sum of the individual intensities. Standard graphs were prepared relating I/I_{KBr} and percent alite for these two peaks in the absence of C_2S, and standard graphs relating I/I_{KBr} and percent C_2S for these two peaks in the absence of alite. The latter was checked by examining standard patterns in which both alite and C_2S were present and subtracting the contribution due to alite alone.

The method used for cements would be to estimate alite from the peaks at 29.4° 2θ, and 30.1° 2θ, and to subtract the intensity due to alite alone from the total intensity at 32.6° 2θ and 34.4° 2θ. The amount of C_2S is determined from the residual intensity. We do not always get good agreement between the three results obtained for C_2S and at the moment our data for the peak at 34.4° 2θ are suspect. Two simultaneous equations can be written for the interfering peaks and solved for alite and C_2S. These results are not always in good agreement with results obtained on the other peaks, and have only been used in interpreting patterns obtained from set portland cement mortars when the line due to alite at 29.4° 2θ can be obscured by calcite whose main peak occurs at the same position.

At the moment there is some difficulty in determining low C_3A contents in the presence of high ferrite content since severe ferrite and β-C_2S interference means that no definite C_3A peak need be apparent, and at the time of writing this has not been solved to our complete satisfaction.

Using the methods outlined in this note and scanning each sample three times the following coefficients of variation of the mean were obtained:

Alite, 5 percent
β-C_2S, 11 percent
C_3A, 3 percent
Ferrite, 6 percent

The methods outlined have been used on two series of cements, one of old cements (some more than 25 years old) used by Midgley [8] in his work on ferrites, and a second series of modern British portland cements of various kinds.

Result of X-Ray Examination of Cements

The results given by the three methods of compound determination are given in tables 2 and 3.

TABLE 2. *Compound composition of old cement clinkers*

Compounds \ Cement No.		A.40	P. 893	A.5	539 S. R. P. C.	540 S. R. P. C.	520	512	Dg
Alite	Diff [a]	65	58	59	56	39	59	53	50
	Mod	70	68	61	52	31	46	53	36
	Bogue		66		56	34.5			
β-C_2S	Diff	13	16	11	17	32	16	21	30
	Mod	7	7	9.1	20	41	29	22	37
	Bogue		8		17	38.3			
C_3A	Diff	11.5	3.7	13.5	4.8	4.5	11	12.1	14
	Mod	9.5	5.8	15.4	3.0	4.7	9.6	10.7	15
	Bogue		2.5		0.7	0.9			
Ferrite	Diff	8.5	17.5	10.5	17.5	16.5	6.4	8.8	9
	Mod	9.2	15.2	10.2	17	16.6	6.2	6.3	10
	Bogue		18		19	19.3			
Ferrite comp., wt % C_2F by diffractometer 141 reflection		57	66	54	62	67	56	56	56

(N.B. Where the C_2F content is nearly equal to C_4AF no modified calculation is shown as it would be the same as by the Bogue calculation.)

[a] Diff =by Diffractometer
Mod =by Modified Bogue calculation
Bogue=by Bogue calculation

TABLE 3. *Compound composition of modern British cement clinkers*

Compounds \ Cement No.		(1)	(2)	(3)	(4)	(5)	(6)	(7)	(8)	(9)
		572 O.P.C.[a]	625 O.P.C.	580 R.H.P.C.	615 O.P.C.	561 O.P.C.	569 O.P.C.	597 L.H.P.C.	592 O.P.C.	A. S. R. S.R.P.C.
Alite	Diff	53	54	49	53	43	60	35	53	55
	Mod	47	42.5	44	48	42.5	48	26	56	50
	Bogue		42			42			55	53
β-C_2S	Diff	24	24	27	23	30	27	45	23	17
	Mod	28	25	32	23	29	29	49	21.5	20
	Bogue		26			30			22	18
C_3A	Diff	9.3	12.8	8.3	14.5	9.8	9.7	8.8	9.7	3.6
	Mod	8.4	12.1	8.8	13.1	10.0	9.5	9.2	9.1	4.0
	Bogue		12.9			10.9			9.7	0.9
Ferrite	Diff	9.5	11.0	6.2	9.0	12.5	7.6	6.9	7.5	17.5
	Mod	9.2	9.9	6.6	7.3	9.7	6.3	6.6	6.1	17.1
	Bogue		9.2			9.0			5.6	19.6
Ferrite comp., wt % C_2F		56	52	56	56	52	56	56	51	64

[a] O.P.C. = Ordinary portland cement
R.H.P.C. = Rapid hardening portland cement
L.H.P.C. = Low heat portland cement
S.R.P.C. = Sulfate resisting portland cement

Conclusions

Although all three methods of estimating the compound composition of portland cement clinker are still subject to errors, there appears to be a better agreement between the modified method of calculation from chemical analysis and direct diffractometry, than between the Bogue method and either of the other two.

The great errors in the Bogue method appear in those cements with the lowest C_3A. In these cements the ferrite appears to be rich in C_2F, making the Bogue estimate of C_3A too low.

The diffractometry measurement of C_3A in these cases (539, 540, A.S.R.) is not yet satisfactory but the modified calculation shows agreement with the diffractometer estimate.

References

[1] R. H. Bogue (1929), Calculation of compounds in portland cement, Ind. Eng. Chem. Anal. Ed. **1,** 192–7.

[2] F. M. Lea and T. W. Parker (1935), The quaternary system CaO–Al_2O_3–SiO_2–Fe_2O_3 in relation to cement technology, Building Research Technical Paper **16.**

[3] J. H. Welch and W. Gutt (1960), The effect of minor components on the hydraulicity of the calcium silicates, This symposium, Paper II–S1.

[4] N. A. Toropov, L. D. Markov, and N. A. Shishakov, (1937), The binary system $5CaO{\cdot}3Al_2O_3$-$4CaO{\cdot}Al_2O_3{\cdot}Fe_2O_3$ (in Russian), Tsement No. 1, 28.

[5] T. Yamauchi (1938), A study on the celite part (in Japanese),
I. The system CaO-Fe_2O_3, J. Japan. Ceramic Assoc. **45,** 279.
II. Brownmillerite **45,** 361–375.
III. The system $3CaO{\cdot}Al_2O_3$-$2CaO{\cdot}Fe_2O_3$, **45,** 433–436.
IV. The system $5CaO{\cdot}3Al_2O_3$-$2CaO{\cdot}Fe_2O_3$, **45,** 614–631.
V. System $3CaO{\cdot}Al_2O_3$-$5CaO{\cdot}3Al_2O_3$-$2CaO{\cdot}Fe_2O_3$, **45,** 880–896.
VII. Systems CaO-Al_2O_3-Fe_2O_3 and CaO-Al_2O_3-Fe_2O_3-SiO_2, **46,** 66.

[6] G. Malquori and V. Cirilli (1954), The ferrite phase, Third International Symposium on the Chemistry of Cement, London, 1952, pp. 137–150.

[7] M. A. Swayze (1946), A report on studies of (1) the ternary system CaO-C_5A_3-C_2F, (2) the quaternary system CaO-C_5A_3-C_2F-C_2S; (3) the quaternary system modified by 5 percent magnesia, Am. J. Sci., **244,** pt 1, 1–30, pt 2, 65–94.

[8] H. G. Midgley (1954), Contribution to paper on the ferrite phase, Third International Symposium on the Chemistry of Cement, London, 1952, pp. 140–143.

[9] H. G. Midgley (1958), The composition of the ferrite phase in portland cement, Mag. Concrete Research, **10** (28), 13–16.

[10] M. Von Euw (1958), Analyse quantitative des clinkers de ciment portland par les rayons X, Silicates Inds. **23,** 643–9.

[11] L. E. Copeland, S. Brunauer, D. L. Kantro, E. G. Schulz, and C. H. Weise (1959), Quantitative determination of the four major phases of portland cement by combined X-ray and chemical analysis, Anal. Chem. **31,** 1521–1530.

[12] T. W. Parker and J. F. Ryder (1954), private communication.

[13] H. G. Midgley and J. F. Ryder (1954), private communication.

[14] H. G. Midgley (1957), A compilation of X-ray powder diffraction data of cement minerals, Mag. Concrete Research **9** (25), 17–24.

[15] N. Fratini and R. Turriziani (1956), Esame rontgenografico della fase ferrica del cemento portland, La Ricerca Sci. **26,** 2747–2751.

[16] F. Keil and F. Gille (1939), Über das Verhalten von Schlackengläser gegen Ammon- und Aminosalze organischer Säuren, Zement **28,** 429.

[17] L. Alexander and H. P. Klug (1948), Basic aspects of X-ray absorption, in quantitative diffraction analysis of powder mixtures, Anal. Chem. **20,** 886.

[18] L. E. Copeland and R. H. Bragg (1958), Quantitative X-ray diffraction analysis, Anal. Chem. **30,** 196.

Discussion*

D. L. Kantro, L. E. Copeland, and Stephen Brunauer

Quantative Analysis of Portland Cements by X-rays

Over the past few years, experimental work has been performed at a number of laboratories throughout the world in an effort to apply the method of X-ray quantitative analysis to portland cement. Much of this work has already been discussed by Dr. Nurse. However, at the time of his writing, Dr. Nurse did not have at his disposal our paper on an extension of our previously published quantitative method combining X-ray and chemical data [1][1] to the pure X-ray method [2]. We should like to discuss the results of this latter work, including data heretofore unpublished, on a recently analyzed group of cements. In addition, we should like to present a few sidelights arising from our investigations in this field.

Experimental Problems in X-ray Cement Analysis

The X-ray diffraction pattern of a portland cement involves many complexities. A portion of a pattern of a normal portland cement is reproduced in figure 1. A number of strong lines are evident, one of which, at 2.71 A (33°2θ) represents tricalcium aluminate, and one, in the vicinity of 2.67 A (33.7°2θ) represents the calcium aluminoferrite solid solution phase.[2] The ferrite and aluminate lines overlap, so that the area designated as "tricalcium aluminate peak" in figure 1 contains a considerable contribution from the ferrite phase. In spite of this serious overlap problem, we had to use these lines, because we were unable to find other lines of either of these materials sufficiently strong and sufficiently unhampered as to be useful for quantitative analysis.

The ferrite-aluminate overlap problem is complicated by the fact that the amount of overlap depends upon the composition of the ferrite solid solution phase. This composition can be expressed in terms of the A/F ratio of the phase. The d-spacings of the ferrite phase lines are dependent on the A/F ratio, and may be used for the evaluation of this quantity. For the whole cement, only the line at 2.67 A may be used, but if the cement is fractionated, either chemically [3,4] or magnetically [3], other lines may be used. However, there is always the possibility of a disproportionation in a separation procedure, if the ferrite phase is not homogeneous. The A/F ratio may also be evaluated from combined X-ray intensity and chemical data [1]. In a pure X-ray method, however, a d-spacing determination must be used.

The other strong lines in the pattern shown in figure 1, besides the silicon line, are due to the calcium silicates. Actually, each of these strong lines contains a contribution from each of the silicates: only a weak line, at 31°2θ, is due to but one of the silicates, β-dicalcium silicate. Thus, a serious overlap problem exists for the silicates as well. However, because of the relatively numerous strong lines of these constituents of portland cement, some selection of lines is possible.

Thus, there are three basic experimental problems associated with the X-ray quantitative analysis of portland cement. These are: (1) resolution of the C_3A and ferrite phase lines, (2) precise determination of the d-spacing of a ferrite line, and (3) selection of suitable silicate lines. It would seem that the differences in results reported by various investigators are based on the different attacks on these three basic problems.

There is a fourth problem, though not as serious as those enumerated above, the selection of a suitable internal standard. Von Euw [5] used the 2.81 A line of NaCl; Midgley, Rosaman, and Fletcher [3] used the 3.30 A line of KBr. During the first year of our investigations we also used the latter as the internal standard, but we discarded it later in favor of the 3.14 A line of silicon. Because of the height of the KBr peak relative to the heights of the cement compound peaks, a weight ratio of 0.05 g of KBr/g of cement was used; when we substituted silicon, we could use twice as much internal standard. This has resulted in a larger area for the silicon line, and

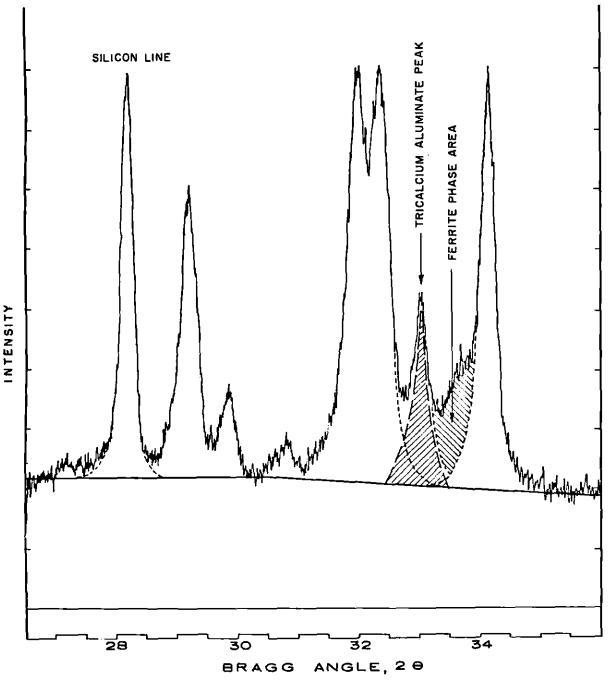

FIGURE 1. *X-ray diffraction pattern of a portland cement.*

* This discussion discusses papers II-1, "Phase Equilibria and Constitution of Portland Cement Clinker" by R. W. Nurse, and II-82, "X-Ray Diffraction Pattern of Portland Cement Clinker" by H. G. Midgley, D. Rosaman, and K. E. Fletcher.

[1] Figures in brackets indicate the literature references at the end of this paper.

[2] All angles refer to locations of reflections obtained with CuKα radiation.

in an improved precision of the data. In addition, it was not infrequent that we obtained anomalously high peaks with KBr, perhaps because of concentration of KBr in the surface layer of the mixture. Whatever the cause, this difficulty has not bothered us since we use silicon with the technique described earlier [2].

Calibration With the Internal Standard

In general, the calibration procedure is to observe intensity ratios for known weight ratios of cement compound to standard. However, it is equally important that the characteristics of the patterns from which the calibration data are obtained are as nearly like those of cement patterns as is possible. This is necessary not only because of the overlap between ferrite and C_3A lines, but also, as will be seen later, because we could not obtain linear relationships between relative intensities of lines and weight ratios of the silicates. Thus, one cannot simply make binary mixtures of each cement compound with internal standard and get usable data. Von Euw [5], Midgley and his coworkers [3] and ourselves [1] have all calibrated from mixtures of the cement compounds in proportions such as occur in portland cement.

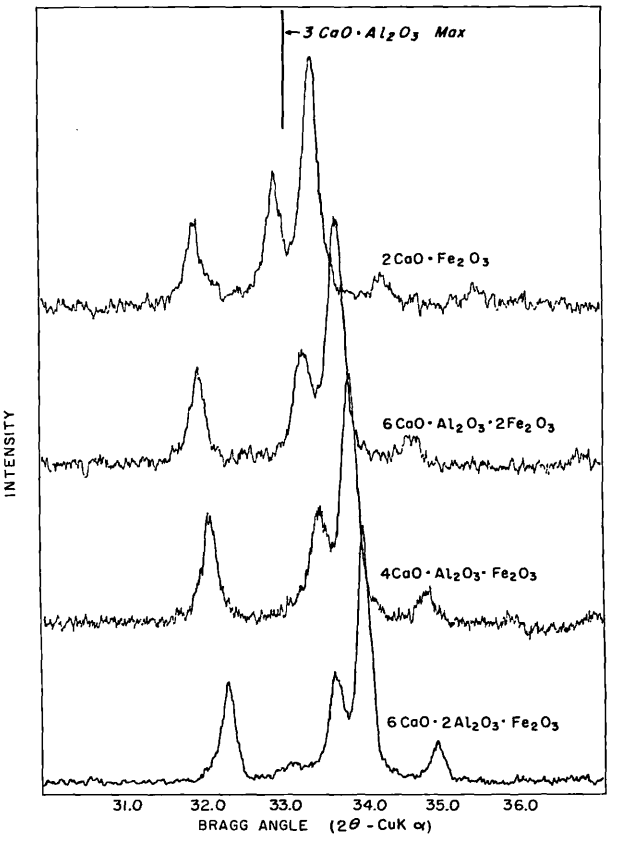

FIGURE 2. *X-ray diffraction patterns of calcium aluminoferrites.*

1. The calibration of the ferrites and aluminates requires, as was pointed out above, a consideration of the complex overlap situation that exists. As a first approximation, one may consider that the overlap correction may be obtained by a simple graphical procedure such as is illustrated in figure 1. Such a graphical procedure was used by Midgley, Rosaman, and Fletcher [3]. If this is the case, the calibration equations would take the form

$$\frac{P_F}{P_0}=\mu\frac{I_F}{I_0}=\mu R_F \qquad (1)$$

where P_F/P_0 is the weight ratio of ferrite to internal standard, μ is a proportionality constant, and R_F is the intensity ratio of the ferrite line to the standard line.

On the other hand, the fact of the matter is that the ferrite region, actually composed of two ferrite lines, may strongly overlap the C_3A line and extend to even lower angles than that at which the C_3A peak occurs, as can be seen from figure 2. Thus, there may be an intensity contribution to the apparent C_3A peak which cannot easily be corrected graphically. As a second approximation, then, some equation may be set up to account for this phenomenon. We have adopted an empirical form

$$\frac{P_F}{P_0}=\mu[R_F+g(\nu)R_A] \qquad (2)$$

where $g(\nu)$ is a function of ν, the molar A/F ratio, and R_A is the intensity ratio of the C_3A line to standard line.

Midgley, Rosaman, and Fletcher [3] found it expedient in their calibration to use C_4AF to represent all of the ferrites. As a first approximation, over a narrow molar A/F ratio range about unity, this is a simple and straightforward approximation, represented by eq (1) with μ independent of A/F ratio. Over the entire range of A/F values from 0 to 2, however, μ is not independent of A/F. Smith [6] has shown that there are A/F-ratio dependent intensity variations in ferrite diffraction lines, these variations being the results of crystallographic changes in symmetry caused by the substitution of aluminum for iron in C_2F. The dependence of μ on A/F ratio is of course a result of this phenomenon, and is illustrated in figure 3, the data for which were obtained from binary mixtures of C_2F, C_6AF_2, C_4AF and C_6A_2F with silicon. With the dependence of μ on A/F ratio taken into consideration, eq (2) becomes

$$\frac{P_F}{P_0}=g_1(\nu)[R_F+g_2(\nu)R_A] \qquad (3)$$

where $g_1(\nu)$ and $g_2(\nu)$ are both empirical functions of ν, the A/F ratio. The use of such an equation

avoids introduction of a systematic error proportional to the deviation of the A/F ratio from unity, which would result from the assumption of a μ value independent of the A/F ratio.

A similar expression may be set up for C_3A, wherein, however, the quantity μ' is independent of A/F ratio. Thus

$$\frac{P_A}{P_0}=\mu'[R_A-f(\nu)R_F] \tag{4}$$

where P_A/P_0 is the weight ratio of C_3A to internal standard and $f(\nu)$ is some empirical function of the A/F ratio. In this equation R_A is corrected for the overlapping ferrite line in such a way that systematically high C_3A results are avoided in low overall A/F ratio cements.

2. The calibration of the silicates presents a different problem. As was stated before, all of the strong lines of either silicate coincide with lines of the other.

There is a reasonably strong line at 29°2θ, which is predominantly a C_3S line, though C_2S also makes a contribution to it. For equal weights of C_3S and C_2S, the contribution of C_3S to the intensity of the line is about 8 times that of C_2S. Midgley, Rosaman, and Fletcher [3], as well as Von Euw [5], have used this line for their determinations of C_3S. Neglect of the β-C_2S contribution to this line by Von Euw introduces only a small error for cements high in C_3S, but somewhat more significant errors for low C_3S cements (type IV).

At the beginning of our investigations we also used the same line, though we always considered the contributions of both C_3S and C_2S to the line. We discarded the line later because we found that calcium sulfate hemihydrate and gypsum, with strong lines at 2.98 A and 3.06 A, respectively, made significant contributions to the intensity of the line [7]. At the suggestion of Katharine Mather, we adopted the line at 51°2θ, instead.

There is a rather weak line at 31°2θ, which is a pure C_2S line. Midgley, Rosaman, and Fletcher, as well as Von Euw, have used this line for their determination of C_2S. We also tried this line, but found it unsatisfactory. Von Euw found it so unsatisfactory that he did not report any C_2S results in his paper. Midgley and his coworkers used the 32 and 34°2θ C_3S-C_2S lines, in addition to the 31°2θ line, to evaluate C_2S. The three results did not always agree well, and they especially suspected the 34°2θ results. In our early work, we tried both the 32 and 34°2θ lines, and we did not find either line satisfactory.

In our final work, we have adopted the 41°2θ C_3S-C_2S line and the already mentioned 51°2θ line for the quantitative determination of C_3S and C_2S. The use of two lines permits the simultaneous solution of two equations of the type

$$\frac{I_1}{I_0}=\alpha_1\frac{w_1}{w_0}+\alpha_2\frac{w_2}{w_0} \tag{5}$$

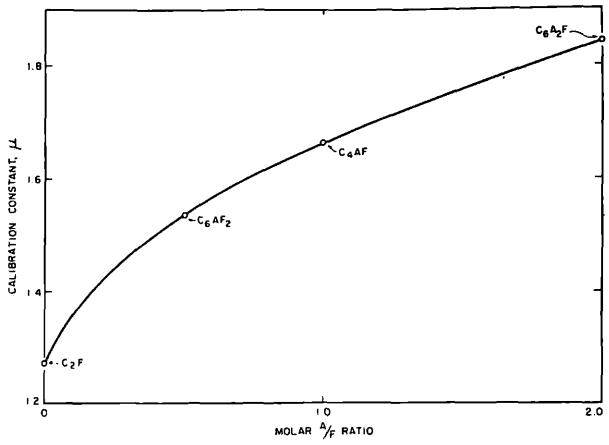

FIGURE 3. *Dependence of ferrite calibration constant on molar A/F ratio.*

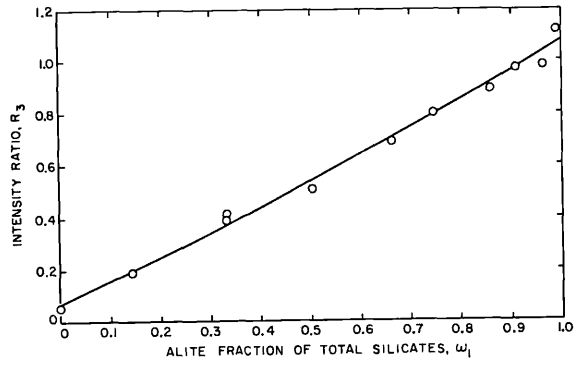

FIGURE 4. *Dependence of ratio of intensities of 51° 2θ line to 41° 2θ line on relative amounts of alite and belite in silicate calibration mixtures.*

$$\frac{I_2}{I_0}=\beta_1\frac{w_1}{w_0}+\beta_2\frac{w_2}{w_0} \tag{6}$$

where I_1, I_2 and I_0 are the intensities of the two selected lines and the standard line, respectively. α_1, α_2, β_1, and β_2 are proportionality constants, and w_1/w_0 and w_2/w_0 are the weight ratios of C_3S and C_2S to standard, respectively. In our work, I_1 is the intensity of the line at 51.6°2θ, and I_2 that of the line at 41.1°2θ. I_0 is the intensity of the (111) silicon line (28.4°2θ).

Even though suitable lines are found from which interpretable X-ray data can be obtained, certain calibration problems still exist. It is not certain that the alite form of C_3S found in one cement is identical with that found in another cement; the same is true of the belite (C_2S) phase. That differences do exist is clearly shown by the results obtained when the calibration is carried out on preparations designed to give certain alite/belite ratios upon burning. These preparations were described previously [1]. On the basis of eqs (5) and (6) it can be shown that I_1/I_2, the ratio

of the 52°2θ line to the 41°2θ line should be a linear function of w_1, the alite fraction of the total silicates. A plot of I_1/I_2 $(=R_3)$ against w_1 is shown in figure 4. It can be seen that a curvilinear plot is obtained. This deviation from expectation indicates that there is a structural variation of either alite or belite or both as a function of composition. This was accounted for by the modification of eq (5) which we described in detail in an earlier publication [1]. Experimental evidence shows that the curvature of R_3 is caused by a curvature in I_1. Within experimental error, I_2 varies with composition in a linear manner.

The alite used for this work had the approximate composition $52C_3S{\cdot}C_6AM$, as contrasted to the composition $16C_3S{\cdot}C_6AM$ reported by Jeffery at the last symposium [8]. However, his results, and the results of other investigators, including ourselves, who have attempted to make alite of this composition indicated the presence of a significant amount of C_3A. We have prepared materials with overall A/S ratios of 1/52 ($52C_3S{\cdot}C_6AM$) which, while still demonstrating the alite diffraction pattern, contain negligible amounts of C_3A. These results are in quantitative agreement with those reported by Von Euw [5].

We have prepared alite using ferric oxide and magnesia instead of alumina and magnesia. The F/S ratio was 1/52. So far we have not investigated the iron stabilized alite, but it is clear that the presence of ferric oxide in alite may cause further complications.

Because of the possible variations in alite and belite structures due to the solution of different impurities, the calibration curves obtained for the silicates are not strictly applicable to the determination of alite and belite in portland cements. A somewhat better approximation is described in our second paper [2], in which the alite-belite results obtained for 20 portland cements by the combined X-ray and chemical analysis method were used for calibration purposes.

Analysis of Cements

Composition of the Ferrite Phase

The X-ray quantitative analysis of a cement is carried out in two steps: (1) determination of the composition of the ferrite phase and (2) determination of the amounts of the four major phases.

The results of the determinations of A/F ratio for 36 cements are given in table 1. The results are expressed in this table as molar A/F ratio, designated ν (columns 2, 3, and 4) and as mole percent C_2F, designated n (columns 5, 6, and 7). Values were obtained in two ways: (1) by determination of the d-spacing of the (141) ferrite line (ν_d and n_d, columns 2 and 5, respectively), and (2) by calculation from the intensity of this line and the total iron in the cement, as was described previously [1] (ν_1 and n_1, columns 3 and 6, respectively). The average values from these

TABLE 1. *Ferrite phase compositions in portland cements*

1	2	3	4	5	6	7
Cement	ν_d	ν_1	ν_{avg}	n_d %	n_1 %	n_{avg} %
LTS-11	0.733	1.362	1.047	57.7	42.3	48.9
LTS-12	1.000	1.000	1.000	50.0	50.0	50.0
LTS-13	1.212	----------	1.212	45.2	--------	45.2
LTS-14	0.980	----------	0.980	50.5	--------	50.5
LTS-15	1.150	0.738	.944	46.5	57.5	51.4
LTS-16	0.949	1.180	1.064	51.3	45.9	48.4
LTS-17	.764	0.928	0.846	56.7	51.9	54.2
LTS-18	1.445	1.129	1.287	40.9	47.0	43.7
LTS-19C	0.862	0.983	0.922	53.7	50.4	52.0
LTS-21	1.096	1.058	1.077	47.7	48.6	48.1
LTS-22	0.815	1.178	0.997	55.1	45.9	50.1
LTS-23	.740	0.641	.690	57.5	60.9	59.2
LTS-24	.984	.966	.975	50.4	50.9	50.6
LTS-25	.805	.765	.785	55.4	56.7	56.0
LTS-31	1.170	1.014	1.092	46.1	49.7	47.8
LTS-33	0.920	1.254	1.087	52.1	44.4	47.9
LTS-34	.838	1.214	1.026	54.4	45.2	49.4
LTS-41	.865	0.939	0.902	53.6	51.6	52.6
LTS-42	1.150	----------	1.150	46.5	--------	46.5
LTS-43	0.815	.979	0.897	55.1	50.5	52.7
LTS-43A	.923	1.122	1.023	52.0	47.1	49.4
LTS-51	.764	0.923	0.844	56.7	52.0	54.2
SBR-15754	1.440	----------	1.440	41.0	--------	41.0
SBR-15698	0.742	.450	0.596	57.4	69.0	62.7
SBR-15622	.709	.920	.814	58.5	52.1	55.1
SBR-15497	.897	.842	.869	52.7	54.3	53.5
SBR-15669	1.217	.974	1.096	45.1	50.7	47.7
LS-1	0.300	.452	0.376	76.9	68.9	72.7
LS-2	.300	.442	.371	76.9	69.3	72.9
B-H	.835	.651	.743	54.5	60.6	57.4
B-L	1.070	.830	.950	48.3	54.6	51.3
BR-A	0.880	1.156	1.018	53.2	46.4	49.6
BR-B	.894	1.050	0.972	52.8	48.8	50.7
BR-C	1.008	0.970	.990	49.8	50.8	50.3
BR-D	0.613	.659	.636	62.0	60.3	61.1
BR-E	.783	----------	.783	56.1	--------	56.1

two methods, ν_{avg} and n_{avg} are given in columns 4 and 7, respectively. The determination of ν_1 involves the solution of a quadratic equation. In a few cases, a real solution could not be obtained because of the occurrence of a negative discriminant. In such cases, no value for ν_1 is given.

The median value of ν_d for the first 27 cements listed in table 1 is 0.96; that for ν_1 (23 of the first 27 cements) is 0.98. The median of the average values for the first 27 cements is 1.00, while the average of the average values is 0.99. In terms of mole percent, the average values of n_d, n_1 and n_{avg} are 51.4, 51.1, and 50.7 percent. These n values correspond to ν values of 0.95, 0.96, and 0.97, respectively. The mean deviation from the average is 2.7 percent.

Because there is only one ferrite diffraction line in the cement pattern amenable to d-spacing determination, and because even this determination can become quite uncertain when only a small amount of ferrite phase is present, other investigators have developed methods for separating a cement fraction containing a high percentage of ferrite. Thus, there is the chemical separation method of Fratini and Turriziani [4] and the magnetic separation method of Midgley [9]. These methods permit unencumbered observation of weaker diffraction lines.

Midgley, Rosaman, and Fletcher [3] have employed the chemical separation method, the

magnetic separation method, and observations on the whole cement to determine the ferrite compositions for a group of 15 cements. They considered that their results by the magnetic separation method contained a bias on the C_2F side compared with results by the other techniques. This would indicate an inhomogeneous ferrite phase. Certainly a few cements are of this type as can be ascertained from the lack of sharpness of the (141) peak, as was pointed out by both Midgley [9] and ourselves [1]. Midgley, Rosaman, and Fletcher also observe, however, that their chemical separation results are in good agreement with the results from observation of the whole cement. At the same time they point out that the rate of solution of ferrite phase in the chemical medium used to dissolve away the silicates depends on the A/F ratio of the ferrite. On the basis of these two facts it would appear that the ferrite phase is homogeneous. Thus one may draw two conflicting conclusions from the results.

In spite of the claim of the C_2F bias of the results by the magnetic separation technique, only 7 of the 14 values reported indicate higher C_2F contents than the corresponding direct observation values, and 7 indicate lower C_2F contents. The molar A/F ratios corresponding to the mean weight percentages of C_2F for the 14 cements, obtained by magnetic separation, chemical separation and direct observation are 0.97, 1.00 and 1.00, respectively. These values are in excellent agreement with each other and are also in excellent agreement with our results.

One may, therefore, conclude that at least in the great majority of portland cements the ferrite phase is homogeneous. Because, however, there may be some cements in which the ferrite phase is not uniform [1, 9], it is safest to use the method of direct observation on the whole cement.

The constancy of A/F ratio after chemical extraction of the silicates, during which time a part of the ferrite phase is also dissolved, is consistent with the evidence presented by Copeland, Kantro, and Verbeck [10], showing that the A/F ratios of unhydrated residues of partly hydrated cement pastes are the same as those of the original cements.

The Quantities of the Four Major Phases

Analyses of 36 cements have been obtained by the combined chemical and X-ray method (CCX) [1] and by the method utilizing only X-ray data [2]. The primary calibration was that published by us originally [1], and the secondary calibration was that based on 20 of the 36 cements and published by us recently [2]. The results are given in table 2.

The conclusions based on the results from 36 cements are unchanged from those previously published. The CCX silicate data, given in columns 6 and 8 are those obtained by the total silica calculation described previously [1]. A comparison of the X-ray with the CCX results shows that the systematic errors of the pure X-ray ferrite,

TABLE 2. *Compositions of portland cements*

1	2	3	4	5	6	7	8	9
Cement	Ferrite, percent		C_3A, percent		C_3S, percent		C_2S, percent	
	CCX	X-ray	CCX	X-ray	CCX	X-ray	CCX	X-ray
LTS-11	7.5	9.2	8.4	7.6	57.3	60.0	19.0	19.9
LTS-12	7.3	7.3	7.9	7.9	51.0	48.3	27.4	26.0
LTS-13	7.0	8.3	6.8	6.8	50.2	53.8	27.6	29.7
LTS-14	9.0	11.1	3.2	3.2	57.1	55.2	26.0	25.1
LTS-15	7.4	6.0	9.9	10.4	60.9	63.5	12.5	13.0
LTS-16	11.0	11.7	4.3	3.9	54.5	58.7	22.8	24.5
LTS-17	8.8	9.6	7.6	7.3	58.6	53.4	20.2	18.5
LTS-18	7.9	7.6	7.4	7.6	52.5	53.2	26.5	26.9
LTS-19C	8.5	9.0	6.2	6.0	57.7	54.1	20.8	19.6
LTS-21	10.1	10.0	3.6	3.6	45.7	49.6	35.6	38.6
LTS-22	11.8	13.4	3.1	2.3	49.4	50.2	29.9	30.4
LTS-23	14.2	13.3	2.2	2.6	55.6	55.5	23.2	23.2
LTS-24	14.4	14.4	2.1	2.2	48.8	50.3	26.4	27.2
LTS-25	13.5	13.2	0.2	0.3	38.7	37.6	43.0	41.8
LTS-31	6.6	6.3	7.6	7.7	57.7	56.7	17.1	16.8
LTS-33	7.9	8.7	7.4	7.0	55.8	58.7	17.6	18.5
LTS-34	10.2	11.4	3.6	3.0	61.3	62.8	13.6	13.9
LTS-41	14.6	15.0	0.2	0.0	25.4	25.6	52.4	52.8
LTS-42	8.8	10.0	1.3	1.3	31.6	33.2	52.4	55.0
LTS-43	13.1	14.1	3.0	2.5	30.2	33.9	47.9	53.7
LTS-43A	9.5	10.1	1.6	1.2	29.9	30.2	53.6	54.1
LTS-51	9.4	10.1	0.6	0.2	49.7	48.2	36.4	35.2
SBR-15754	8.0	10.0	7.1	7.1	52.0	52.3	25.2	25.3
SBR-15698	6.2	5.0	8.3	8.7	65.0	54.2	16.4	13.6
SBR-15622	11.7	13.1	0.0	0.0	52.6	51.9	30.6	30.3
SBR-15497	7.5	7.2	8.9	9.0	55.6	59.2	16.2	17.3
SBR-15669	6.0	5.7	0.7	0.9	29.7	30.4	57.8	59.1
LS-1	11.5	13.1	.0	.0	65.3	66.8	17.9	18.3
LS-2	10.8	12.2	.0	.0	70.0	63.9	12.3	11.2
B-H	13.2	11.8	6.4	7.0	56.6	55.2	23.8	23.3
B-L	8.6	7.7	9.0	9.3	51.8	56.4	28.6	31.2
BR-A	6.8	7.6	11.8	11.5	44.1	42.9	26.8	26.2
BR-B	6.3	6.8	9.3	9.2	41.5	46.6	32.0	36.0
BR-C	8.5	8.4	7.1	7.2	39.5	43.8	35.9	39.8
BR-D	15.3	15.6	0.0	0.0	43.4	42.8	34.6	34.0
BR-E	0.8	2.3	6.4	6.4	59.0	56.8	31.1	29.9

C_3A, C_3S, and C_2S values relative to the CCX values are +0.5, +0.1, +0.3, and +0.5 percent, respectively. The mean deviations are 0.9, 0.3, 2.5, and 1.4 percent, respectively, and the root mean square deviations (standard deviations) are 1.1, 0.4, 3.3, and 1.9 percent, respectively. Because of the nature of the calculations, the ratio of C_3S error to C_2S error is the same as the C_3S/C_2S ratio.

The C_3A contents determined for these cements are in every case lower than the values obtained by the Bogue potential compound calculation. Midgley, Rosaman, and Fletcher [3] reported C_3A values higher than the potential values for cements with low overall A/F ratios. However, one would expect that the C_3A would be the lowest in these very cements because of the tendency of low A/F ratio ferrites to take up additional alumina. As was stated before, the ferrite line may overlap the C_3A line in such a way as to be unresolvable graphically. As can be seen from figure 2, this would be the case all the more if the ferrite has a low A/F ratio. Hence, the Midgley, Rosaman, and Fletcher result appears to be a manifestation of an increasing high systematic error in C_3A content with decreasing ferrite A/F ratio.

TABLE 3. *Sums of oxides and major phases in portland cements*

Cement	Oxide sum	CCX sum	X-ray sum
	Percent	*Percent*	*Percent*
LTS-11	92.3	92.2	96.7
LTS-12	93.6	93.6	89.6
LTS-13	93.0	91.6	98.5
LTS-14	94.0	95.4	94.6
LTS-15	94.5	90.8	92.9
LTS-16	93.3	92.5	98.8
LTS-17	94.9	95.2	88.7
LTS-18	93.6	94.3	95.3
LTS-19C	92.2	93.3	88.7
LTS-21	95.5	95.0	101.8
LTS-22	93.9	94.3	96.2
LTS-23	95.7	95.3	94.6
LTS-24	91.8	91.8	94.0
LTS-25	94.2	95.4	92.9
LTS-31	90.3	89.0	87.6
LTS-33	91.5	88.7	92.9
LTS-34	90.9	88.6	91.1
LTS-41	92.6	92.5	93.4
LTS-42	94.4	94.1	99.4
LTS-43	94.1	94.2	104.3
LTS-43A	95.0	94.5	95.6
LTS-51	94.8	96.0	93.7
SBR-15754	92.0	92.2	94.7
SBR-15698	93.1	95.9	81.6
SBR-15622	94.6	95.0	95.3
SBR-15497	90.9	88.2	92.8
SBR-15669	94.4	94.3	96.1

The combined chemical and X-ray method has the advantage of restricting the error in the system somewhat by the limitations imposed by the oxide analysis. There are, however, a number of minor oxides in portland cement which may be dissolved in one or more of the four major phases. The CCX method does not take these into account. On the other hand, the X-ray method, not limited by the oxide analysis, measures the total amount of each of the major phases, regardless of the presence of minor oxides. Thus, a comparison of the sum of the major and minor oxides, corrected for substances known not to occur in the major phases [2], with the sums of the major phases obtained by the CCX and X-ray methods is useful in illustrating the overall accuracy of the methods. These sums are given in table 3. The CCX sums are on the average 0.3 percent smaller than the oxide sums, while the X-ray sums are on the average 0.8 percent greater. This implies that at least some of the minor oxides in the cement are dissolved in the four major phases. The mean deviations of the CCX and X-ray sums from the oxide sums are 1.0 and 2.6 percent, respectively, and the root mean square deviations (standard deviations) are 1.5 and 4.4 percent, respectively. It is to be expected that the CCX deviations would be smaller than the X-ray deviations because of the restrictions imposed on the system by the method.

Finally, the oxide results indicate that there is no significant amount of amorphous material in cement. The material designated as glass or glassy phase is actually microcrystalline, and hence detectable by X-rays.

References

[1] L. E. Copeland, Stephen Brunauer, D. L. Kantro, Edith G. Schulz, and C. H. Weise, Quantitative determination of the four major phases of portland cement by combined X-ray and chemical analysis, Anal. chem. **31,** 1521–30 (1959).

[2] Stephen Brunauer, L. E. Copeland, D. L. Kantro, C. H. Weise, and Edith G. Schulz, Quantitative determination of the four major phases in portland cement by X-ray analysis, Proc. ASTM, **59,** 1091–1100 (1959).

[3] H. G. Midgley, D. Rosaman, and K. E. Fletcher, X-ray diffraction examination of portland cement clinker. This symposium, paper II–S2.

[4] N. Fratini and R. Turriziani, X-ray investigation of the ferric phase in portland cement (In Italian), La Ricerca Sci. **26,** 2747–2751 (1956).

[5] M. Von Euw, Quantitative analysis of portland cement clinker by X-rays (In French), Silicates inds. **23,** 643–9 (1958).

[6] Deane K. Smith, Crystallographic changes with the substitution of aluminum for iron in dicalcium ferrite, (To be published).

[7] X-ray Powder Data File, ASTM, Philadelphia, 1959.

[8] J. W. Jeffery, The tricalcium silicate phase, Proceedings of the Third International Symposium on the Chemistry of Cement, London, 1952, pp. 30–48 (Cement and Concrete Association, London, 1954).

[9] H. G. Midgley, The composition of the ferrite phase in portland cement, Mag. Concrete Research **9,** 17–24 (1957).

[10] L. E. Copeland, D. L. Kantro, and G. J. Verbeck, Chemistry of the hydration of portland cement, This symposium, paper IV–3.

Discussion

H.-G. Smolczyk

Methods of X-ray investigation were the subject of several discussions at the Symposium. Although I discussed the matter several times with different gentlemen I shall try to combine some of these different discussions about preparation methods in one contribution. I should like to offer this discussion as a supplement to the very interesting paper of the Building Research Station.

At the Forschungsinstitut für Hochofenschlacke at Rheinhausen we fully agree to the opinion that the technique of preparing the samples is one of the most important parts of a quantitative X-ray diffraction analysis, and that wet grinding has important advantages.

Therefore, I want to report about the good experience we have had—for about 4 years—with a very simple wet grinding method for X-ray powder samples.

We use an ordinary small closed agate ball mill with a volume of 100 ml. In it, 1 cm^3 of the coarsely ground material together with 30 cm^3 of benzene (C_6H_6) are ground for 40 min. Then the benzene is removed and the very fine powder (2–6μ) dried quickly in a flow of dry air or in a

vacuum. Afterwards the powder is placed in an ordinary sample holder with a rectangular window and is densely compacted. Careful precautions are taken to obtain an entirely even surface.

Some smaller advantages of this method are the short grinding time, the easy separation of the powder, with its higher density, from the lower density benzene, and the chemical inactivity of the benzene which excludes any reaction with the cements or with their hydration products.

The two main advantages will be described in detail:

(1) By carefully using this preparation technique a high degree of reproducibility is obtained. Moreover, the preferred orientations of some hydrates—e.g., calcium hydroxide or ettringite—are reproducible, too, and diagrams obtained with these substances can be used even for quantitative analysis. Care must be taken, however, that the X-ray pattern of the mineral used for comparison shows the same degree of preferred orientation.

To give an impression of the accuracy that can be obtained by this method, two examples from our practice are given. Each sample was prepared four times, and the intensity of the $Ca(OH)_2$ peak at $2\theta=18°$ (CuKα) of each of the 8 specimens obtained was measured. The results were as follows (in percent of $Ca(OH)_2$):

Sample A: 21.8; 20.1; 18.8; 19.4; average, 20.0 $\pm$0.7

Sample B: 0.9; 1.3; 1.5; 1.2; average, 1.2 $\pm$0.2

$$\left(\text{Error calculated by } E=\pm\sqrt{\frac{\Sigma\Delta^2}{n(n-1)}}\right).$$

It must be mentioned here that the 18° peaks showed intensities which were approximately five times higher than normal, due to the effect of preferred orientation. The determination of 1.2 percent of $Ca(OH)_2$ was possible, however, only by using this orientation effect. Otherwise the low peak would have been disturbed too much by the high statistical background.

(2) In spite of the material being ground to an extremely fine powder, this method is nondestructive, and even the hydrates are not destroyed. Ettringite ($32H_2O$), which was nearly destroyed by 1 hr of dry grinding, did not change its intensities after having been ground in benzene for 10 hr (fig. 1a, 1b, and 1c). In order to detect a possible change of the diagram with time of exposure, the intense X-ray beam (CuKα; 30 kv) was directed on the surface of the sample for 12 hr. Even then, however, the X-ray diagram did not change at all.

It should be added that after the Symposium it was learned that for the last two years, a similar method of wet grinding has been used in the laboratories of the Portland Cement Association at Skokie, Illinois (cf. L. E. Copeland, and R. H. Bragg, ASTM Bull. No. 228, Feb. 1958, pp. 56–60).

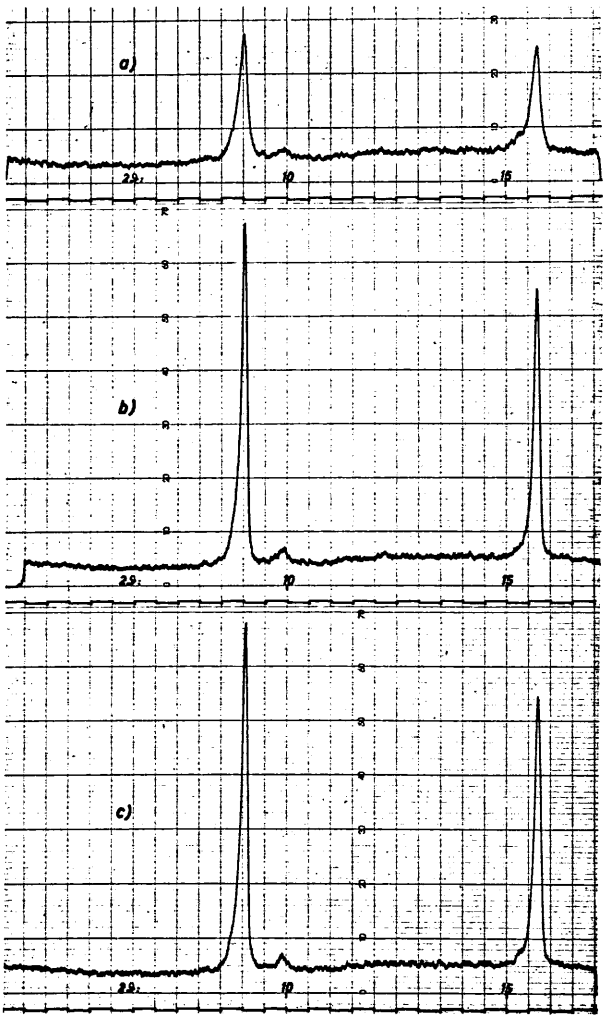

FIGURE 1. *Ettringite (X-ray diagrams).*

(a) 1 hr dry grinding
(b) 40 min grinding in benzene
(c) 10 hr grinding in benzene

Paper III–S2. The Composition of Ettringite in Set Portland Cement*

H. G. Midgley and D. Rosaman

Synopsis

X-ray powder diffraction patterns and differential thermograms of synthetic calcium sulfo- and hydroxyaluminate hydrates of known chemical composition were recorded and compared with the X-ray spacings and peak temperatures of the "ettringite" phase in set portland cement.

Using the calibration curves for X-ray spacing and normalized peak temperature obtained from the synthetic compounds, the composition of the "ettringite" phase in setting portland cements has been determined.

For three cements it was found that the phase first precipitated was very near to the pure calcium sulfoaluminate hydrate composition, but as the cements were stored for longer periods the composition changed, the solid solution containing more of the calcium hydroxy-aluminate hydrate.

Résumé

L'exposé présente des diagrammes de diffraction des rayons X à travers de la poudre et des thermogrammes différentiels d'hydrates synthétiques de sulfo- et hydroxy-aluminate de calcium de composition chimique connue. Ils sont ensuite comparés aux espacements des rayons X et aux températures des crochets des courbes pour la phase "ettringite" dans le ciment Portland pris.

La composition de la phase "ettringite" dans des ciments Portlands en train de prendre est déterminée par des courbes d'étalonnage pour l'espacement des rayons X et la température normalisée du crochet obtenue à partir des composés synthétiques.

On trouva que pour trois ciments la phase précipitée d'abord était très proche de la composition du sulfo-aluminate de calcium hydraté pur. Mais à mesure que les ciments étaient conservés pendant de plus longues périodes, la composition changeait et la solution solide contenait une plus forte proportion d'hydrate d'hydroxy-aluminate de calcium.

Zusammenfassung

Röntgendiagramme von Pulvern und Differentialthermogramme der synthetischen Kalzium-Sulfo- und Hydroxyaluminathydrate bekannter chemischer Zusammensetzung wurden aufgezeichnet und mit den Röntgenbeugungslinien und den Spitztemperaturen für die sogenannte Ettringitphase im abgebundenen Portlandzement verglichen.

Bei Anwendung der Eichkurven für die Röntgenbeugungslinien und der normalisierten Spitztemperaturen der synthetischen Verbindungen war man in der Lage, die Zusammensetzung der sogenannten Ettringitphase im abbindenden Portlandzement zu bestimmen.

In drei Zementen wurde gefunden, daß die zuerst präzipitierende Phase beinahe die Zusammensetzung des reinen Hydrats des Kalziumsulfoaluminats hat, daß aber, wenn die Zemente für längere Zeiten abgelagert wurden, die Zusammensetzung sich verändern würde, sodaß die feste Lösung mehr Hydrat des Kalziumhydroxylaluminat enthält.

Introduction

The mineral ettringite occurs in set portland cement as a result of the reaction between the hydrating calcium aluminates and the calcium sulfate. It was first observed by Candlot, and since it is formed in large quantities during the destructive attack of sulfate solutions on cement mortars and concretes it has been called the "cement bacillus." The usually accepted formula for ettringite is $3CaO{\cdot}Al_2O_3{\cdot}3CaSO_4{\cdot}32H_2O$, although Kalousek [1][1] has suggested that there is a solid solution between $3CaO{\cdot}Al_2O_3{\cdot}3CaSO_4{\cdot}aq.$ and $3CaO{\cdot}Al_2O_3{\cdot}3Ca(OH)_2{\cdot}aq.$ and a solid solution between the "low sulfate" sulfo-aluminate $3CaO{\cdot}Al_2O_3{\cdot}CaSO_4{\cdot}aq.$ and $3CaO{\cdot}Al_2O_3{\cdot}Ca(OH)_2{\cdot}aq.$ Of these compounds $3CaO{\cdot}Al_2O_3{\cdot}3CaSO_4{\cdot}aq.$, $3CaO{\cdot}Al_2O_3{\cdot}CaSO_4{\cdot}aq.$, and $3CaO{\cdot}Al_2O_3{\cdot}Ca(OH)_2{\cdot}aq.$ are well established. $3CaO{\cdot}Al_2O_3{\cdot}3Ca(OH)_2{\cdot}aq.$ was first described by Flint and Wells, [2] who did not give any X-ray powder data but described it as having a pattern indistinguishable from that given by $3CaO{\cdot}Al_2O_3{\cdot}3CaSO_4{\cdot}aq.$

It had been noticed by the present authors that the X-ray pattern given by the ettringite phase in set portland cement mortars and concretes had d values a little lower than those for the pure calcium sulfoaluminate hydrate, and also the temperature of the differential-thermal-analysis peak was higher than for the pure compound.

This paper is a report on the investigations undertaken to find an explanation for these differences.

*Fourth International Symposium on the Chemistry of Cement, Washington, D.C., 1960. Contribution from the Building Research Station, Department of Scientific and Industrial Research, Watford, England.

[1] Figures in brackets indicate the literature references at the end of this paper.

Methods

The two methods used in this investigation were X-ray powder diffraction and differential thermal analysis (DTA). The X-ray analyses were carried out with cylindrical Debye-Scherrer cameras, diameter 10 cm. or 11.4 cm.; the radiation used was Cobalt K alpha filtered with iron foil. The long spacing at about 9.7 A was found to be of most use.

The differential thermal analyses were carried out with ceramic crucibles, chromel-alumel thermocouples, alpha alumina as the inert substance, and a heating rate of 10 ± 1 °C/min.

Thermograms for some of the compounds likely to be met with in this investigation are given in figure 1. The problem of specifying the temperature of the peak for each of the substances was solved in the following manner. Samples of the pure compounds were diluted with alpha-alumina, a known weight was placed in the DTA crucible and the analysis was carried out. From the thermograms it was discovered that for any one substance the following relationship between the peak area and the peak temperature existed; $T = a + b \ln A$, where T is peak temperature in °C, a and b are two arbitrary constants, and A is the area of the peak. This means that peak temperatures may be compared in relation to some arbitrary area; for this investigation 1,000 sq mm was used, and the corresponding temperature is called the normalized peak temperature. The results for the compounds met with in this investigation are given in figure 2, from which it may be seen that an unknown substance present in a mixture at an unknown concentration may be identified by finding on which of the curves it lies.

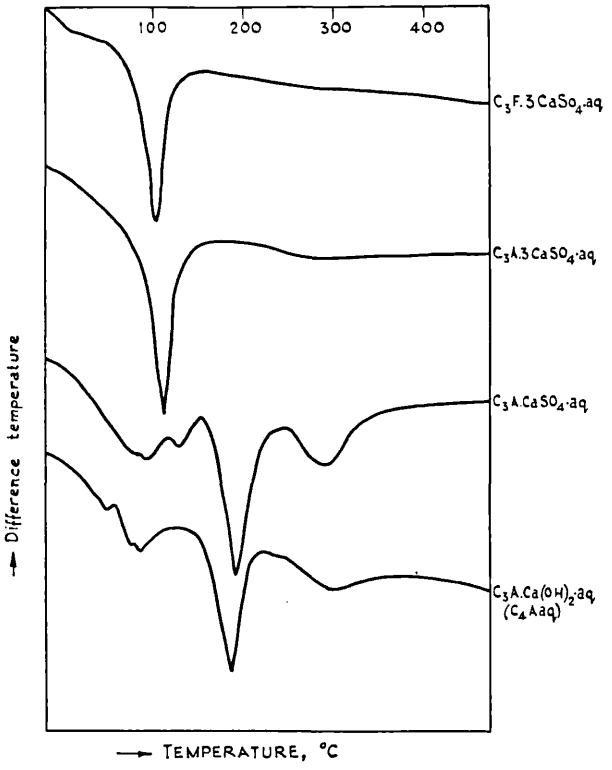

FIGURE 1. *Differential thermograms of pure calcium aluminate salt hydrates*

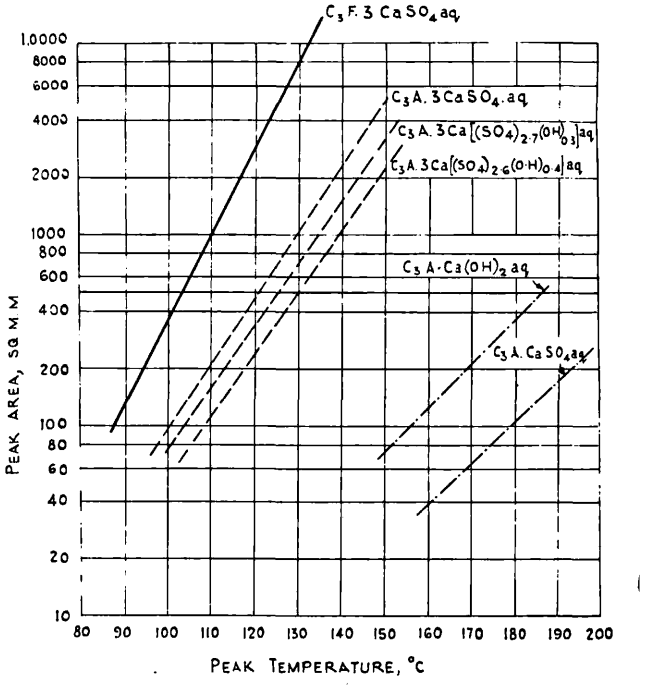

FIGURE 2. *Peak area and peak temperature for calcium sulfo- and hydroxyaluminate hydrates*

Portland Cements

TABLE 1. *Normalized peak temperature and d value of long spacing of ettringite phase in set portland cement cured at 18 °C in water*

Age	1 day	7 days	14 days	28 days	3 mo.	6 mo.
Normalized peak T °C	136	144	149	152	156	156
d A	9.75	9.75	9.73	9.67	9.65	9.63

A series of DTA and X-ray examinations of a set portland cement of different ages was carried out. From a series of DTA's of different dilutions, the set of curves given in figure 3 was obtained.

The normalized peak temperatures of ettringite for a series of set portland cements stored at 18 °C in water are given in table 1.

The normalized peak temperature of ettringite is shown to increase with age of storage. This change in peak temperature could be caused by two factors: by a change in the grain size of the ettringite crystals, or by a change in the composition of the ettringite phase. X-ray powder-diffraction analyses of the same cements gave the *d* values for the longest spacing as in table 1. This result would seem to support the view that there is a change in composition of the ettringite solid solution. It has not been possible to separate the ettringite phase from the cement, so analysis was impossible. An attempt was therefore made to discover the identity of the solid solution responsible for the change in the X-ray pattern. The compounds investigated included $C_3F{\cdot}3CaSO_4{\cdot}aq.$, $C_3A{\cdot}CaSO_4{\cdot}aq.$, and $C_4A{\cdot}aq.$ The normalized peak temperature (from figure 2) and the *d* values are given in table 2.

TABLE 2

Compound	Normalized peak temperature	*d*
	°C	A
$C_3F{\cdot}3CaSO_4{\cdot}32H_2O$	111	9.78
$C_3A{\cdot}CaSO_4{\cdot}12H_2O$	224	8.95
$\beta C_3A{\cdot}Ca(OH)_2{\cdot}12H_2O$	200	7.94

None of these compounds fitted the data given by the ettringite solid solutions in set portland cement.

Another possible compound is $C_6A{\cdot}aq.$ (or $C_3A{\cdot}3Ca(OH)_2{\cdot}aq.$) which may be regarded as ettringite having all its sulfate ions replaced by hydroxyl ions. This compound was first described by Flint and Wells [2] who said that its X-ray pattern was almost indistinguishable from that of ettringite, although they gave no detailed X-ray or DTA data.

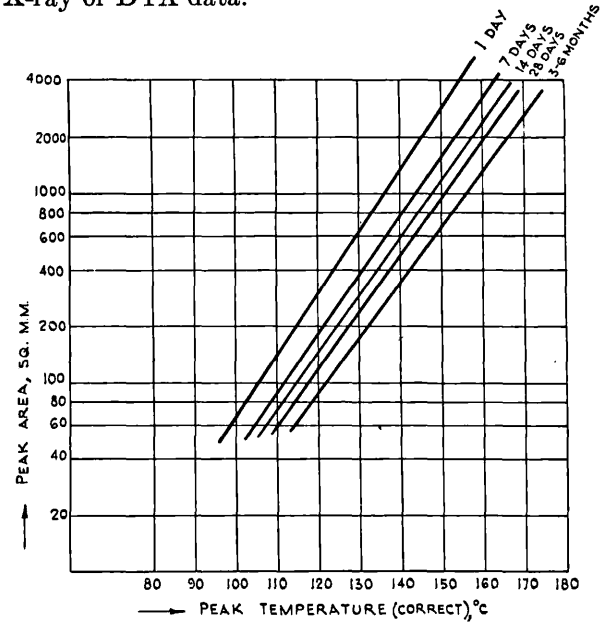

FIGURE 3. *Plot of peak area vs. peak temperature of ettringite in cement No. 555*

All attempts by the present authors to prepare this compound were unsuccessful.

Attempts were also made to prepare members of the solid solution $C_3A{\cdot}3CaSO_4{\cdot}aq.$-$C_3A{\cdot}3Ca(OH)_2{\cdot}aq.$ by preparing a lime-sugar solution containing 16.6 g CaO/l, adding 1.45 g and 0.38 g of gypsum respectively to two separate 450-ml portions and then adding 450 ml of calcium aluminate solution to each. The calcium aluminate solution was prepared by shaking 10 g of "Secar 250" white high-alumina cement with 1 liter of air-free distilled water for 24 hrs at 25 °C. The filtered solution gave the following analysis; 1.026 g CaO/l and 1.815 g Al_2O_3/l. After shaking the reactants in polyethylene bottles for 7 days, the white precipitate was filtered off and chemically analyzed. Differential thermograms and X-ray powder-diffraction patterns of each solid were recorded after the solids had been stored over saturated ammonium sulfate (R.H. 81 percent) for one week. The two compounds E and F produced the following data: (table 3).

TABLE 3

Component	Molar ratios		
	E	F	Ettringite (theoretical)
CaO	5.50	5.96	6.0
Al_2O_3	1.00	1.00	1.0
SO_3	2.58	2.72	3.0
X-ray diffraction, *d*A			
	9.70	9.75	9.75
Normalized peak temperature, °C			
	140	135	130

These results indicate that there is a solid solution, at least part of the way, between $C_3A{\cdot}3CaSO_4{\cdot}aq.$ and $C_3A{\cdot}3Ca(OH)_2{\cdot}aq.$

A relationship between the normalized peak temperatures and composition of these pure compounds can be obtained, figure 4. From this relationship the formula of a solid solution of unknown composition may be inferred from the differential thermogram. To check the validity of this assumption, the composition of six "ettringites" in a setting portland cements were obtained in this manner; the values of the long spacing on the X-ray diffraction pattern were also obtained. The results of change in X-ray *d* value and composition are given in figure 5 and are in reasonable agreement, indicating that the composition given by DTA cannot be very far out.

This method of obtaining the compositions of the "ettringite" phase in setting portland cement has been carried out on three cement types; a) normal 545, b) rapid hardening 549, and c) sulfate resisting 555. The results of this composition determination in relation to the age of the set cement are given in figure 6.

All samples show the same trend; the ettringite first produced is nearest to the pure sulfate end member, but with increasing time of hydration the ettringite phase becomes more substituted by hydroxy end member.

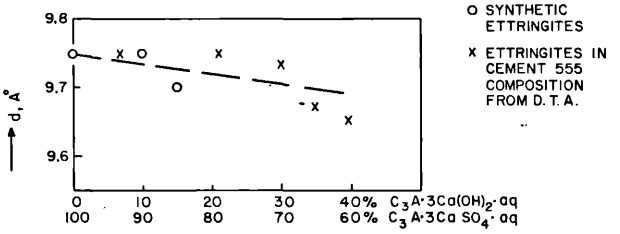

FIGURE 5. *Relation of d value for longest spacing of ettringite solid solutions to composition.*

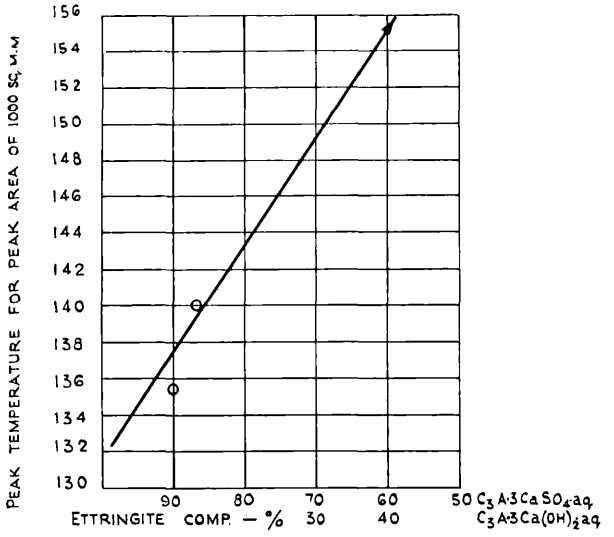

FIGURE 4. *Relationship between normalized peak temperature of endotherm and composition of ettringite solid solution.*

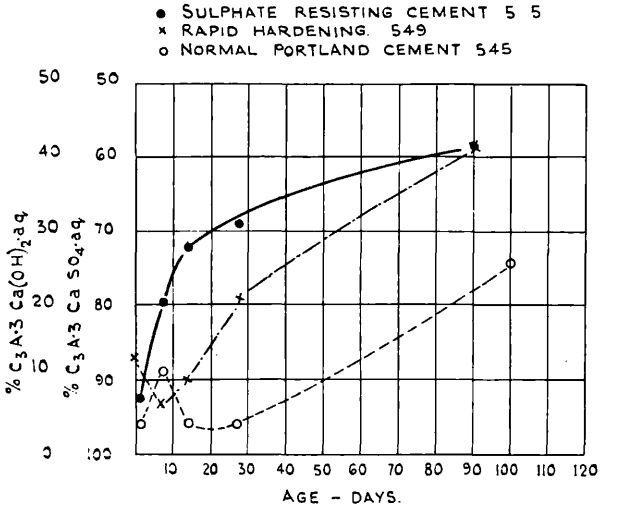

FIGURE 6. *Change in composition of ettringite composition with age of set portland cements.*

References

[1] G. L. Kalousek, Thesis, University of Maryland, 1941.

[2] E. P. Flint and Lansing S. Wells, Analogy of hydrated calcium silicoaluminates and hexacalcium aluminate to hydrated calcium sulfoaluminates, J. Research NBS **33** 471 (1944).

[3] J. D'Ans and H. Eick, The behavior of the system $CaO–Al_2O_3–H_2O$ at 20 °C and the hardening of high-alumina cement (in German), Zement-Kalk-Gips **6** (6), 197 (1953).

Paper IV–S2. The Mineralogical Examination of Set Portland Cement*

H. G. Midgley

Synopsis

The methods used for the mineralogical examination of set portland cement at the Building Research Station are microscopy, differential thermal analysis, X-ray diffraction, infrared absorption spectrometry, and electron microscopy and diffraction. By a combination of the methods it is possible to get a semiquantitative estimate of the various constituents of the cement paste of neat cements, mortars, and concretes. Differential thermal analysis appears to be the most sensitive and most likely to give quantitative results for the calcium silicate hydrate. The results so obtained are indicative that the main calcium silicate hydrate formed is a gel-like phase related to tobermorite, probably with a $CaO:SiO_2$ ratio greater than 1.5. The calcium aluminates formed are C_4AH_x with varying water content, ettringite solid solutions, and low-sulfate sulfoaluminate. There seems some evidence that all these crystalline aluminates can be formed at any age and that kinetic conditions such as CaO and SO_3 concentrations at the C_3A crystal face may govern the phase produced.

Résumé

Les méthodes dont dispose la *Building Research Station* pour l'examen minéralogique de la prise du ciment Portland sont la microscopie, l'analyse différentielle thermique, la diffraction des rayons X, la spectrométrie d'absorption infra-rouge, et la diffraction et la microscopie électronique. En combinant ces méthodes il est possible de faire une évaluation semi-quantitative des constituants variés de la pâte de ciment des ciments purs, des mortiers et bétons. Il semble que ATD est la méthode la plus sensible et la plus susceptible de donner des résultats quantitatifs pour l'hydrate de silicate de calcium. Les résultats obtenus jusqu'à présent indiquent que le principal hydrate de silicate de calcium formé est une phase comparable à un gel semblable au tobermorite, avec un rapport de $CaO:SiO_2$ probablement plus grand que 1.5. Les aluminates de calcium formés sont C_4AH_x avec une teneur en eau variable, ettringite, et le sulfo-aluminate avec une teneur plus basse en sulfate. Certains faits semblent prouver que tous ces aluminates cristallins peuvent être formés à tout âge et que les conditions cinétiques telles que les concentrations en CaO et SO_3 à la facette du cristal peuvent régir la phase produite.

Zusammenfassung

Die Methoden für die mineralogische Analyse des erstarrten Portlandzements, die in der *Building Research Station* angewandt werden können, sind die Mikroskopie, die differentielle Thermalanalyse, die Röntgenbeugungsbestimmungen, die Ultrarotabsorptionsspektrometrie, die Elektronenmikroskopie und die Elektronenbeugung. Durch eine Kombination der Methoden ist man in der Lage, eine halbquantitative Abschätzung der Bestandteile der Zementpaste des Purzements, des Mörtels und des Betons vorzunehmen. Die differentielle Thermalanalyse scheint die größte Empfindlichkeit zu haben, sie gibt wahrscheinlich die besten quantitativen Ergebnisse für Hydrate des Kalziumsilikats. Die Ergebnisse, wie sie bis jetzt erhalten worden sind, besagen, daß das Haupthydrat des Kalziumsilikat, welches sich formt, eine gelähnliche Phase ist, die mit Tobermorit verwandt ist, und in der das Verhältnis $CaO:SiO_2$ vermutlich größer als 1.5 ist. Die gebildeten Kalziumaluminate sind C_4AH_x mit verschiedenen Wassergehalten, Ettringit und der gering sulfatige Sulfoaluminat. Vermutlich können sich alle diese kristallinen Aluminate in jedem Alter bilden; die kinetischen Bedingungen, wie die CaO- und SO_3-Konzentrationen an der Kristalloberfläche des C_3A beeinflussen vermutlicherweise die gebildete Phase.

Introduction

The mineralogical method of examining set portland cement has a long and important history. The use of the thin section and the petrographic microscope was described by Parker and Hirst [1][1], who also extended the work of dye absorption to help differentiate the cementitious phase, called by them gel. About the same time Brown and Carlson [2] carried out a very comprehensive petrographic study of set portland cement pastes. These two papers probably represent all the data that may be obtained by such methods.

Alternative methods were now needed to advance the knowledge of the mineralogy of set portland cement. Ordinary powder X-ray diffraction analysis had not proved very successful. Firstly, the cameras in normal use did not record low angles, and secondly, the diffraction patterns of any possible cement hydrate minerals were swamped by the patterns of the still remaining unhydrated cement minerals.

The next big step forward in technique for mineralogical examination of set cements came

*Fourth International Symposium on the Chemistry of Cement, Washington, D.C., 1960. Contribution from the Building Research Station, Department of Scientific and Industrial Research, Watford, England.

[1] Figures in brackets indicate the literature references at the end of this paper.

from Kalousek, who with Davis and Schmertz [3] in 1949 used the method of differential thermal analysis (DTA) for the first time. By this method these workers were able to identify in setting portland cement pastes the minerals ettringite, $3CaO{\cdot}Al_2O_3{\cdot}3CaSO_4{\cdot}32H_2O$, and $Ca(OH)_2$. Although in the same paper they investigated the thermograms given by synthetic calcium silicate hydrates, they were unable to use the DTA method to identify the calcium silicate hydrate in set portland cement.

Although a considerable amount of data was known [4–6] on the phase chemistry of the systems $CaO–SiO–H_2O$, $CaO–Al_2O_3–H_2O$, and $CaO–Al_2O_3–SO_3–H_2O$, it was not until 1947 that the team under Bernal began its work on the crystallography of the minerals of the system $CaO–SiO_2–H_2O$. This work, summarized by Bernal, Jeffery, and Taylor [7] and Taylor and Heller [8], led to an attempt to identify the calcium silicate hydrate in set portland cement. Nurse and Taylor [9] reported X-ray diffraction data on a number of set cements, indicating that the calcium silicate hydrate present was of the tobermorite type. The method of separation used was very involved and tedious, involving elutriation and continuous centrifuging in very large quantities of anhydrous alcohol. Taylor [10] later made a separation using only limited quantities of material and centrifuging in bromoform-benzene mixtures. By this method Taylor identified the calcium silicate hydrate as CSH I or II.

Another important method of investigation available is electron microscopy and diffraction, and although a large amount of work has been done on calcium silicate hydrates it is only recently that attention has been paid to set portland cement pastes or mortars. Gille, et al. [11] have investigated set portland cement pastes by replica methods and have identified the plates of calcium hydroxide. Grudemo [12], one of the most important workers in this field, has recently published pictures of calcium aluminate hydrate and calcium silicate hydrate from set portland cement pastes.

The other methods available for mineralogical examination—infrared absorption analysis, nuclear-magnetic-resonance spectrometry and microprobe technique—so far have not been used extensively to determine the mineralogy of set portland cements. Hunt [13] has given infrared absorption spectra of some of the cement minerals, and the author of this paper has used the method extensively and reports the results here for the first time.

Using the techniques described before, together with a much more refined X-ray diffraction method involving X-ray diffractometers instead of film cameras, Turriziani [14] and Copeland, Kantro, and Verbeck [15] have recently described the mineralogy of set portland cements.

This paper sets out the methods and results obtained in similar studies at the Building Research Station.

Methods of Investigation

Microscopy

Reflection microscopy is not yet of great value in investigating the mineralogy of set portland cements, although the method is of some value in determining the microhardness of the minerals. The technique for preparing polished surfaces of set portland cements is under investigation, and a method of preparing good surfaces has been evolved. The method is simple—the section is cut on a high speed, resin-bonded diamond wheel, and the surface is then lapped on a similar diamond high speed plate.

For thin-section work, the required section should be as thin as possible; by the usual techniques sections of about 30μ are possible, but by a technique evolved by Smith [16] at the Building Research Station sections of about 10μ thickness have been prepared. Farran [18] has used microscopy in his investigations into the binding of cement paste and aggregate, but he was not able to deduce anything of the mineralogy of set portland cement from the microscope.

X-ray Diffraction

X-ray diffraction methods have been used extensively in the study of set portland cement pastes, mortars, and concretes. Most of the work has been done using cylindrical Debye-Scherrer cameras of varying radii, but all capable of recording at least 20A with copper K-alpha radiation. More recently some work has been done using a recording diffractometer. This latter method gives greater resolution and gives a better idea of quantities of identifiable minerals, but is not as good as photographic techniques in differentiating weak reflections from background.

An adjunct to X-ray diffraction identification is the possibility of concentrating the cementitious minerals. The method found most effective with concretes and mortars is to crush the sample with an iron pestle and mortar and sieve the fragments first through a 14-mesh sieve; further crushing and passing through a 100-mesh sieve removes a considerable quantity of the aggregate. This method of course precludes the quantitative determination of the cementitious minerals.

A further concentration of the cementitious phases has also been attempted using the technique described by Taylor [10]. This involves centrifuging of a benzene-ground sample in appropriate bromoform-benzene mixtures to produce a light fraction in which the cementitious hydrates are concentrated.

Differential Thermal Analysis

The differential thermal analysis (DTA) of set portland cements has been carried out in an apparatus especially designed for the purpose. The furnaces are of nichrome winding capable of reaching 1,000 °C; they are programed to give better than 10/min ±1 °C accuracy, the temperature of the sample and the amplified difference temperature between the sample and the inert body are recorded on a 0–50 mv, potentiometric recorder. The crucible and thermocouple setup received special attention (figure 1). The crucibles used were ceramic (fired alpha alumina), which were found to give better resolution than metal crucibles. By using two thermocouples, one in the sample and one in the inert body, a high degree of symmetry was obtained. The thermocouples found to be best for this work were chromel-alumel. Care was also taken to match the heat properties of the sample and the inert body. For most of the work about 0.7 g of sample was used. By these methods it has been possible to resolve the low-temperature endotherm around 120 °C into three peaks (figure 2). This resolution is repeatable, and full reliance can be given to the resolution.

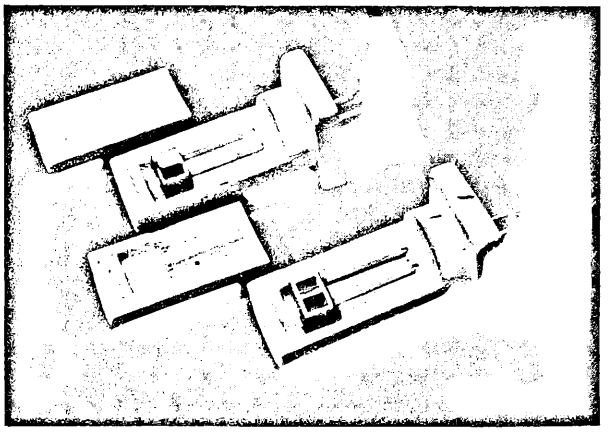

FIGURE 1. *DTA ceramic crucibles and holders showing two symmetrically disposed thermocouples.*

Infrared Absorption Spectrophotometry

For these investigations a commercial spectrometer, recording between 2.5- and 15-μ wavelength, was used.

Three methods of sample preparation were used. In the first, about 10 mg of sample was pressed with about 1 g of anhydrous KBr into a disc of 13-mm diameter by means of a vacuum press[17] This method was successful for anhydrous minerals, but there appeared to be interfering chemical reactions when hydrates were tried.

The second method was to mill the sample with an inert oil and make a thin film of the suspension between sodium chloride plates. This method gave good resolution but strong absorptions at 3.6, 7.0, and 7.4 μ due to the oil interference with the pattern.

The third method was to mill the sample with isopropyl alcohol. A sample was pipetted onto a NaCl disk and the alcohol allowed to evaporate. This method gave very good resolution at wavelengths greater than 5 μ, but owing to the specular reflection due to the difference in retractive index between the sample and air, there was a considerable absorption at less than 5 μ. This reflection, however, did not interfere with that part of the spectrum (around 10 μ) of most value in differentiating between the different minerals.

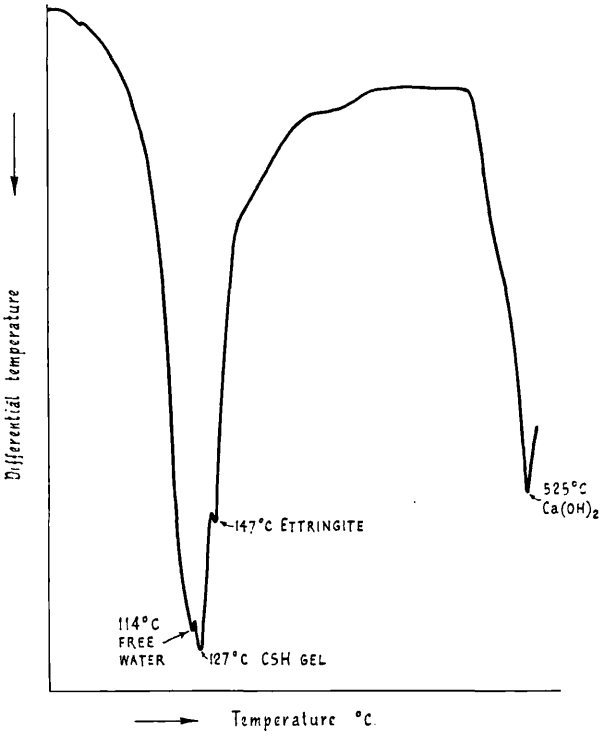

FIGURE 2. *Differential thermogram of set portland cement.*

Experimental Results

Microscopy

With the advent of very thin sections prepared by the Smith method, a new interest has been aroused in thin-section microscopy. Sheaths of isotropic gel have been seen around $3CaO{\cdot}SiO_2$ and $2CaO{\cdot}SiO_2$ grains, as is shown in figure 3. These are taken to be reaction rims of what is probably the calcium silicate hydrate gel phase.

FIGURE 3. *Photomicrograph of thin section of set portland cement paste (normal water-cement ratio) showing rim of calcium silicate hydrate gel around silicate grains.*

X-Ray Diffraction

By film techniques it is possible to detect the presence or absence of the unhydrated minerals; the data used are those of Midgley [19]. Of the hydrate minerals, ettringite ($3CaO{\cdot}Al_2O_3{\cdot}3CaSO_4{\cdot}aq.$–$3CaO{\cdot}Al_2O_3{\cdot}3Ca(OH)_2{\cdot}aq.$) can be detected by its reflection at 9.8A, and the solid-solution composition can be detected by a change in the value of this reflection [20], although DTA would be more accurate. The low-sulfate sulfoaluminate $3CaO{\cdot}Al_2O_3{\cdot}CaSO_4{\cdot}12H_2O$ is detected by its reflection at 8.92A, and the carbonate-aluminate $3CaO{\cdot}Al_2O_3{\cdot}CaCO_3{\cdot}12H_2O$ can be detected by the change in value of the reflection to 7.59A. The $4CaO{\cdot}Al_2O_3{\cdot}aq.$ series [21] can be detected by their reflection in the region of 8.05A. Calcium hydroxide and calcium carbonate are easily recognized from their patterns.

Calcium silicate hydrates have not been identified by this method so far. The only strong reflection for CSH I or II at 3.06A is very close to the strong reflections of alite and calcite, so that, if there is more than a trace of either of these minerals, any possible CSH reflection is masked.

In counterdiffractometry the aluminate and aluminate salt hydrates are detectable using the same reflections as by film camera technique, but it is also possible to make quantitative estimates of the amounts.

Figure 4 is the trace given by a neat cement paste 7 days old. The ettringite peak at 9.1 °2θ (d=9.7Å) and the C_4AH_{13} peak at 10.84 °2θ (d=8.13A) are clearly seen. Similarly, figure 5 is for a neat cement paste 3 years old. Here the ettringite peak is seen again at 9.1 °2θ and the aluminate peak is spread between 10.4° and 11.0 °2θ, suggesting that more than one hydration state is present.

In both these samples no aggregate was used, and great care was taken to keep CO_2 away so that the amount of calcium carbonate present is very small. So in the case of the cement paste 3 yr old, which is fully hydrated, calcium silicate

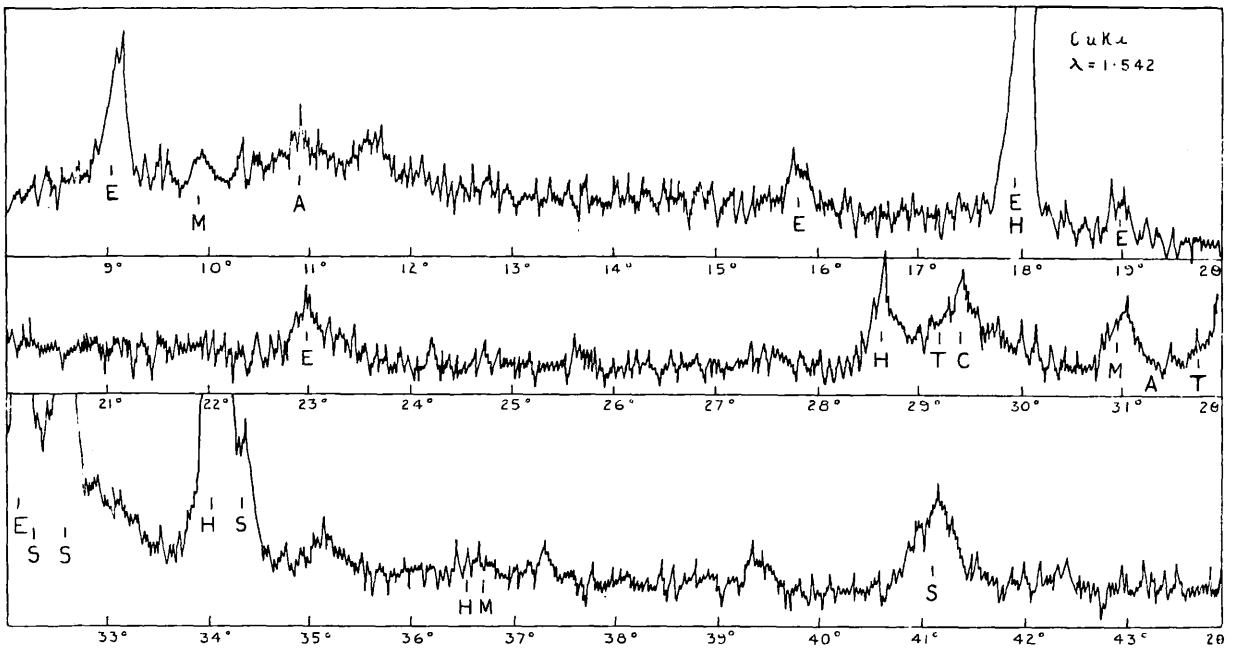

FIGURE 4. *X-ray diffractometer trace of set portland cement, neat; w/c 0.45.*
Made 2/6/60; examined 8/6/60 (see figure 5 for key).

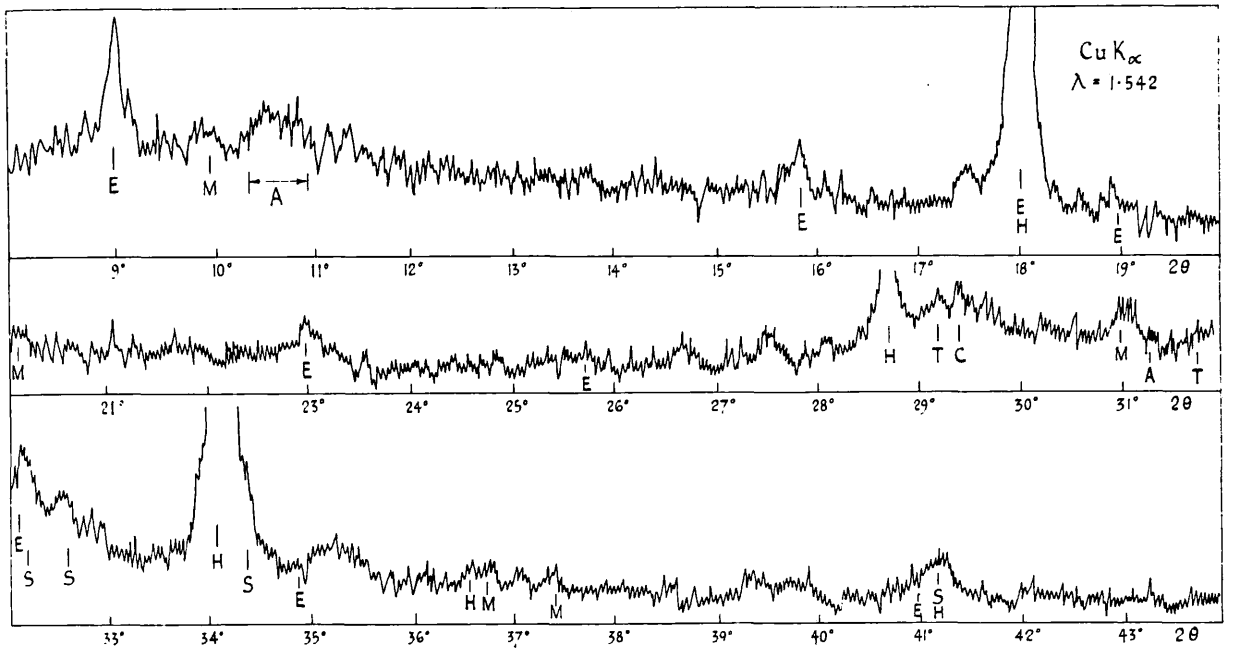

FIGURE 5. *X-ray diffractometer trace of set portland cement, neat; w/c 0.45.*
Made 10/4/57; examined 4/6/60. Key: E=Ettringite, M=$C_3A{\cdot}CaSO_4{\cdot}13H_2O$, H=$Ca(OH)_2$, T=CSH, C=$CaCO_3$, A=C_4AH_x, S=βC_2S, L=Alite, Q=Quartz.

hydrate is detected by the 3.06A reflection at 29.2 °2θ (fig. 5). Even in this sample where only a very small quantity of anhydrous silicate β-$2CaO{\cdot}SiO_2$, is detected the peak size for the CSH phase is disappointingly small.

The diffraction trace of the sample 7 days old shows that the CSH phase is undetectable owing to the presence of beta dicalcium silicate.

As the samples referred to above were stored in CO_2-free atmospheres, there is no calcite interference. In normal mortars and concretes CO_2 will not be absent, and figure 6 shows what happens when a 1:3 mortar is stored without precautions. After 3 and 6 days water storage the possible detection of CSH at 29.2 °2θ (d= 3.06Å) is masked by the alite peak (L) at 29.55 °2θ (d=3.03A). Prolonged storage in conditions which would allow carbonation gives patterns such as shown at 3 and 6 months. Here any possible detection of CSH is masked by the very strong calcite peak at 29.4 °2θ (d=3.04A).

Similar results are obtained from the cement fraction extracted from a concrete, figure 7. The concrete was from a roadway and was about 4 yr old. The diffraction pattern shows that ettringite, $Ca(OH)_2$, and calcite, together with quartz from the aggregate, may be detected.

Taylor [10] has shown that a concentration of the hydrate minerals is possible, but repeated attempts by the author and some of his colleagues have failed to repeat Taylor's results.

Recently, Fletcher [22] has modified the method and made an extraction. The method is similar to Taylor's but after grinding the cement in benzene the suspension is put into a centrifuge

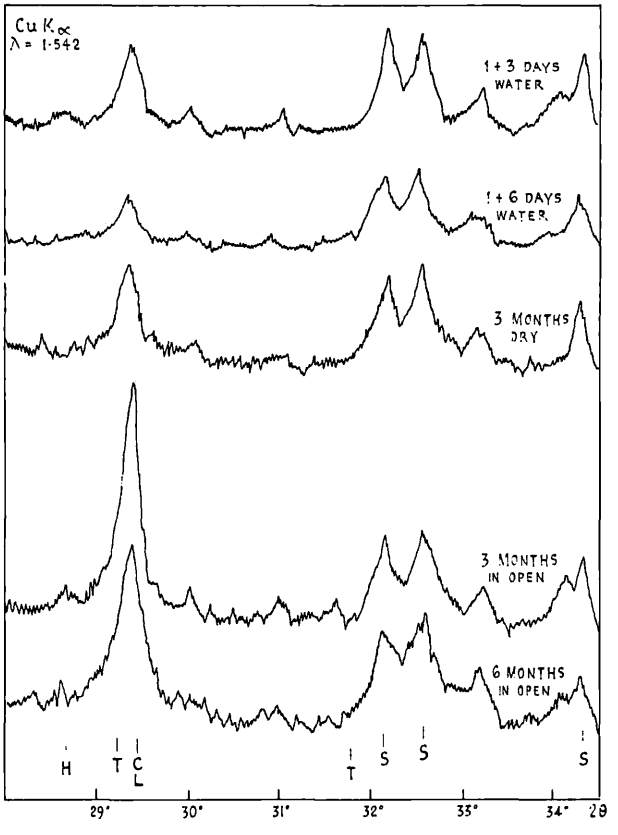

FIGURE 6. *X-ray diffractometer trace of cement fraction from portland cement mortars.*
1:3 standard sand; w/c 0.52 (see figure 5 for key).

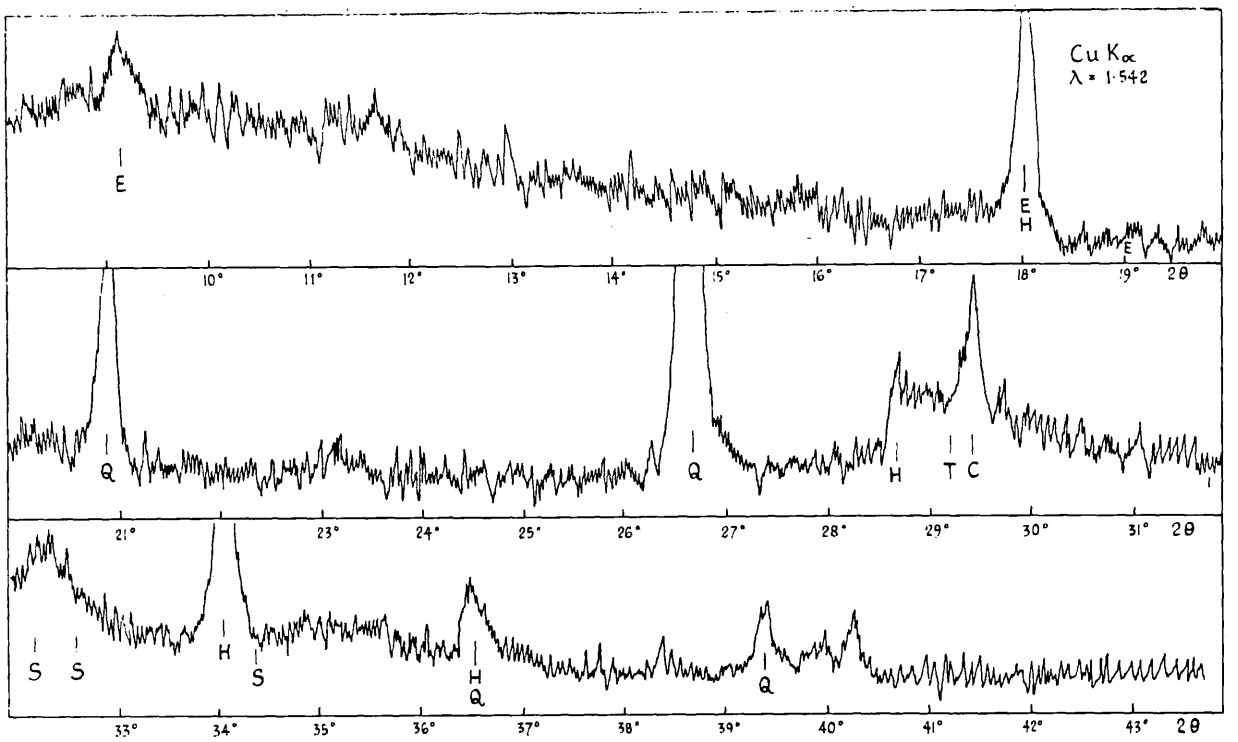

FIGURE 7. *X-ray diffractometer trace of cement fraction from concrete.*
(See figure 5 for key.)

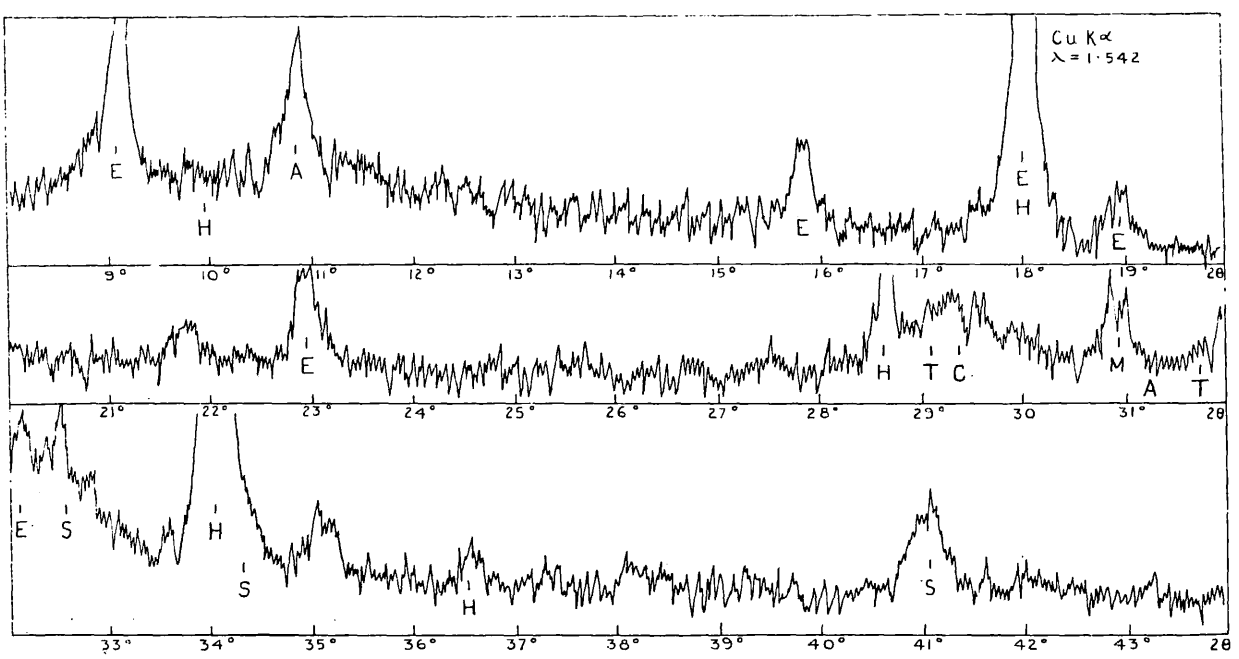

FIGURE 8. *X-ray diffractometer trace of set portland cement, neat; w/c 0.45.*
Made 2/6/60; examined 8/6/60. Light fraction from bromoform-benzene S.G. 1-78 (see figure 5 for key).

tube and drops of bromoform added until a separation is effected. The light fraction contains the concentration of hydrates. In the experiments reported here the specific gravity of the liquid used was 1.78, much lower than that used by Taylor. These experiments seem to suggest that each separation has to be taken on its own and a suitable liquid density determined by trial and error.

A diffraction pattern obtained from such a separation is given as figure 8. This sample is the light fraction of the same cement as shown in figure 3, a neat portland cement paste 7 days old. The C_4AH_{13} is considerably concentrated, and to a lesser extent the ettringite and the calcium hydroxide, but there does not appear to be any concentration of the CSH phase. The beta dicalcium silicate is reduced.

By X-ray methods it is therefore possible to detect the calcium aluminate and aluminate salt hydrates, $Ca(OH)_2$, and $CaCO_3$, and in favorable circumstances the CSH phase may be just identified.

Differential Thermal Analysis

The problems associated with the DTA of set portland cements are the interpretation of the low-temperature endotherms, for, as can be seen from figure 2, the endotherm is made up of three peaks. The temperatures of the peaks on DTA's are known to vary with quantity of mineral present, and it has been suggested by various authors, Keith and Tuttle [23] for example, that the characteristic temperature of a DTA peak should be the inflection point on the low-temperature side of the peak. This point is found to be consistent irrespective of amount. In the case of multiple peaks such as those given by a set portland cement, the inflections of the second and third peaks are not measurable, and the only easily measured parameter is the peak temperature.

If the peak temperature is plotted against the logarithm of the peak area, for reasonable dilutions, a straight line is obtained. This plotting has been done in figure 9 for the important constituents likely to occur in a set portland cement. The ettringite (pure end member $3CaO{\cdot}Al_2O_3{\cdot}3CaSO_4{\cdot}aq.$), C_4AH_{13}, and $C_3A{\cdot}CaSO_4{\cdot}aq.$ were prepared in the normal way. The free water was ordinary distilled water added to alpha alumina in the DTA crucible. (In all cases reported in this paper, alpha alumina was used as diluent.) The phase labeled tobermorite gel caused some difficulty, for although the middle of the three peaks in figure 2 was thought to be due to a calcium silicate hydrate [24, 25], some difficulty was experienced in preparing a synthetic sample.

Calcium silicate hydrate I prepared by double decomposition and by shaking silica sol with $Ca(OH)_2$ produced gels which contained very large quantities of free water, giving peaks on the DTA which agreed with the "free water" line on the graph. All attempts to dehydrate the sample by drying at various humidities caused the sample to crystallize and produce tobermorite which was well crystallized, that is, gave good basal spacings at about 11A on an X-ray diffraction diagram.

The only sample of calcium silicate hydrate which gave an endothermic peak anywhere near the middle of the three endotherms found in set portland cement (fig. 2) was CSH II. The sample was prepared by hydrating pure C_3S for 2 yr in a paste at room temperature. The sample was analyzed for $Ca(OH)_2$ and $CaCO_3$ by DTA and thermogravimetry, and the remainder was assumed to be calcium silicate hydrate of the formula $1.77CaO{\cdot}SiO_2{\cdot}3.00H_2O$. ($CaO/SiO_2=1.77$). The X-ray pattern is of a poorly crystallized tobermorite type, reflections occurring only at 3.06, 2.98, and 1.83A. This mineral is equivalent to the CSH II of Taylor [26] and the tobermorite gel of Midgley and Chopra [24, 25].

Using the results obtained from the pure synthetic minerals and the graph in figure 9, it is possible to interpret the DTA thermograms of set portland cements.

Figure 10 shows the interpretation of the DTA thermogram given by a portland cement paste 14 days old. The scale of the curves given for the pure substances has been adjusted so that the peaks are of about the size of those given by the minerals in set portland cement. From this diagram it may be seen that free water, tobermorite gel (CSH II), ettringite, and $Ca(OH)_2$ may be detected. (In these experiments no attempt has been made to determine the ettringite composition by the method of Midgley and Rosaman [20].)

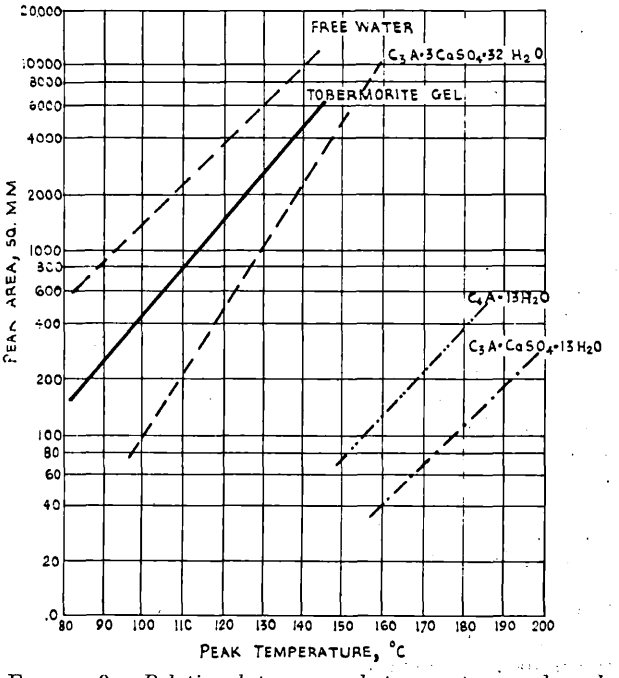

FIGURE 9. *Relation between peak temperature and peak area.*

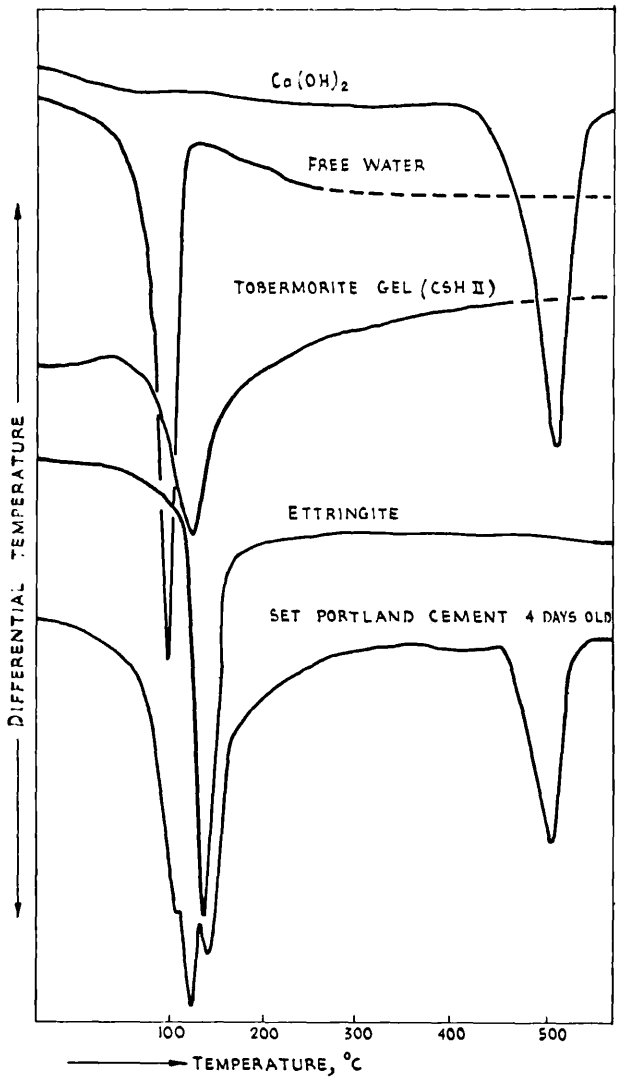

FIGURE 10. *Differential thermograms of set portland cement and constituents.*

A similar interpretation is shown in figure 11 for a portland cement paste 1 yr old, where tobermorite gel, ettringite, and low-sulfate sulfoaluminate are detected.

Now that it is possible to identify the peaks on a DTA, some quantitative estimate of the minerals present can be made by setting up calibration curves for the DTA apparatus, relating peak area to mass of mineral. This calibration has been done for all the important constituents mentioned so far. There is one serious difficulty not wholly overcome; that there is no simple way of determining the constituent parts of a triple peak. The method used in this paper is to construct graphically with reference to standard peaks the two outside peaks (free water and ettringite) giving the remainder as tobermorite gel. This method, although not very precise, is the best available at the moment, and has been employed on a series of setting portland cements stored at 18 °C in water, with the results shown in table 1.

TABLE 1. *Weight percent of cement hydrate minerals in a hydrating 1:3 mortar, w/c 0.52*

Age	Wt percent of		
	tobermorite	ettringite	$Ca(OH)_2$
1 day	1	10	9
3 days	2	35	10
7 days	14	27	10
28 days	18	28	8

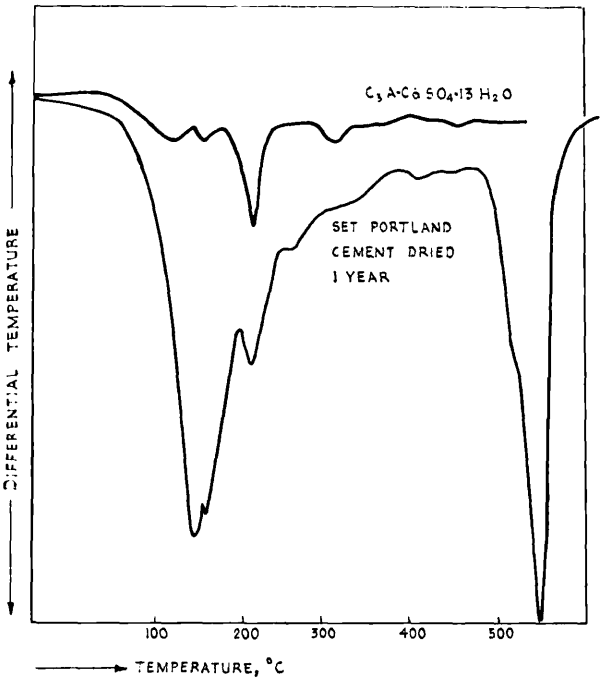

FIGURE 11. *Differential thermogram showing presence of* $C_3A \cdot CaSO_4 \cdot 13H_2O$ *in set portland cement.*

Infrared Absorption Spectroscopy

Absorption curves for all the compounds likely to be met in set portland cement have been prepared. These curves have been obtained for the four main components of portland cement clinker, C_4AF, C_3A, C_2S, and C_3S, shown in figure 12; for gypsum, and hemihydrate, figure 13; and for quartz, MgO, CaO, $Ca(OH)_2$, and calcite, in figure 14. The absorption spectrograms for some of the possible calcium silicate hydrates—Flint's CSH(A), C_2S gamma hydrate, C_2S beta hydrate, and C_2S alpha hydrate—are given in figure 15, C_3SH_2 and tobermorite plus afwillite in figure 16, and crystalline tobermorite and tobermorite gel in figure 17. The spectra for the two important aluminate hydrates are given in figure 18.

The data published here for the first time agree well with the data of Hunt [13] given in his as yet unpublished thesis.

The absorption spectrum of a set portland cement paste is given in figure 19. It is possible to identify the contributions of the various minerals as follows:—unhydrated C_3S by its peak at 10.5 μ; tobermorite gel by its peak at 10.0 μ; (ettringite by its peak at 9 μ, and also possibly calcite from the peak at 11.3 μ. The tobermorite peak is distinguished from the other calcium silicate hydrates by the simplicity of the peak at 10 μ and also by the presence of the double peak at 6.6 and 7.1 μ. Both Hunt [13] and Kalousek and Roy [27] have observed that the ratio of the peak absorption at 7 μ to that at 10 μ is related to the $CaO:SiO_2$ ratio of the tobermorite. Where the 7-μ peak is almost equal to the 10-μ peak, the $CaO:SiO_2$ ratio is highest.

The evidence from the absorption curve of set portland cement 4 days old is that the tobermorite has a high $CaO:SiO_2$ ratio.

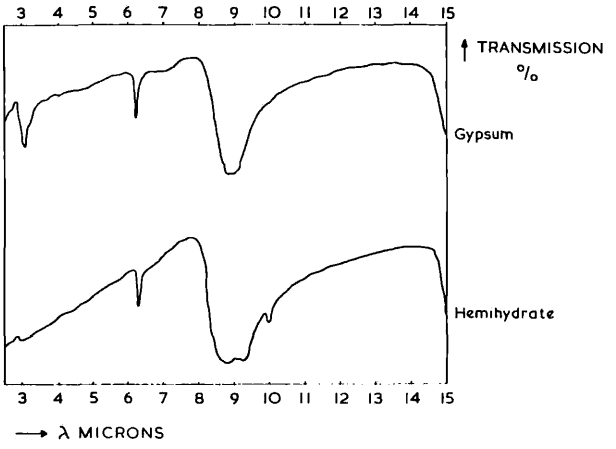

FIGURE 13. *Infrared absorption curves.*

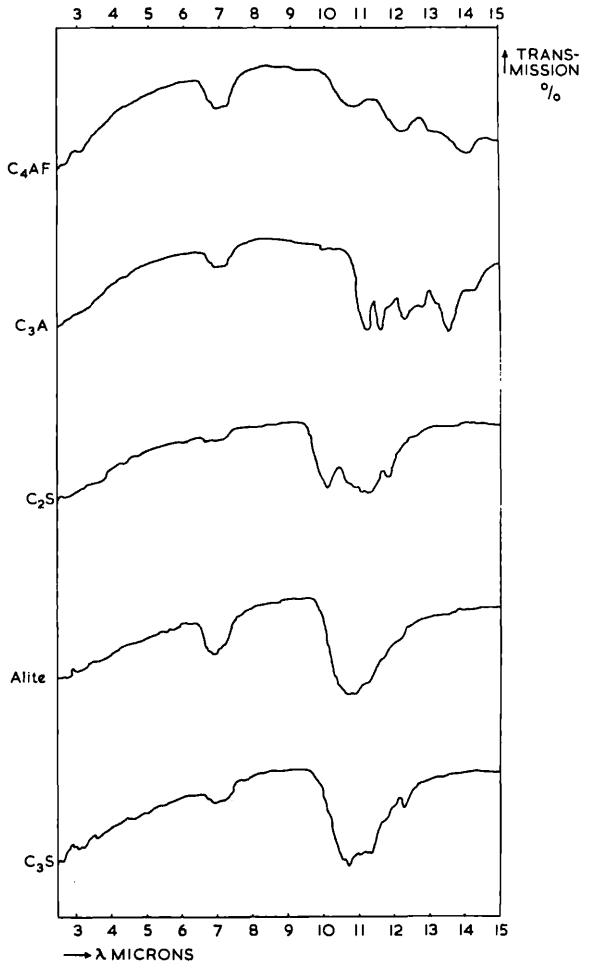

FIGURE 12. *Infrared absorption curves.*

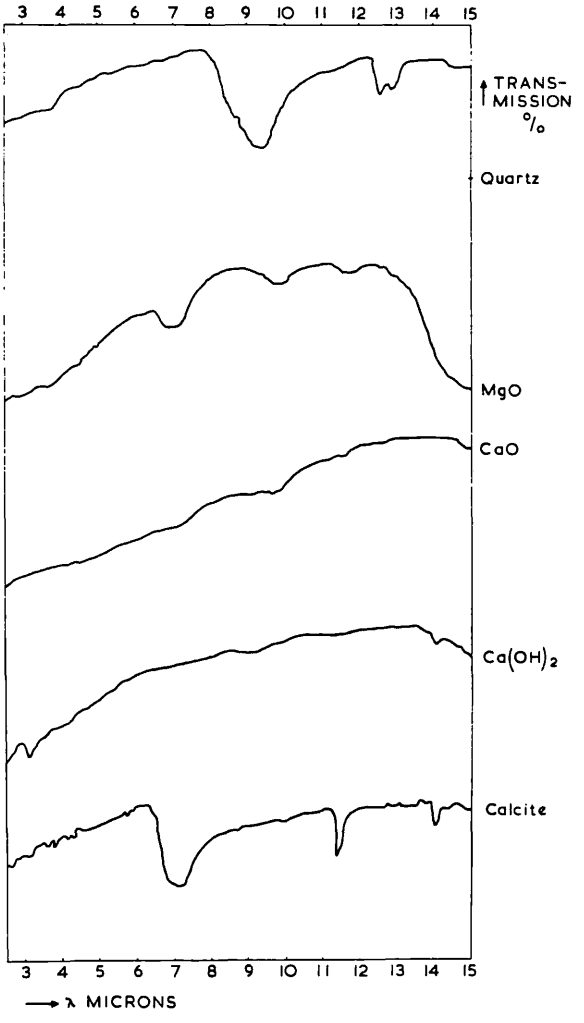

FIGURE 14. *Infrared absorption curves.*

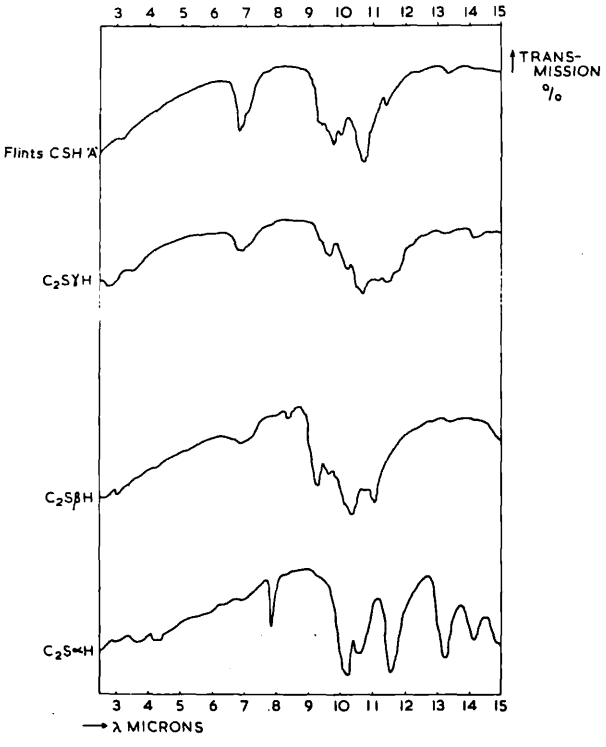

FIGURE 15. *Infrared absorption curves.*

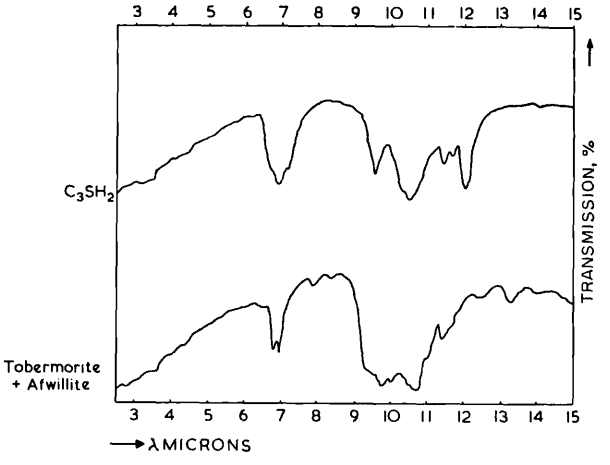

FIGURE 16. *Infrared absorption curves.*

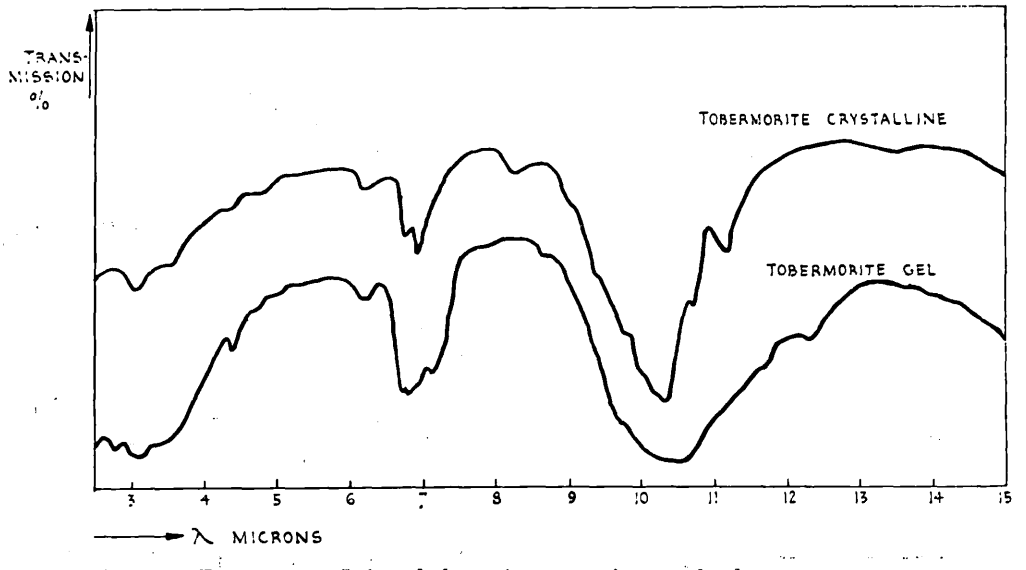

FIGURE 19. *Infrared absorption curve of set portland cement.*

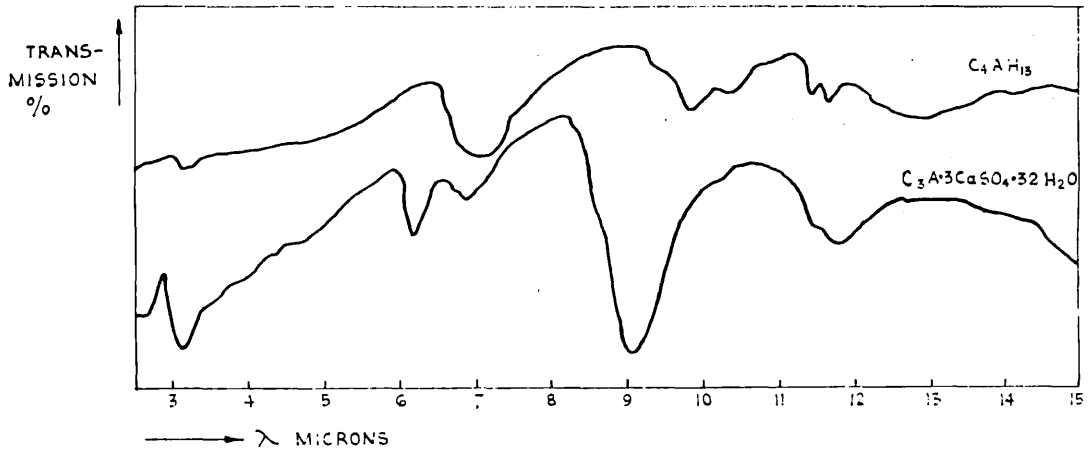

FIGURE 17. *Infrared absorption curves.*

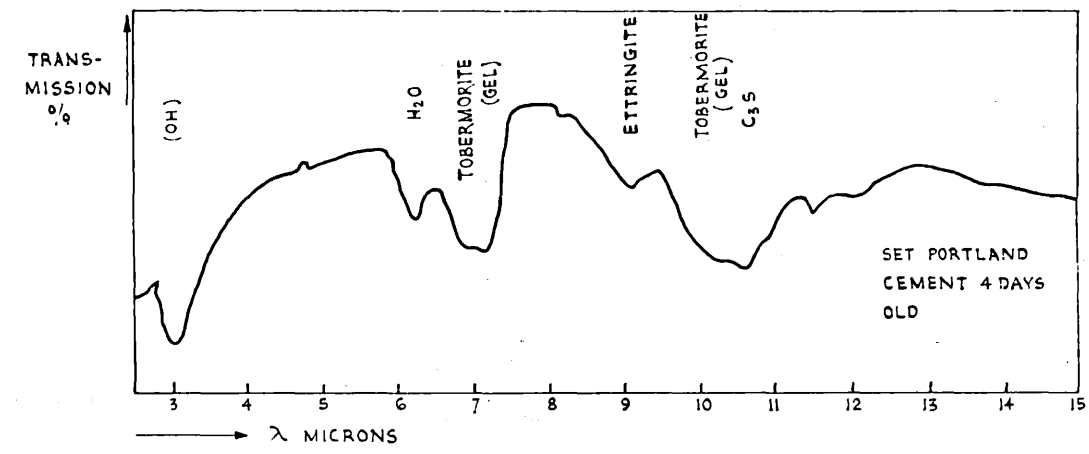

FIGURE 18. *Infrared absorption curves.*

Mineralogy of Set Portland Cements

All the various methods of examining the set portland cement pastes seem to indicate that the main calcium silicate hydrate formed is a gel-like phase related to tobermorite, probably with a $CaO:SiO_2$ ratio greater than 1.5; the calcium aluminates formed are C_4AH_x with varying water, ettringite, and low-sulfate sulfoaluminate. There seems some evidence that all these crystalline aluminates can be formed at any age, and that kinetic conditions, such as CaO and SO_3 concentrations at the C_3A crystal surface, may govern the phase formed.

References

[1] T. W. Parker and P. Hirst, Preparation and examination of thin sections of set cements, Cement and Cement Manuf. **8,** 235–241 (1935).

[2] L. S. Brown and R. W. Carlson, Petrographic studies of hydrated cements, Am. Soc. Testing Materials Proc. **36,** 2, 332–350 (1936).

[3] G. L. Kalousek, C. W. Davis, and W. E. Schmertz, An investigation of hydrating cements and related hydrous solids by differential thermal analysis, J. Am. Concrete Inst. **20,** 693–712 (1949).

[4] H. H. Steinour, The reactions and thermochemistry of cement hydration at ordinary temperature, Proc. 3rd International Symposium Chem. of Cement, London, 261–289 (1952).

[5] G. E. Bessey, Discussion of paper by P. Schlapfer, Effect of water on portland cement, Proc. 2nd International Symposium Chem. of Cement, Stockholm, 285–288 (1938).

[6] F. E. Jones, The quaternary system $CaO-Al_2O_3-CaSO_4-H_2O$ at 25 °C, J. Phys. Chem. **48,** 311–356 (1944).

[7] J. D. Bernal, J. W. Jeffery, and H. F. W. Taylor, Crystallographic research on the hydration of portland cement, Mag. of Concrete Research **4,** 49–54 (1952).
[8] L. Heller and H. F. W. Taylor, Crystallographic data for calcium silicates, (Her Majesty's Stationery Office, London. 1956).
[9] R. W. Nurse and H. F. W. Taylor, Discussion of paper by H. H. Steinour, The reactions and thermochemistry of cement hydration at ordinary temperature, Proc. 3rd International Symposium Chem. of Cement, London, 311–318 (1952).
[10] H. F. W. Taylor, Études sur l'hydratation du ciment Portland, (in English), 27e Congrès chimie industrielle, Brussels, 1954; Ind. chim. belge, **20,** Spec. No. 3, 63–66 (1954).
[11] F. Gille, W. Czernin, U. Danielsson, and F. Grasenick, Electron microscope studies on hydrated cements, Zement u. Beton **16,** 21–24 (1959).
[12] Å. Grudemo, The microstructure of hardened paste, this Symposium, paper V–2.
[13] C. M. Hunt, The infrared absorption spectra of some silicates, aluminates, and other compounds of interest in portland cement chemistry, Thesis, Univ. of Maryland, 1959, 84 pp.
[14] R. Turriziani, The process of hydration of portland cement, (in Italian), Ind. ital. cemento **29,** 185–189, 219–223, 244–246, 276–282 (1959).
[15] L. E. Copeland, D. L. Kantro, and G. Verbeck, Chemistry of hydration of portland cement, this Symposium, paper V–3.
[16] J. J. Smith, Private communication.
[17] U. Schiedt and H. Reinwein, Zur Infrarot-Spectroscopie v. Aminosäuren, Z. Naturforsch. **7B,** 270–277 (1952).
[18] J. Farran, Contribution minéralogique a l'étude de l'adhérence entre les constituants hydratés des ciments et les matériaux enrobés, Rev. Mat. Construction, No. 490–491, 155–172; No. 492, 191–209 (1956).
[19] H. G. Midgley, A compilation of X-ray powder diffraction data of cement minerals, Mag. of Concrete Research **9,** 17–24 (1957).
[20] H. G. Midgley and D. Rosaman, The ettringite phase in set portland cement, this Symposium, paper III–S2.
[21] M. H. Roberts, New calcium aluminate hydrates, J. Appl. Chem. **7,** 543–546 (1956).
[22] K. E. Fletcher, Private communication.
[23] M. L. Keith and O. F. Tuttle, Significance of variation in the high-low inversion of quartz, Am. J. Sci. **250A,** 203–280 (1952).
[24] H. G. Midgley and S. K. Chopra, Hydrothermal reactions in the lime-rich part of the system CaO-SiO_2-H_2O, Mag. of Concrete Research **12,** 19–26 (1960).
[25] H. G. Midgley and S. K. Chopra, Hydrothermal reactions between lime and aggregate, Mag. of Concrete Research **12,** 73–82 (1960).
[26] H. F. W. Taylor, Hydrated calcium silicates. I. Compound formation at ordinary temperatures, J. Chem. Soc. 3682–3690 (1950).
[27] G. L. Kalousek and R. Roy, Crystal chemistry of hydrous calcium silicates. II. Characterization of interlayer water, J. Am. Ceram. Soc. **40,** 236–239 (1957).

Discussion

H. Dutz

I will make a brief discussion of the very interesting paper of Midgley.

In the infrared spectrum of calcium hydroxide in figure 14, most of the sample must have consisted of $CaCO_3$. The absorption bands at 7, 11.4, and 14 μ are typical of $CaCO_3$. It is very difficult to get a calcium hydroxide free of carbonate. Therefore, the relation of the absorption bands in figure 19 based on that examination is partly incorrect.

(Editor's note: The comments by Dr.-Ing. Dutz are applicable only to the original version of the paper presented at the Symposium. The author subsequently submitted a corrected copy of figure 14, in which a new absorption spectrum for $Ca(OH)_2$ was substituted.)

RESEARCH SERIES 14

Building Research

CURRENT PAPERS

THE ROLE OF ALUMINA AND MAGNESIA IN THE POLYMORPHISM OF TRICALCIUM SILICATE

By H.G. Midgley, M.Sc., Ph.D., F.G.S., and K.E. Fletcher

Reprinted from: Transactions of the British Ceramic Society, 1963, vol. 62(11), pp. 917-37

BUILDING RESEARCH STATION

DEPARTMENT OF SCIENTIFIC & INDUSTRIAL RESEARCH

Building Research CURRENT PAPERS are produced in four series

CONSTRUCTION SERIES
DESIGN SERIES
ENGINEERING SERIES
RESEARCH SERIES

Details of Current Papers issued are given, with summaries, in the Station's QUARTERLY LIST OF PUBLICATIONS, which may be obtained regularly on application to:

The Director,
Building Research Station,
Garston, Watford, Herts.

Extra copies of this paper are available; a charge may be made for supplies in quantity.

THE ROLE OF ALUMINA AND MAGNESIA IN THE POLYMORPHISM OF TRICALCIUM SILICATE

by

H.G. Midgley

and

K.E. Fletcher

SUMMARY

Tricalcium silicate is an important constituent of basic steelmaking slags some types of basic refractories and Portland cement, and it occurs in three polymorphic modifications depending on the temperature, passing from triclinic to monoclinic and to trigonal with increasing temperature. Aluminium and magnesium ions may be incorporated in the lattice and cause a high-temperature modification to be stabilized at room temperature. The roles of magnesia and alumina have been investigated at 1.500°C. It has been found that Mg^{2+} substitutes directly for Ca^{2+} with a limit of replacement of about 2.0% MgO, the monoclinic polymorph being stabilized at room temperature by 1.5% MgO. With alumina the substitution is more complicated: $3Al^{3+}$ replaces $3Si^{4+}$ and the balance of charge is maintained by the introduction of Al^{3+} in interstitial positions. The substitution may be represented by a solid solution series between C_3S and a hypothetical $C_{4.5}A$. The substitution by Al^{3+} does not affect the polymorphism, only the triclinic form was encountered at room temperature. The limit of solubility for Al_2O_3 is about 0.9%. Magnesia and alumina together also form solid solutions with C_3S. When the C_3S phase is saturated with alumina, only 1.0% magnesia is required to stabilize the monoclinic form at room temperature, but if both magnesia and alumina are reduced below about 0.75 of their individual saturation limits, the triclinic form occurs at room temperature.

1. INTRODUCTION

Tricalcium silicate is a constituent of basic steelmaking slags and of some types of basic refractories, and any polymorphic inversions might possibly affect the stability of these materials. It is of most interest, however, in connection with Portland cement, being the principal cementing mineral present. It can be shown that C_3S † occurs in three crystallographic modifications at room temperature: the triclinic modification occurs in synthetic preparations of pure C_3S, the monoclinic form commonly occurs in Portland cement clinker, the trigonal phase has been observed to occur in open hearth slags and by the present authors in some cement clinkers. X-ray diffraction examination of pure synthetic C_3S at increasing temperatures shows the transformations from triclinic, first to monoclinic and then to trigonal. The stabilization of the monoclinic and trigonal modifications at

† In the text the cement chemists' shorthand notation is used: C = CaO; S = SiO_2; A = Al_2O_3; M = MgO. Where the simple compound exists as a phase the normal notation is used.

room temperature is a result of solid solution of other compounds in C_3S. In 1952 Jeffery [1,2] investigated the crystal structure of C_3S and proposed the formulation $C_{54}S_{16}AM$ for the monoclinic variety as found in Portland cement which he called alite[7]. It has been found that Jeffrey's formulation, if synthesized at 1,500°C, gives a product containing considerable quantities of lime and C_3A despite repeated reburning[3-6] and since 1952 this problem has been constantly under examination.

Yamaguchi and his co-workers[7] in 1957 examined by means of X-ray analysis and d.t.a. the products obtained by replacing part of the CaO in C_3S by MgO. They indicated a maximum solubility of 2.4 mole% of MgO giving a contraction of interplanar spacings of 0.38%. Differential thermal analysis showed that the endothermic peaks they detected in C_3S at 925° and 985°C were lowered to 895° and 940°C by such a solution, and that an exothermic peak then occured at 905°C.

Naito, Ono and Iiyama[8] in 1957 studied the series $(Ca_{3-x-y}Mg_xAl_y)_3(Si_{1-3y}Al_{3y})O_5$, and concluded that Al^{3+} alone could stabilize the monoclinic structure and that Mg^{2+} alone could not. They presented a diagram showing the combined effect of Al^{3+} and Mg^{2+}.

In 1958 Von Euw[3] indicated that a progressive simplification of the C_3S X-ray diffraction pattern occurred with MgO, C_3A solid solution, and concluded that the addition of 2% C_3A and 1% MgO to C_3S was the best means of stabilizing the monoclinic structure although to facilitate saturation all his preparations were made with an excess of lime.

Locher[4] in 1960 showed by means of free-lime determinations that Mg^{2+} replaces Ca^{2+} in the C_3S lattice, giving progressive simplification of the X-ray pattern eventually stabilizing the monoclinic form at room temperature. He stated the C_3A alone had little or no effect on the C_3S pattern. He concluded that C_3S could contain 2% C_3A and 2.5% MgO at 1,500°C; the solubility of MgO dropped to 1.5% at 1,420°C.

Kantro, Copeland and Brunauer[6] in 1960 reported the preparation of a material of the composition $52C_3S.C_6AM$ called "$\frac{1}{3}$J. Alite", which they claimed gave the monoclinic diffraction pattern and contained negligible amounts of C_3A.

Yamaguchi and Miyabe[9] in 1960 carried out a high-temperature X-ray diffraction examination of C_3S, and indexed the C_3S solid solution produced from the formulation $C_{54}S_{16}AM$. Their observations on C_3S can be summarised diagramatically as in Figure 1.

---

[7] There is some discrepancy in nomenclature. Alite was originally described as a phase which occurrs in Portland cement clinker; it was subsequently demonstrated to be essentially C_3S, then shown to be usually the monoclinic form. Thus many authors use alite to be synonomous with monoclinic C_3S, but it has been shown by Midgley, Fletcher and Cooper[14] that the C_3S may occur in Portland cement clinker as any of the crystallographic modifications; to avoid confusion it is proposed to use the terms trigonal, monoclinic, or triclinic C_3S where the form is known, and the term alite for the C_3S in Portland cement clinker irrespective of crystal modification.

$C_{54}S_{16}AM$ gave a doublet at 51°2θ CuKα_1 at room temperature and was considered to be monoclinic. They indexed the reflection of lowest angle in the region 51-52°2θ as 620 and that at the higher angle as 040. Using this indexing of the solid-solution data they then indexed the pure triclinic C_3S. But in their high temperature work on pure C_3S they showed that it was the high-angle reflections of the triplet that came together to eventually form a doublet. This implies that in the monoclinic form observed at high temperature the reflection at the lower angle is 040 and that at the higher angle 620. Their indexing for the monoclinic form stabilized at high temperature and that stabilized by solid solution is thus reversed. It is shown later in this paper that it is the higher angle reflections in the triplet which come together to give a doublet and these are therefore referred to in this paper as 620, $\bar{6}20$ reflections, in agreement with the high-temperature observations of Yamaguchi and Miyabe.

Yannaquis and co-workers[13] have recently carried out an investigation of polymorphism of C_3S by means of d.t.a. and a high-temperature attachment on an X-ray focusing camera. The use of strictly monochromatic radiation enabled them to make precise observations of changes in structure. They observed sudden changes in the structure of the triclinic polymorph at 615° and 750°C, triclinic to monoclinic transformation at 917°C, a sudden change in the monoclinic structure at 973°C to give a form which was almost trigonal, and a final monoclinic to trigonal transformation at 1,050°C. The transformations at 750° and 1,050°C were not accompanied by a detectable thermal reaction.

In the present paper d.t.a. observations on pure C_3S indicate endothermic reactions occuring at 595°, 747°, 916° and 969°C (Table 2). Thus the change in triclinic structure found by Yannaquis about 750°C is confirmed. A delay in the final clarification of the trigonal pattern until about 1,050°C was observed during an attempt to repeat the high-temperature observations of Yamaguchi and Miyabe. It was attributed to the existence of a range of temperature within the sample, the observation of a clear trigonal pattern not being possible until the whole sample was above 969°C. The same reservation must apply to the observation of Yannaquis and his co-workers, since adequate temperature control and measurement is difficult under the conditions of the experiment.

The present paper reports an investigation into the role of alumina and magnesia in the stabilization of the monoclinic C_3S polymorph and provides a basis for subsequent investigation of the effect of solid solution by other compounds. A more precise evaluation of the limits of solid solution of Mg^{2+} and Al^{3+} has been attempted together with an interpretation of the accompanting structural changes.

2. EXPERIMENTAL

If solid solution occurs between C_3S and another component, a partial join must exist within the phase diagram between $CaO\text{-}SiO_2$ and the third component. If preparations are made whose compositions do not fall on the join or in which the third component is present in excess of its solubility, phases other than tricalcium silicate will be present.

In the work reported here, solid solution caused a slight progressive change in the unit-cell dimensions of C_3S, detected by means of the X-ray powder diffraction pattern; and also caused a lowering of the temperature at which polymorphic changes

occured, as measured by d.t.a. Appropriate techniques were used to detect and estimate phases other than C_3S which were likely to occur.

Preparations were made from calcium carbonate, magnesia and alumina, given in Table 1.

The reagents were homogenized in a vibratory mixer and decarbonated by heating in a platinum crucible at 1,000°C for 1 h; then ground in an agate mortar to pass a 200-mesh B.S. Sieve, and reburnt at 1,500°C. The sample was removed from the furnace after 1 h, air-quenched to room temperature and reground to pass a 200-mesh B.S. sieve. The procedure of heating at 1,500°C, air-quenching, and grinding was repeated until the free-lime content had reached a minimum value. In the early stages of the reaction, free lime was detected by means of the X-ray diffractometer; for the final stages it was estimated by the Lerch and Bogue[10] method.

The samples were then examined by means of X-ray techniques, microscope point counting and d.t.a. It is important to note that the basic results obtained apply to samples air-quenched from 1,500°C to room temperature. The effect of varying the cooling conditions is considered separately.

2.1 X-ray Techniques

An X-ray diffraction trace of the region 65-18°2θ $CuK\alpha_1$ was made using a Philips X-ray diffractometer; more accurate observations of the peaks in the region of the 040, 620, $\bar{6}20$ reflections at about 51° 2θ $CuK\alpha_1$ were made. For the latter observations about 15% silicon powder was mixed with the sample to act as an internal standard. The $CuK\alpha_1$ radiation was generated at 40kV 20 mA and passed through a nickel filter. The instrument settings were: scanning rate, $^1/_8$°/min; scatter slits, 1°, receiving slit, 0.1mm; rate-meter, 8 counts; time constant, 8 sec; multiplier, 0.6; chart speed, 800 mm/h. Silicon reflections occuring at 56.122° 2θ $CuK\alpha_1$ and 47.302° 2θ $CuK\alpha_1$ were used to bracket and correct the observed angular values for the 040, 620, $\bar{6}20$ reflections. For the general trace from 65°-18° 2θ $CuK\alpha_1$ no internal standard was used; the multiplier setting was 1.0 and the chart speed 200 mm/h.

C_3A was estimated using an X-ray technique established for the estimation of the compounds present in Portland cement[5], and requiring measurement of the intensity of the reflection at 33.2° 2θ $CuK\alpha_1$. It was observed that in C_3S itself and in C_3S preparations containing magnesia a weak reflection of consistent intensity occurred at this position, which could not be attributed to C_3A since no Al_2O_3 was present. The reflection was considered to be part of the pattern due to C_3S and, when C_3A was estimated, allowance was made. Its intensity was equivalent to the presence of about 1.5% C_3A.

Magnesia was detected and estimated by means of its strong reflection at 42.8° 2θ $CuK\alpha_1$, using the C_3S reflection at 41.3° 2θ $CuK\alpha_1$ as the reference standard.

2.2 Microscope Point Counting

The sample was cast in a cold-setting resin, a polished surface was prepared and was etched with HF vapour. With the correct conditions of etchings C_3S was coloured pale yellow, C_2S deep blue, and interstitial material was detected by its greater reflectivity. The point-counting technique of successive equal intercepts was used to estimate the amount of C_2S present in the sample.

2.3 Differential Thermal Analysis (d.t.a.)

Differential thermal analysis was carried out using furnaces with nichrome windings capable of reaching 1,000°C with a rate of heating of 10°C/min 1°C. Alpha alumina was used as the inert reference material. The sample temperature together with the amplified temperature difference between the sample and the reference material were recorded on a 0-50 mV potentiometric recorder.

2.4 The Solid Solution of Magnesia in Tricalcium Silicate

The most likely form of solid solution was thought to be a simple substitution of Mg^{2+} for Ca^{2+}. Therefore mixes were investigated along a line between C_3S and a hypothetical M_3S. Any deviation from the assumed solid-solution series would result in crystallization of either C_2S or CaO, and the end of the series would be marked by the simultaneous appearance of C_2S and MgO, or the appearance of MgO and a decrease in the amount of CaO.

The result obtained after heat treatment as previously described are shown in Table 2. The mixes are based on an oxygen content of 260; $C_3S = Ca_{156}Si_{52}O_{260}$.

Figure 2 shows the relationship between the positions of the 040, 620, $\bar{6}20$ reflections and composition. The mix represented by $C_{146}M_{10}S_{50}$ gave a mixture of C_3S, C_2S and MgO, and from the amounts of MgO and C_2S detected the composition of the monoclinic C_3S was calculated as $C_{148.8}M_6S_{52}$. The results indicate that Mg^{2+} replaces Ca^{2+} in the C_3S lattice with a resulting decrease in the divergence of the γ and α angles from 90° until the monoclinic form becomes stabilized at room temperature between about $C_{152}M_4S_{52}$ and $C_{151}M_5S_{52}$, that is when containing about 1.5% MgO. The limit of solid solution for the 1,500°C preparation is $C_{150}M_6S_{52}$ which contains about 2.0% MgO. The mix of composition $C_{152}M_4S_{52}$ probably contains a mixture of the monoclinic and triclinic modifications at room temperature. D.t.a. examinations were made; the results are plotted in Figure 3 and confirm the suggested limit of solid solution.

The triclinic-monoclinic and monoclinic-trigonal inversions are both lowered in temperature by solid solutions of MgO and tend to come closer together. Composition $C_{152}M_4S_{52}$ which under the standardized heat treatment gave a mixture of phases, when annealed at 800°C for 4 h became clearly triclinic and, on reheating, two endotherms were detected at 889° and 906°C. No exsolution of MgO was noted. Composition $C_{150}M_6S_{52}$ remained monoclinic after 4 h at 800°C but was converted to triclinic after 19 h. On re-heating to 1,500°C and air-quenching it was again monoclinic. The metastable-phase boundaries are probably as shown in Figure 3: trigonal-monoclinic inversion rapid, monoclinic-triclinic inversion sluggish.

2.5 The Solid Solution of Alumina in Tricalcium Silicate

Starting with the assumption that Al replaces Si, preparations were made whose compositions fell on the line C_3S-"C_6A" (Table 3). From the amounts of the phases present the composition of the trialcium silicate phase was calculated. The results are given in the last column and indicate a maximum solubility of about 0.9% Al_2O_3 and a CaO/Al_2O_3 ratio for the matter in solid solution of 3.5-4.5. A second series of preparations was made in which alumina was present at about its limit of solubility and where composition fell on different possible joins towards the system $CaO-Al_2O_3$ (Table 4). D.t.a. was not considered necessary for these preparations.

Although the results are variable, a CaO/Al_2O_3 ratio of 4.5 in the solid solution is again indicated (it will be shown that there is a theoretical justification for this ratio).

A final series of preparations was made in the join C_3S-$C_{4.5}A$. Because of the structural findings reported later their compositions are expressed in terms of a constant oxygen content, conveniently 260, as $Ca_{156}Si_{52-3/4x}Al_xO_{260}$ or $(C_{156}S_{52-3/2y}A_y)$. (See Table 5 and Figures 4 and 5). The results indicate that there is only a very slight change of cell dimensions with solid solution of alumina.

3. STRUCTURAL IMPLICATIONS

The Mg^{2+} solid solution is a direct ionic replacement of Mg^{2+} for Ca^{2+} without affecting the charge balance. The solid solution C_3S-$C_{4.5}A$ can be accounted for by replacing $3Si^{4+}$ by $4Al^{3+}$ in the C_3S lattice and could take place in two ways:

(1) Keeping the oxygen content of the unit cell constant, which with this mode of substitution results in the calcium content also being constant. Then Si^{4+} is replaced by Al^{3+} in the ratio 3:4, the balance of charge being maintained.

(2) Keeping the $(Si^{4+} + Al^{3+})$ content of the unit cell constant; this results from a replacement of Si^{4+} by Al^{3+}, the balance of charge being maintained by the omission of Ca^{2+} and O^{2-} in the ratio 3:5.

To determine which of these possibilities was the most likely, the densities of the two preparations C_3S and $C_{156}S_{50.5}A$ were compared..

Assuming the same unit-cell volume for both compositions (as confirmed by X-ray results), the difference in density between C_3S and $C_{156}S_{50.5}A$ would be:

(1) Oxygen constant +0.10%

(2) Si^{4+} and Al^{3+} constant -0.65%

The determined density of C_3S was 3.1351 and of $C_{156}S_{50.5}A$ 3.1368 $g.cm^{-3}$. The standard deviation of the density determination was 0.0048 and the standard deviation of the mean was 0.0024. Taking 99% probability limits, the greatest possible difference between the two figures arising from experimental errors was 0.47%. There is therefore a strong probability that the structure is based on a constant O and Ca packing.

If $3Si^{4+}$ at the centres of oxygen tetrahedra are replaced by $3Al^{3+}$, the extra Al^{3+} will probably be placed in the interstitial positions which Jeffery indicated as possible sited for Mg^{2+}.

3.1 The Solid Solution of Magnesia and Alumina in Tricalcium Silicate

Solid solutions of C_3S in the system $CaO-SiO_2-MgO-Al_2O_3$ were investigated by means of mixes near the plane $C_3S-M_3S-C_{4.5}A$.

All the preparations shared the presence of other phases, C_2S, CaO, MgO or C_3A, and from the amounts of them the CaO/Al_2O_3 ratio of the solid solution end member was calculated. In this series of mixes there was a considerable scatter in the CaO/Al_2O_3 ratio, owing to the limitations of the experimental techniques used. It was concluded that the solubilities of Al_2O_3 and MgO and their modes of substitution are almost unaffected by the presence of each other.

When the C_3S phase is saturated with Al_2O_3, only about 1.0% of MgO is required to stabilize the monoclinic form at room temperature. If MgO and Al_2O_3 are both reduced below their saturation limits, at about 0.75 of their saturation limits the triclinic form probably occurs (Figure 6). No endothermic reactions were detected in the preparations saturated with both Al_2O_3 and MgO, which may be related to the observation reported by Nurse et al[12], who found that a cement containing a large amount of C_3S gave no detectable transformation peaks.

A final series of preparations was made in which alumina was kept at its limit of solubility and in which the magnesia content was gradually increased. The compositions based on 260 oxygens in the form $C_{156-x}M_xS_{51-3/2y}A_y$ and the results obtained are given in Table 6, the X-ray results are plotted in Figure 7. In this series will be found the purest preparations of the Al_2O_3 and MgO stabilized monoclinic phase that have been prepared in the present investigation. Figures 7 and 8 show that the interpretation is not so explicit as that for the MgO series. But, considering the evidence for that series, a similar interpretation has been applied.

Preparations in the series $C_{156-x}M_xS_{50.5}A$ were cooled from 900°C to room temperature at a rate of about 3°C/min. and then re-examined. The X-ray results (Figure 9) indicate the relative instability of the monoclinic form previously obtained from mix $C_{153}M_3S_{50.5}A$. Rather more significant results (Table 7) were obtained from quenching experiments similar to those carried out for the magnesia series.

These results agree with the interpretation of the X-ray and d.t.a. results. There was no detectable decomposition of the samples or exsolution of MgO or Al_2O_3 after 19 h at 800°C. A Portland cement containing C_3S in the monoclinic form was also annealed at 800°C for 19 h and air-quenched. Almost complete decomposition of the C_3S phase into CaO and C_2S had occurred, but the C_3S remaining appeared still to be monoclinic. The discrepancy between the rate of decomposition of the monoclinic phase in synthetic preparations and in Portland cements stresses the need for investigation into the effect of other ions in the stabilization of the monoclinic C_3S phase.

The evidence for the solid solution of MgO and Al_2O_3 in C_3S, together with their limits of solubility, can be incorporated into a single diagram indicating the type of C_3S occurring at room temperature when the preparations are quenched from 1,500°C. to room temperature (Figure 6).

The monoclinic form observed at room temperature is probably metastable for three co-existing reasons:

(1) Suspension of the monoclinic-triclinic transition occurring at about 850°C.

(2) Possible supersaturation with respect to both magnesia and alumina.

(3) Reported instability of C_3S below about 1,250°C.[12]

3.2 Jeffery's Formula for Alite

Jeffery determined a structure for alite using crystals grown by Nurse at the Building Research Station from cement clinker dissolved in $CaCl_2$. The diffraction pattern of these crystals cannot be distinguished from that given by $C_{151}M_5S_{50.5}A$, although Jeffery's structure and the chemical analysis both indicated a formula $C_{54}S_{16}AM$. The present research shows that a mix of this composition processed at 1,500°C would yield a monoclinic solid solution with 4.5% C_3A and 4.8% CaO. However, neither CaO nor C_3A can be detected in Jeffery's crystals, which would suggest that either the chemical analysis is in error or that, under the conditions of formation of the crystals, the solubility of MgO and Al_2O_3 was markedly greater than in the present experiments at 1,500°. This would not be surprising, as Nurse's crystals were grown in the presence of liquid and at a much lower final temperature.

A mixture of Jeffery's formula was synthesized and processed at 1,500°C and as shown in Table 8 gave the results expected on the basis of the present investigation, according to the following equation:

$$C_{54}S_{16}AM \longrightarrow 0.317(C_{152.84}M_{3.16}S_{50.5}A) + 0.683C_3A + 3.501\ CaO.$$

3.3 P.C.A. Formulation 1/3 J Alite, $C_{162}S_{52}AM$

Kantro, Copeland and Brunauer[6] prepared a large sample of what they described as 'a good sample of alite containing little C_3A'. This sample has been widely circulated and we are grateful to Dr. Copeland for supplying us with a sample of his material. If the findings reported in this paper are correct then at 1,500°C this sample should give a triclinic solid solution and lime according to the equation:

$$C_{162}S_{52}AM \longrightarrow 1.03(C_{155.03}M_{0.97}S_{50.51}A_{0.97}) + 2.2CaO$$

Having made allowance for the presence of a small peak due to the C_3S phase itself, no C_3A was detected in this sample; there was also less than 0.2% C_2S. The results of the examination are given in Table 9 and compared with the results predicted.

The C_3S phase is in the triclinic form as predicted.

4. CONCLUSIONS

(1) Mg^{2+} can enter the structure of C_3S to the extent of 2.0% MgO at 1,500°C. Mg^{2+} replaces Ca^{2+}, and can stabilize the monoclinic form on quenching to room temperature, about 1.5% MgO being required.

(2) Al^{3+} can enter the structure of C_3S to the extent of about 0.9% Al_2O_3 at 1,500°C. $4Al^{3+}$ replaces $3Si^{4+}$, the balance of charge is maintained, and the O and Ca packing in the unit cell is unchanged. Al^{3+} alone does not stabilize the monoclinic form on quenching to room temperature.

(3) In the presence of Al^{3+} to the extent of 0.9% Al_2O_3 about 1% MgO can stabilize the monoclinic form on quenching to room temperature. Further MgO substitution can occur up to a maximum of about 1.7% MgO, resulting in a slight change in the monoclinic structure. The conclusions regarding the mode of substitution of Mg^{2+} and Al^{3+} alone still apply whenthey are introduced together.

(4) If Mg^{2+} and Al^{3+} together are reduced below about 0.75 times the amount required to saturate the structure, the triclinic form occurs on quenching to room temperature.

REFERENCES

1. JEFFERY, J.W., 'The crystal structure of tricalcium silicate', Acta Cryst., 5, 26, 1952.

2. JEFFERY, J.W., 'The tricalcium silicate phase', Third International Symposium on the Chemistry of Cement (London, 1952).

3. VON EUW, M., 'Quantitative analysis of Portland cement clinker by X-rays', Silicates Industriels, 23, 643, 1958. (Translated from French by D. Kantro, Portland Cement Association Foreign Literature Study No. 326).

4. LOCHER, F.W., 'Solid solution of alumina and magnesia in tricalcium silicate', Fourth International Symposium on the Chemistry of Cement (Washington, 1960).

5. MIDGLEY, H.G., ROSAMAN, D., and FLETCHER, K.E., 'X-ray diffraction examination of Portland cement clinker', Fourth International Symposium on the Chemistry of Cement (Washington, 1960).

6. KANTRO, D.L., COPELAND, L.E., and BRUNAUER, STEPHEN, Discussion of the papers 'Phase equilibria and constitution' (Nurse), 'X-ray diffraction examination of Portland cement clinker' (Midgley, Rosaman and Fletcher), Fourth International Symposium on the Chemistry of Cement (Washington, 1960).

7. YAMAGUCHI, G., IKEGAMI, H., SHIROSUGA, K., and AMANO, K., 'Effects of the addition of magnesia or calcium fluoride on the thermal properties of tricalcium silicate', Semento Gijutsu Nenpo, 11, 24, 1957; Chem. Abstr., 52, (18), 15319, 1958.

8. NAITO, R., ONO, Y., and IIYAMA, T., 'A study on alite phase by X-ray powder diffraction', Jap. Cem. Eng. Ass. Rev., 11, Meeting, Tokio 1957.

9. YAMAGUCHI, G., and MIYABA, H., 'Precise determination of the $3CaO.SiO_2$ cells and interpretation of their X-ray diffraction patterns', J. Amer. Ceram, Soc., 43, 219, 1960.

10. LERCH, W., and BOGUE, R.H., Ind. Eng. Chem. Analyst., 2, 296, 1930.

11. COPELAND, L.E., and BRAGG, ROBERT H., 'Quantitative X-ray diffraction analysis', Anal. Chem., 30, 196, 1958.

12. NURSE, R.W., MIDGLEY, H.G., and WELCH, J.H., 'Polymorphism of tricalcium silicate and its significance in cement hydration', Building Research Station Note No. A 95.

13. YANNAQUIS, N., REGOARD, M., MAZIERES, Ch., and GUINIER, A., Bull. Soc. Franc. Miner, Crist., 83, 271, 1962.

14. MIDGLEY, H.G., FLETCHER, K.E., and COOPER, A.G., (in the press), Symposium on the analysis of Calcareous Materials (April, 1963).

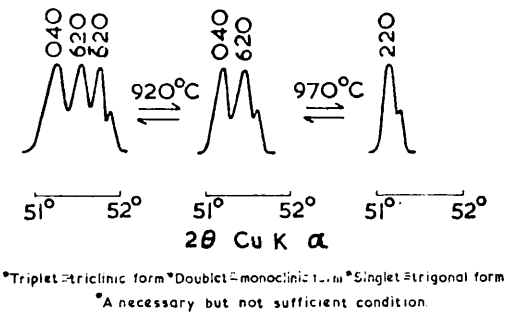

FIGURE 1.

Diagrammatic representation of the 040, 620, $\bar{6}20$, reflections of the three polymorphs of C_3S

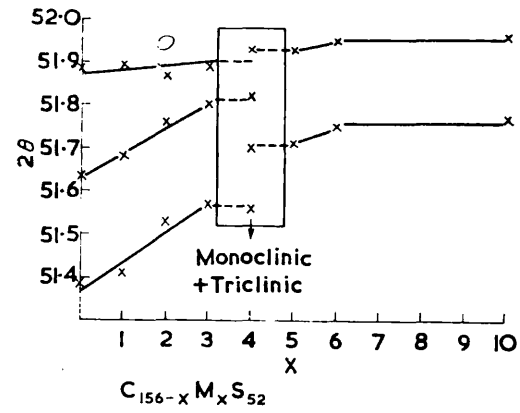

FIGURE 2.

Relationship between position of 040, 620, $\bar{6}20$ reflections (Cu $K\alpha_1$ radiation) and composition in magnesium-substituted C_3S.

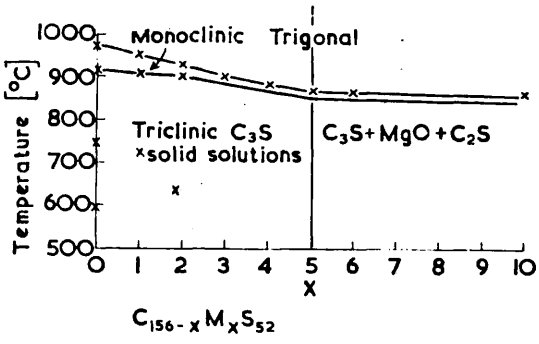

FIGURE 3.

D.t.a. peak temperatures and a suggested phase diagram.

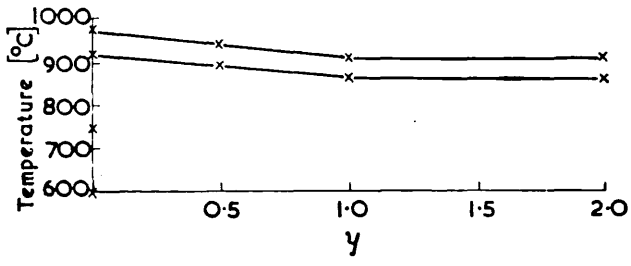

FIGURE 4.

D.t.a. results of mixes of composition $C_{156}S_{52-3/2y}A_y$.

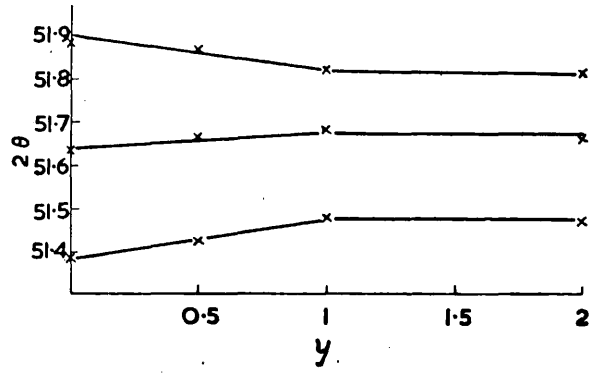

FIGURE 5.

X-ray diffraction results of the 040, 620, $\bar{6}20$ reflections (Cu$K\alpha_1$ radiation) of mixes of composition $C_{156}\ S_{52-3/2y}A_y$.

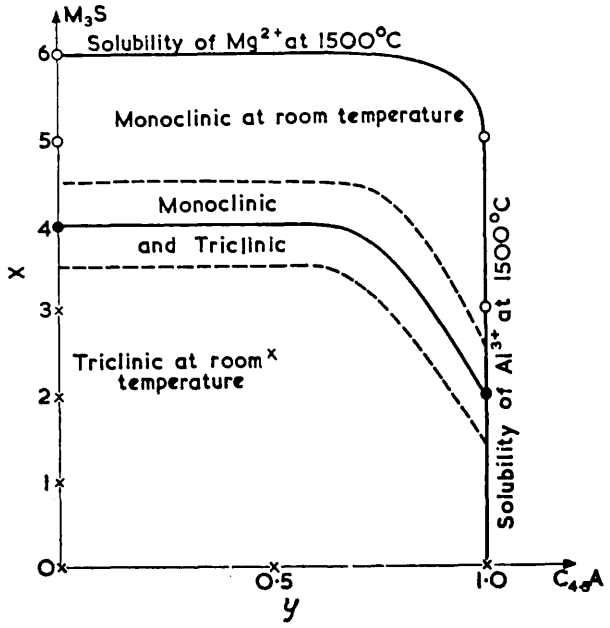

FIGURE 6.

Polymorphic phases obtained at room temperatures as a result of air quenching preparation of composition $C_{156-x}M_xS_{52-3/2y}A_y$ from 1,500°C.

o denotes monoclinic form at room temperature.
× denotes triclinic form at room temperature.
● denotes triclinic and monoclinic form at room temperature.

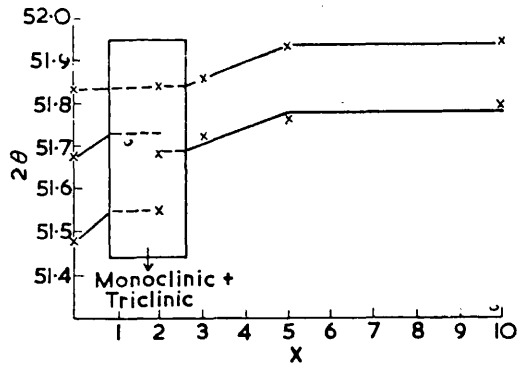

FIGURE 7.
X-ray diffraction data of the 040, 620, $\bar{6}20$ reflections (Cu $K\alpha_1$ radiation) of mixes of composition $C_{156-x}M_xS_{50\cdot5}A$.

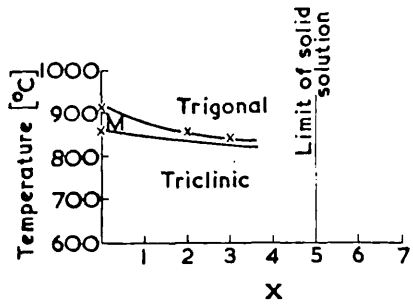

FIGURE 8.
D.t.a. results on mixes of composition $C_{156-x}M_xS_{50\cdot5}A$.

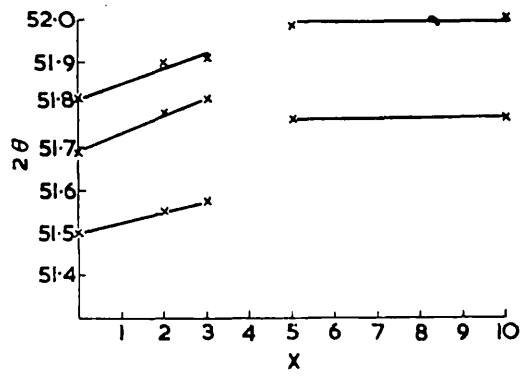

FIGURE 9.
X-ray diffraction data of the 040, 620, $\bar{6}20$ reflections (Cu $K\alpha_1$ radiation) of mixes of composition $C_{156-x}M_xS_{50\cdot5}A$ cooled from 900°C at 3°C/min.

Table 1
Analyses of Reagents used in Mixes

Calcium carbonate (%)		*Silica* (%)		*Magnesia* (%)		*Alumina* (%)	
CaO	56·08	SiO_2	> 99·90	MgO	> 97·94	Al_2O_3 (by difference)	> 99·6
R_2O_3	< 0·02	Loss at 1,200°C	0·04	SiO_2	0·05	SiO_2	0·03
Fe_2O_3	< 0·01	Fe_2O_3	< 0·01	Fe_2O_3	< 0·01	Fe_2O_3	0·04
MgO	≯ 0·10	Na_2O	< 0·01	TiO_2	< 0·01	CaO	< 0·03
Na_2O	< 0·03	K_2O	< 0·01	Al_2O_3	0·03	MgO	< 0·03
K_2O	< 0·03			CaO	0·02	Na_2O	< 0·02
SO_3	< 0·01			Na_2O	0·02	K_2O	< 0·03
Chloride	< 0·01			K_2O	0·004	TiO_2	< 0·01
				Mn_2O_3	< 0·01	P_2O_5	< 0·01
				Acid-soluble SO_3	< 0·01	SO_3	< 0·01
				Chloride	Absent	Chloride	< 0·01
				Loss at 1,000°C	1·68	HNO_3 soluble Loss at 1,200°C (carbon present)	0·18
				Loss at 1,150°C	1·91		
				Carbonate	0·54		

Table 2

X-ray, D.t.a. and Composition Data on Magnesium-substituted C_3S

Sample	Minor phases present			X-ray diffraction 2θ CuKα1			D.t.a. temps at which endothermic reactions are observed (°C)			
	C_2S	CaO	MgO	040	620	$\bar{6}20$				
C_3S	0·5	0·05	0	51·381	51·642	51·890	595	747	916	969
$C_{155}MS_{52}$	1·4	0·13	0	51·41	51·68	51·89	—	721	911	954
$C_{154}M_2S_{52}$	0	0·03	0	51·53	51·76	51·87	—	663	907	923
$C_{153}M_3S_{52}$	2·2	< 0·03	0	51·57	51·80	51·89	—	—	901	—
$C_{152}M_4S_{52}$	1·1	< 0·03	0	51·56	51·70	51·82 51·93	—	—	886	—
$C_{151}M_5S_{52}$	1·0	0·13	0	51·71	51·93		—	—	871	—
$C_{150}M_6S_{52}$	1·3	0·06	0	51·75	51·95		—	—	864	—
$C_{146}M_{10}S_{52}$	4·7	< 0·03	1·5	51·77	51·96		—	—	860	—

Table 3

X-ray, D.t.a. and Composition Data in the System C_3S–"C_6A"

Sample (Mole per cent)		Minor phases present			X-ray diffraction 2θ CuKα1			D.t.a. temps at which endothermic reactions were observed (°C)				Solid solution in form 98 mole % C_3S 2 mole % C_zA_y	
C_3S	C_6A	C_2S	CaO	C_3A	040	620	$\bar{6}20$					C_zA_y	z/y
100	0	0·5	0·05	0	51·381	51·642	51·890	595	747	916	969	—	—
99	1	0·2	0·63	0	51·45	51·64	51·87	*(466)		886	936	$C_{1·84}A_{0·52}$	3·6
98	2	0	0·66	0	51·50	51·72	51·84	(476)		856	908	$C_{4·79}A_{1·04}$	4·6
97	3	0·5	1·31	0·4	51·50	51·70	51·85	(470)		857	904	$C_{6·47}A_{1·42}$	4·6
96	4	0·4	2·88	1·4	51·50	51·70	51·84	(466)		856	906	$C_{4·75}A_{1·51}$	3·2
94	6	0·3	3·49	3·0	51·50	51·71	51·84	(466)		856	904	$C_{7·85}A_{1·92}$	4·1

* The reaction observed at 466°C is due to $Ca(OH)_2 \longrightarrow CaO + H_2O$.

Table 4

X-ray, D.t.a. and Composition Data in the Systems of C_3S with Hypothetical Calcium Aluminates of Various Compositions

Sample 98 mole % C_3S 2 mole % x	Minor phases present			X-ray diffraction 2θ CuKα1			Solid solution in the form 98 mole% C_3S 2 mole% C_zA_y	
x	C_2S	CaO	C_3A	040	620	$\bar{6}20$	C_zA_y	z/y
C_3A	2·5	0·06	0	51·49	51·70	51·82	$C_{4·92}A_{1·06}$	4·6
C_4A	1·1	0·10	0	51·49	51·71	51·84	$C_{4·63}A_{1·105}$	4·2
$C_{4·5}A$	1·1	0·03	0	51·48	51·68	51·83	$C_{5·4}A_{1·02}$	5·3
C_5A	0·8	0·03	0	51·49	51·70	51·83	$C_{5·55}A_{1·01}$	5·5
C_6A	0	0·66	0	51·50	51·71	51·84	$C_{4·79}A_{1·04}$	4·6

Table 5

X-ray, D.t.a. and Composition Data in the System C_3S towards $C_{4·5}A$

Sample $C_{156}S_{52-3/2y}A_y$	Minor phases present			X-ray diffraction 2θ CuKα1			D.t.a. temps at which endothermic reactions were observed (°C)				Solid solution in form 98 mole% C_3S 2 mole% C_zA_y	
	C_2S	CaO	C_3A	040	620	$\bar{6}20$					CA_y	z/y
C_3S	0·5	0·05	0	51·381	51·642	51·890	595	747	916	969	—	—
$C_{156}S_{51·25}A_{0·5}$	1·6	0·03	0	51·43	51·67	51·87	—	—	896	941	$C_{2·62}A_{0·51}$	5·14
$C_{156}S_{50·5}A$	1·1	0·03	0	51·48	51·68	51·83	—	—	869	916	$C_{5·4}A_{1·02}$	5·29
$C_{156}S_{49}A_2$	0	0·98	2·5	51·49	51·70	51·82	(468)*	—	864	911	$C_{4·23}A_{1·105}$	3·83

* Decomposition of $Ca(OH)_2$.

Table 6

X-ray, D.t.a. and Composition Data for Mixes of Composition $C_{156-x}M_xS_{50·5}A$

Sample	Minor phases present				X-ray diffraction 2θ CuKα1			D.t.a. temps at which endothermic reactions were observed				Solid solution in form $C_{156-x}M_xS_{52}C_zA_y$	z/y
	C_2S	CaO	MgO	C_3A	040	$\bar{6}20$	$\bar{6}20$						
$C_{156}S_{50·5}A$	1·1	0·03	0	0	51·48	51·68	51·83	—	—	864	911	$C_{156}S_{52}C_{5·4}A_{1·02}$	5·3
$C_{154}M_2S_{50·5}A$	2·0	0·03	0	0	51·55	51·68	51·84	—	—	854		$C_{153·8}M_{2·2}S_{52}C_{5·4}A_{1·07}$	5·0
$C_{153}M_3S_{50·5}A$	1·2	0·03	0	0	51·72	51·86		—	—	842		$C_{153}M_3S_{52}C_{5·3}A_{1·00}$	5·2
$C_{151}M_5S_{50·5}A$	0·4	0·13	0	0	51·76	51·93		No endothermic reactions detected				$C_{151}M_5S_{52}C_{4·4}A_{1·00}$	4·4
$C_{146}M_{10}S_{50·5}A$	4·0	0·03	1·5	0	51·79	51·94						$C_{150·2}M_{5·8}S_{52}C_{2·9}A_{1·05}$	2·8
												Mean	4·5

Table 7

Relative Stabilities of Polymorphic Modifications in the Series $C_{156-x}M_xS_{50\cdot5}A$

	Annealed for 4 h at 800°C air-quenched	*Annealed for 19 h at 800°C air-quenched*	*Annealed for 10 min. at 1500°C, air-quenched*
$C_{153}M_3S_{50\cdot5}A$	Mainly monoclinic, some triclinic	Triclinic	Monoclinic
$C_{151}M_5S_{50\cdot5}A$	Monoclinic	Mainly monoclinic, some triclinic	Monoclinic
$C_{146}M_{10}S_{50\cdot5}A$	Monoclinic	Monoclinic	Monoclinic

Table 8

X-ray, D.t.a. and Composition Data for the Formulation $C_{54}S_{16}AM$ processed at 1,500°C

	CaO	C_3A	*X-ray diffraction 2θ CuKα₁*		*D.t.a. temp (°C) of endothermic reaction due to a C_3S transition*
			040	*620*	
Predicted	4·8	4·5	51·72	51·88	838
Found	4·7	4·5	51·70	51·90	832

Table 9

X-ray, D.t.a. and Composition Data for the Formulation $C_{162}S_{52}AM$

	CaO	*X-ray diffraction 2θ CuKα₁*			*D.t.a. temp (°C) of endothermic reaction due to a C_3S transition*
		040	*620*	*$\bar{6}20$*	
Predicted	1·0	51·55	51·71	51·83	870
Found	1·3	51·55	51·72	51·85	864

CURRENT PAPERS

RESEARCH SERIES

1. The system $CaO-Al_2O_3-H_2O$ at $25^{\circ}C$
2. Some experiments on model piled foundations in clay
3. Measurement and control of moisture content by microwave absorption
4. The measurement of wind pressures on tall buildings
5. The reverberation times of some English cathedrals
6. Hysteresis in the moisture characteristics of porous bodies
7. New data on synthetic mullites
8. An improved solution for the determination of thermal conductivity by Vernotte's dynamic method.
9. International comparisons of the cost of housebuilding.
10. The horizontal propagation of sound from a jet engine close to the ground, at Radlett
11. Warm air heating in local authority flats, 1961-2
12. Determination of heat of hydration of low heat slag cements
13. The point counting microscopic method for the quantitative determination of the silicate phases in Portland cement clinker

MIDGLEY (H.G.)
D.Sc. 1967.

26

CHAPTER 3

The Formation and Phase Composition of Portland Cement Clinker

H. G. MIDGLEY

Building Research Station, Garston, Watford, Hertfordshire, England

CONTENTS

26

I. Introduction

Portland cement is produced by the high-temperature reaction of a lime-bearing material with one containing silica, alumina, and some Fe_2O_3. Reaction is effected in kilns of various types, normally under oxidizing conditions. The product, which is known as clinker, is afterwards ground with gypsum to give cement. The main phases in the clinker are tricalcium silicate (C_3S), β-dicalcium silicate (β-C_2S), tricalcium aluminate (C_3A) and a ferrite phase belonging to the C_2F–C_2A solid solution series. Also present in many clinkers are smaller amounts ($< 3\%$) of free lime (CaO), periclase (MgO) and alkali sulphates. The presence of glass, in amounts ranging up to 20% or even higher, has also frequently been postulated, but recent work casts doubt on this conclusion.

It is now well established that none of the major phases has an exact composition; all are modified by solid solution, both by the major oxides and by minor components.

II. The Phases in Clinker

A. Tricalcium Silicate

The main phase in most modern Portland cement clinkers is a form of tricalcium silicate, originally described as "alite" by Törnebohm [*1*], who studied it by thin-section microscopy. General agreement that alite was essentially C_3S was reached by about 1930. In 1952 Jeffery [*2*] showed that pure C_3S is triclinic but that small amounts of solid solution cause it to become monoclinic or trigonal; he found the monoclinic form in a Portland cement clinker. The three polymorphs differ only slightly in structure. He suggested that, with pure C_3S, the triclinic form is stable relative to the others at room temperature, the monoclinic form at moderate temperatures and the trigonal form at high temperatures. This was later confirmed by Yamaguchi and Miyabe [*3*], who used a high-temperature X-ray diffractometer. Midgley [*4*] investigated 20 Portland cement clinkers by X-ray diffraction using film, and showed that in all of these the C_3S was monoclinic. More recent work by Midgley and Fletcher [*5*], using X-ray diffractometry, showed that the C_3S in Portland cement is usually monoclinic but that, even in ordinary clinkers, the triclinic and trigonal forms may occur.

Jeffery [*2*] proposed that the alite in Portland cement clinker had the composition $C_{54}S_{16}AM$, but von Euw [*6*] showed that material of this

composition contained C_3A as an impurity. He suggested that alite formed in the presence of excess CaO had the composition of C_3S with about 2% C_3A and 1% MgO. Naito, Ono and Iiyama [7] reported the maximum substitutions of Mg and Al in the series

$$(Ca_{1-x-y}Mg_xAl_y)_3 \cdot (Si_{1-3y}Al_{3y})O_5$$

to be $x = 0{\cdot}025$ and $y = 0{\cdot}0075$. Brunauer *et al.* [8] investigated the incorporation of Al and Mg into C_3S in an effort to produce an "alite" suitable for use as a standard in the X-ray diffractometry of clinkers, and concluded that the correct formulation was $52C_3S.C_6AM$; that is, the type of substitution proposed by Jeffery but with one-third the amounts of Al_2O_3 and MgO. Locher [9] studied the solid solution of MgO and C_3A in C_3S at various temperatures and found that the solubility of MgO varies from 2·5% at 1500° C to 1·5% at 1420° C; that of C_3A was 2% at 1500° C. He relied mainly on the determination of free lime by chemical means to estimate the limits of solubility and gave no details of the crystal structures.

Midgley and Fletcher [5] have investigated the effect of substitution of Mg and Al in C_3S prepared at 1500° C and subsequently studied at room temperature. They showed by X-ray diffractometer studies that Mg can replace Ca directly in C_3S and that as the amount of Mg increases there is a change in the lattice parameters of the triclinic form, until at about 1·7% MgO the lattice becomes monoclinic. Further incorporation of Mg causes changes in the monoclinic lattice parameters until about 2% MgO is reached, beyond which no further substitution takes place. Midgley and Fletcher also showed that the substitution of Al in the attice is not caused by solid solution of C_3A in C_3S, but by solid solution within the series C_3S–$C_{4\cdot5}A$; that is, three-quarters of the Al replaces Si directly, the number of oxygens remains constant and the remaining one-quarter of the Al goes into interstitial positions. Substitution of Al causes a change in lattice parameters but not in symmetry. Lafuma [10] and Midgley and Fletcher [5] have shown that Fe_2O_3 may also enter into solid solution with C_3S to a limited extent.

Midgley and Fletcher [5] studied the effects of simultaneous substitution of Mg for Ca and of $C_{4\cdot5}A$ for C_3S. There were changes in cell parameters and symmetry similar to those observed when only the first of these substitutions was made. The trigonal form has not so far been observed in this work. These results, together with those of studies on cement clinkers, suggest that the alite in Portland cement can vary considerably in composition and symmetry. The changes in symmetry can affect the strength produced by the phase; experiments have shown that the differences are of the order of 10%.

Substitution in C_3S is further discussed in Chapter 4.

Alite decomposes into C_2S and CaO below about 1275° C, but this reaction is usually sluggish and C_3S can therefore occur metastably at room temperature. Woermann [*11*] has investigated the effect of substitution on the rate of decomposition and has shown that divalent ions of radius greater than 0·7 Å increase the rate of decomposition while smaller ones do not.

Jander [*12*] suggested that the strength produced by the alite in a cement might depend not only on the presence of ions in solid solution but also on the occurrence of structural defects and of cracks and irregularities of colloidal dimensions. No experimental evidence to support or refute this has so far been presented. Grzymek [*13*] believes that small and elongated crystals of alite can hydrate more rapidly, even if ground to the same specific surface as large and more equant crystals. So far this has not been confirmed by other workers in the field.

B. Dicalcium Silicate

Most of the work on dicalcium silicate in recent years has been on laboratory preparations; little work has been done on C_2S from clinker. Dicalcium silicate can occur in four polymorphic modifications: α, α', β and γ. Nurse [*14*] has shown that the γ-form is almost inert, that β hydrates at a rate depending on the kind of stabilizer, that α' gives very poor strength and that α is non-hydraulic. Budnikov and Azelitskaya [*15*] declare that γ-C_2S has hydraulic properties, but the general view is that it has not.

The usual form of dicalcium silicate in Portland cement clinker is the β-modification. Metzger [*16*] has observed small quantities of α'-C_2S by microscopic investigation, and Midgley and Fletcher [*17*] have found this phase by X-ray methods in commercial clinkers. A phase of approximate composition $KC_{23}S_{12}$ has also been formed in commercial clinkers; as shown later, this is probably a form of α'-C_2S.

Dicalcium silicate can take into solid solution many substances, and the presence of these must modify the structure. Nurse [*14*], Kukolev and Mel'nik [*18, 55*] and Welch and Gutt [*20*] have shown that the strength obtained from β-C_2S depends on the nature of the stabilizer. The substances that might most obviously occur in solid solution with the β-C_2S of Portland cement clinker are magnesia and alumina [*8, 21, 22*] P_2O_5 [*23*], Na_2O, CaO and K_2O [*19, 24–26*]. Yannaquis and Guinier [*26*] suggested that β-C_2S may also be stabilized by crystal size alone. Most work on the pure compound has been on material stabilized with B_2O_3, but it is not likely that this form occurs in Portland cement. Midgley,

Fletcher and Cooper [*27*] showed that the X-ray pattern of the β-C_2S present in Portland cement clinkers differs significantly from that given by C_2S stabilized by B_2O_3.

C. The Ferrite Phase

The ferrite phase in Portland cement clinker, also called brownmillerite, is a solid solution which is usually taken to belong to the series C_2F–C_2A. The limiting composition at the iron-rich end is C_2F. There is some disagreement as to the limit at the alumina-rich end but, from the work of Toropov, Shishakov and Merkov [*28*], Yamauchi [*29*], Swayze [*30*] and Malquori and Cirilli [*31*], summarized by Nurse [*32*], it must occur at a composition slightly more aluminous than C_6A_2F. This problem is also discussed in Chapter 2.

The clinker mineral has been studied by X-ray diffraction methods by Midgley [*33–35*] and by Kato [*36*], who showed that it can vary in composition and may show zoning—a variation in composition within each crystal. This work has been extended by Brunauer *et al.* [*8*], Copeland *et al.* [*32*] and Midgley, Rosaman and Fletcher [*37*], who have made quantitative estimations of the minerals in Portland cement.

Midgley [*35*] has shown that the composition of the ferrite phase from clinker may extend to very near the alumina-rich limit. Cirilli and Brisi [*38*] and Santarelli, Padilla and Bucchi [*39*] suggest that the limit may be C_4AF, although the first-named authors showed that in the presence of 3% MgO the limit may extend approximately to C_6A_2F. Kato [*36*] has shown that about 1·5% MgO may substitute for CaO in the ferrite phase, and Royak [*40*] showed that Na_2O may enter into solid solution.

D. Tricalcium Aluminate

Tricalcium aluminate has no polymorphic modifications, and the only effects observed by Volkonskii [*41*] on heating C_3A to 1500° C in the high-temperature X-ray diffraction camera were caused by thermal expansion. Tröjer [*42*] observed zoning in C_3A in a microscope examination.

Two compounds that are closely allied to C_3A are NC_8A_3 [*43*] and KC_8A_3 [*44–46*]; both give X-ray diffraction patterns very similar to but slightly modified from that of pure C_3A. Suzukawa [*44–46*] showed that SiO_2 and MgO also enter into solid solution, resulting in a change in lattice parameter. Müller-Hesse and Schwiete [*47*] give the solubility of MgO in C_3A as 2·5%.

E. Minor Phases

Calcium oxide (CaO) and magnesium oxide (periclase; MgO) are both undesirable phases in a cement clinker, because they are liable to hydrate slowly after the cement has hardened, causing expansion. The composition of the raw mix must therefore be such that these phases are absent or nearly absent in the product; this question is discussed in Chapter 2. CaO is nevertheless probably present in small amounts in all Portland cement clinkers, generally because of incomplete reaction. MgO, where present, is usually derived from the $MgCO_3$ of the original limestone. As shown later, the harmful effect of MgO can be somewhat reduced by rapid cooling of the clinker.

The clays and shales used in the manufacture of Portland cement usually contain small amounts of sulphates and sulphides, and the fuel used frequently contains sulphur compounds, so that in the kiln at the clinkering temperatures SO_3 is produced. This reacts with any alkalis present, either from the raw materials or the fuel, to produce alkali sulphates. Taylor [*48*] detected K_2SO_4 in commercial clinkers; other alkali sulphates which might reasonably be present include Na_2SO_4, $3K_2SO_4.Na_2SO_4$, and K_2SO_4–Na_2SO_4 solid solutions, which are stable at high temperatures. The subject has been reviewed by Newkirk [*49*], who concluded that the alkali sulphate produced probably depends on the Na/K ratio of the raw materials and the amount of SO_3 available. He also considered that there was a tendency for the alkalis to combine with the entire content of SO_3 in the approximate molar ratio $K_2O/Na_2O_3 = 3$, subject to the availability of the three components involved. In contrast, Suzukawa [*44–46*] concluded that the SO_3 reacts with K_2O in preference to Na_2O. In most clinkers the molar ratio $(Na_2O + K_2O)/SO_3$ exceeds unity. The excess of Na_2O and K_2O is likely to enter the silicate or aluminate phases; this is discussed on pp. 97–99.

III. Effect of Minor Components

The minor components in the raw materials of Portland cement clinker affect the product mainly by ionic substitution in the major phases. These modifications may or may not affect the hydraulic properties. Recently the study of the effects of minor components has become prominent because of the increasing use of impure raw materials.

A. Phosphates

The chemical analyses of most Portland cements show small percentages of phosphates, expressed as P_2O_5. In recent years the role of

phosphates has assumed greater interest because of the exploitation of difficult limestone deposits, or the desire to use various trade wastes as raw material in cement manufacture. The effect of phosphate in Portland cement has been reviewed by Steinour [*50*], who concluded that the rules put forward by Nurse [*51*] are a sufficiently accurate guide to practice. Nurse showed that most of the P_2O_5 is present in solid solution with the

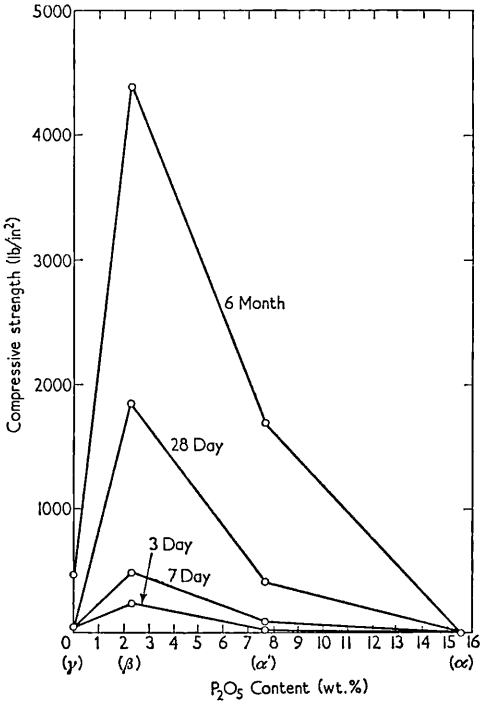

FIG. 1. Compressive strengths on $\frac{1}{2}$-in (12-mm) 1:3 mortar cubes of preparations on the join C_2S–C_3P, showing effect of C_2S polymorphism.

C_2S and that as a consequence the amount of C_3S is markedly reduced. Nurse, Welch and Gutt [*23*] published a diagram showing a series of solid solutions between α-C_2S and a previously unknown high temperature form of C_3P isomorphous with α-C_2S.

Toropov and Borisenko [*52*] also investigated the effect of P_2O_5 on C_3S at high temperatures and found the latter to be decomposed to C_2S and CaO. These authors also found that there was no reaction with the ferrite phase. Simanovskaya and Shpunt [*53*] investigated reactions

with P_2O_5 and found the same decomposition of C_3S; they also followed the reaction in a kiln.

Erschov [*54*] found that a rapid-hardening Portland cement could be produced by adding 0·2–0·3% P_2O_5 to the raw material. Kukolev and Mel'nik [*55*] found that addition of 0·3–1·5% P_2O_5 to the raw meal used for making clinker by the wet process increased the hydraulic activity of the resultant cement. They attributed the increased activity to the production of lattice defects in the C_2S due to the substituting ions; as already stated, Jander [*12*] considered that this would increase the activity. Welch and Gutt [*20*] investigated the effect of P_2O_5 on C_3S

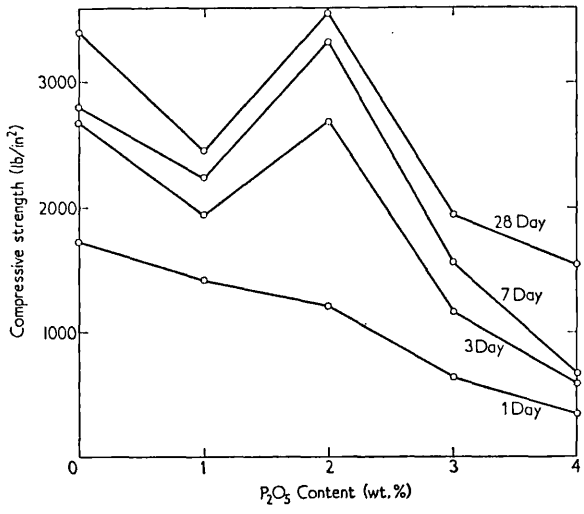

FIG. 2. Compressive strengths on ½-in (12-mm) 1:3 mortar cubes of preparations on the join from C_3S to 24·1 weight % C_3P, 75·9 weight % C_2S, in the system $CaO–SiO_2–P_2O_5$. Mean results of determinations on duplicate preparations containing 1% and 2% P_2O_5 are plotted.

and C_2S; they found that small amounts of P_2O_5 enhanced the strength obtained from C_2S, while large amounts decreased it. As an explanation they showed that with no P_2O_5 the C_2S was in the γ-form; with 2% it was in the β-form; and with 7 and 15% it was in the α'- or α-form (Fig. 1). With C_3S they report that addition of small amounts of phosphate causes a fall in the compressive strength, but that as addition continues the strength rises again, the composition 71·7 CaO, 26·3 SiO_2, 2·0 P_2O_5 (wt %) giving by a small margin the highest strength of the series at 3, 7 and 28 days. Further addition of up to 4% P_2O_5 is detrimental to strength (Fig. 2).

In interpreting the results with C_3S, allowance must be made for the increasing proportions of α'-C_2S occurring in mixes of increasing P_2O_5 content. In the 2% mix, for example, the α'-C_2S content can be estimated as about 30% by weight of the total. So far it has not been possible to isolate the C_3S, which may be modified by the incorporation of P_2O_5, and it has therefore been necessary to use mixes containing the additional phase and to make appropriate corrections. Since the α'-C_2S is comparatively inert hydraulically, the fall in strength of the mixes progressing from 2 to 4% P_2O_5 can be accounted for by the increasing dilution of the C_3S with almost non-hydraulic material. The 2% P_2O_5 mix, although diluted with some 30% of α'-C_2S, gives strengths comparable with those obtained with pure C_3S, so that the form of C_3S present in this mix can be considered to possess enhanced hydraulic value. The authors therefore deduce that limited amounts of P_2O_5 can enhance the hydraulicity of C_3S.

B. Fluorides

Fluorides are occasionally found as impurities in limestone. They may also be added deliberately as a flux or whitening agent or to offset the deleterious effect of P_2O_5.

Yamaguchi *et al.* [*56*] showed that both C_3S and C_3A can exist in the presence of CaF_2 and that CaF_2 can substitute in C_3S, causing a contraction of the lattice parameters. Toropov and his co-workers [*57*, *58*] showed that C_3A is decomposed at high temperatures by 5% addition of CaF_2 and that members of the ferrite solid solution series are also acted upon by CaF_2, being decomposed to $C_{12}A_7$ and a ferrite of composition near to C_6AF_2. Moore [*59*] showed that the addition of 1–3% fluorspar to raw meal ensured assimilation of the free CaO at a much lower temperature; the fluoride is retained by the clinker.

Welch and Gutt [*20*] found that in the presence of phosphatic calcium silicate minerals some of the fluorine is lost on heating. They also found that fluoride ion greatly accelerates the formation of C_3S; increasing fluoride content alters the lattice parameters of the triclinic C_3S, causing the X-ray pattern to become more like that of monoclinic C_3S. They also found that excess CaF_2 decomposed the C_3S to α- and α'-C_2S.

C. Alkali Oxides

The effects of alkali have been widely studied, partly because of reported reactions between the alkali from Portland cement clinker and certain types of aggregate. Newkirk [*49*] summarized work up to 1951.

As already stated (p. 94), the alkali oxides combine preferentially with SO_3 from the fuel or raw materials, forming sulphates. Taylor [*48, 60*] reported the preparation of a compound $KC_{23}S_{12}$, optically similar to β-C_2S but distinguishable from it by X-rays; he considered that any K_2O not present as sulphate was likely to occur in this form. Nurse [*14, 32, 61*] and Suzukawa [*44–46*] concluded, however, that this product was not a distinct compound but a potassium-stabilized form of α'-C_2S.

Brownmiller and Bogue [*62*] described a compound NC_8A_3, the X-ray powder pattern of which was closely similar to that of C_3A. Phase equilibrium studies [*62–65*] indicated that any excess of Na_2O was likely to occur in this form. Newkirk [*49*] concluded that alkalis not present as sulphates occurred mainly as $KC_{23}S_{12}$ and NC_8A_3; he discussed the effects which the formation of these phases had on the potential phase composition of the clinker. Because of the low proportions of alkali in $KC_{23}S_{12}$ and NC_8A_3, small amounts of alkalis in the clinker could markedly affect the potential phase composition; thus, in the absence of SO_3, addition of 1% of K_2O to a CaO–Al_2O_3–Fe_2O_3–SiO_2 mixture could cause the formation of over 20% of $KC_{23}S_{12}$ and decrease the potential C_2S content by a comparable amount. Addition of 1% Na_2O could similarly cause the formation of over 10% of NC_8A_3, with a comparable decrease in potential C_3A. The presence of alkalis could also cause small increases in the potential C_3S content, and in certain cases might lead to the formation of free CaO where this would not otherwise appear. Newkirk considered that the presence of alkalis affected the burning process in three ways: by the formation of new compounds, as mentioned above, by the lowering of the temperature of liquid formation, and by the shifting of the primary phase boundaries. This last effect might cause the CaO primary phase region to be enlarged, and thereby make the complete combination of CaO more difficult to achieve.

The interpretation of the large changes in potential compound composition which are brought about by addition of alkali clearly depends on whether the phases $KC_{23}S_{12}$ and NC_8A_3 differ appreciably in chemical behaviour from β-C_2S and C_3A, respectively. Newkirk stated that the alkali phases hydrate rapidly, and considered that one or more of them might contribute to high early strength. Nurse [*14, 61*], in contrast, found that $KC_{23}S_{12}$ inverted so rapidly to β-C_2S that it was doubtful whether it could exist in clinker; he also considered the phase to be a K_2O-stabilized form of α'-C_2S, and showed that α'-C_2S prepared in other ways had poor hydraulic properties.

The alkali phases in cement clinker have recently been reinvestigated by Suzukawa [*44–46*]. The latter confirmed the existence of the com-

pound NC_8A_3 and also prepared an analogous compound, KC_8A_3. As already stated, he concluded in agreement with Nurse that the phase $KC_{23}S_{12}$ was not a distinct phase but a K_2O-stabilized form of α'-C_2S.

Suzukawa confirmed previous reports that the alkali oxides combine preferentially with SO_3. As already mentioned, he found that the SO_3 combined with K_2O in preference to Na_2O. For rapidly cooled clinkers any excess of K_2O occurred as KC_8A_3 or in solid solution in α- or α'-C_2S; any excess of Na_2O tended to occur as NC_8A_3 which, in his view, contained some SiO_2 due to partial replacement of CaAl by NaSi. Slow cooling led to the formation of C_3A and Na_2SO_4 instead of NC_8A_3. Suzukawa agreed with previous investigators that the presence of Na_2O could cause an increase in the C_3S content of the clinker.

D. Heavy Metal Oxides

Kukolev and Mel'nik [*55*] investigated the effects of Cr_2O_3, P_2O_5, V_2O_5 and BaO on the C_2S in wet process clinker. They found that 0·3–1·5% additions of P_2O_5, V_2O_5 and BaO all increased the hydraulic activity; they attributed this to the production of structural defects in the C_2S.

Mn_2O_3 probably substitutes for Fe_2O_3 in Portland cement. A compound $4CaO.Al_2O_3.Mn_2O_3$ is known to exist; it is analogous to C_4AF, with which it forms a continuous series of solid solutions [*66*]. Newman and Wells [*67*] showed that up to 8% of Mn_2O_3 could also be incorporated in solid solution in C_2S. The α–α' inversion temperature is considerably lowered and the β–γ inversion totally inhibited as a result of the substitution. MnO can be incorporated in C_3S. The limiting solubility is not known; the X-ray pattern is changed in the direction of that of alite [*68*].

IV. The Burning of Portland Cement

The burning of Portland cement begins as a series of reactions between intimately mixed solids, and it is only in the later stages of burning that any liquid is formed, causing the reactions which produce the cement compounds to take place more rapidly. Lea [*69*] has indicated that "the production of Portland cement by a clinkering process in which only a minor proportion of the mix becomes liquid is dependent on three factors: (1) the chemical composition of the mix; (2) the physicochemical state of the raw constituents; (3) the temperature and period of burning; a fourth condition which influences the resulting clinker is the rate of

cooling." Most research on the burning of Portland cement has been carried out in the laboratory with small-scale mixes of oxides, but a few authors have reported work with commercial kilns.

A. Reactions in the Kiln

The following discussion applies primarily to rotary kilns, the main features of which were described in Chapter 1. The reactions occur in stages, which were summarized by Lea [*69*] as follows:

Temperature (°C)	Process	Thermal change
100°	Evaporation of free water	Endothermic
500° and above	Dehydroxylation of clay minerals	Endothermic
900° and above	Crystallization of products of clay mineral dehydroxylation	Exothermic
	Decomposition of $CaCO_3$	Endothermic
900–1200°	Reaction between $CaCO_3$ or CaO and aluminosilicates	Exothermic
1250–1280°	Beginning of liquid formation	Endothermic
Above 1280°	Further liquid formation and completion of formation of cement compounds	Probably endothermic on balance

Other authors are in general agreement, though there are some significant differences; Bogue [*70*] considers that reactions giving cement compounds begin at as low a temperature as 600° C. The first stage (evaporation of free water) is quickly completed in a dry process kiln, but with the wet process it occupies roughly the first half of the length of the kiln.

The maximum temperature is reached in the "burning zone" some 5–12 m from the exit end of the kiln, and is normally between 1300° and 1500° C. It is chosen so as to produce a degree of melting sufficient to cause the material to cohere into small balls or lumps of clinker, and is therefore known also as the clinkering temperature. Between 20% and 30% of the material is normally molten at this temperature. Overburning, i.e. operating at a higher temperature, is generally considered undesirable, as it can lead to difficulties in running the kiln and possibly yields a less reactive product, owing to the formation of larger crystals or ones containing fewer defects [*71*]. Beyond the burning zone the temperature falls, and the clinker normally enters the cooler at 1000–1300° C. The

mixture takes about 2·5 h to pass through a kiln 60 m long, and the time during which it is at the clinkering temperature is, at the most, 20 min [*69*].

Information on the course of reaction in commercial kilns has been obtained by sampling at various points, either after stopping the kiln and allowing it to cool or, better, during normal operation [*72*, *73*]. Temperatures at various points can be determined by inserting thermocouples through the lining. The results of such studies show that the content of free CaO rises to a maximum at a point somewhat before the burning zone. This suggests that at 900–1000° C decomposition of the $CaCO_3$ occurs more rapidly than reaction of the resulting CaO with aluminosilicates. Immediately before the burning zone the free CaO content drops again and the temperature rises sharply to about 1250° C. Both effects are probably caused by the exothermic reaction of the CaO with the aluminosilicates. The mixture then passes through the burning zone at 1300–1500° C, where this reaction is completed and the free CaO content drops almost to zero.

The product at the clinkering temperature consists essentially of crystals of C_3S and C_2S, formation of which is largely completed at this stage, together with a liquid containing CaO together with all or most of the Al_2O_3, Fe_2O_3 and MgO, but relatively little SiO_2. The aluminate and ferrite phases therefore form only during cooling. Other processes that occur, or can occur, during cooling include polymorphic transitions, especially in the C_2S, crystallization of periclase and reaction between the liquid and the C_3S or C_2S crystals already formed. This last process will alter the ratio of C_3S to C_2S.

Alumina and iron oxide are the main fluxes in cement burning; without them the silicates could only be formed at much higher temperatures or in much longer times. The relations between the Al_2O_3/Fe_2O_3 weight ratio of the mix and the amounts of liquid formed at different temperatures are discussed by Lea [*69*]. At a clinkering temperature of 1400° C, rather more liquid is formed for each per cent by weight of Al_2O_3 than of Fe_2O_3, but this situation can be reversed in the earlier stages of liquid formation below about 1300° C. There is also some evidence that Fe_2O_3 can be more effective in promoting solid–solid reactions.

The exact sequence of reactions by which the cement compounds are formed is not well understood. It was at one time generally supposed that they were formed almost wholly by crystallization from the liquid and that little or no interaction occurred before melting began, but Bogue [*70*] has suggested that reactions of solid phases, either with each other or with the melt, may also be important. There is general agreement that, whatever the mechanism, equilibrium conditions are closely

approximated to at the clinkering temperature, assuming that grinding, mixing and burning are properly carried out.

B. Effect of Raw Material

As has already been mentioned in Chapter 1, the reactivity of a raw mix depends not only on its chemical composition, but also on the mineral composition and the size of the particles. It may also be affected by the state of crystallinity of individual minerals; defects in a crystal are likely to make it more reactive.

Most work has been concerned with the effects of varying particle size of the limestone and of quartz, which is likely to be one of the least reactive constituents of the clay or other acidic constituents. If the material which is introduced into the kiln is not sufficiently well mixed, reaction will be incomplete. This usually results in a lowering of the C_3S content, C_2S and CaO being formed instead in different parts of the clinker nodules. The commonest cause of incomplete reaction is probably the presence of large particles of quartz, which can produce bands rich in C_3S and C_2S (Plate 1). The remedy is better grinding of the raw materials.

Toropov and Luginina [*74*] investigated the influence of particle size of the raw mix on the processes of combination of calcium oxide in Portland cement burning. They showed that care had to be taken to prevent the fine material from remaining in the clinkering zone too long, as this caused kiln rings to be produced. They later investigated the effect of rapid burning, which they showed to accelerate the combination of the raw materials [*75*]. Heilmann [*76*] showed that not more than 0·5% of silica particles above 0·2 mm nor more than 1% between 0·09 and 0·2 mm should be present in raw mixes with a lime saturation factor (Chapter 1, p. 32) as high as 0·95, but for lower lime saturation factors twice these amounts might be allowed. Up to 5% of pure calcite particles greater than 0·15 mm in size can be tolerated, while impure siliceous limestones of greater size can be used without detrimental effects.

C. Effect of Reducing Atmospheres

In general, oxidizing conditions are maintained in cement kilns, and the iron in the resulting clinker is predominantly in the ferric state. Reducing conditions can occur, however, especially in shaft kilns of certain types. They have several effects on the properties of the clinker, all of which are undesirable.

Woermann [*11*] found the main effect to be a marked acceleration of the decomposition of alite during cooling. C_3S is unstable relative to

C_2S and CaO below 1250° C, but with clinkers prepared under oxidizing conditions the process is much too sluggish to be significant under technical conditions. With kilns run under moderately reducing conditions, microscope examination of the clinker often shows that many of the alite crystals have been decomposed to pseudomorphs containing β-C_2S, CaO and ferrite. Woermann considered that the Ca^{2+} in C_3S was partially replaced by Fe^{2+}. During cooling, the conditions became more oxidizing. The Fe^{2+} was oxidized to Fe^{3+}, which could not be accommodated in the alite structure and was precipitated as ferrite; the C_3S was decomposed by C_2S and CaO.

A second effect, observed by Woermann [*11*] and also by Suzukawa and Sasaki [*77*], was a tendency for the β-C_2S to invert to γ-C_2S on cooling. This can probably be attributed to the fact that Fe^{2+} substitutes for Ca^{2+} more readily in γ-C_2S than in β-C_2S. Woermann noted several other effects. Considerably more periclase was produced; it contained appreciable FeO in solid solution. There were also changes in the properties of the ferrite phase and in the relative amounts of ferrite and aluminate phases. Lastly, sulphides (CaS and iron sulphides) are sometimes formed.

If the conditions are sufficiently strongly reducing, the iron is converted to the metal [*11*, *77*]. The clinker formed under these conditions is white and decomposition of the alite does not occur; $C_{12}A_7$ may be produced [*77*].

D. Effect of Cooling Rate

In Chapter 2 it was shown that the rate of cooling of a cement clinker might be expected to influence the compound composition. In the following discussion it will be assumed that the four major constituents have the exact compositions C_3S, C_2S, C_3A and C_4AF. If it could further be assumed that equilibrium is reached at the clinkering temperature and continuously maintained during cooling (except that no decomposition of C_3S into C_2S and CaO occurs), the four products would be formed in the amounts given by the Bogue calculation (p. 77). With sufficiently rapid cooling, the liquid present at the clinkering temperature might be expected either to crystallize independently of the solids already formed or to solidify to a glass. Lea and Parker [*78*] derived methods for calculating the liquid content of a clinker of given composition at any desired temperature, and the corrections that should be applied to the results of the Bogue calculation for each of the types of non-equilibrium cooling mentioned above. Further possibilities of non-equilibrium cooling were considered by Dahl [*79*].

Table I gives the chemical analyses of two cement clinkers, together with the potential compound compositions given by the Bogue calculation and the results of applying Lea and Parker's corrections. It will be seen that independent cooling of the liquid would be expected to produce small amounts of $C_{12}A_7$, while complete vitrification of the liquid would produce substantial amounts of glass.

TABLE I

Calculation of cement composition with varying conditions of cooling

Cement composition	$CaO = 68\%$, $SiO_2 = 23\%$, $Al_2O_3 = 6\%$, $Fe_2O_3 = 3\%$		
	Complete crystallization	1450° C; liquid quenched to glass	1450° C; liquid crystallized independently
C_3S	57·5	59·6	59·6
C_2S	22·6	15·6	21·0
C_3A	10·8	0	9·8
C_4AF	9·1	0	9·1
CaO	0	0	0
$C_{12}A_7$	0	0	0·5
Glass	0	24·8	0
Cement composition	$CaO = 66\%$, $SiO_2 = 24\%$, $Al_2O_3 = 7{\cdot}5\%$, $Fe_2O_3 = 2{\cdot}5\%$		
C_3S	32·4	38·5	38·5
C_2S	44·5	33·3	39·9
C_3A	15·7	0	10·6
C_4AF	7·6	0	7·6
CaO	0	0	0
$C_{12}A_7$	0	0	3·5
Glass	0	28·1	0

The extent to which either of these forms of non-equilibrium cooling occurs in practice is uncertain. There is little doubt that the technical properties of cement clinkers are affected by the rate of cooling; studies by Lerch and Taylor [*80*], Lerch [*81*], Parker [*82*] and others have shown three main effects. First, cements made from certain slowly cooled clinkers and ground with gypsum in the ordinary way show flash set, i.e. rapid setting with marked evolution of heat to give a mixture that is difficult to work and that gives poor early strength; cements made from rapidly cooled but otherwise similar clinkers set normally. Secondly, if the clinker is relatively high (2·5–5·0%) in MgO, slow cooling may

give an unsound cement, i.e. one that gradually expands after hardening and thereby becomes weakened or disintegrates. Thirdly, cements made from rapidly cooled clinkers may be more resistant to attack by sulphate solutions. Slow cooling may also cause "dusting", i.e. inversion of the C_2S to the γ-form. In all these respects it would appear that rapid cooling is likely to yield a better product. On the other hand, it has been reported that slowly cooled clinkers may be easier to grind.

These effects on the technical properties of the clinker could reasonably be attributed to differences in glass content, in accordance with the predictions of Lea and Parker. The flash setting and poor sulphate resistance of cements made from the slowly cooled clinkers could be attributed to the formation of too much C_3A, and the unsoundness to the presence of MgO. The contents of C_3A and MgO would both be lowered if glass was present. It would appear reasonable to suppose that, in a rapidly cooled clinker, the position is somewhere between the three extremes of equilibrium crystallization, independent crystallization of the liquid and solidification of the liquid to a glass.

Microscopic studies, discussed later in this chapter, give results which appear to be in general accord with this conclusion. The rapidly cooled clinkers consist largely of crystals of C_3S and β-C_2S embedded in a matrix consisting of the ferrite phase together with glassy material; with slowly cooled clinkers the glassy material is partly or wholly replaced by detectably crystalline phases, including as a rule C_3A and MgO. One recent investigation [*84*] has, however, given a contrary result, in that slow cooling from 1150° C to 750° C was reported to increase the proportion of glass.

Calorimetric evidence has also been considered to support the view that rapidly cooled clinkers contain glass; Lerch and Brownmiller [*83*] used a calorimetric method for the approximate determination of the glass content. They showed that rapidly cooled clinkers had higher heats of solution than the same clinkers which had been reheated and annealed. The difference was attributed to the heat of crystallization of the glass; this quantity was determined separately for a glass of appropriate composition and the percentage of glass in the clinker was thereby obtained. While there are some discrepancies between the results given by the various methods, it would appear both from the effects on the technical properties and from the results of microscopic and calorimetric studies that rapid cooling can lead to the formation of glass at the expense especially of C_3A and MgO.

Recent work nevertheless casts some doubt on the correctness of this view. Quantitative X-ray studies, discussed later in this chapter, do not support the view that commercial clinkers, whether slowly or rapidly

cooled, contain any substantial proportions of glass. Moreover, commercial clinkers, including those which have been rapidly cooled, do not normally contain appreciable amounts of $C_{12}A_7$ unless they have been made under reducing conditions. The microscopic detection of glass in clinker is fraught with uncertainty, as material that appears glassy under the microscope may really be microcrystalline. The higher heats of solution and different technical behaviour of rapidly cooled clinkers may be caused, not by the presence of glass, but by the occurrence of disordered or defective crystalline states in the C_3A and other phases separating from the liquid. It is also possible that unstable, though persistent, new phases may be formed as a result of rapid cooling of a liquid; it has been suggested that a crystalline C_3F, structurally similar to C_3A, can be formed in this way [*85*]. The whole question of glass in clinker needs re-assessment after many more systematic, quantitative X-ray studies of the phase compositions of clinkers cooled in different ways have been completed.

V. Qualitative Examination of Clinker

A. Visual Examination

Portland cement clinker as it comes from the kiln forms rounded pellets if a dry process is used and irregular lumps if a wet process is used. Considerable information may be obtained by direct observation of the clinker without resort to apparatus. If the kiln is running satisfactorily, the clinker should be black and dark for a normal Portland cement; if the kiln is running under reducing conditions, however, the clinker will be a reddish brown. If the clinker is being under-burned, the clinker will show white or light coloured patches. Information about the state of the kiln can also be obtained on breaking the clinker nodules. Bad mixing of the raw material and the results of failure to reach equilibrium or of segregation can sometimes be seen with the naked eye.

Some indication of the running of the kiln can be obtained from the bulk density, known in the cement industry by the name of litre weight. The clinker sample is roughly packed into a drum of known capacity and weighed. This shows whether too much dust is coming out from the kiln.

B. Microscopy

The binocular stereoscopic microscope is a most useful instrument for more detailed visual examination of the clinker. The petrological microscope provides further information; it was by the examination of thin sections that the phases in Portland cement were first identified.

Törnebohm [*1*] named four phases: alite, belite, celite and felite. It was shown later by Insley [*86*] that alite was C_3S, that belite and felite were two different habits of C_2S and that celite was a ferrite phase then thought to be C_4AF. The greatest use of the thin section today is in the identification of the minor modifications of the phases. Thus, Nurse, Midgley and Welch [*87*] examined the types of C_3S in Portland cement clinkers and found that optically they were different from those in slags and laboratory preparations.

Most of the work on the microscopic examination of Portland cement clinker has dealt with the examination of polished and etched surfaces under the reflecting microscope. After the pioneering work of Insley [*86*], Parker and Nurse [*88*] and Tavasci [*89*] the method has become almost routine. The methods used have been summarized by Insley and Frechette [*90*] and in Volume 2, Chapter 20. Plate 2 shows a typical polished surface of a quickly cooled clinker, etched with water followed by 0·25% HNO_3 in alcohol. The material consists essentially of crystals of C_3S and β-C_2S up to 100 μ in size, embedded in a matrix of interstitial material. The various phases detectable optically in this and other clinkers will now be described.

1. Tricalcium Silicate

This occurs mainly as relatively large, euhedral crystals (Plate 2). They frequently appear pseudo-hexagonal, and when etched with water followed by alcoholic HNO_3 are lighter than the crystals of β-C_2S. They are sometimes zoned. In thin section they are colourless.

2. β-Dicalcium Silicate

This also occurs mainly as relatively large crystals (Plate 2). Unlike those of the C_3S, they are anhedral or subhedral; the outlines can be smooth and rounded, as in Plate 2, or fingered. They appear darker than C_3S crystals when seen in polished sections etched with water followed by alcoholic HNO_3. In thin sections they tend to be slightly yellow, brown or green. They usually show striations due to polysynthetic twinning. Several varieties have been distinguished; at one time these were thought to be different polymorphs of C_2S, but Insley [*86*] showed that all were forms of β-C_2S. The commonest form, called Type I by Insley, shows two or more sets of interpenetrating striations, and probably represents crystals which have originally formed as α-C_2S. The crystals seen in Plate 2 are of this type. Type II crystals show only one set of striations and are rare in commercial clinkers. Type III crystals are untwinned and are sometimes found as overgrowths on

crystals of Type I; they have possibly crystallized from the melt during cooling. In a further type, called Ia [*91*], there are inclusions of apparently exsolved material along traces of twinning planes.

β-C_2S also occurs as rims of small crystals on the surfaces of C_3S grains and as very small, rounded particles dispersed in the interstitial material; both forms can be seen in a clinker which has been slowly cooled (Plate 3). The rims have possibly been formed by reaction between C_3S crystals and liquid during cooling, while the dispersed particles have crystallized from the liquid or glass. β-C_2S also occurs as inclusions in C_3S (Plate 4).

In some clinkers the C_3S and β-C_2S crystals tend to occur in separate aggregates which are probably relicts of coarser particles in the raw material. That shown in Plate 2 is of this type. An extreme case of inhomogeneity, attributable to inadequate grinding and mixing, is shown in Plate 1.

3. Interstitial Material

This is the material that was liquid at the clinkering temperature. It is undifferentiated, or only slightly differentiated, in a quickly cooled clinker (Plate 2), but in a slowly cooled clinker (Plate 3) distinct regions are more easily observed. The interstitial phases were reviewed by Insley [*92*]; the following types of material have been recognized.

(a) *Light interstitial material.* This is the ferrite phase. It is unaffected by most etching reagents and has a high reflectance; it therefore appears very bright in reflected light. It is seen as the lightest coloured regions in Plates 2 and 3. The ferrite phase in clinkers is sometimes prismatic but more often forms irregular aggregates. In thin sections it is reddish in colour, birefringent and pleochroic.

(b) *Dark interstitial material.* This has been further subdivided into three types known as rectangular, prismatic and amorphous. The rectangular type is C_3A and is seen most readily in slowly cooled clinkers of high Al_2O_3/Fe_2O_3 ratio. The prismatic form (Plate 3) is probably a form of C_3A modified by incorporation of alkali, perhaps NC_8A_3. The "amorphous" form (Plate 2) is the material generally described as glass; this has been discussed earlier (pp. 103–106).

(c) *MgO.* This usually occurs in the interstitial material and is visible as small, angular, highly reflecting grains in an unetched, polished section (Plate 5). MgO also occurs as inclusions in other phases; the triangular surface of a crystal included in C_3S is visible in Plate 1.

4. CaO

This is only present in quantity in cements that are incompletely burned. It forms rounded crystals which occur singly or in groups and

are often as large as the C_2S grains. Plate 6 shows its appearance on an unetched polished section.

The use of the microscope for quantitative estimation of the phases will be discussed later.

C. Chemical Separation

In recent years some attempt has been made to separate the phases chemically. Jander and Hoffman [*93*] evolved a method for obtaining a separation of the non-hydraulic silicates CS and C_3S_2 from a mixture with C_3S and C_2S, but they did not succeed in separating C_3S from C_2S. Midgley [*94*] managed to separate C_2S from a clinker by differential hydration, but although no other crystalline phases were present it seemed likely that a film of alumina gel was left on the surfaces of the grains.

Chemical methods have been sought to separate, or at least concentrate, the ferrite phase sufficiently to make it possible to determine the composition. Fratini and Turriziani [*95*] described a reagent consisting of 25 ml water, 65 ml ammonia, and 10 g ammonium citrate which preferentially dissolves the silicates from Portland cement, leaving a residue consisting mainly of C_3A and the ferrite phase. The treatment as described by them consists of shaking 1 g of cement sample with 100 ml of reagent for 12 h. The solution is decanted from the residue, which is then shaken with a further 100 ml of reagent for a further 12 h. The residue is then filtered off in a sintered glass crucible, washed rapidly with ammonia and dried at 110° C. Midgley *et al.* [*37*] investigated the method and found that the rates of solution of the ferrites C_6AF_2, C_4AF and C_6A_2F differed (Fig. 3). They also found that C_3A dissolves more rapidly even than C_6A_2F. These authors also studied the effect of lowering the sample weight; they found that a single three-hour extraction, with the initial weight of sample reduced to 0·2 g in 100 cm^3 of reagent, left a residue of about 22%. X-Ray diffraction showed the complete removal of the crystalline silicates.

More recently two further methods have been put forward for the separation of the aluminate phases. Royak, Nagerova and Kornienko [*96*] suggested the use of 5% boric acid solution to remove the silicate phases and of acetic acid to remove the ferrite phase and the glass, presumably leaving the C_3A. This method does not appear to have been followed up. Takashima [*97*] investigated the dissolution of the silicate phases in solutions of salicylic and picric acids in mixtures of toluene and acetone. The cement sample was stirred with the solvent for 1 h and allowed to stand for 1 day; the residue was washed with toluene, methyl

ethyl ketone or methanol, which dissolved the reaction products. It was suggested that by varying the concentrations of the acid and the final solvent it is possible to remove successively free lime, alite, β-C_2S and amorphous silicates.

From these experiments it seems that the calcium silicate phases can be removed by either acid or alkaline treatment, and it is not easy to see why these methods should work. It has been suggested that the much

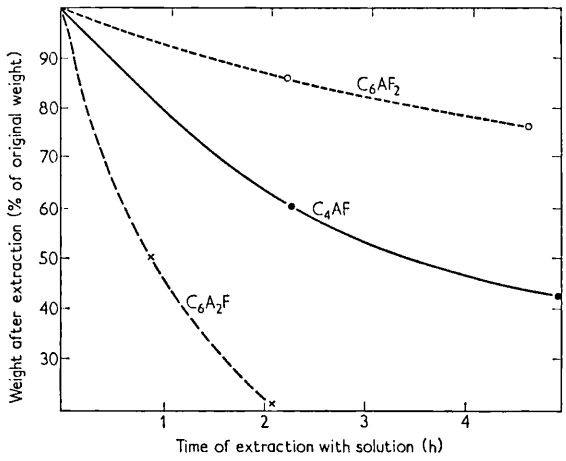

FIG. 3. Rates of solution of ferrites in "Fratini and Turriziani" solution.

more rapid dissolution of the silicate phases can effectively deactivate the reagent before the solution of the other phases has proceeded to any extent.

One very sensitive chemical method exists for detecting free lime; White's reagent (a solution of 5 g phenol in 5 ml nitrobenzene + 2 drops of water) will form calcium phenate in the presence of CaO or $Ca(OH)_2$. Calcium phenoxide occurs in tetragonal, acicular prisms which have a high birefringence and show up on a polarizing microscope under crossed nicols. The crystals form rapidly if much free lime is present, but may require an hour to form if only traces occur.

D. PHYSICAL SEPARATION

The physical separation of the constituent clinker minerals is extremely difficult, since the individual crystals are frequently smaller than 1 μ.

The most obvious method is based on the use of heavy liquids, since the four main minerals have different densities (C_3S 3·13 g/cm^3, C_2S 3·28 g/cm^3, C_4AF 3·77 g/cm^3, and C_3A 3·00 g/cm^3). This means that with liquids of suitable densities, e.g. methylene iodide–benzene mixtures, it should be possible to effect some separation. Guttmann and Gille [*98*] made an effective separation of the alite phase from a Portland cement clinker and showed it to be essentially C_3S.

Attempts at the Building Research Station by Midgley and Smith [*99*] have not been very successful; a complete separation of the silicate phases has never been effected. A nearly complete separation of the ferrite phase was made, but the method was so long and tedious that it was not repeated. These authors have found that one of the major difficulties in separation is the small crystal size, which necessitates the use of powder of less than 300 B.S. sieve size. This is much finer than is generally considered suitable for gravity separation. They found that a contributing cause of non-separation was the non-wettability of the cement grains; this could be overcome by the addition of a wetting agent.

With some Portland cement clinkers it can be seen on microscopic examination that the silicate phases differ greatly in particle size; this suggests that a mixture of particle size separation and gravity separation should be possible. Midgley and Smith [*99*] carried out such a separation on a normal Portland cement clinker in which the C_2S had grown to a much larger crystal size than the C_3S. The sample was ground to less than 10 μ and then separated into two fractions of 5–10 μ and less than 5 μ. Each fraction was then separated by means of the centrifuge and heavy liquids; the parts having a density less than 3·2 g/cm^3 were retained. The amounts of the phases present were estimated microscopically as follows:

Less than 5μ	C_3S	85%	C_2S	7·5%	Interstitial material 7·5%
5–10μ	C_3S	4%	C_2S	91%	Interstitial material 5%

It was thus possible to concentrate but not to separate the phases.

Another property which has been used to separate the phases is magnetic susceptibility; Midgley [*33*] concentrated the ferrite phase in clinkers to enable the weak X-ray lines of the ferrite to be recorded. Malquori and Cirilli [*31*] suggested that the concentration found by Midgley could have been due, not to the differing magnetic susceptibilities of the ferrite and silicate phases, but to included free iron in the ferrite phase. This method has now been superseded by ones based on chemical separation. Other possible methods of separation which have not been investigated are electrostatic separation and froth flotation.

E. X-Ray Examination

1. General Points

The use of X-ray diffraction methods for determining the phase composition dates back to the pioneer work of Bogue and Brownmiller [*100*], who used a powder camera to identify C_3S, C_2S, C_3A and C_4AF in clinker. Various experimental techniques are now available for powder work which give differing degrees of information about the crystalline modifications of the phases. It must be emphasized that with Debye–Scherrer cameras the best results will be obtained only if special care is taken with the preparation of specimens and accurate centring in the cameras. At the Building Research Station it has been found possible to use cellulose acetate capillaries 0·2 mm in diameter for the mounting of specimens, and with these the resulting lines are quite sharp. In much of the more recent work either focusing cameras or diffractometers have been used.

In Portland cement the predominant mineral is tricalcium silicate, which gives a very strong pattern and dominates the diffraction pattern. Midgley [*34*] concluded that, with simple Debye–Scherrer techniques, the limits of detection are C_3S 5%, C_2S 15%, C_4AF 3%, C_3A 5%. By using focusing cameras or diffractometers these limits can be lowered. Midgley *et al.* [*27*], using a proportional counter with pulse height analysis, found that the limits of detection were about C_3S 3%, β-C_2S 5–6%, ferrite 2%, C_3A 1%; phases other than C_3S, β-C_2S, C_3A and ferrite were also detected. Yannaquis [*101*] reported detection of γ-C_2S. Midgley and Fletcher [*17*], using X-ray diffraction methods, have reported the presence of α'-C_2S (bredigite) in cements made from a phosphatic limestone. They identified the bredigite by the occurrence of a reflection at 3·16 Å; the limit of detection in this case was estimated to be about 5%.

Yannaquis [*101*] heated a clinker to 1150–1200° C to decompose the C_3S to β-C_2S and CaO; the X-ray diagram of the residual β-C_2S was identical with that of a synthetic product. He also eliminated the C_3S by hydration; the product so obtained was found to contain β- and γ-C_2S. In an effort to obtain better X-ray diffraction diagrams, Yannaquis also made a mechanical separation under the microscope of both C_3S and C_2S. He found that the X-ray patterns from homogeneous specimens so obtained were simpler than those of the pure synthetic silicates. He also deduced that, because of superposition of the stronger lines, the identification of C_2S in the presence of C_3S could only be made on lines of medium intensity.

2. *Tricalcium Silicate*

As already stated, C_3S occurs in more than one polymorphic modification. Simons, quoted by Jeffery [2], concluded that alite has single lines at 1·761 and 1·485 Å, while pure C_3S has doublets; by examinations of these lines the polymorphic state can be determined. In a more recent study Yamaguchi and Miyabe [3] showed that the line at about 1·761 Å ($52°2\theta$ for CuK_α radiation) is a singlet for the trigonal modification, a doublet for the monoclinic one and a triplet for the triclinic one. Midgley and Fletcher [5] used a diffractometer to study the profile of this line for a number of cement and clinker samples and also for two samples of alite having the appropriate limiting compositions (Table II). The MgO contents are significant and are included where available. In all these samples alumina was present in excess of the amount required to stabilize the monoclinic modification. The work showed that the C_3S in samples 1–6 and also in sample 10 was monoclinic, in samples 7–9 triclinic, and in samples 11 and 12 trigonal. The 2θ values for samples 1–4 fell within the range defined by the synthetic preparations. Sample 6, which contained about 73% of alite, did not contain sufficient magnesia to stabilize the monoclinic form, but as it was a white cement it may have contained other ions which could have this effect. Samples 7, 8 and 9 did not contain sufficient magnesia to stabilize the monoclinic form and the triclinic modification was present. No explanation for the occurrence of the trigonal modification in a clinker can be put forward. X-Ray diffractometry can therefore be used to determine the type or modification of the C_3S present in the clinker.

3. *Dicalcium Silicate*

The identification of β-C_2S in mixtures is difficult, since its strong lines almost coincide with those of alite, and the identification therefore depends on weak lines. The most useful lines are the pair at 2·448 and 2·403 Å; one of these (2·448) almost coincides with a weak C_3S line at 2·449 Å, but the line at 2·403 Å is clear except for a weak line of C_3A at 2·39 Å. Since C_3A is usually present in small quantities, this weak line does not show in patterns from a cement clinker.

4. *Ferrite*

The ferrite phase is a solid solution series ranging in composition from C_2F to just beyond C_6A_2F. X-Ray powder data for the solid solution series show that there is a change in the lattice spacing with composition; a determination of the necessary lattice constants therefore gives the

TABLE II

2θ values of X-ray reflections for alite in some Portland cements

Sample	Modifications of monoclinic C_3S		Portland cements						High C_3S clinkers			Clinkers		
			1	2	3	4	5	6	7	8	9	10	11	12
	$C_{153}M_6S_{52}A$	$C_{156}M_3S_{52}A$	Sulphate resisting	High C_3A	High C_3S	Normal	Normal	White						
Reflections at about 52° 2θ (CuK_α radiation)	51·92 51·78	51·87 51·70	51·95 51·73	51·88 51·73	51·86 51·70	51·90 51·71	51·85 51·70	51·78 51·63	51·94 51·79 51·69 51·55	51·91 51·78 51·67 51·52	51·91 51·82 51·68 51·55	51·73 51·64	 51·63	 51·66
MgO%	1·7	0·9	2·8	2·3	1·3	1·2	1·1	0·5	1·5	0·8	0·6	—	—	—

composition. The relationship between spacing and composition has been studied by several investigators [*22*, *31*, *33–35*, *102–105*]. The strongest line, 141,† occurs at 2·63–2·68 Å but is very close to the 2·70 Å line of C_3A and the 2·60 Å line of the C_3S; the position is complicated further by the fact that a moderately strong line of the ferrite, 200, occurs at 2·66–2·71 Å, thus overlapping the C_3A line. If enough resolution can be obtained, it is nevertheless possible to use the position of the 141 line to determine the composition. Figure 4 shows the relationships

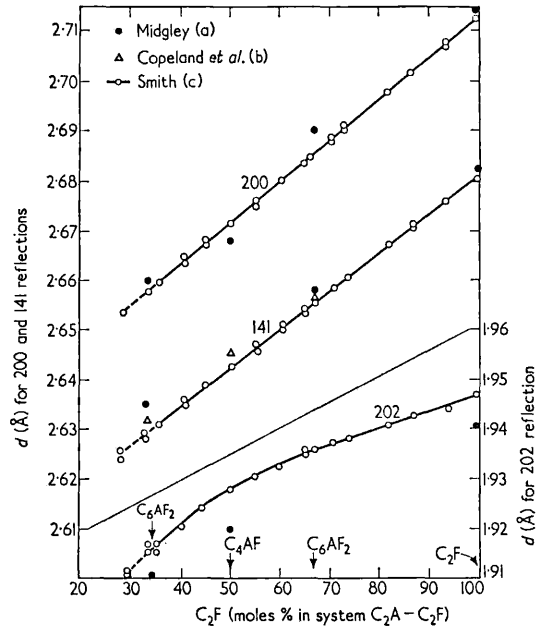

FIG. 4. Relationship between composition and X-ray powder spacings for the ferrite phase. (a) New data; (b) reference [*22*]; (c) reference [*103*].

between composition and spacing for the 141, 200 and 202 reflections. If the resolution is insufficient, the ferrite phase can be concentrated by drawing a bar magnet through the ground clinker. Lines of lower *d* spacing, such as 202, may then be used.

Copeland *et al.* [*22*] determined the composition of the ferrite phase in a number of cements from the position of the 141 line, and also by a calculation based on the intensity of this line and the total iron content

† The 141 line was wrongly indexed as 200 in some of the earlier investigations. There is a drafting error in the relevant figure of reference [*35*].

of the cement. Midgley [*35*] made a similar study, using the 202 line of a magnetic fraction; a Debye–Scherrer camera was employed. Later Midgley *et al.* [*37*] studied the same series of clinkers, using a diffractometer; in this work they used the 141 and 202 reflections from concentrates obtained by Fratini and Turriziani's method, and also the 141 reflections from the untreated clinkers. Table III compares the results of the various methods.

TABLE III

Weights % of C_2F in ferrite phase determined by X-ray diffraction

Clinker	Camera; magnetic fraction; 202 reflection	Diffractometer; untreated clinker; 141 reflection	Diffractometer; product of Fratini and Turriziani extraction	
			141 reflection	202* reflection
A. 9	56	54	52	48
A. 10	65, 39 (52)	56, 47 (51)	60, 54 (57)	50, 42 (46)
A. 20	66	60, 48 (54)	61, 51 (56)	No distinct peak
A. 35	71, 39 (55)	57	58, 53 (55)	50
A. 36	74, 39 (57)	56, 48 (52)	50	48
A. 37	66	63, 47 (55)	56	46, 35 (40)
A. 39	66	50	54, 50 (52)	49, 41 (45)
A. 40	66	63, 52 (57)	56	46
A. 143	65, 39 (52)	59, 50 (55)	56, 48 (52)	48, 42 (45)
A.F.	56	73, 59 (66)	64	62
A. 141	65, 39 (52)	62, 50 (56)	63, 55 (59)	45
A. 7	54, 39 (47)	64, 46 (55)	62, 52 (57)	No distinct peak
A. 35	54, 39 (47)	62, 54 (58)	54	48
A. 33	71, 39 (55)	68, 51 (59)	63, 57 (60)	37, 33 (35)
A. 113	—	70, 54 (62)	70, 46 (58)	66, 46 (56)

* The use of the 202 reflection is not very satisfactory for diffractometric techniques with KBr or Si as an internal standard, as both KBr and Si give peaks close to the ferrite 202 reflection. 2θ values for CuK_α radiation: Ferrites (46·6–47·5)°; KBr 45·60° and 47·74°; Si 47·30°.

5. *Other Phases*

Tricalcium aluminate can usually be detected by its strongest line at 2·70 Å; this is frequently the only detectable line due to this compound. The overlap of this line with the 200 line of the ferrite causes certain difficulties, which were discussed by Copeland *et al.* [*22*].

Midgley and Fletcher [*106*] found a significant variation in the spacing of the strongest X-ray powder reflection given by the C_3A in a number of commercial cement clinkers; the spacing was shifted from 2·699 Å in pure C_3A to 2·692, 2·695 and 2·695 Å in three clinkers studied. The 95% probability range for these results was 0·001 Å. They suggested that the shift might be due to MgO or Al_2O_3 or both. K_2O and Na_2O substitutions shift the reflection to higher d values in, for example, NC_8A_3. The shift to lower values in the C_3A of Portland cement may therefore be the algebraic sum of shifts up and down. This would mean that the measurement of the d spacing for C_3A in a Portland cement clinker cannot be used alone to determine the composition of the phase. Mather [*107*] found that with some clinkers the strong C_3A reflection occurred at spacings significantly higher than 2·699 Å. She obtained evidence that this was due, not to the occurrence of substituted forms of C_3A, but to overlap of the C_3A peak with a peak of spacing 2·720–2·725 Å attributable to some other phase. This phase was probably a calcium silicate.

MgO can be detected by its line at 2·106 Å and CaO by that at 1·390 Å. The 1·390 Å line is one of the weaker lines of the compound; the strongest line, at 2·405 Å, coincides with a line of β-C_2S. If more than about 5% of CaO is present, the 1·390 Å line becomes very strong.

F. Other Methods

1. *Infra-red Absorption*

The use of infra-red absorption spectrometry in the study of cements is comparatively recent. Hunt [*108*], Lehmann and Dutz [*109*], Lazarev [*110*], Midgley [*111*] and Roy [*112*] have reported data for cement minerals; Midgley's results are given in Fig. 5. Lehmann and Dutz [*109*] and Midgley [*111*] also investigated Portland cements. Lehmann and Dutz report that the cement they examined "consists essentially of β-C_2S which can be identified by the bands at 10·1 and 11·8 μ. Bands at 10·9 and 11·25 μ have the same intensity in β-C_2S as that at 10·05 μ. In Portland cement, however, they are better revealed, an indication that alite is present, whose bands are superimposed on those of β-C_2S at 10·9 and 11·2 μ. All maxima are displaced by 0·05–0·1 μ in the direction of longer waves as compared with pure minerals. Flat absorptions at

13·35 and 14·0 μ are attributable to vibration of AlO_6 octahedra." Midgley [*113*] showed that the four main constituents of Portland cement can be detected by measuring the absorptions at 10·2, 10·8, 13·5

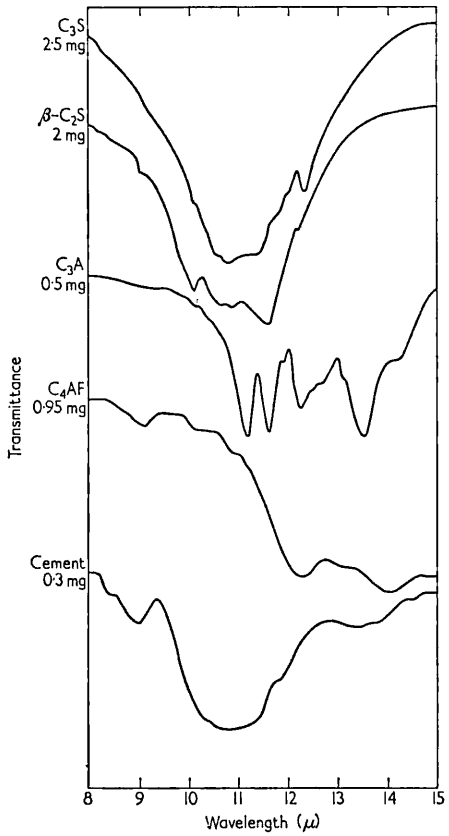

FIG. 5. Infra-red absorption spectra for clinker minerals and for a typical cement.

and 14·0 μ and then solving simultaneous equations. This method can possibly be used quantitatively and is discussed later.

2. *Electron Microscopy*

Very little work has been done on Portland cement clinker with the electron microscope. The only recent work seems to be that of Fahn [*114*], who examined powder mounts of clinker minerals. The present writer has attempted to make replicas of polished surfaces. The usual tech-

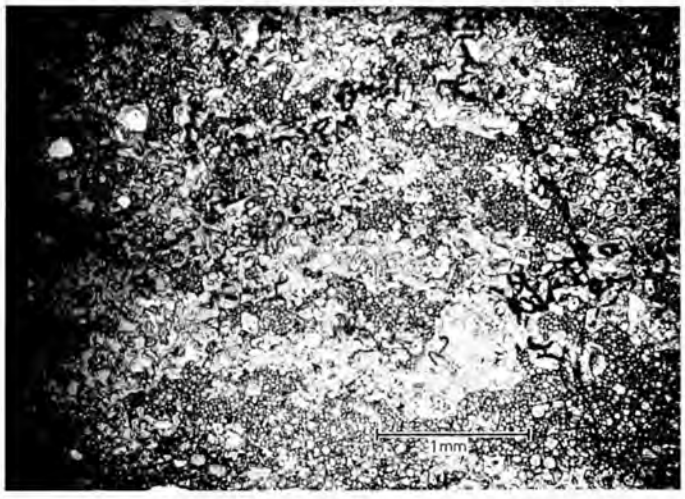

PLATE 1. Thin section of a Portland cement clinker showing bands rich in C_3S and C_2S produced by poor mixing of the raw material. Ordinary light.

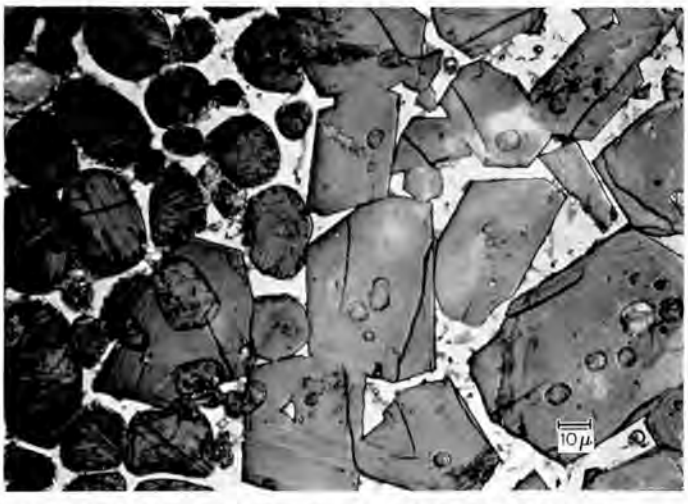

PLATE 2. Polished and etched surface of a quickly cooled Portland cement clinker, showing crystals of C_3S (right) and β-C_2S (left) embedded in a matrix of interstitial material which is only slightly differentiated.

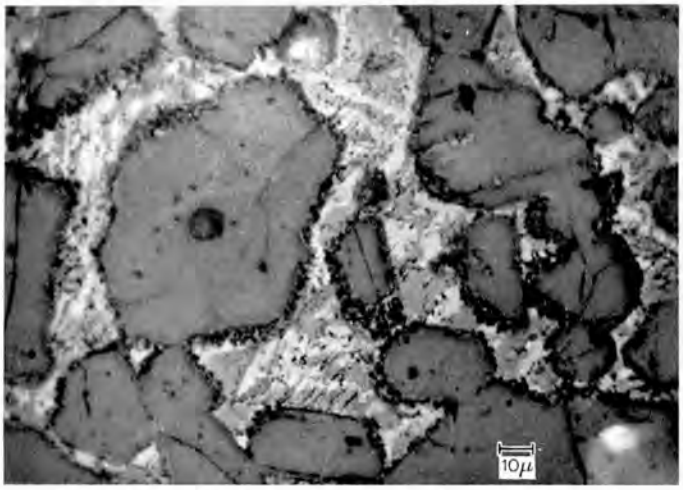

PLATE 3. Polished and etched surface of a slowly cooled Portland cement clinker, showing C_3S crystals with reaction rims of β-C_2S, embedded in a matrix of strongly differentiated interstitial material.

PLATE 4. Polished and etched surface of a Portland cement clinker, showing inclusions of β-C_2S in C_3S (centre and bottom right).

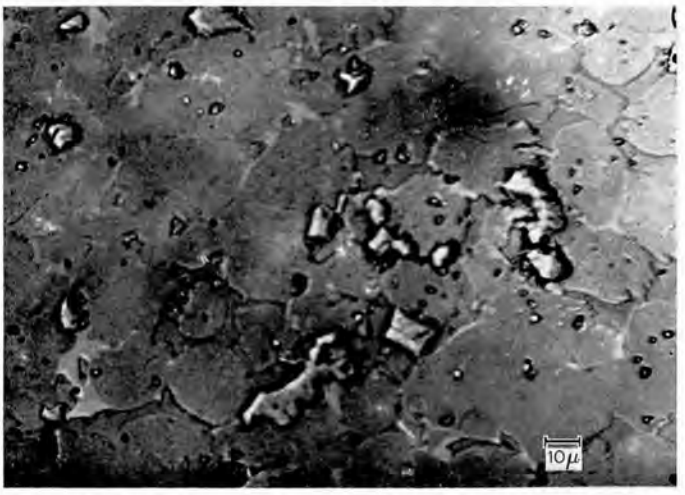

PLATE 5. Polished, unetched surface of a Portland cement clinker, showing MgO.

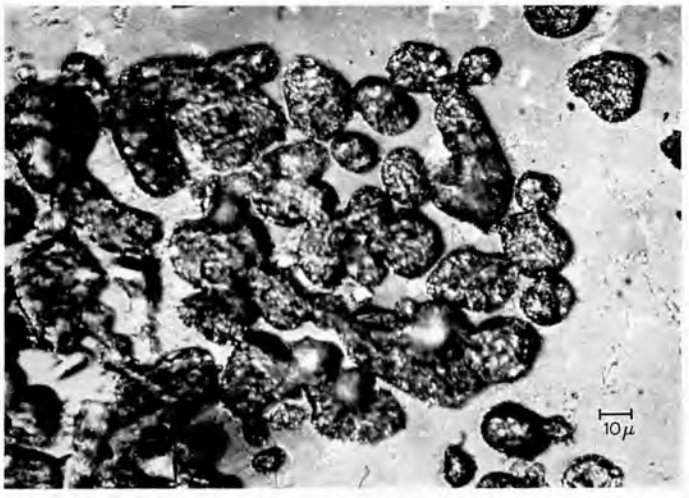

PLATE 6. Polished, unetched surface of a Portland cement clinker, showing CaO.

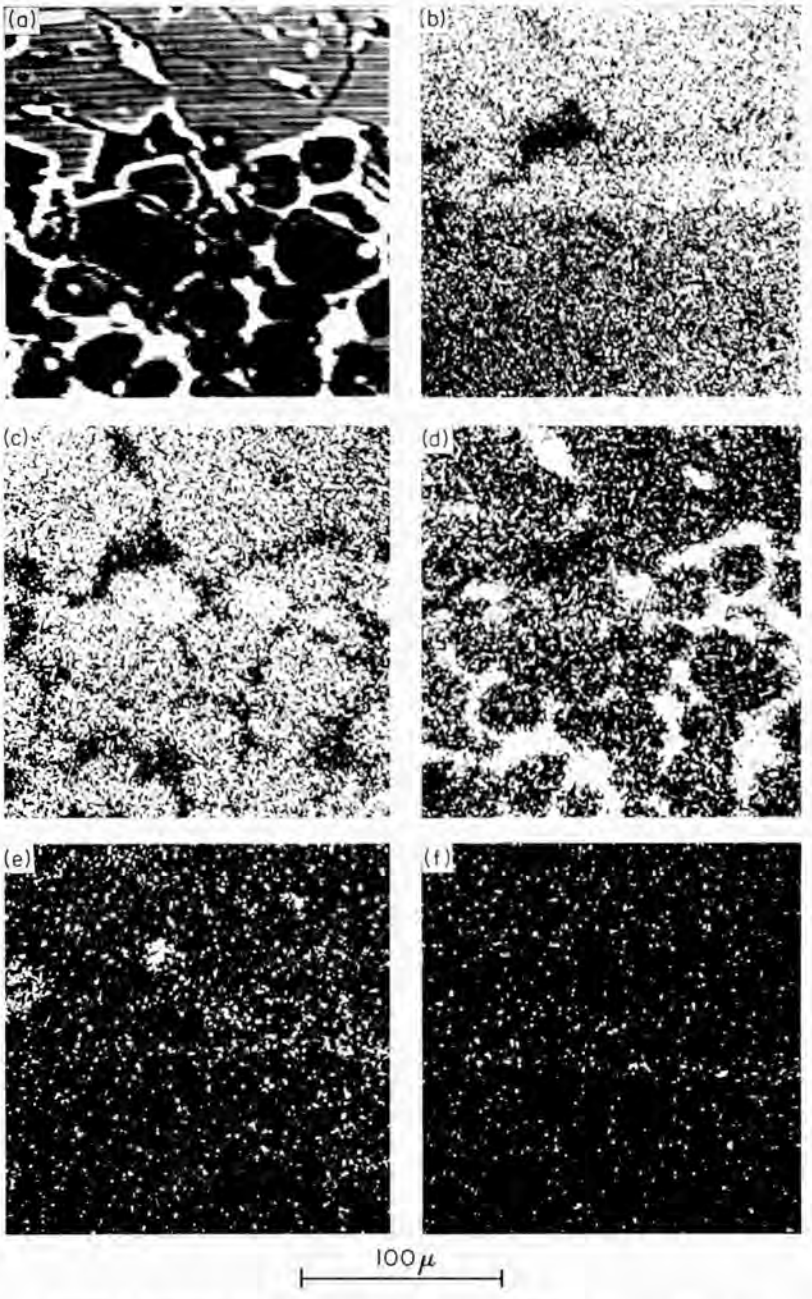

PLATE 7. Electron probe results for a polished surface of cement clinker (Japan Electron Optics Laboratory Co. Ltd.). (a) Absorbed electron image; (b)–(f) characteristic X-ray images for (b) CaK_α, (c) SiK_α, (d) FeK_α, (e) AlK_α, (f) TiK_α.

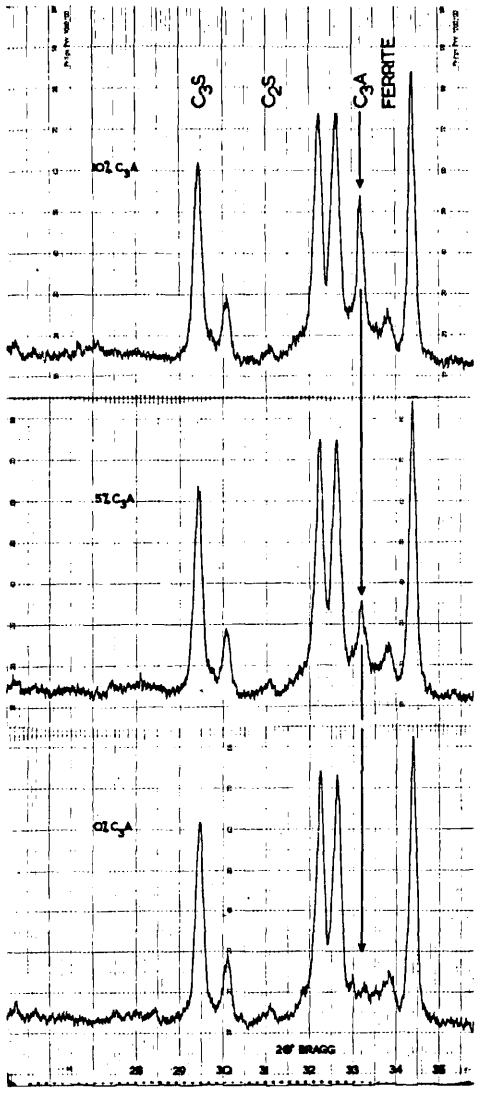

PLATE 8. Diffractometer traces of Portland cements of differing C_3A content.

niques proved unsuccessful but one technique, a modification of that of Hall [*115*], who had used it for teeth, proved possible. A replica is made from collodion in amyl acetate, backed with gelatine in water, and a carbon layer deposited *in vacuo*. The gelatine is removed with warm water and the collodion with amyl acetate. This work is still in its early stages and much additional research is required to perfect the technique.

3. Electron Probe Analysis

Electron probe analysis has not been in use long enough to have been applied systematically to research on clinkers. Some preliminary experiments have been carried out for the author by Wright [*116*], using an AEI (Associated Electrical Industries, Britain) X-ray microanalyser, and by the Japan Electron Optics Laboratory, using a JXA-3 instrument. With an electron probe the polished surface of the specimen is scanned by an electron beam. It is possible to measure continuously the intensity of the electrons scattered or absorbed and to display the results on a cathode-ray tube, the beam of which is synchronized with that scanning the specimen. The absorption of electrons by the specimen increases with the mean atomic number of the material, and the image produced in the cathode ray tube is so arranged that material of high mean atomic number appears bright. Mean atomic numbers for clinker compounds are: CaO 14·0; C_4AF 13·2; C_3S 12·7; C_2S 12·3; C_3A 12·2. In Plate 7(a), the dark, rounded areas at the bottom represent C_2S and the lighter areas at the top represent C_3S. The interstitial material, which is rich in ferrite, appears white. There are also indications of free CaO (white inclusions in C_2S) and of C_3A (very dark areas corresponding to the dark areas in Plate 7(b)).

If the beam scanning the specimen is of sufficiently high energy, characteristic X-rays are also emitted and may be analysed with a crystal spectrometer, the output from which can be fed to a cathode-ray tube as in the previous case. Bright areas in the resulting image represent parts of the specimen where the concentration of the element producing the X-rays of the wavelength isolated is high. Plate 7(b–f) shows the results thus obtained for Ca, Si, Fe, Al and Ti, using the same specimen as in Plate 7(a) The Ca concentration is high in the C_3S, lower in the C_2S and lower still in the C_3A. The Si concentration is low and the Fe concentration high in the interstitial material. The Al concentration is high in the C_3A.

If the electron beam is kept stationary, the intensities of the characteristic X-rays can be measured and the results used to give a quantitative chemical analysis of the material in the small region of the specimen

irradiated. In this way Wright [*116*] found 55·2% (theoretical, 52·7%) for Ca in C_3S, and 45·4% (theoretical, 46·5%) for Ca in C_2S.

VI. Quantitative Estimation of Phases

A. Chemical Analysis

As has been shown earlier, it has not been found possible to effect a complete mechanical separation of the phases, and other methods of determining the quantitative phase composition of clinker have therefore been evolved. The most important and the most widely used is the recasting of a chemical analysis into a phase composition by means of the Bogue calculation (p. 77). As has already been indicated, this method, at least in its original form, is subject to errors of two main kinds. First, the phase composition obtained is only a potential one because equilibrium crystallization is assumed. This question was discussed on pp. 103–106. Secondly, it is assumed that the principal phases have the exact compositions C_3S, C_2S, C_3A and C_4AF. This assumption is only approximately true, especially in regard to the ferrite phase.

A refinement is clearly possible if the true composition of the ferrite

Table IV

Typical results obtained by Bogue and modified Bogue calculations

	%		A %	B %
SiO_2	20·15	C_3S	49·9	46·0
Al_2O_3	4·47	C_2S	20·1	23·1
Fe_2O_3	6·44	C_3A	0·9	5·7
TiO_2	0·23	Ferrite	19·6	15·7
MgO	2·81	Gypsum	4·1	4·1
CaO	61·51	CaO	0·8	0·8
Na_2O	0·19	MgO	2·8	2·8
K_2O	0·64	Unassigned (TiO_2, alkalis, part of ignition loss)	2·0	2·0
SO_3	1·95			
Ignition loss	1·80			
Total	100·19		100·2	100·2
Free CaO	0·8			

A. Results of the original type of Bogue calculation, assuming the phases to be C_3S, C_2S, C_3A, C_4AF, $CaSO_4.2H_2O$, CaO and MgO.

B. Results of modified Bogue calculation [*37*], assuming the ferrite phase to be $C_4A_{0·72}F_{1·28}$.

phase is known [*37*]. Table IV gives the chemical analysis of a typical Portland cement (containing gypsum), with the results obtained from Bogue calculations of the original type and modified to take into account the true composition of the ferrite phase. If the ferrite composition is wrongly assumed to be C_4AF, the main error introduced is usually in the content of C_3A, the calculated value of which will be high if the molar Al_2O_3/Fe_2O_3 ratio of the ferrite phase exceeds unity and low if it is less than unity. Corrections have also been suggested on the basis of assumptions regarding the alkali phases, and also the SO_3 in the case of clinker [*49, 117*].

The uncertainties inherent in the calculation of the phase composition from the chemical analysis have led to the development of independent methods of determination. The most important of these are based on optical microscopy and X-ray diffraction; infra-red spectroscopy provides a possible additional method.

B. Microscopic Examination

As described earlier, it is possible to identify the C_3S, C_2S, ferrite and possibly the C_3A phases on polished surfaces under the microscope. Once this identification has been made, it is a short step to try to measure the amounts. The first method was that of Rosiwal [*118*]: the area of each constituent on a surface is estimated by measuring the intercepts made by each mineral on a series of equally spaced lines. Various types of aid were invented to help with this method, the most popular being the integrating stage which moved the sample along by micrometers. Parker and Nurse [*88*] used this method to determine the constituents in 12 cements. This method became standard practice, but it was subject to a serious error, as the limits of each individual grain had to be accurately located.

Chayes [*119*] in 1949 made popular the Glagolev statistical method. This method substitutes points for lines in the estimation of areas. A point grid is superimposed on the area to be measured, and the mineral under each point is identified and recorded. In practice, the points of the grid are successively presented to the microscope. Various types of apparatus have been invented recently to carry out this task mechanically (see Chayes [*120*]) in which the specimen is moved across the stage and each mineral when identified is recorded on some form of counter. All these methods give volume percentages of the constituents. Conversion to weight percentages is necessary for comparison with other methods.

The reproducibility of the method may be judged from a series of

measurements made on one clinker sample at the Building Research Station. This clinker was examined by nine operators and the standard deviations of the mean for one result were for C_3S 1%, for C_2S 1·5% and for interstitial material 2·25%. This clinker gave the following volume percentages: C_3S 60·3%, C_2S 24·5%, interstitial material 15·0%. In weight per cent this is equivalent to C_3S 60·4%, C_2S 25·2%, interstitial material 14·3%.

C. Infra-red Absorption

Infra-red absorption spectrometry has been used extensively for quantitative analysis in organic chemistry, but, although the method has been used more and more for qualitative and structural studies in mineralogy, it has had little use in quantitative mineralogy. Lyon, Tuddenham and Thompson [*121*] have reported a method for the analysis of a granite, using infra-red absorption, and this method could be used for the analysis of Portland cements.

Midgley [*113*] concluded that the infra-red absorption spectra for the four main constituents were well established and that the spectra differed sufficiently to allow analysis to be attempted. To carry out the investigation samples of the pure minerals C_3S, C_2S, C_3A and C_4AF were ground to less than 2 μ; since all the minerals under investigation were anhydrous, the KBr disk method could be used. Various weights of the preground minerals were added to either 0·5 or 1·0 g of KBr and blended in a vibratory shaker. The disks were produced by vacuum die pressing. The cement clinker sample was dealt with in the same way. The absorption curves were run on a Perkin-Elmer Type 137 Infra-cord spectrometer.

The absorption curves for the four constituents are given in Fig. 5. Experiment established that Beer's Law held for these minerals. As four components are being investigated, the absorption at four points, 10·2, 10·8, 13·5 and 14 μ, is measured and then from four simultaneous equations the amounts of the four components may be established. These equations may be solved for the minerals present in cement, a typical curve for which is included in Fig. 5. The results so far obtained show only moderate agreement with those obtained by other methods, but the method is still in an early stage of development.

D. X-Ray Diffraction

1. Methods

The quantitative estimation of the phases, using X-ray diffraction, is based on the fact that the integrated intensity of a reflection is directly

proportional to the amount of the substance producing it [*122*, *123*]. This may be expressed as $I_1/I_0 = aw_1/w_0$ where I_1 is the intensity of a given peak of one constituent of which w_1 is the weight percentage, I_0 and w_0 similarly relate to a second constituent, and a is a constant. In practice, calibration mixtures are prepared by taking the four principal clinker compounds in varying known proportions and adding to each a fixed percentage of an internal standard. A given peak is then chosen for the determination of each compound and its intensity (I_1) is measured relative to that (I_0) of a selected peak of the internal standard. From a plot of I_1/I_0 against w_1/w_0 the constant a is obtained. Difficulties occur because of the overlapping of peaks from different compounds, which makes it difficult to find suitable peaks, and also because of the possibility that the patterns of the clinker compounds may differ significantly on account of isomorphous replacement from those of the preparations used in the calibration mixtures.

Table V summarizes the experimental methods that have been used by the various investigators and shows the peaks selected for the various compounds. Most of these peaks have d spacings between 3·1 and 2·6 Å (29–34°2θ for CuK_α radiation). Plate 8 shows traces covering this region for three different clinkers of varying C_3A content.

Von Euw [*6*] used a photographic technique and determined intensities with a microdensitometer. He did not correct for interfering peaks and gave the following coefficients of variation: alite ±3%, β-C_2S ±6–9%, C_3A ±0·7%, ferrite ±1·5%. Brunauer, Copeland and coworkers [*8*, *22*] used a diffractometer with a Geiger counter and ratemeter. They corrected for overlapping peaks by mathematical equations based on the diffraction intensities of individual phases. The method which they used at first [*22*] was based partly on X-ray intensities and partly on chemical analyses for certain oxides. Later they employed a modified method [*8*] which permitted the direct determination of the four major phases and also that of the composition of the ferrite phase. Possible errors arising from differences between the alite and β-C_2S used for standardization and the phases present in the cement were corrected for by adjustments to the constants in the equations. These were made by a process of successive approximation in which the results of the earlier method based partly on chemical analysis were also employed.

Midgley *et al.* [*37*] used initially a diffractometer with Geiger counter and ratemeter. They corrected graphically for interfering peaks. For the ferrite phase separate calibration curves were obtained for different compositions. Difficulties were encountered in grinding silicon satisfactorily for use as an internal standard, and KBr was used. Subsequently Midgley *et al.* [*27*] improved the technique. A better method of grinding

TABLE V

X-Ray diffraction methods used by various authors

Author	Apparatus	Radiation	Reflections used, spacings (Å) and 2θ values				Standard	
			C_3S	C_2S	C_3A	Ferrite		
Von Euw [6]	Guinier camera + photometer	CoK_α	3·07 (34·2°)	2·88 (36·2°)	2·70 (38·6°)	2·66* (39·4°)*	NaCl	2·82 (37·1°)
		CuK_α	3·07 (29·1°)	2·88 (31·1°)	2·70 (33·2°)	2·66* (33·7°)*	NaCl	2·82 (31·8°)
Midgley *et al.* [37]	Geiger counter + ratemeter	CuK_α	3·04 (29·4°) 2·98 (30·0°)	2·88 (31·1°)	2·70 (33·2°)	2·66* (33·7°)*	KBr	3·29 (27·1°)
Copeland *et al.* [22]	Geiger counter + ratemeter	CuK_α	2·19 (41·2°) 1·78 (51·2°) Both reflections common to both phases		2·70 (33·2°)	2·66* (33·7°)*	Si	3·14 (28·4°)
Smolczyk [124]	Geiger counter + counting rate computer	CuK_α	1·76 (51·8°)	2·88 (31·1°)	2·70 (33·2°)	2·66* (33·7°)*	Al_2O_3	1·74 (52·6°)
Midgley *et al.* [27]	Proportional counter + discriminator	CuK_α			2·70 (33·2°)	2·66* (33·7°)*	Si	3·14 (28·4°)

* Approximate values.

permitted the use of silicon, and the Geiger counter was replaced by a proportional counter with pulse height analyser. A 30% increase in peak-to-background ratio was obtained, and the background stability improved. They concluded that the graphical method of correction for interfering peaks was still the best available. The coefficients of variation claimed were as follows (values claimed by Midgley *et al.* [*37*] in parentheses): alite ±5(5)%, β-C_2S ±5(11)%, C_3A ±1(3)%, ferrite ±2(6)%.

Smolczyk [*124*] used a diffractometer with Geiger counter and counting rate computer. He used Al_2O_3 as internal standard and found an improvement in the determination of C_3A. He gave the following coefficients of variation: alite ±2%, β-C_2S ±3%, C_3A ±1%, ferrite ±1%. Kheĭker, Konstantinov and Alekseev [*125*] have suggested the use of a scintillation counter.

2. Results

Brunauer, Copeland and co-workers [*8, 22*] found a reasonably close agreement between the two methods employed. They reported that the C_3A contents were always lower than those predicted by the Bogue calculation. The totals for the four main phases in 20 cements, as determined by their direct method, were on the average 0·8% greater than the sums of the contents of the major oxides (usually 90–95%). They concluded that some of the minor oxides were dissolved in the four main phases and also that no significant amounts of glass were present.

Midgley *et al.* [*37*] found that, in general, the phase compositions determined by X-rays agreed quite well with those given by a modified Bogue calculation in which the observed composition of the ferrite phase was taken into account. They agreed less well with those given by the normal Bogue calculation. Like Copeland *et al.* [*22*], they found no evidence of the presence of appreciable amounts of glass; the sums of the four main phases in 17 clinkers of differing kinds ranged from 90 to 104%. In contrast to Copeland *et al.*, they found no fixed bias between the X-ray results and those of the normal Bogue calculation, except that the latter tended to underestimate C_3A in cements low in this phase. This could be attributed to the fact that in such cements the ferrite phase tended to be rich in C_2F. Smolczyk [*124*] also compared his results with those given by the normal and modified forms of the Bogue calculation; his conclusions were similar to those of Midgley *et al.*

To sum up, the established method of compound determination is the Bogue calculation. This method has been shown to be in error, owing to the very variable ferrite composition; if the composition of the ferrite can be determined separately, however, the modified calculation can be

of use. If independent estimates of the compounds are required, the silicate phases can be determined by point counting with a microscope, but the aluminate phases cannot be determined accurately by this method. X-Ray diffractometry can be used for all four phases; it is most accurate for the aluminate phases and less accurate for the silicate phases. Infra-red absorption can be used, but does not yet appear to give accurate results.

REFERENCES

1. Törnebohm, A. E. (1897). *TonindustrZtg* 1148.
2. Jeffery, J. W. (1952). *Acta cryst.* **5**, 26; (1954). *Proceedings of the Third International Symposium on the Chemistry of Cement, London 1952*, p. 30. Cement and Concrete Association, London.
3. Yamaguchi, G. and Miyabe, H. (1960). *J. Amer. ceram. Soc.* **43**, 219.
4. Midgley, H. G. (1952). *J. appl. Phys.* **3**, 277.
5. Midgley, H. G. and Fletcher, K. E. (1963). *Trans. Brit. Ceram. Soc.*, in press.
6. von Euw, M. (1958). *Silicates industr.* **23**, 647.
7. Naito, R., Ono, Y. and Iiyama, T. (1957). *Semento Gijutsu Nenpo* **11**, 20.
8. Brunauer, S., Copeland, L. E., Kantro, D. L., Weise, C. H. and Schulz, E. G. (1959). *A.S.T.M. Bull.* **59**, 1091.
9. Locher, F. W. (1962). *Chemistry of Cement, Proceedings of the Fourth International Symposium, Washington 1960*, p. 99. National Bureau of Standards Monograph 43. U.S. Department of Commerce.
10. Lafuma, H. (1961). Centre d'Études et de Récherches de l'Industrie des Liants hydrauliques, Note d'information 17.
11. Woermann, E. (1962). *Chemistry of Cement, Proceedings of the Fourth International Symposium, Washington 1960*, pp. 104, 119. National Bureau of Standards Monograph 43. U.S. Department of Commerce.
12. Jander, W. (1938). *Angew. Chem.* **51**, 696.
13. Grzymek, J. (1953). *Cement-Wapno-Gips.* **9**, 162.
14. Nurse, R. W. (1954). *Proceedings of the Third International Symposium on the Chemistry of Cement, London 1952*, p. 56. Cement and Concrete Association, London.
15. Budnikov, P. P. and Azelitskaya, R. D. (1956). *Dokl. Akad. Nauk S.S.S.R.* **108**, 515.
16. Metzger, A. (1953). *Zement-Kalk-Gips* **6**, 269.
17. Midgley, H. G. and Fletcher, K. E. (1960). D.S.I.R. Building Research Station Note D707. HMSO, London.
18. Kukolev, G. V. and Mel'nik, M. T. (1956). *Dokl. Akad. Nauk S.S.S.R.* **109**, 1012.
19. Funk, H. (1958). *Angew. Chem.* **70**, 655.
20. Welch, J. H. and Gutt, W. (1962). *Chemistry of Cement, Proceedings of the Fourth International Symposium, Washington 1960*, p. 59. National Bureau of Standards Monograph 43. U.S. Department of Commerce.
21. zur Strassen, H. (1961). *TagungsBer. Zementindustr.* **21**, 1.
22. Copeland, L. E., Brunauer, S., Kantro, D. L., Schulz, E. G. and Weise, C. H. (1959). *Analyt. Chem.* **31**, 1521; Kantro, D. L., Copeland, L. E. and Brunauer, S. (1962). *Chemistry of Cement, Proceedings of the Fourth International Symposium, Washington 1960*, p. 75. National Bureau of Standards Monograph 43. U.S. Department of Commerce.

23. Nurse, R. W., Welch, J. H. and Gutt, W. (1959). *J. chem. Soc.* **220**, 1077.
24. Thilo, E. and Funk, H. (1953). *Z. anorg. Chem.* **273**, 28; (1953). *Naturwissenschaften* **40**, 241.
25. Funk, H. and Thilo, E. (1955). *Z. anorg. Chem.* **281**, 37.
26. Yannaquis, N. and Guinier, A. (1959). *Bull. Soc. franç. Minér. Crist.* **82**, 126.
27. Midgley, H. G., Fletcher, K. E. and Cooper, A. C. (1963). Symp. Anal. Calcareous Materials, London.
28. Toropov, N. A., Shishakov, N. A. and Merkov, L. D. (1937). *Tsement, Moscow* **5**, No. 1, 28.
29. Yamauchi, T. (1937). *J. Jap. ceram. Soc. (Ass.)* **45**, 279, 361, 433, 614.
30. Swayze, M. A. (1946). *Amer. J. Sci.* **244**, 1, 65.
31. Malquori, G. and Cirilli, V. (1954). *Proceedings of the Third International Symposium on the Chemistry of Cement, London 1952*, p. 120. Cement and Concrete Association, London.
32. Nurse, R. W. (1962). *Chemistry of Cement, Proceedings of the Fourth International Symposium, Washington 1960*, p. 9. National Bureau of Standards Monograph 43. U.S. Department of Commerce.
33. Midgley, H. G. (1954). *Proceedings of the Third International Symposium on the Chemistry of Cement, London 1952*, p. 140. Cement and Concrete Association, London.
34. Midgley, H. G. (1957). *Mag. Concr. Res.* **9**, 17.
35. Midgley, H. G. (1958). *Mag. Concr. Res.* **10**, 13.
36. Kato, A. (1958). *Semento Gijutsu Nenpo* **12**, 17.
37. Midgley, H. G., Rosaman, D. and Fletcher, K. E. (1962). *Chemistry of Cement, Proceedings of the Fourth International Symposium, Washington 1960*, p. 69. National Bureau of Standards Monograph 43. U.S. Department of Commerce.
38. Cirilli, V. and Brisi, C. (1953). *Industr. ital. Cemento* **23**, 289.
39. Santarelli, L., Padilla, E. and Bucchi, R. (1954). *Industr. ital. Cemento* **24**, 55.
40. Royak, G. S. (1958). *Tsement, Moscow* **24**, No. 5, 21.
41. Volkonskii, B. V. (1956). *Rep. Symposium on the Chemistry of Cement, Moscow*, p. 83.
42. Tröjer, F. (1953). *Zement-Kalk-Gips* **6**, 312.
43. Brownmiller, L. T. and Bogue, R. H. (1935). *Amer. J. Sci.* **26**, 260.
44. Suzukawa, Y. (1956). *Zement-Kalk-Gips* **9**, 345.
45. Suzukawa, Y. (1956). *Zement-Kalk-Gips* **9**, 390.
46. Suzukawa, Y. (1956). *Zement-Kalk-Gips* **9**, 433.
47. Müller-Hesse, H. and Schwiete, H. E. (1956). *Zement-Kalk-Gips* **9**, 386.
48. Taylor, W. C. (1942). *J. Res. nat. Bur. Stand.* **29**, 437.
49. Newkirk, T. F. (1954). *Proceedings of the Third International Symposium on the Chemistry of Cement, London 1952*, p. 151. Cement and Concrete Association, London.
50. Steinour, H. H. (1957). Portland Cement Assoc. Res. Dev. Labs (Chicago), Bull. 85.
51. Nurse, R. W. (1952). *J. appl. Chem.* **2**, 708.
52. Toropov, N. A. and Borisenko, A. I. (1954). *Tsement, Moscow* **20**, No. 6, 10.
53. Simanovskaya, R. E. and Shpunt, S. Ya. (1955). *C.R. Acad. Sci. U.R.S.S.* **101**, 917.
54. Erschov, L. D. (1955). *Tsement, Moscow* **21**, No. 4, 19.

55. Kukolev, G. V. and Mel'nik, M. T. (1956). *Tsement, Moscow* **22**, 16.
56. Yamaguchi, G., Ikegami, H., Shirasuka, K. and Amano, K. (1957). *Semento Gijutsu Nenpo* **11**, 24.
57. Toropov, N. A., Volkonskii, B. V. and Sadkov, V. I. (1955). *Tsement, Moscow* **21**, No. 4, 12.
58. Toropov, N. A. and Skue, E. R. (1954). *Dokl. Akad. Nauk S.S.S.R.* **98**, 415.
59. Moore, R. E. (1960). *Rock Prod.* **63**, 108.
60. Taylor, W. C. (1941). *J. Res. nat. Bur. Stand.* **27**, 311.
61. Nurse, R. W. (1954). *Proceedings of the Third International Symposium on the Chemistry of Cement, London 1952*, p. 169. Cement and Concrete Association, London.
62. Brownmiller, L. T. and Bogue, R. H. (1932). *Amer. J. Sci.* **23**, 501.
63. Greene, K. T. and Bogue, R. H. (1946). *J. Res. nat. Bur. Stand.* **36**, 187.
64. Eubank, W. R. and Bogue, R. H. (1948). *J. Res. nat. Bur. Stand.* **40**, 225.
65. Eubank, W. R. (1950). *J. Res. nat. Bur. Stand.* **44**, 175.
66. Parker, T. W. (1954). *Proceedings of the Third International Symposium on the Chemistry of Cement, London 1952*, p. 143. Cement and Concrete Association, London.
67. Newman, E. S. and Wells, L. S. (1946). *J. Res. nat. Bur. Stand.* **36**, 137.
68. Gutt, W. Private communication.
69. Lea, F. M. and Desch, C. H. (1956). "The Chemistry of Cement and Concrete", 2nd Ed., revised by F. M. Lea. Arnold, London.
70. Bogue, R. H. (1954). *Proc. International Symposium on the Reactivity of Solids, Gothenburg, 1952*, p. 639.
71. Jander, W. and Wuhrer, J. (1938). *Zement* **27**, 73.
72. Lacey, W. N. and Woods, H. (1929). *Industr. Engng Chem. (Industr. Ed.)* **21**, 1124.
73. Lacey, W. N. and Shirley, H. E. (1932). *Industr. Engng Chem. (Industr. Ed.)* **24**, 332.
74. Toropov, N. A. and Luginina, I. G. (1953). *Tsement, Moscow* **19**, No. 1, 4.
75. Toropov, N. A. and Luginina, I. G. (1953). *Tsement, Moscow* **19**, No. 2, 17.
76. Heilmann, T. (1962). *Chemistry of Cement, Proceedings of the Fourth International Symposium, Washington 1960*, p. 87. National Bureau of Standards Monograph 43. U.S. Department of Commerce.
77. Suzukawa, Y. and Sasaki, T. (1962). *Chemistry of Cement, Proceedings of the Fourth International Symposium, Washington 1960*, p. 83. National Bureau of Standards Monograph 43. U.S. Department of Commerce.
78. Lea, F. M. and Parker, T. W. (1935). D.S.I.R. Building Research Technical Paper No. 16. HMSO, London.
79. Dahl, L. A. (1938–1939). *Rock Prod.* **41–42**.
80. Lerch, W. and Taylor, W. C. (1937). *Concrete, N.Y.* **45**, 199, 217.
81. Lerch, W. (1938). *J. Res. nat. Bur. Stand.* **20**, 77.
82. Parker, T. W. (1939). *J. Soc. chem. Ind. Lond.* **58**, 203.
83. Lerch, W. and Brownmiller, L. T. (1937). *J. Res. nat. Bur. Stand.* **18**, 609.
84. Yung, V. N., Butt, Yu. M. and Tunastov, V. V. (1957). *Trud. khim-tekh. Inst. Mendeleeva* **24**, 25.
85. McMurdie, H. F. (1941). *J. Res. nat. Bur. Stand.* **27**, 499.
86. Insley, H. (1936, 1940). *J. Res. nat. Bur. Stand.* **17**, 353; **25**, 295.
87. Nurse, R. W., Midgley, H. G. and Welch, J. H. (1961). D.S.I.R. Building Research Station Note A95.

88. Parker, T. W. and Nurse, R. W. (1939). *J. Soc. chem. Ind. Lond.* **58**, 255.
89. Tavasci, B. (1939). *Chim. e Industr.* **21**, 329.
90. Insley, H. and Frechette, van D. (1955). "Microscopy of Ceramics and Cements". Academic Press, New York.
91. Insley, H., Flint, E. P., Newman, E. S. and Swanson, J. A. (1938). *J. Res. nat. Bur. Stand.* **21**, 355.
92. Insley, H. (1954). *Proceedings of the Third International Symposium on the Chemistry of Cement, London 1952*, p. 172. Cement and Concrete Association, London.
93. Jander, W. and Hoffmann, E. (1933). *Angew. Chem.* **46**, 76.
94. Midgley, C. M. (1952). *J. appl. Phys.* **3**, 9, 277; see also Nurse, R. W. (1954). *Proceedings of the Third International Symposium on the Chemistry of Cement, London 1952*, p. 75. Cement and Concrete Association, London.
95. Fratini, N. and Turriziani, R. (1956). *Ric. Sci.* **26**, 2747.
96. Royak, S. M., Nagerova, E. I. and Kornienko, G. G. (1952). *Trud. vsesoyuz. nauch.-issled. Inst. Tsement* No. 5, 58.
97. Takashima, S. (1958). Ann. Rep. 12th Gen. Meeting Jap. Cement Engng Assoc., p. 12.
98. Guttmann, A. and Gille, F. (1931). *Zement* **20**, 144.
99. Midgley, H. G. and Smith, J. J. Private communication.
100. Bogue, R. H. and Brownmiller, L. T. (1930). *Amer. J. Sci.* **20**, 241.
101. Yannaquis, N. (1955). *Rev. Matér. Constr.* **480**, 213.
102. Newkirk, T. F. and Thwaite, R. D. (1958). *J. Res. nat. Bur. Stand.* **61**, 233.
103. Smith, D. K. (1962). *Acta cryst.* **15**, 1146.
104. Toropov, N. A. (1962). *Chemistry of Cement, Proceedings of the Fourth International Symposium, Washington 1960*, p. 113. National Bureau of Standards Monograph 43. U.S. Department of Commerce.
105. Bertaut, E. F., Blum, P. and Sagnières, A. (1959). *Acta cryst.* **12**, 149.
106. Midgley, H. G. and Fletcher, K. E. (1961). D.S.I.R. Building Research Station Note A94. HMSO, London.
107. Mather, K. (1962). *Chemistry of Cement, Proceedings of the Fourth International Symposium, Washington 1960*, p. 34. National Bureau of Standards Monograph 43. U.S. Department of Commerce.
108. Hunt, C. M. Doctoral dissertation, Maryland University (1959).
109. Lehmann, H. and Dutz, H. (1962). *Chemistry of Cement, Proceedings of the Fourth International Symposium, Washington 1960*, p. 513. National Bureau of Standards Monograph 43. U.S. Department of Commerce.
110. Lazarev, A. N. (1960). *Optika i Spektroskopiya* **9** (2), 195.
111. Midgley, H. G. (1962). *Chemistry of Cement, Proceedings of the Fourth International Symposium, Washington 1960*, p. 479. National Bureau of Standards Monograph 43. U.S. Department of Commerce.
112. Roy, D. M. (1958). *J. Amer. ceram. Soc.* **41**, 293.
113. Midgley, H. G. (1962). D.S.I.R. Building Research Station Note D811.
114. Fahn, R. (1956). *TonindustrZtg u. keram. Rdsch.* **80**, 171.
115. Hall, D. M. (1957). *Brit. J. appl. Phys.* **8**, 295.
116. Wright, P. W. Private communication.
117. Satou, S. and Tagai, H. (1961). *J. Jap. ceram. Soc.* (*Ass.*) **69**, 102.
118. Rosiwal, A. (1898). *Verh. geol. ReichsAnst.* (*StAnst.*) *Wien* 143.
119. Chayes, F. (1949). *Amer. Min.* **34**, 1.
120. Chayes, F. (1956). "Petrographic Modal Analysis". New York.

121. Lyon, R. J. P., Tuddenham, W. M. and Thompson, C. S. (1959). *Econ. Geol.* **54**, 1047.
122. Alexander, L. and Klug, H. P. (1948). *Analyt. Chem.* **20**, 886.
123. Copeland, L. E. and Bragg, R. H. (1958). *Analyt. Chem.* **30**, 196.
124. Smolczyk, H. G. (1961). *Zement-Kalk-Gips* **12**, 558.
125. Kheĭker, D. M., Konstantinov, I. E. and Alekseev, V. A. (1959). *Kristallografiya* **4**, No. 1, 54.

CHAPTER 20

Optical Microscopy

H. G. MIDGLEY

Building Research Station,
Garston, Watford, Hertfordshire, England

and

H. F. W. TAYLOR

Department of Chemistry,
University of Aberdeen, Scotland

CONTENTS

I. Introduction

Optical microscopy has several uses in the field covered by this book: it can provide information about the morphology and texture of a material, that is, the sizes and shapes of the particles of which it is composed and the way in which they are arranged; it can generally show whether particles are amorphous or crystalline; crystalline materials can be identified by their optical properties; and in favourable cases information about the crystal symmetry can be obtained.

Four main techniques are of use in the present field.

(a) The binocular microscope is useful for the preliminary examination of hand specimens, but provides no detailed information.

(b) The polarizing (or petrographic) microscope can be used for examining small fragments of material in transmitted light. This method provides the most complete information about the optical properties of transparent substances, but it is not the best way of studying the texture of an inhomogeneous material such as a natural rock or cement clinker.

(c) The polarizing microscope can also be used with thin sections (usually about 25 μ thick) of transparent materials; this method can be used to determine all the optical properties other than refractive index, and also provides information about texture.

(d) The reflected light (or metallurgical) microscope can be used to study polished sections in polarized light; this is the equivalent of method (c) for use with opaque materials. It has also proved the most useful single method for studying cement clinker.

We shall not discuss here the optical principles underlying microscopy, nor the detailed design, care and use of microscopes, nor the use of the microscope for studying crystal morphology. For these matters, and for a fuller treatment of many of the subjects that are discussed, specialist texts must be consulted [*1–4*]. Unless otherwise stated, it will be assumed that white light is used.

II. Examination of Crushed Material

(By H. F. W. T.)

A. General

Unlike biological microscopes, the polarizing microscope is designed for the determination of optical properties rather than for very high magnification and resolution. The main special features (Fig. 1) are the inclusion of (a) the polarizer and analyser; (b) the Bertrand lens and converger, which permit the study of crystals in a convergent beam of polarized light; (c) one or more slots to take accessories such as the gypsum plate; and (d) a rotating stage with a vernier scale calibrated in degrees. As an alternative to (d), the stage can be fixed and provision made for the synchronous rotation of polarizer and analyser. The polarizer and analyser are usually called *nicols* (Nicol prisms), although in modern microscopes they are generally made from polaroid. The term *polars* is also encountered. They are often used with their vibration directions perpendicular to each other, thus giving a dark field; this arrangement is described as *crossed nicols.* The eyepiece is provided with cross-wires perpendicular to the two vibration directions. Polarizer, analyser, Bertrand lens and converger can each be brought in or out of the optical system at will, though it is rarely necessary to take the polarizer out of the system.

Crushed or powdered material is usually best examined in suspension in an *immersion liquid*; grains of the material are placed on a microscope slide and covered over with a cover glass, and a drop of the immersion liquid is introduced at the edge of the cover glass, under which it flows by capillary action. The optimum grain size is about 100–150μ, but this varies with the shape and other properties. For the study of optical

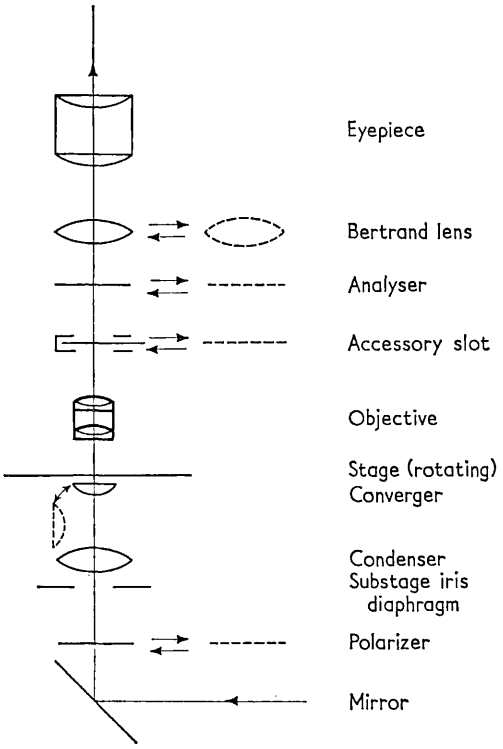

FIG. 1. The polarizing microscope (diagrammatic).

properties it is highly desirable that the grains be single crystals or fragments of single crystals.

As immersion liquids, involatile organic substances which do not react with the grains are generally used. It is convenient to have a series of liquids with refractive indices varying in steps of 0·01 or 0·02; the following mixtures are satisfactory.

Refractive indices 1·48–1·63: medicinal paraffin + α-chloronaphthalene
Refractive indices 1·63–1·66: α-chloronaphthalene + α-bromonaphthalene
Refractive indices 1·66–1·74: α-bromonaphthalene + methylene iodide
Refractive indices 1·74–1·78: methylene iodide + sulphur

For refractive indices above 1·78 it is difficult to find suitable liquids; various solutions in methylene iodide and also low melting solids have been described [*2*]. In all cases the refractive index can be checked against standard glasses or determined using an Abbé or other type of refractometer, which may itself be checked against suitable organic liquids of high purity.

As regards optical properties, all solid substances fall into one or other of two categories: *isotropic* and *anisotropic*. With isotropic substances the optical properties are independent of the direction of vibration of the light; with anisotropic substances this is not so. Crystals belonging to the cubic system and amorphous substances are normally isotropic; crystals of all other systems are anisotropic. Amorphous substances and cubic crystals can, however, become anisotropic if they have undergone certain kinds of thermal or mechanical treatment, and are usually then said to have become "strained"; glass fibres provide an example of this.

Particles can also be described according to their morphology (e.g. platy, needle-like, etc.) or, if crystalline, according to the extent to which external faces are developed. The terms *euhedral*, *subhedral* and *anhedral* denote full development, partial development and non-development, respectively, of external form. Cubic crystals can sometimes be distinguished from amorphous particles by their euhedral or subhedral appearance, but care is necessary, as crystals can become anhedral due to crushing or irregular growth, while amorphous particles can develop a distinctive morphology.

B. Isotropic Substances

Apart from the study of the shape, size, colour, etc. of the grains, the only property which can be determined is the refractive index. This is most easily done by employing the principle that the relief of the grain is at a minimum when the latter is immersed in a liquid having the same refractive index as itself. The analyser must be out; it does not matter whether the polarizer is in or out. To find whether a grain has a refractive index higher or lower than that of the liquid, the method of *Becke lines* is used: when the microscope objective is racked upwards, or the stage lowered, so that the object goes out of focus, a bright line appears on the edges of the grain and moves into the medium of higher index. If the objective is lowered or the stage raised, the line moves into the medium of lower index. It is usually best to close partially the substage iris diaphragm and to use an objective of only moderately high power. The Becke line method makes it possible to narrow down the range within which the index of the grain lies, by bracketing. In the final

stages mixtures of immersion liquids can be made and their indices determined with a refractometer. With white light the index can often be found to $\pm 0{\cdot}005$. For greater precision it is essential to use monochromatic light; sodium vapour lamps are commonly used. The temperature must also be controlled, as the refractive indices of immersion liquids change rapidly with temperature. Precision methods of refractive index determination employing changes in refractive index with temperature or wavelength or both have been described [*1*].

C. Anisotropic Substances

1. Birefringence

If an anisotropic substance is viewed between crossed nicols in white light, its appearance normally changes as the stage is rotated. Four times in each revolution, at 90° intervals, the crystal appears dark; these settings are called *extinction positions*. In the intervening *45° positions*, the crystal appears white or coloured. This is caused by the fact that the light is split into two rays, which travel at different speeds within the crystal. The vibration directions of these rays are mutually perpendicular and are controlled by the crystal's structure; extinction occurs when the vibration directions in the crystal are parallel to those of the nicols. The vibration directions within the crystal are therefore also called *extinction directions*.

If an acicular crystal has its extinction directions parallel and perpendicular to its length (i.e. if it extinguishes when either cross-wire is parallel to its length), it is said to show *straight* or *parallel extinction*. Crystals of the orthorhombic, hexagonal, tetragonal and trigonal systems, as well as some monoclinic crystals in certain orientations, frequently show parallel extinction. If the extinction directions are not parallel and perpendicular to the length, extinction is said to be *inclined*. The *extinction angle* is the angle between some prominent morphological feature, such as the long axis of a needle-shaped crystal, and the nearest extinction direction. Inclined extinction is shown predominantly by triclinic crystals and by monoclinic crystals in certain orientations.

Since the two rays travel within the crystal at different speeds, the crystal has a different refractive index for each. The difference between these two refractive indices is called the *birefringence*; its value depends, not only on the substance, but also on the direction of travel of the light. The product of the birefringence and the thickness of the crystal in the direction of the light's travel is called the *retardation*. The colour which is shown by the crystal in the 45° positions depends directly on the retardation (Fig. 2). Hence, if the colour can be recognized and the

thickness of the crystal measured, the birefringence can be obtained. The thickness can be measured by focusing on the top and bottom surfaces of the crystal in turn or by turning the latter on edge (e.g. by mounting it

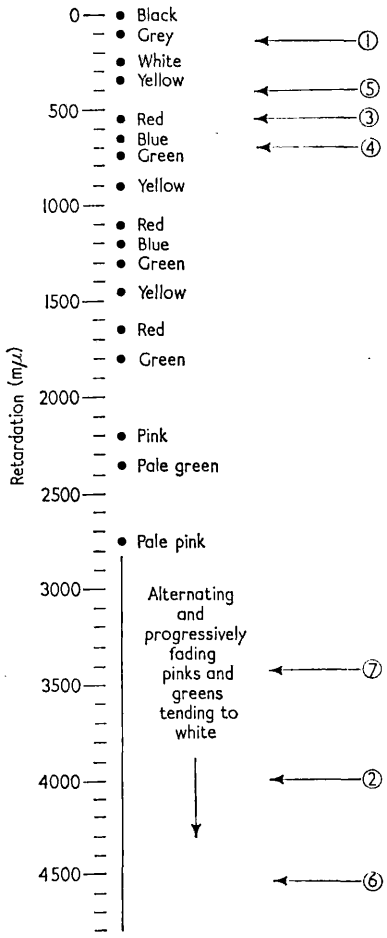

FIG. 2. Scale of interference colours (called also "Newton's scale"): 1, Typical low white; 2, typical high white; 3, gypsum plate; 4, gypsum plate + low white (additive); 5, gypsum plate − low white (subtractive); 6, gypsum plate + high white (additive); 7, gypsum plate − high white (subtractive).

on some simple type of rotation apparatus) and using a micrometer eyepiece.

The two rays into which the light is split within the crystal are called

the *slow* and *fast* rays, and the corresponding vibration directions are called the slow and fast directions. The slow direction corresponds to the higher refractive index. To find which is the slow and which the fast direction, *compensators* are used. One of the simplest of these is a plate of gypsum, which is cut so as to have a retardation of about 550 mμ, and its slow direction either parallel or perpendicular to its length (with British manufacturers, usually parallel). The plate is inserted into the accessory slot of the microscope (Fig. 1), which is so arranged that the length of the plate makes an angle of 45° to the vibration directions of the nicols. With crossed nicols in use the field becomes red, as this colour corresponds to the retardation of 550 mμ (Fig. 2). If a crystal is now viewed in a 45° position, the retardations of plate and crystal add if the slow directions of the two are parallel to each other, and subtract if they are perpendicular. If, as is very common, the crystal has a retardation in the low white range, addition produces a blue colour and subtraction a yellow one (Fig. 2). The slow and fast directions in the crystal can thus be identified.

If an acicular crystal has the slow direction parallel or nearly parallel to its length, it is said to have *positive elongation* or to be *length-slow*. If the fast direction is parallel or nearly parallel to the length, the crystal is said to have *negative elongation* or to be *length-fast*. These signs are called *signs of elongation*.

The gypsum plate can also be used to distinguish a low white from a high white colour. In the former case, when the plate is introduced, the colour changes to blue or yellow as already described. A high white colour, in contrast, is little affected by the introduction of the gypsum plate (Fig. 2). This is useful for identification, especially of calcite. Most of the substances encountered in cement chemistry have birefringences below 0·01 for any orientation, so that crystals of normal thickness (10–30 μ) show colours in or near the low white range (retardation 100–300 mμ). Calcite, in contrast, has an exceptionally high maximum birefringence of 0·17 and generally shows a high white colour ($>$ 3000 mμ).

Several other types of compensator are in common use, the mica plate (retardation about 150 mμ) and quartz wedge being especially important. The quartz wedge has a retardation which varies along its length from almost zero at one end to about 2500 mμ at the other. If it is gradually pushed into the accessory slot, thin end first, between crossed nicols and with no crystal in view, the entire sequence of colours shown in Fig. 2 is observed. If a crystal is now brought into view, in a 45° position and with its retardation opposing that of the wedge, a dark band appears when the crystal is optically superimposed on the part of the wedge which has a retardation equal to its own. This is a useful way of determining the

retardation, especially if the latter is fairly high; it makes it possible, for instance, to distinguish the green at 800 mμ from that at 1300 mμ. The Berek compensator [*2*, *3*] is an alternative to the quartz wedge.

2. The Optical Indicatrix

Anisotropic crystalline substances fall into two groups, *uniaxial* and *biaxial*. Crystals of the trigonal, tetragonal and hexagonal systems are uniaxial; those of lower symmetry are biaxial. The optical properties of both groups are most easily understood by reference to the *optical*

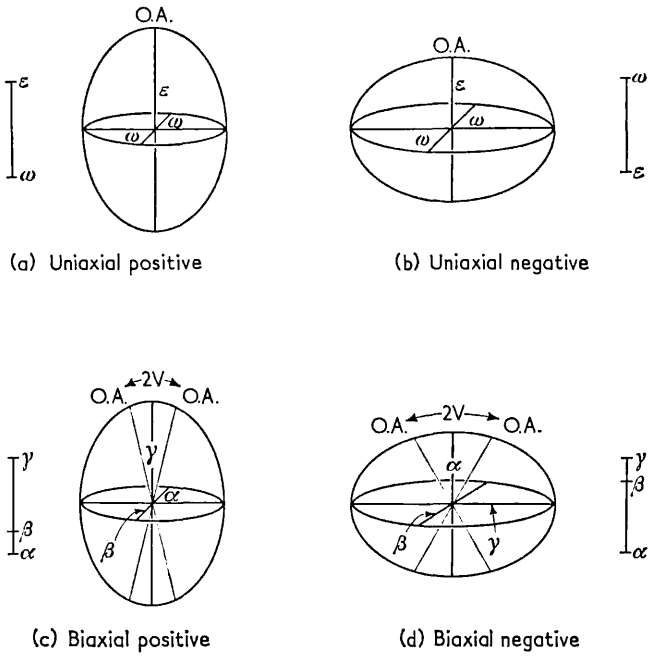

FIG. 3. Indicatrix ellipsoids.

indicatrix. This is defined as the surface whose radius vector in any direction represents the refractive index for light vibrating in that direction. The light must, of course, travel in a direction perpendicular to the radius vector. For isotropic substances the indicatrix is a sphere. With anisotropic crystals it is an ellipsoid. When light passes through the crystal, the vibration directions of the two rays into which it is resolved are parallel to the major and minor axes of the elliptical section which passes through the origin. In certain cases this ellipse reduces to a circle, and the crystal then behaves as if it were isotropic.

(a) *Uniaxial crystals.* The indicatrix is an ellipsoid of revolution (Fig. 3(a) and (b)). The unique axis is called the *optic axis* and coincides with the crystallographic *c*-axis. For light travelling along this direction the crystal behaves as if it were isotropic; for light travelling in any other direction it behaves in the way described in the previous section. Two *principal refractive indices*, ω and ϵ, suffice to define the indicatrix surface. If $\epsilon > \omega$, the *optic sign* is said to be positive (Fig. 3(a)); if $\omega > \epsilon$, the optic sign is negative (Fig. 3(b)).

The two commonest habits adopted by uniaxial crystals are flakes with basal cleavage and prisms with length *c*. The former appear isotropic when lying flat on the slide, and determination of refractive index gives ω. If they are viewed edge on, ω and ϵ can both be determined. To do this, the polarizer of the microscope is employed but not the analyser. If the crystal is set so that the length of the flake is parallel to the vibration direction of the polarizer, refractive index determination will give ω; if the length of the flake is perpendicular to this direction, ϵ will be obtained. The same principles apply with uniaxial crystals which crystallize as prisms. For a prismatic uniaxial crystal, extinction is always parallel and the optic sign is the same as the sign of elongation.

(b) *Biaxial crystals.* The indicatrix is a triaxial ellipsoid (Fig. 3(c) and (d)). There are two optic axes, i.e. directions of travel for which the crystal appears isotropic. Sections of the indicatrix passing through the origin and normal to these directions are circular. Three principal refractive indices, α, β and γ†, define the indicatrix surface: β is the index for light whose vibration direction lies in the intersection of the two circular sections; α, β and γ are mutually perpendicular; and, by definition, $\alpha < \beta < \gamma$. The acute angle between the optic axes is called 2V; if the line bisecting it (the *acute bisectrix*) is α, the optic sign is negative (Fig. 3(d)), and if this line is γ, the optic sign is positive (Fig. 3(c)). In theory 2V and the optic sign can always be calculated if α, β and γ are known. In practice it is usual to determine them independently, because small errors in the indices have a large effect on 2V and can even affect the sign. For a biaxial positive crystal β is closer to α than to γ; for a biaxial negative crystal it is closer to γ than to α (Fig. 3).

For an orthorhombic crystal the vibration directions α, β and γ must each be parallel to crystallographic *a*, *b* or *c*; there are no rules as to which optical direction is parallel to a given crystallographic direction. For monoclinic crystals either α, β or γ must be parallel to *b*, but there are no other restrictions on the orientation of the indicatrix. For triclinic crystals there are no restrictions at all on the orientation of the indicatrix. These laws are the reason for the frequent occurrence of parallel extinction with

† Other symbols are sometimes used; for a concordance table see reference [3].

orthorhombic crystals and of inclined extinction with triclinic crystals, and for the intermediate situation observed with monoclinic crystals.

In favourable cases α, β and γ can be determined by observing the crystal in each of two orientations, each of which will give two of the indices. This procedure is a simple extension of that mentioned for use with uniaxial crystals and can often be applied with orthorhombic crystals. With monoclinic or triclinic crystals determination of the three refractive indices is more difficult and specialist texts must be consulted. For any random orientation one of the observed indices will always lie between α and β, and the other between β and γ.

With an acicular biaxial crystal the optic sign is not necessarily the same as the sign of elongation. This position differs from that observed with uniaxial crystals.

3. Use of Convergent Light

If the Bertrand lens and the converger (Fig. 1) are brought into the optical system of the microscope and a high-power objective used, the image of an anisotropic crystal is replaced by an interference figure. This is a pattern in which each point represents a different direction of travel of light within the crystal. Interference figures can provide much information, including whether a crystal is uniaxial or biaxial, the orientation of the indicatrix, the optic sign and the approximate value of 2V. These uses are particularly important with biaxial crystals.

Only two very simple cases will be described here, to illustrate the uses of the method. Figure 4(a) shows the interference figure given by a uniaxial crystal viewed along the direction of the optic axis. The pattern consists of a black cross superimposed on a circularly symmetrical sequence of interference colours. With rotation of the stage the pattern remains unchanged. The arms of the cross are called *isogyres* and represent directions for which extinction occurs. The circular bands of colour join points representing directions of equal retardation. If a gypsum plate or other compensator is introduced, the colours undergo changes which may be used to determine the optic sign. With biaxial crystals the simplest case is for light travelling parallel to the acute bisectrix (Fig. 4(b)). In this case the isogyres may again form a cross, but only if the crystal is in an extinction position for parallel light. If the stage is rotated, the cross opens and two separate isogyres are seen. As with uniaxial crystals, the isogyres are superimposed on a pattern of coloured bands and the optic sign can be found by studying the effect of compensators on the pattern. The maximum separation between the isogyres occurs in the 45° position; from its value 2V can be determined. The method is not of high accuracy but is the one most frequently used.

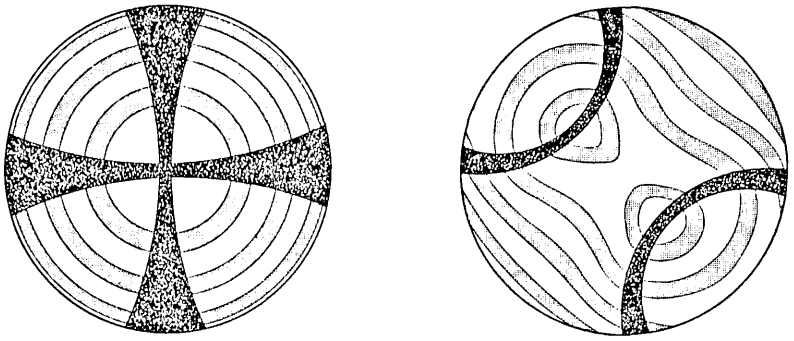

FIG. 4. Interference figures: (a) Uniaxial crystal viewed along optic axis; (b) biaxial crystal viewed along acute bisectrix (for a 45° position of the stage).

4. Additional Considerations

(a) *Pleochroism.* This denotes variation in absorption with the direction of vibration of the light. The occurrence of pleochroism can be recognized by rotating the stage with the polarizer in and the analyser out; the depth and sometimes also the shade of the colour change. The shade changes if the way in which absorption varies with direction depends on the wavelength.

(b) *Dispersion.* This denotes variation in the indicatrix surface with wavelength. For isotropic substances this reduces to variation in refractive index. For uniaxial and orthorhombic crystals the directions of the indicatrix axes are fixed and only their lengths can vary; for monoclinic and triclinic crystals both the lengths of the axes and their orientations (apart from that of the one parallel to *b* in the monoclinic case) can vary. With both uniaxial and biaxial crystals the different indicatrix axes may be affected to differing extents. Dispersion is most conveniently studied by its effects on the interference figure, and can be used to distinguish the three possible crystal systems in the case of biaxial crystals. Either dispersion or pleochroism, or the two together, can cause abnormal colours to appear when a crystal is viewed between crossed nicols in parallel light.

(c) *The universal stage.* This is an attachment to the microscope in which the specimen is placed between two glass hemispheres, enabling its orientation to be adjusted over a wide range of angles; graduated scales for determining changes in orientation are provided. The use of the

universal stage is described in references [*1*, *2*]. It is almost essential for the precise determination of the optical properties of crystals of the less symmetrical systems.

5. *Incomplete Optical Studies*

To describe the optical properties of a crystal fully, it is necessary to have defined completely the optical indicatrix in terms of the optic sign together with ω and ϵ, or α, β, γ and 2V. It is also necessary to have determined the orientation of the indicatrix axes relative to the crystallographic axes, and to have given an adequate description of any pleochroic or dispersive effects. Properties relating the optical directions to the external form, such as the sign of elongation and extinction angles, should also be given for important orientations of the crystal. Lastly, though not strictly relevant to the matters discussed in this chapter, any morphological features such as crystal shape, cleavage, inclusions or twinning should be described.

It is often necessary to be content with incomplete information, usually because of small crystal size. Two cases are especially important with calcium silicates and aluminates.

(a) Crystals are found which grow as fibrous aggregates. The individual crystallites all have one axis parallel or nearly parallel, but are rotated at random around this axis. It is impossible to observe individual crystallites. Aggregates of this type necessarily have parallel extinction, even though individual crystals would have inclined extinction. Only three optical properties can usually be determined: the sign of elongation, and the refractive indices for light vibrating parallel and perpendicular to the fibre. It is better to call these n_1 and n_2, rather than α and γ, as they are not necessarily equal to the principal refractive indices of a single crystal.

(b) Crystals are found which contain two or more phases intergrown in a definite orientation, on a sub-optical scale. Such crystals can be recognized by X-ray methods. Their optical properties are, in general, intermediate between those of their constituents, and optical methods do not distinguish them from solid solutions.

(c) Many substances can be prepared in a condition intermediate between crystalline and amorphous; many topotactically formed products come into this category (Chapter 5). The optical properties of these products often differ grossly from those of the corresponding well crystallized materials; in general, they have much lower refractive indices.

III. Thin and Polished Sections

(By H. G. M.)

A. Thin Sections

This method is widely used by geologists for the study of rocks. A small chip of the material, ideally about 25 mm × 25 mm × 3 mm, is first obtained by breaking with a hammer or cutting with a diamond saw. In the latter case a lubricant or coolant is needed; water is normally used, but with hydraulic materials such as cement clinker, liquid paraffin should be employed.

Before proceeding further, porous materials such as cement clinker must be impregnated with a resin. Even where it is not absolutely necessary, setting in resin is a convenient method of obtaining a specimen which can be handled easily and marked for identification. A piece of material about 40 mm × 40 mm × 40 mm, or alternatively about 6 small chips, is placed in a glass specimen tube in a desiccator fitted with a two-holed rubber bung which bears a tap funnel and a tube for evacuation. The desiccator is evacuated for one hour, and resin (Bakelite R0014) is then run into the specimen tube from the funnel until the sample is covered. The specimen tube and contents are removed and heated in an oven for 4 hr at 50° C, followed by 24 hr at 100° C. Cold-setting resins such as Ceemar† may also be used. These are mixed according to the manufacturer's instructions, run into a specimen tube containing the specimen, if necessary under vacuum, and allowed to harden in a normal laboratory atmosphere. They harden more rapidly than thermosetting resins, and the product is transparent and in some other ways superior. The hardened resin containing the specimen is removed from the tube by breaking the glass.

With either the chip, slice or impregnated specimen, one surface is ground flat until of sufficient area. This may be done on a rotating metal lap, or by hand on a glass or metal plate, with successively finer grades of silicon carbide powder; it is important to clean the surface thoroughly before changing from one grade to the next. Final polishing is done by hand on a glass plate with 4F grade silicon carbide (about 10μ). When a perfectly even surface is obtained, the specimen is cleaned and allowed to dry. It is then mounted. The traditional mounting medium for this purpose is Canada Balsam; its use is described in references [*1*, *2*]. Recently, media such as Lakeside No. 70C‡ have become available and are easier to use. With this latter medium the microscope slide

† E. M. Cromwell & Co. Ltd., Bishops Stortford, Herts., England.

‡ Obtained from Hugh Courtright and Co., 7600, Greenwood Avenue, Chicago 19, Illinois.

(75 mm × 25 mm) is placed on a hot plate at 140° C and a small amount is melted on to its surface. The specimen is then lowered on to the mounting medium, polished side downwards, and the slide is removed from the hot plate, pressed to remove air bubbles, and allowed to cool.

The second side of the specimen is then ground in the same way as the first. Initial grinding with 60 grade followed by 120 grade silicon carbide is carried on until the section is just transparent; great care is needed to keep the thickness of the section uniform and to avoid breaking away the surrounding mounting medium, which protects its edges.

When the section is just transparent, it is thoroughly cleaned and final grinding is carried out by hand on the glass plate, using 4F grade silicon carbide. As the section becomes thinner, repeated examinations on a polarizing microscope are made and grinding is continued until the minerals give the desired interference colours when viewed between crossed nicols. It is usual to make sections about 20 μ thick; at this thickness quartz, C_3S, and most melilites have white or grey polarization colours.

A cover glass is placed on top of the finished section for protection. The slide and cover glass are placed on the hotplate and a little of the mounting medium is placed on the cover glass. When the mounting medium has attained the right consistency, the cover glass is inverted on to the specimen with a hinge action. After the mounting medium has spread out evenly, the slide is removed from the hotplate and the cover glass pressed into its final position.

Broadly speaking, methods of examination are the same as with crushed material, though it is not possible to determine refractive indices except qualitatively in relation to that of the mounting medium. Thin sections of hydrated Portland cement, about 30 μ thick, can be made in the manner just described but are not very informative, because the thickness greatly exceeds the crystal size ($< 1\ \mu$). By using great care in polishing, J. J. Smith has succeeded at the Building Research Station in preparing specimens under 5 μ thick. With these specimens reaction rims around the clinker grains can be seen (Plate 1).

B. Polished Sections

1. Preparation

Friable materials are first mounted in resin as for the preparation of thin sections. The surface is then ground by the following successive operations: (a) mechanical grinding on a rotating steel lap with 120 grade silicon carbide (about 150 μ) and water; (b) hand grinding on a glass plate with 220 grade silicon carbide and water; (c) hand grinding

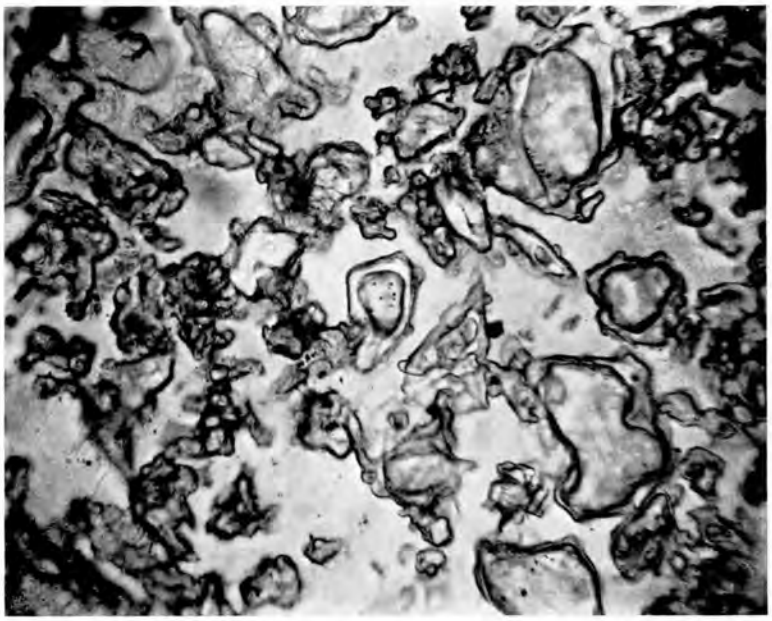

PLATE 1. Very thin section of a hydrated Portland cement paste, showing reaction rims round C_3S grains (J. J. Smith; × 400).

on a glass plate with 4F grade silicon carbide and water; (d) grinding on a rotating cloth-covered lap, using Sira abrasive,† grade 4; and (e) grinding on a rotating cloth covered lap, using chromium(III) oxide (Cr_2O_3) and water, and finally polishing until dry. For very soft materials freshly ignited magnesia is better than chromium(III) oxide for stage (e), and it may be found better to omit stage (d). With Portland cement clinker or other reactive materials it is advisable to use alcohol instead of water in stage (e). The best cloth to use on the lap is well washed linen or twill; a lap speed of about 1500 rev/min is suitable. If the number of polished sections to be made is not large, a rotating lap is not needed for stages (a), (d) and (e); all grinding can be done by hand.

With a slow speed grinding machine, such as is used in metallurgical work, more perfect surfaces can be obtained, but the method is slow. For hard materials, such as blastfurnace slags or high-alumina cement, slow grinding offers little advantage over the high speed cloth covered lap, but for softer materials such as Portland cement clinker some advantages are obtained. The most useful polishing agent is cerium dioxide, used with liquid paraffin as lubricant. This produces excellent surfaces free from scratches. Polishing is slow, but the machine is automatic and may be left running unattended. The slow speed machine may also be used with "plastic laps", where the polishing agent is embedded in a plastic (usually acrylic) lap, no further polishing agent being then added.

2. Optical Properties in Reflected Light

The reflected light microscope is provided with a prism or semi-reflecting glass plate above the objective, which allows the light to be directed through the latter on to the object. Polarizer, analyser, rotating stage and Bertrand lens are provided, as with the petrographic microscope. Focusing is usually done by moving the stage. Only a brief indication of reflected light techniques can be given here; for fuller details see reference [*4*].

(a) *Properties observed with the analyser out of the system.* These include colour, reflectivity, bireflectance and hardness. Opaque substances reflect much of the light and appear silvery-white, grey or yellow. Transparent substances appear dark grey or black; the lower the refractive index, the darker the substance appears. The *reflectivity*, R, is defined as the ratio of the intensity of the light reflected to that of the incident light and can be determined using a Berek slit microphotometer. A colour filter, which is usually red, is employed, and measurements are made relative to a standard substance of known reflectivity.

† Obtainable from U.K. Optical Bausch and Lomb Ltd., Bittacy Hill, London, N.W.7.

For an isotropic substance of refractive index n

$$R = \frac{(n-N)^2-n^2K^2}{(n+N)^2+n^2K^2}$$

where N is the refractive index of the immersion medium and K is the absorption coefficient of the material. In most transparent or semi-transparent substances n^2K^2 is small enough to be neglected. A simple test of this assumption is to determine R, using both a dry and an oil-immersion objective; if the two values of n so obtained agree to $\pm 0{\cdot}1$, the assumption is justified.

Many anisotropic substances vary in brightness or colour, or both, as the stage is rotated. This property is called *bireflectance* and its magnitude is related to the birefringence. It therefore depends on the crystal orientation. The birefringence of the ferrite phase in cement clinkers has been determined in this way, but it is difficult to find crystals showing the maximum bireflectance.

When a polished surface is made on an inhomogeneous material, the harder constituents are ground down less than the others. The relative *polishing hardnesses* (resistances to abrasion) can be found from a test analogous to the Becke line test in transmitted light; on racking down the stage, a bright line appears at the boundary and moves towards the softer constituent.

(b) *Properties observed using crossed nicols.* In theory, an isotropic substance should remain dark for all positions of the stage and an anisotropic one should (except in certain orientations) show four extinction positions, as with transmitted light. In practice, with transparent or semi-transparent materials such as cement clinker some light penetrates the surface and is reflected internally at crystal boundaries. This effect masks any true reflection polarization phenomena arising from anisotropy of the crystals. True polarization effects have, however, been observed with polished surfaces of synthetic melts. The use of an oil-immersion objective is helpful and critical adjustment of polarizer and analyser is important. The surface may be observed in parallel light, or interference figures may be studied, using the Bertrand lens.

3. *Etching Techniques for the Study of Cement Clinkers*

Since thin sections of either anhydrous or hydrated cements are difficult to make and to interpret, the polished section technique was introduced [5–7] and has become widely used. With a Portland cement clinker very little can be seen on a normally polished surface, but the outlines of the crystals can be made visible by differential etching.

(a) *General.* The etching reagent is poured into a small watch glass and the specimen is rapidly immersed in it, polished surface down, care being taken to avoid trapping air bubbles on the surface. The watch glass is gently rocked. The specimen is then removed and rinsed, in alcohol if the etch reagent is made up in alcohol, otherwise in water. Many of the etch reactions depend on the formation of a thin film on the surface of the crystals, which produces interference colours. Care must be taken when drying the specimen not to scratch the film. The best method is to dab gently on lens cleaning tissue or on a soft cloth. Where the etch acts by removal of a surface film, the surface is not harmed by gentle wiping. A method sometimes used is to expose the surface to HF vapour. The specimen is placed face down on a lead, plastic or platinum crucible half filled with the acid and a larger crucible is inverted over it.

When using high magnifications, trouble may be caused by the objective misting over. This can be avoided by a final drying of the specimen with a jet of warm air.

(b) *Portland cement clinker.* When the unetched specimen is examined, two constituents, appearing white against the grey matrix, are differentiated by their high reflectivity. The commoner is the ferrite phase, which occurs as small needle- or spear-shaped crystals; the other, MgO, is rare and occurs as squares or triangles, often rounded at the angles. The MgO may be more definitely identified by buffing the specimen on a cloth lap, when it will be left in relief, owing to its hardness.

Free CaO may also be seen in unetched specimens; it is darker than the ground mass, and often shows scratches because of its relative softness. After the buffing described above the free CaO will be pitted. It often occurs in aggregates and may be found in contact with any of the other constituents of the clinker. Free CaO is etched in about 2 sec by distilled water, which causes it to appear pitted and to display interference colours.

C_3S and free CaO are etched by immersing the specimen for 3 hr in a mixture of equal volumes of ethylene glycol and absolute alcohol. Another and quicker method is to immerse the specimen for 10 sec in 10% $MgSO_4$ in water, followed by a rapid wash in water, followed by alcohol, and drying. A disadvantage is that this reagent also etches the ground mass, but with experience this ceases to be a difficulty.

C_2S is etched to a blue or red colour (depending on the time of etching) by holding the specimen over a crucible containing 40% HF in water and allowing the vapour to come in contact with the polished surface. About 10–20 sec produces the blue, and somewhat longer periods the red colour. At this later stage differentiation of the ground mass also occurs and C_3S assumes a straw colour.

A modification of the double etch described by Insley is useful. The specimen is immersed in distilled water for 5 sec, washed in alcohol and then immersed in 0·25% HNO_3 in alcohol. The surface is finally washed in alcohol and dried by blotting. The acid colours the calcium silicates, while the water affects mainly the C_3A and glass of some glass compositions. The ferrite phase is unattacked. There is some doubt as to the effect on the glass. Nurse and Parker concluded that glasses of high iron content are not etched but that those low in iron and high in alumina contents are etched. Insley [*6*] and Tavasci [*5*] claimed to be able to distinguish glass specifically. A more certain method of distinction is based on measurement of reflecting power (see below).

(c) *High alumina cements.* Much useful information can be obtained by the examination of a polished surface of high alumina cement, even before etching, as the wider range of refractive indices produces more contrast between the various constituents than is the case with slag or Portland cement clinker. This contrast can be considerably increased by the use of oil immersion objectives.

CA may be identified by etching with boiling 10% NaOH at 100° C for 20 sec. It is coloured blue or brown, depending on the crystal orientation. The characteristic twinning can also be noted. The phase sometimes described as "unstable C_5A_3", the fibrous phase, or "pleochroite" is also faintly etched by this reagent but can readily be distinguished by its elongated crystal shape.

After immersion in boiling 1% borax for 30 sec., $C_{12}A_7$ is etched dark grey, C_2S light blue. The effect of "pleochroite" varies from a slight darkening in some specimens to a strong blue or yellow coloration in others. The effect of the etch possibly depends on the degree of solid solution or on the orientation of the crystal.

The HF vapour etch as used for C_2S in Portland cement can also be used with high alumina cements, with a similar effect, but a more specific etch for this compound is to use 10% $MgSO_4$ at 50° C. This etches only the C_2S.

Tavasci [*5*] described an etch reagent for C_2AS consisting of 2 g NH_4Cl and 2 g $Na_2HPO_4.12H_2O$ in 100 cm^3 distilled water. The specimen is immersed in the boiling solution for from 3 to 5 min. The C_2AS is etched blue or brown and generally shows considerable zoning. Other aluminates are also etched but do not become so strongly coloured.

(d) *Polished thin sections.* This technique makes it possible to study the action of etching reagents and thus to obtain the information given in the previous section. A thin section is polished and etched. Particular crystals can then be identified by thin section methods in transmitted light and the effect on them of etching can be studied in reflected light.

The technique is not difficult, but it is too troublesome for routine use.

A thin section about 20 μ thick is first prepared, but no cover glass is put on. The top surface has now to be polished; this can be done on a felt lap, using the usual polishing agents. The only difficulty is to hold the glass slip on the fast rotating lap. A simple method is to cement a cork on to the back of the glass microscope slide with shellac; the latter melts at a low temperature and does not interfere with the mounting medium. It is usually not possible to run the lap at the normal speed, so that a much longer time than usual is required, but with patience a perfect polished thin section can be made. The normal etch reactions may then be employed, and the thin section can also be observed in transmitted light.

REFERENCES

1. Hartshorne, N. H. and Stuart, A. (1960). "Crystals and the Polarising Microscope. A handbook for chemists and others", 3rd Ed. Arnold, London.
2. Rogers, A. F. and Kerr, P. F. (1942). "Optical Mineralogy", 3rd Ed. McGraw-Hill, New York.
3. Bloss, F. D. (1961). "An Introduction to the Methods of Optical Crystallography". Holt, Rinehart and Winston, New York.
4. Cameron, E. N. (1961). "Ore Microscopy". Wiley, New York.
5. Tavasci, B. (1934). *G. Chim. industr.* **16**, 538.
6. Insley, H. (1936). *J. Res. nat. Bur. Stand.* **17**, 353.
7. Parker, T. W. and Nurse, R. W. (1939). *J. Soc. chem. Ind., Lond.* **58**, 255.

MIDGLEY (H.G.) 28

Reprinted from *Analysis of Calcareous Materials.*

D.Sc. 1967.

THE IDENTIFICATION AND DETERMINATION OF ALITE IN PORTLAND CEMENT CLINKER

By H. G. MIDGLEY,* K. E. FLETCHER*
and A. G. COOPER**

A difficulty arising in the quantitative determination of cement constitution by *X*-ray methods is that the principal mineral present (alite) varies in composition and even to a slight extent in crystal structure. The present paper describes how this difficulty can be minimised.

The alite phase of Portland cement clinker is essentially tricalcium silicate modified by solid solution and occurs in three polymorphic forms, triclinic, monoclinic and trigonal.

So far, experiments have shown that magnesium, aluminium and ferric oxides go into solid solution, and the quantities present influence the polymorphism.

Only the triclinic and monoclinic polymorphs have been synthesised artificially using the above oxides. Alites from Portland cement clinkers have been found to occur in the trigonal form, but the possible composition is not known.

Introduction

In order to establish a procedure for standardising the *X*-ray method of determining the constituents of cement, it has been necessary to investigate the variations in chemical constitution and atomic structure which can occur in the principal constituent, alite, an impure form of tricalcium silicate.

In one of the key investigations into the constitution of Portland cement clinker Tornebohm[1] described four phases which occurred, the most important of which he called 'alite'. Le Chatelier[2] showed that it probably had the formula $3CaO,SiO_2$. There were a number of dissenters to this proposition but by 1929 Guttmann & Gille[3] had separated the phase and concluded that 'alite is tricalcium silicate'.

However, there was considerable evidence that C_3S† could take up other constituents in solid solution. Jeffery[4] summarised the position up to 1952 and concluded that the composition of alite in Portland cement clinker was $C_{54}S_{16}AM$: he also suggested that pure tricalcium silicate occurred in three polymorphic modifications, the trigonal form of highest symmetry occurring metastably

* Building Research Station.
** A.P.C.M. Research Fellow at Building Research Station.

† The usual cement chemists' shorthand notation will be used, C_3S = $3CaO,SiO_2$, C_2S = $2CaO,SiO_2$, F = Fe_2O_3, M = MgO, etc.

28

above 980°, a monoclinic form between 923° and 980°, and a triclinic form below 923°.

It came to be accepted that the phase which occurred in Portland cement was the monoclinic modification and that the term alite was synonymous with the monoclinic C_3S. It would seem more correct to use the term 'alite' for the mineral which occurs in Portland cement clinker irrespective of its structural nature for, as will be shown later, the C_3S phase in Portland cement occurs in all three modifications. In this paper the term 'alite' will refer to the phase in Portland cement, the crystal modification will be indicated by a modifying adjective.

There are thus three problems concerning the phase in Portland cement clinker; firstly the composition, secondly the polymorphic modification and thirdly the quantity. Each of these factors may influence the strength of a cement made from the clinker.

Composition of alite in Portland cement

The composition of the alite phase in Portland cement clinker can be estimated in two ways, by a direct analysis of the phase or by analogy.

For the direct determination, until recently the only possible way was by an analysis of a separated sample. With the advent of the *X*-ray microscanning apparatus an analysis of an alite is probably possible, but so far no analyses have been reported.

Three analyses of alites from Portland cement clinkers have been reported, two by Guttmann & Gille[3] and one by Nurse (see Jeffery[5]). The former separated the alite part from two Portland cement clinkers by centrifuging in a methylene iodide–acetylene tetrabromide mixture. They were unable to make a complete separation: the material was thought to be 86·7 and 93·1% alite for the two cements, the remainder being C_3A and CaO. Guttmann & Gille[3] suggested that Mg^{2+} and Na^{+} substituted for Ca^{2+}, and Ti^{4+} substituted for Si^{4+}. The data they obtained enabled them to show that the alite of Portland cement clinker was essentially C_3S.

Nurse[6] separated an alite from a commercial clinker by dissolving it in molten calcium chloride and allowing the solution to cool slowly so that the alite recrystallised in large enough crystals to be hand sorted. The chemical analysis of the separated alite is given in Table I, column A, ignoring the $CaCl_2$ and recalculating to a total of 100 in B. This is equivalent to $C_{54}S_{16}AM$ if the FeO is added to MgO, and Fe_2O_3 to Al_2O_3. It was on this basis and on crystallographic arguments that Jeffery[4] proposed his composition for 'alite'.

Table I

	% Composition		
	A	B	Molar ratios
CaO	71·6	73·25	1·3062
SiO_2	23·0	23·53	0·3918
Al_2O_3	1·94	1·98	0·0194
Fe_2O_3	0·40	0·41	0·0026
FeO	0·05	0·05	0·0006
MgO	0·85	0·87	0·0216
$CaCl_2$	1·65		

To obtain some idea of the composition of an alite by analogy is difficult, but such a method may be useful if for some purpose a simulated compound is required, as for instance in *X*-ray counter diffraction analysis. With the increasing interest in *X*-ray counter diffractometry methods for obtaining quantitative estimates of the phases in Portland cement clinker, it has become a necessity to produce alites for standardisation which closely resemble the phase actually present in the cement. Jeffery's proposed formula, $C_{54}S_{16}AM$, has been used by a large number of workers, many of whom found it not entirely satisfactory. For instance, von Euw[7] found it to contain about 5% of C_3A. He showed that a progressive simplification of the C_3S *X*-ray diffraction pattern occurred with magnesium oxide and C_3A solid solution and concluded that the addition of 2% C_3A and 1% magnesium oxide to C_3S was the best formulation for a monoclinic C_3S similar to the alite in cement. Locher[8] found that Mg^{2+} replaces Ca^{2+} in the C_3S lattice, giving a progressive simplification of the *X*-ray pattern eventually stabilising the monoclinic form at room temperature. He also showed that Mg^{2+} replaces Ca^{2+} in the presence of C_3A to the same extent, and stated that C_3A had little or no effect on the C_3S pattern. He concluded that C_3S could contain 2% of C_3A and 2·5% of magnesium oxide at 1500°; the solubility of magnesium oxide dropped to 1·5% at 1420°.

Kantro *et al.*[9] reported the preparation of a material of the composition $52C_3S,C_6AM$ which they claimed demonstrated the alite (monoclinic C_3S) *X*-ray diffraction pattern and contained negligible amounts of C_3A.

Midgley & Fletcher[10] have continued this work and found that the monoclinic C_3S phase may be stabilised by magnesium oxide alone, Mg^{2+} replacing Ca^{2+} directly. Aluminium oxide will not

stabilise the monoclinic modification but there is a solid solution between C_3S and a hypothetical C_9A_2.

Magnesium and aluminium oxides together will stabilise C_3S in the monoclinic form. This last solid solution has proved to be the best simulation so far obtained of the monoclinic alite of Portland cement; it may be written as $C_{302}M_{10}S_{101}A_2$, that is a solid solution $(CM)_3S$–C_9A_2.

Some explanation of the difference between this last formulation and the analysis of alite by Nurse given above is required.

Synthetic preparations compounded to $C_{54}S_{16}AM$ and processed by sintering at 1500° always contain about 5% of C_3A according to the diffraction pattern. Midgley & Fletcher[10] suggest that such a preparation will give a monoclinic C_3S of composition $C_{305\cdot7}M_{6\cdot3}S_{101}A_2$, 4·5% of C_3A, and 4·8% of CaO. On the other hand, they have investigated by *X*-ray counter diffraction the remainder of the crystals prepared by Nurse for Jeffery and could detect no other phases except monoclinic C_3S. A chemical analysis on such a small quantity could of course be in error, but since the analysis agreed well with the *X*-ray calculations, it seems more likely that Nurse's crystals were in equilibrium at a different temperature and were able to take up more solid solution.

Polymorphism of alite in Portland cement clinker

Simons[11] demonstrated that by powder *X*-ray diffraction using a cylindrical camera and photographic technique it was possible to distinguish between the various forms of C_3S using the reflections at 1·77Å. Midgley[12] using this method 'examined a series of twenty Portland cement clinkers and found in every case alite (monoclinic alite) and not the pure C_3S phase'.

Von Euw[7] presented microdensitometer traces from C_3S and clinkers. Using a Guinier focusing camera the 2·78Å line was resolved into a quadruplet or triplet from the triclinic phase and a doublet for the alite (? monoclinic) from a Portland cement clinker.

Yamaguchi & Miyabe[13] using a high-temperature *X*-ray counter diffraction apparatus indexed the triplet at 1·77Å as the 040, 620 and $\bar{6}20$ reflections of the triclinic cell; they demonstrated that the triplet became a doublet when the cell was monoclinic and a singlet when the cell was trigonal. This then gave a sensitive method of determining the symmetry of the alites in Portland cement clinkers.

The present authors have analysed the 1·77Å (52° 2θ CuKα) peak in the diffraction patterns from 62 Portland cement clinkers. The

important data which can be measured are, the crystal symmetry, the position of one of the peaks (the 040), and the distance apart of the $\bar{6}20$ and 040 in the monoclinic variety. The latter will indicate how near the alite comes to being trigonal. Measurements were made to an accuracy of $\pm 0{\cdot}02°$ 2θ. Of the 62 cements, one was triclinic; 56 were monoclinic and five trigonal. The position of the 040 (or 220 if trigonal) reflection ranged from 51·66 to 51·74° 2θ CuKα1, the largest number having a value of 51·70° 2θ.

In the monoclinic alites, the difference between 040 and 620 ranged from 0·09 to 0·18° 2θ CuKα1, the largest number having a difference of 0·15° 2θ.

For comparison the data for the synthetic alites of Midgley & Fletcher[10] are: $C_{302}M_{10}S_{101}A_2$, 040 at 51·76° 2θ, difference 0·17° 2θ, $C_{306}M_6S_{101}A_2$, 040 at 51·72° 2θ, difference 0·14° 2θ. This shows that the shape of the alite diffraction trace is matched reasonably by the compositions proposed. It is to be expected that other substituting ions than those considered here will affect the shape of the peak to some extent.

All the cements examined were normal in their behaviour.

Quantitative estimation of alite in Portland cement clinker

The most commonly used method of estimating the alite is to recast an oxide analysis into standard minerals, as suggested by Bogue.[14] The standard minerals are C_3S, C_2S, C_3A and C_4AF. As has been shown earlier in this paper, the alite in Portland cement clinkers is not pure C_3S but is modified by magnesium oxide and aluminium oxide solid solution. These solid solutions could affect the calculation of alite content, and considerably affect the C_3A estimate. Direct physical estimations are required; the most used in the past has been microscopy, but *X*-ray diffraction methods have come into use more recently.

Midgley *et al.*[15] gave the method in use at the Building Research Station (B.R.S.) in 1959, but since that time there have been considerable changes in method. That in use in 1962 is based on standardisation with mixes containing synthetic preparations of the main components of Portland cement clinkers and a fixed proportion of silicon to act as internal standard. An examination of the superimposed *X*-ray diffraction patterns of the four main phases shows that for each component there are a few reflections which suffer little or no interference from the other components and whose intensity can be used for quantitative estimation. Such reflections which are currently used at B.R.S. are alite 29·4°, 30·1°; β-C_2S 31·0°; C_3A 33·2°; ferrite 33–34°; silicon 28·4° 2θ CuKα. The in-

tegrated intensity (peak area) is measured using a planimeter and expressed as a fraction of the integrated intensity due to a standard silicon peak. The calibration graph is then I_x/I_{si}, plotted against weight percentage of x. The β-C_2S reflection at 31·0° 2θ CuKα is extremely weak, but it is the only one which does not suffer interference, so attempts have been made to use various combinations of interfering and non-interfering peaks to obtain a better C_2S estimation. The results obtained have been disappointing, but it seems inevitable that such a method using all measurable reflections and a computer to evaluate the results must eventually be used.

The ferrite phase is not necessarily C_4AF but a member of a solid solution series ranging in composition from C_2F to C_6A_2F. The lattice constants vary continuously between the end members, thus the exact measurement of the position of any particular reflection can be used to determine the chemical composition of the ferrite concerned. The reflections used are the 141 varying between 33·42 and 34·01° and the 002 varying between 32·97 and 33·66° 2θ CuKα. For quantitative determination, the combined intensity of the 141 and 002 reflections are measured. It is found that the slope of the calibration graph I_x/aI_{si} against wt.-% of x varies continuously between the end members, thus the quantitative determination is completed after determining the composition of the ferrite phase. The relationship between the intensities of the 002 and 141 reflections has been determined for different ferrite compositions. The majority of clinkers examined fall within the range C_4AF–C_6AF_2 and for this range the intensity due to the 002 reflection is taken to be 0·5 that of the 141 reflection. These data are used in interpreting diffraction patterns in which the 002 reflection overlaps the C_3A reflection at 33·2° 2θ. It is unfortunate that this normally occurs with a clinker of very low C_3A content. In clinkers where the ferrite diffraction pattern is diffuse there is difficulty in determining the composition of the ferrite, that is the position of the 141, 002 reflections. In this case, the silicate phases can be partially or completely removed by chemical dissolution using a modified version of the Fratini & Turriziani extraction method.[15] The residual ferrite and C_3A phases are then re-examined and the diffraction pattern due to the ferrite phase is much more clearly defined. Since there is also a considerable amorphous residue, this method cannot be used quantitatively. The strongest reflection due to magnesium oxide occurs at 42·9° 2θ CuKα and if more than about 2% of magnesium oxide is present this will be detected. This is such an unusual occurrence that no calibration has been attempted for cement clinkers.

The strongest reflection due to calcium oxide occurs at 37·4° 2θ and completely overlaps a weak β-C_2S reflection. If more than about 3% of calcium oxide is present this will be detected, but since most clinkers have less than 3% of calcium oxide this is best determined by one of the extraction methods.

Samples are prepared by pregrinding in an agate mortar to pass a 300-mesh B.S. sieve and then incorporating silicon, preground to pass a 300-mesh B.S. sieve, in the ratio 12 : 1. About 2 g of the mixture are then placed in a 100-ml polythene bottle together with six fused silica rods of ½ in. diameter and about 5 ml of isopropyl alcohol to act as a grinding aid. The bottle is then placed in the ½-litre pot of a vibratory mill. Samples are reduced from 50 μ to less than 5 μ by about 4 h grinding. The particle size is then checked under the microscope to ensure adequate grinding. The alcohol is evaporated away, the sample is sieved through a 300-mesh B.S. sieve to break up coarse aggregates and is then ready for diffractometry. In a series of experiments to avoid preferred orientation the sample was loosely packed into the holder using the method described by Copeland & Bragg.[16]

In a further series, dense packing was used and no evidence of preferred orientation could be detected so this method is now preferred. It gives about the same peak to background ratio as loose packing but slightly better resolution.

A considerable amount of the background radiation occurring with Portland cement clinkers is due to FeKα fluorescence from the sample. This is particularly so in sulphate-resisting clinkers which may have a relatively high ferrite content.

A Geiger counter is less sensitive to lower energy wavelengths and gives some discrimination against FeKα fluorescence. However, by using a proportional counter and pulse height discrimination, complete discrimination against FeKα radiation can be made. The proportional counter gives a pulse whose amplitude is proportional to the energy of the exciting wavelength. A pulse height analyser may be set to pass all pulses greater than a given amplitude or only those pulses lying within a specified amplitude range (channel width or 'window'). In practice an overlap occurs between the CuKα and FeKα radiations and a careful compromise must be made in which most of the FeKα radiation is eliminated without too great a sacrifice of CuKα radiation. Comparative results on a sulphate-resisting clinker are given in Table II.

The increased peak to background ratio obtained by pulse height discrimination has little value of itself, but the accompanying increase in resolution is of considerable value in the interpretation

Table II

Comparison of sample preparation and counting techniques on a sulphate-resisting clinker

Method of packing sample	Detector	*P* Counts per sec at a peak of 34·4° 2θ CuKα reflection due to C_3S+C_2S	*B* Background counts per sec at 35·5° 2θ CuKα	*P*/*B*
loose	Geiger 1550V	144	38	3·8
dense	Geiger 1550V	160	44	3·6
dense	proportional 1650V	183	59	3·1
dense	proportional 1650V +pulse height discrimination	114	16	7·1

of the traces obtained from Portland cement clinker. An *X*-ray diffraction trace of the regions 53–50° 2θ CuKα and 37–25° 2θ CuKα is made using a Philips diffractometer and CuKα radiation. The distance from sample to source and sample to resolving slit is 172 mm. The scatter slits are 1° and the resolving slit is 0·1 mm. Scanning speed is $\frac{1}{8}$° 2θ/min. Full scale chart reading is adjusted to 160 counts per sec., the counts being averaged over 8 sec. A chart speed of 200 mm/h was used for the earlier work but with the improvement in resolution obtained by pulse height discrimination a chart speed of 400 mm/h is more suitable. The reflections at present used for quantitative estimation fall in the region 37–25° 2θ CuKα. The alite reflection at about 51·8° 2θ is used to determine which polymorphic modification of alite is occurring in the sample. The assumption is made that the phase to be estimated corresponds with the synthetic preparation used for standardisation although, as has been shown, this may lead to error in some cases.

Smolczyk[17] has evaluated the possible errors arising from this assumption. If, however, the alite phase in the sample is in the monoclinic form, its quantitative estimation should be reasonably accurate.

We have shown that a weak reflection due to the alite phase occurs at 33·2° 2θ CuKα and is superimposed on the strongest peak of C_3A. It is equivalent to about 1·5% of C_3A in a 100% alite preparation. A more accurate estimate of C_3A can now be made by allowing for this alite reflection. It does, however, impose a lower detection limit of 0·5% for C_3A because of changes in intensity and

peak position with slight variations of alite composition. The difficulty in estimating β-C_2S by multiple peak techniques is probably due to lack of exact correspondence between the synthetic preparation and the form occurring in Portland cement clinkers.

Conclusions

It can be shown that the alite phase of Portland cement clinkers is essentially tricalcium silicate modified by solid solution and occurring in three polymorphic modifications.

So far experiments have shown that magnesium, aluminium and ferric oxides are probably in solid solution, in quantities which may influence the polymorphism. All three polymorphs, trigonal, monoclinic and triclinic, have been identified in commercial Portland cement clinkers, but the monoclinic form is most frequently found. Using the suggested solid solution containing aluminium and magnesium oxide, as a standardising substance, the accuracy of *X*-ray determinations is improved.

References

[1] Tornebohm, A. E., *Tonindustr. Ztg*, 1897, p. 1148
[2] Le Chatelier, H., *C.R. Acad. Sci. Paris*, 1882, **94**, 13
[3] Guttmann, A., & Gille, F., *Zement*, 1931, **20**, 144
[4] Jeffery, J. W., 'The tricalcium silicate phase', Symp. Chem. of Cement (London), 1952, p. 30
[5] Nurse, R. W., in Jeffery, reference 4
[6] Nurse, R. W., *J. sci. Instrum.*, 1952, **26**, 102
[7] Von Euw, M., *Silicates industr.*, 1958, **23**, 543 (in French); P.C.A. Foreign Literature Study No. 326 (in English)
[8] Locher, F. W., Symp. Chem. of Cement (Washington), 1960, p. 99
[9] Kantro, D. L., Copeland, L. E., & Brunauer, S., as reference 8, p. 75
[10] Midgley, H. G., & Fletcher, K. E., *Trans. Brit. ceram. Soc.*, 1963, **62**, 917
[11] Simons, H., in Jeffery, reference 4
[12] Midgley, H. G., in Jeffery, reference 4
[13] Yamaguchi, G., & Miyabe, H., *J. Amer. ceram. Soc.*, 1959, **43**, 219
[14] Bogue, R. H., *Industr. Engng Chem. Analyt. Edn*, 1929, **1**, 192
[15] Midgley, H. G., Rosaman, D., & Fletcher, K. E., as reference 8, p. 69
[16] Copeland, L. E., & Bragg, R. H., *Bull. Amer. Soc. Test. Mat.*, 1958, No. 228
[17] Smolczyk, H.-G., *Zement-Kalk-Gips*, 1961, **12**, 558

Discussion

Dr. H.-G. Smolczyk.—I should like to show the regions between 53° and 51° 2θ in the *X*-ray diagrams of five C_3S samples with different additives (see Fig. 1*), while the exact values of 2θ, the width at $\frac{1}{3}$ of peak height ($h/3$ width), the peak area and the peak height (h) are given in Table I. The intensities are corrected for small amounts of free calcium oxide in the samples.

In the examination of several cement clinkers the largest value

* From *Zement-Kalk-Gips*, 1961, **12**, 558

of 2θ was found to be 51·87° ($h/3$ width 0·47°), and the smallest $h/3$ width 0·29° (2θ 51·70°). I think that in addition to the oxides of aluminium, magnesium or iron there must be other parameters which should be taken into account for an exact quantitative X-ray analysis of this alite peak. In addition, consideration of the polymorphic form of alite could possibly lead to more accurate results.

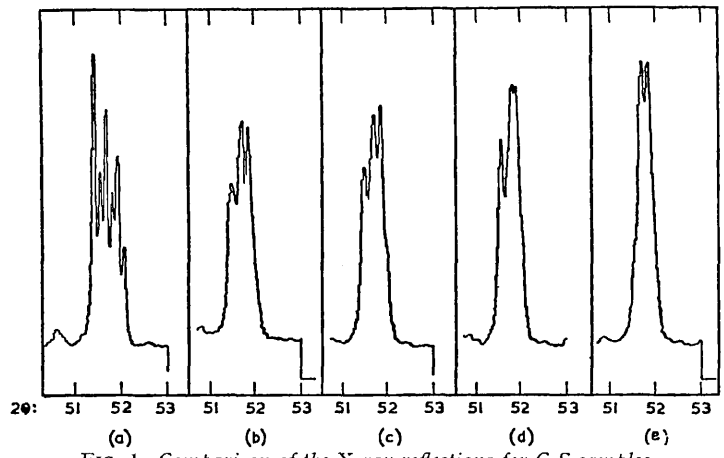

FIG. 1. *Comparison of the X-ray reflections for C_3S samples at about 0·77 Å*

(a) pure C_3S
(b) C_3S+1%Fe_2O_3
(c) C_3S+0·8%Al_2O_3
(d) C_3S+1%MgO
(e) C_3S+1%MgO+0·8%Al_2O_3

Table I

Measurement of the X-ray reflections at about 1·77 Å in various C_3S samples

Material	2θ CuKα	h/3, width	Peak area	Peak height, h
C_3S, pure	51·68°	0·73°	100	(100)
C_3S+1% Fe_2O_3	51·71°	0·61°	98	(95)
C_3S+0·8% Al_2O_3	51·71°	0·60°	97	(100)
C_3S+1% MgO	51·79°	0·57°	98	(110)
C_3S+1% MgO+0·8% Al_2O_3	51·78°	0·46°	92	(120)

The authors: We would like to thank Dr. Smolczyk for his contribution on the X-ray examination of alite peaks. The problem of characterising alite in Portland cement clinkers is by no means fully understood, and we would like to see as many people as possible tackle this problem using as many techniques as possible.

RESEARCH SERIES 55

Building Research

CURRENT PAPERS

DATA ON THE BINARY SYSTEM $3CaO.Al_2O_3$-$Na_2O.8CaO.3Al_2O_3$ WITHIN THE SYSTEM CaO-Al_2O_3-Na_2O

By K. E. Fletcher, H. G. Midgley, and A. E. Moore

Reprinted from:
Magazine of Concrete Research, 1965, vol. 17 (December), pp. 171-6

BUILDING RESEARCH STATION
MINISTRY OF TECHNOLOGY

Building Research CURRENT PAPERS are produced in four series

CONSTRUCTION SERIES
DESIGN SERIES
ENGINEERING SERIES
RESEARCH SERIES

Details of Current Papers issued are given, with summaries, in the Station's QUARTERLY LIST OF PUBLICATIONS, which may be obtained regularly on application to:

The Director,
Building Research Station,
Garston, Watford, Herts.

Extra copies of this paper are available; a charge may be made for supplies in quantity.

UDC 666.94.014 : 541.123

Data on the binary system $3CaO.Al_2O_3$-$Na_2O.8CaO.3Al_2O_3$ within the system CaO-Al_2O_3-Na_2O*

by K. E. Fletcher, H. G. Midgley and A. E. Moore†

MINISTRY OF TECHNOLOGY : BUILDING RESEARCH STATION

SUMMARY

Conwicke and Day showed that partial solid solution occurs in the system C_3A-NC_8A_3 at temperatures below the liquidus. Their results indicated a marked similarity between the X-ray powder diffraction data for a preparation containing more than 3·0% Na_2O and the data given by Moore for a new phase in Portland cements. The present work was almost complete when Conwicke and Day's paper was published. It generally confirms their results but gives more information on the solid solution. At the limit of solid solution at 1,350°C the sodium calcium aluminate which is formed has the composition 91·0 mol % C_3A, 9·0 mol % N_3A and has been indexed on an orthorhombic unit cell with $a = 15{\cdot}314$, $b = 15{\cdot}394$, $c = 15{\cdot}137$ Å.

Introduction

Tricalcium aluminate (C_3A)‡ is an important phase in Portland cements and its presence can cause the cement to be susceptible to sulphate attack. Solid solution of other components in C_3A can cause some variation of the form in which the phase occurs in Portland cements. The study of these changes is of interest since the hydration reactions may be affected. Moreover, since the presence of these forms is mainly detected by a slight change in the X-ray diffraction pattern, quantitative diffractometry could give very inaccurate results if it were wrongly assumed that the phase present was the normal C_3A.

It has been realized since the investigations of Brownmiller and Bogue[1] in 1932 that NC_8A_3 is a phase similar to C_3A which could occur in Portland cements. Moore in 1963 reported the existence of a new constituent, similar to C_3A, in Portland cements and it was this observation which prompted the present investigation of the system C_3A-NC_8A_3.

Brownmiller and Bogue stated that, in spite of the similarity of structure and habit between C_3A and NC_8A_3, no evidence of solid solution between them was found at the liquidus. Bogue[2] (1938) reported that, with slow cooling or prolonged heating at temperatures below the liquidus, microscope investigations indicated the formation of some solid solution between the phases. Greene and Bogue[3] (1946) investigated the system Na_2O-CaO-Al_2O_3-SiO_2. They found that at the liquidus C_3A, NC_8A_3, liquid, C_3S and C_2S could exist together in stable equilibrium but that in samples heated at 1,425°C there was evidence that a reaction had taken place to produce a phase or phases that were neither pure C_3A nor pure NC_8A_3. This was concluded on the basis of necessarily limited X-ray and microscope data. Suzukawa[4] (1956) agreed with the X-ray data of Greene and Bogue but argued that their X-ray data did not indicate solid solution, maintaining that solid solution would be indicated by line shifts rather than by the changes in multiplicity of lines observed by Greene and Bogue.

Moore[5] (1963) produced evidence for a new phase occurring in Portland cements, from material obtained as a residue after selective dissolution of the silicate phases. She concluded that the new phase was a modified C_3A in which additional oxides, Na_2O, K_2O, MgO or even Fe_2O_3 or traces of TiO_2 had lowered the symmetry from cubic to orthorhombic. She showed that there was a fairly good match between the pattern attributable to the new phase and the data given for NC_8A_3 by Brownmiller and Bogue, or the data given for orthorhombic, pseudo-cubic, perovskite.

Conwicke and Day[6] (1964) investigated the system C_3A-NC_8A_3 at 1,250°C, by reacting together C_3A, $C_{12}A_7$ and Na_2CO_3. They found that up to 2·25% of

†Miss Moore is employed in the Research and Development Division of the Cement and Concrete Association.

‡ The cement chemist's shorthand is used: C=CaO; A=Al_2O_3; N=Na_2O; S=SiO_2; except for the simple compound.

Na_2O in C_3A produced no change in the C_3A X-ray diffraction pattern. Between 2·25 and 4·20% Na_2O, there was a mixture of the cubic phase and a phase where the major C_3A reflections had doubled. With more than 4·20% Na_2O, this second phase, which Conwicke and Day called " the split peak phase ", occurred alone. The X-ray diffraction pattern of this phase was similar to the pattern reported by Moore for the new phase in Portland cements. They concluded that in a Portland cement containing 10% C_3A a soda content of only 0·3% would be sufficient to convert the C_3A to a phase with a diffraction pattern similar to that of NC_8A_3, or the new phase of Moore. They were unable to prepare NC_8A_3 as a simple phase (CaO was always found) and thought that the join C_3A-NC_8A_3 as given in the phase diagram Na_2O-CaO-Al_2O_3 could be incorrect. The present investigation was almost complete when the data of Conwicke and Day were published. Although for the present investigation the samples were prepared at 1,350°C, the results confirm many of their data; the region where mixed phases occur is found to be between 2·1 and 4·2% Na_2O in the sodium calcium aluminate, which is in substantial agreement with the values of 2·25 and 4·20% Na_2O found by Conwicke and Day, and both investigations agree that the limiting composition contains less Na_2O than NC_8A_3. The X-ray diffraction pattern produced when there is more than 4·2% Na_2O in the sodium calcium aluminate phase agrees well with Moore's data but the agreement is less when mixtures of the essentially unchanged C_3A phase and the phase showing multiple reflections are present. It seems unlikely that the phase described by Moore could be produced by less than 4·2% Na_2O if solid solution of Na_2O alone were responsible for the modified phase.

The conflicting views of Brownmiller and Bogue, and Suzukawa, are reconciled by the results of the present investigation. There is a change in crystal structure (which results in a change in multiplicity of lines) between C_3A and the composition approximating to NC_8A_3. Each structure also shows slight variation due to solid solution, indicated by line shifts.

Brownmiller and Bogue were not able to prepare a single phase of composition NC_8A_3 although they thought that this was the probable composition. Their choice was influenced by the fact that it implied the replacement of one Ca^{2+} ion by two Na^{1+} ions in one unit cell of C_3A (C_9A_3). The present data confirm that Na_2O replaces CaO; but the composition can vary. This removes the necessity to explain the compositions in terms of simple whole-number ionic replacements in the real unit cell of C_3A, although changes in the structure produced by the substitution can still be conveniently described in terms of changes in an empirical unit cell. The limiting solid solution at 1,350°C was 91·0 mol % C_3A, 9·0 mol % N_3A, rather than 88·9 mol % C_3A, 11·1 mol % N_3A as implied by NC_8A_3.

Experimental work

Preparations were made along the join C_3A-Na_2O in the system CaO-Al_2O_3-Na_2O. C_3A was prepared in the usual manner by repeated heating and grinding of the correct molecular proportions of suitably pure $CaCO_3$ and Al_2O_3 at 1,350°C. A weighed quantity of Analar Na_2CO_3 was mixed with the C_3A and heated in an open platinum boat at 1,000°C for one hour. The sample was remixed and then heated in a sealed platinum envelope for two hours at 1,350°C, then removed and air-quenched. Preliminary experiments indicated that further heatings at 1,350°C produced no further change in the X-ray diffraction pattern and that the sample was effectively at equilibrium. The final sodium content of the samples was determined by chemical analysis: for Na_2O contents of less than about 3% a flame photometer was used; Na_2O contents greater than about 3% were estimated gravimetrically by precipitation with zinc uranyl acetate.

Free CaO that occurred in all the preparations was determined by the Franke[7] method. A Geoscan electron-probe X-ray microanalyser was used to determine the composition of the sodium calcium aluminate occurring in a preparation containing 5·12% Na_2O. This checked the validity of conclusions based on the free CaO content of the preparations. The electron beam was generated at 15 kV with a beam current of 47 μA. A constant specimen current of about 250 millimicroamperes was maintained during single measurements and probe conditions were unchanged for successive comparisons between a standard sample of C_3A and the sodium calcium aluminate. Calcium was estimated by measuring the peak intensity at about 60° 18′ using a quartz analysing crystal. Aluminium was estimated by measuring the peak intensity at about 49° 29′ using a mica analysing crystal. Corrections for fluorescence and absorption are negligible because of the similarity of matrices between the standard and unknown samples.

The X-ray diffraction patterns were determined by means of a Philips PW 1010 diffractometer and a Guinier focusing camera, with CuKα radiation. With samples containing more than 5·9% Na_2O no further change occurred in the X-ray diffraction pattern due to the main phase. For a sample containing 7·1% Na_2O, the position of reflections in its X-ray diffraction pattern was measured with a variety of internal standards—silicon, silver and lithium fluoride. Some very weak reflections detected by the Guinier camera were not discernible in the X-ray diffraction trace; for completeness these are included in Table 1 with an intensity of less than one. This pattern can be indexed on the orthorhombic system with lattice dimensions $a = 15{\cdot}314$, $b = 15{\cdot}394$, $c = 15{\cdot}137$ Å. An Elliot 803 computer was used for this calculation.

For the other samples the positions of the reflections at about 1·56 and 1·92 Å were measured after about

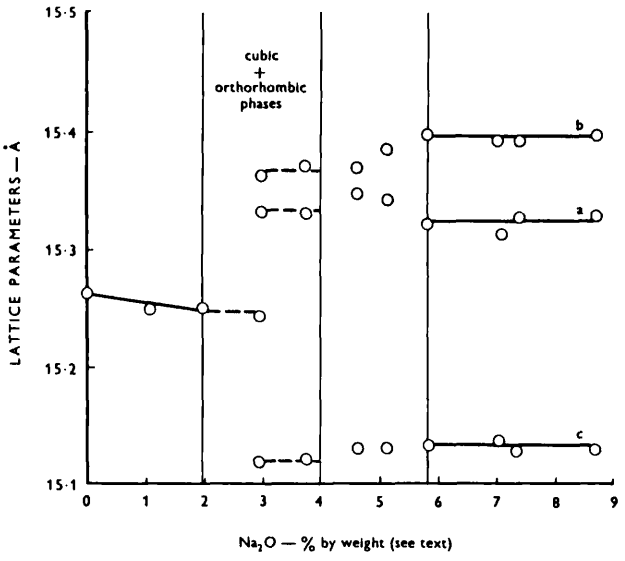

Figure 1: Variation of lattice parameters with sodium content.

20% lithium fluoride had been added to serve as an internal standard; the reflections at 1·424 and 2·013 Å were used to bracket and correct the observed values. Changes in the lattice dimensions were calculated using the data from these two groups of reflections. Samples containing 3·0% Na_2O and 3·7% Na_2O were found to contain mixtures of orthorhombic and cubic phases (Figures 1 and 2). A semi-quantitative estimate of the amounts of cubic and orthorhombic phases present was attempted by measuring the intensities of the 008 and 844 reflections for the cubic phase and the 008 and 448 reflections for the orthorhombic phase (Figure 2). No fine grinding was attempted, since the samples were hygroscopic and no internal standard was added. Intensities were measured on diffraction traces over a band 0·05° two theta wide symmetrical about the peak. This is better than measuring the peak intensity and lessens interference from neighbouring reflections. The intensity measurements were reasonably reproducible. The samples containing 2·0 and 5·12% Na_2O were taken as standards for the quantitative determination since these were near the expected compositions for the mixed phases. Allowance was made for their free CaO content.

Results

The amount of free CaO displaced by Na_2O is shown in Figure 3*. The amount of CaO expected if the displacement is a simple replacement of one mol CaO by one mol Na_2O is also shown. The slight discrepancy between the two plots is consistent with a systematic

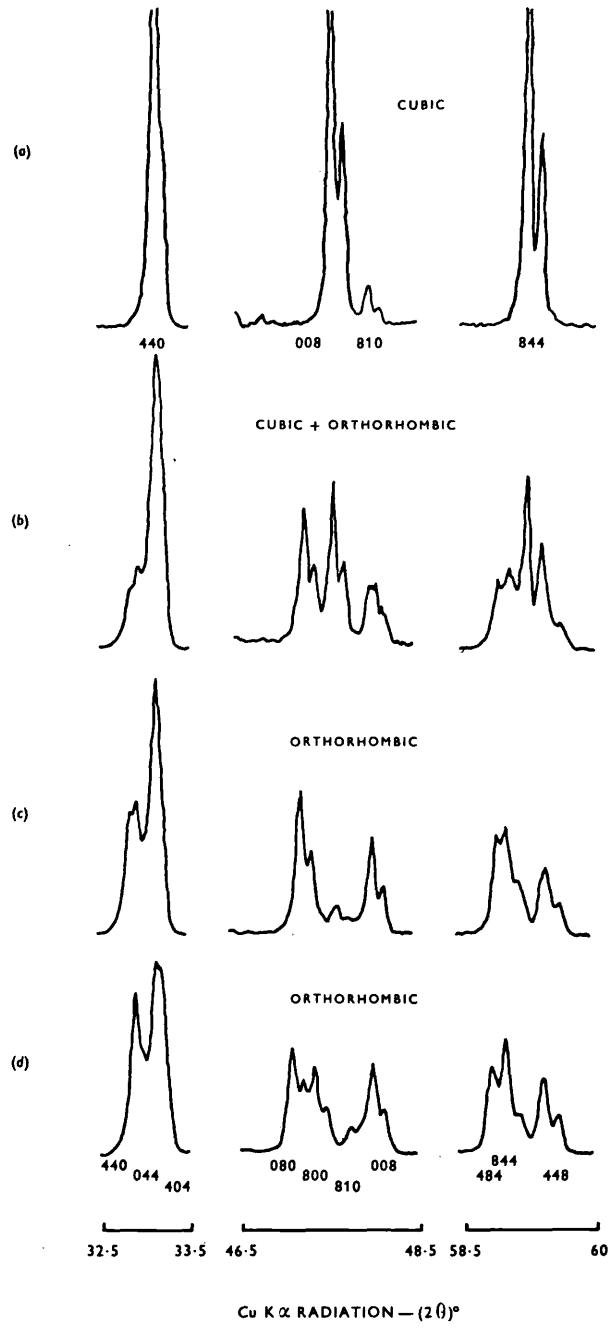

Figure 2: X-ray diffraction traces for samples of C_3A containing Na_2O.

error in the analytical methods. Beyond 5·9% Na_2O the amount of free CaO increases sharply, indicating the limit of solid solution. From the phase diagram NA would be expected to occur, and the rather diffuse reflections at 2·56, 2·61 and 2·94 Å confirmed this. The electron probe microanalysis of the sodium calcium aluminate in a preparation containing 5·12% Na_2O gave 57·07% CaO with a 99% probability range of ±0·66%, and 36·79% Al_2O_3 with a 99% probability range of ±0·84%. Both results are the mean of about 15 separate determinations. If Na_2O replaced CaO, a composition of 57·10% CaO, 37·55% Al_2O_3 would be

* It should be borne in mind that, as these materials were prepared by mixing C_3A and Na_2O (effectively) the percentage of Na_2O found and plotted in Figures 1 and 3 is not the same as the percentage contained by the sodium calcium aluminate; this figure can be deduced by subtracting the free lime figure (and any sodium aluminate) and recalculating to a base of 100.

TABLE 1

hkl	B.R.S. Orthorhombic sodium calcium aluminate of composition 91 mol % C_3A, 9 mol % N_3A			NC_8A_3 Brownmiller and Bogue (1932)		NC_8A_3 Suzukawa (1956)		New C_3A phase* Moore (1963)		3·0% Na_2O ($C_3A + Na_2O$) Cubic phase containing 2·1% Na_2O and orthorhombic phase containing 4·2% Na_2O		C_3A National Bureau of Standards (1955)		
	d calculated	*d* observed	$\frac{I}{I_{100}}$	*d* observed	$\frac{I}{I_{100}}$	*d* observed	$\frac{I}{I_{100}}$	*d* observed	$\frac{I}{I_{100}}$	*d* observed	$\frac{I}{I_{100}}$	*d* observed	$\frac{I}{I_{100}}$	*hkl*
200	7·66	7·66	1					7·62	3			8·82	1	111
								7·31	4					
120	6·89	6·89	1					6·81	3	6·92	3	6·83	5	210
												6·23	3	211
022	5·40	5·39	3							5·44	3	5·40	2	220
221	5·11	5·11	9					5·12	4	5·14	5	5·09	5	221
										4·60	1	4·604	4	113
222	4·41	4·41	5					4·42	6	4·41	2			
										4·24	4	4·235	10	023
023	4·226	4·221	9			4·19	W	4·217	11	4·22	5			
								4·062	3	4·08	7	4·080	16	321
040	3·850	3·845	<1					3·850	3					
												3·816	1	004
322	3·710	3·702	3			3·69	WW	3·694	3	3·70	2	3·705	2	223
								3·652	3·5					
										3·50	1	3·501	2	331
042	3·432	3·430	7					3·427	8	3·43	5			
024	3·399	3·400	4			3·41	W			3·39	1			
142	3·349	3·347	7	3·37	W	3·34	W	3·348	14	3·35	3			
										3·33	3	3·332	5	421
												3·252	1	332
												3·120	<1	422
403	3·051	3·050	10	3·03	W	3·05	W	3·055	7	3·05	6	3·052	3	430
												2·993	3	431
314	2·985	2·980	2			2·984	WW			2·99	2			
511	2·950	2·949	<1					2·900	3					
250	2·858	2·864	<1											
										2·833	2	2·834	6	432
205	2·817	2·811	6					2·813	5	2·815	3			
										2·785	5	2·787	14	521
125	2·773	2·775	3			2·760	WW	2·773	6·5					
440	2·717	2·718	80					2·717	47	2·714	29			
044	2·701	2·699	100									2·700	100	440
404	2·694	2·695		2·68	SS	2·691	SS	2·695	100	2·696	100			
225	2·646	2·648	1					2·647	18					
035	2·610	2·612	3	2·60	W									
153	2·593	2·589	1											
								2·576	2			2·581	3	531
060	2·568	2·569	3											
424	2·542	2·542	1											
610	2·520	2·521	3	2·53	W									
												2·512	<1	610
												2·477	1	611
062	2·432	2·429	3					2·428	4	2·428	2			
602	2·420	2·420	<1			2·419	WW							
				2·41	W					2·410	8	2·413	7	620
261	2·404	2·408	2											
206	2·398	2·398	3					2·398	2					
										2·384	4	2·384	6	621
405	2·376	2·376	5	2·37	W	2·370	WW	2·376	4	2·378	4			
										2·356	2	2·355	2	541
262	2·318	2·320	3											
622	2·309	2·311	<1					2·310	3	2·311	2			
360	2·294	2·292	2											
								2·282	3					
245	2·274	2·273	7			2·66	W	2·270	3	2·271	3	2·277	3	630
444	2·203	2·208	20	2·20	S	2·199	S	2·205	12	2·203	13	2·204	11	444
263	2·191	2·190	1											
170	2·178	2·180	1									2·181	2	632
												2·138	1	711
117	2·121	2·119	2											
046	2·110	2·109	3	2·10	W	2·103	WW	2·107	2			2·097	3	641
633	2·082	2·083	1					2·081	1			2·078	2	721
264	2·046	2·046	3					2·050	4(d)					
										2·037	3	2·040	5	642
426	2·032	2·033	5	2·03	W	2·032	W	2·032	3	2·031	2			
544	2·024	2·025	4											
370	2·019	2·020	2									2·021	1	722
										1·984	2	1·988	4	731
463	1·964	1·964	4					1·960	3	1·963	2			
372	1·951	1·951	1			1·955	W			1·952	2	1·955	4	650
												1·940	1	732
080	1·924	1·924	20											
								1·920	24	1·919	16			
800	1·914	1·914	20	1·915	S	1·916	SS							
												1·908	36	008
810	1·900	1·898	6					1·905	7	1·905	19			
008	1·892	1·891	20	1·888	S	1·885	S	1·890	13	1·890	8	1·893	4	810
												1·865	1	773

TABLE 1 *continued*

hkl	B.R.S. Orthorhombic sodium calcium aluminate of composition 91 mol % C_3A, 9 mol % N_3A			NC_8A_3 Brownmiller and Bogue (1932)		NC_8A_3 Suzukawa (1956)		New C_3A phase* M'oore (1963)		3·0% Na_2O (C_3A+Na_2O) Cubic phase containing 2·1% Na_2O and orthorhombic phase containing 4·2% Na_2O		C_3A National Bureau of Standards (1955)		
	d calculated	*d* observed	$\frac{I}{I_{100}}$	*d* observed	$\frac{I}{I_{100}}$	*d* observed	$\frac{I}{I_{100}}$	*d* observed	$\frac{I}{I_{100}}$	*d* observed	$\frac{I}{I_{100}}$	*d* observed	$\frac{I}{I_{100}}$	*hkl*
446	1·848	1·847	2	1·840	WW									
208	1·837	1·836	1			1·832	WW			1·836	2	1·838	3	821
427	1·829	1·829	1					1·828	4	1·823	2	1·824	3	653
660	1·809	1·810	1											
083	1·798	1·798	2	1·797	WW	1·795	WW					1·799	1	822
381	1·788	1·788	1									1·785	1	830
												1·763	1	751
662	1·760	1·759	1											
283	1·750	1·750	1					1·750	2					
												1·740	2	832
823	1·744	1·744	1	1·746	W	1·742	WW							
												1·727	2	752
663	1·703	1·704	2							1·700	5	1·706	1	840
												1·695	2	841
901	1·691	1·690	2	1·692	Wb									
												1·675	1	911
												1·646	2	921
617	1·641	1·640	1											
483	1·627W	1·627	3	1·628	W							1·627	2	664
922	1·623	1·623	4							1·623	2			
										1·616	2	1·618	1	922
												1·610	1	851
												1·583	1	802
												1·574	1	932
484	1·566	1·566	20							1·566	8			
844	1·562	1·562	24	1·558	SS	1·562	SS	1·564	18	1·561	9			
										1·556	20	1·558	27	844
448	1·552	1·553	18			1·547	S	1·550	11	1·552	13			
608	1·520	1·520	1			1·518	WW					1·519	2	10.1.0
10.2.1	1·495	1·495	1									1·497	2	10.2.0
845	1·491	1·491	1	1·492	W	1·489	W					1·490	2	10.2.1
												1·476	2	951
666	1·470	1·470	1											
												1·462	3	10.3.0
												1·455	2	10.3.1
												1·436	1	10.3.2
												1·429	1	8.7.1
												1·411	1	10.4.1
4.0.10	1·408	1·408	1									1·405	2	10.3.3
873	1·388	1·388	1									1·390	1	962
11.0.2	1·369	1·369	1											
												1·3649	2	10.5.0
880	1·358	1·357	5			1·354	M	1·358	4	1·358	2	1·3596	2	11.2.1
										1·355	2			
088	1·349	1·349	6					1·347	8			1·3491	9	880
808	1·345	1·345	7	1·347	M	1·344	S			1·347	10			
												1·3336	1	11.3.1
												1·3190	1	11.3.2
												1·3087	1	10.6.0
												1·2948	1	11.3.3
11.2.4	1·288	1·288	1											
965	1·284	1·284	1									1·2852	1	11.4.2
												1·2676	2	12.1.0
10.0.7	1·250	1·250	1									1·2506	1	12.2.1
0.2.12	1·245	1·244	1	1·235	W							1·2461	1	11.5.2
												1·2379	2	12.2.2
4.12.0	1·216	1·215	3					1·214	4					
												plus three lines to 1·2064		
0.6.11	1·212	1·212	3	1·210	M	1·212	M			1·213	3			
										1·205	6			
10.8.0	1·198	1·198	3			1·196	W			1·202	3			
888	1·102	1·102	3	1·103	W					1·100	3			
				1·101	W	1·101	W							
988	1·057	1·057	1	1·055	W									
8.12.4	1·026	1·026	3											
10.11.2	1·024	1·024	4			1·023	M							
11.9.5	1·017	1·017	3	1·019	Mb	1·014	W			1·018	5			

Indexed on an orthorhombic unit cell: $a = 15{\cdot}3144$ Å; $b = 15{\cdot}3936$ Å; $c = 15{\cdot}1368$ Å.

*This is the residue from selective dissolution of the silicates and could contain the ferrite phase and other phases.

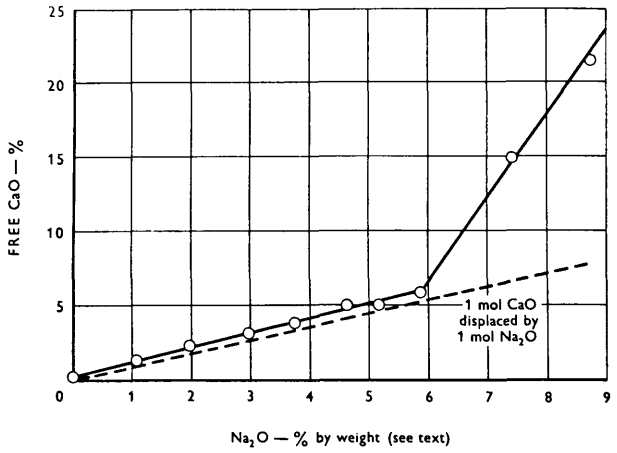

Figure 3: Free CaO displaced by Na_2O.

expected, which agrees with the probe microanalysis.

In view of the large size of the sodium atom and the ability of perovskite-like structures to tolerate oxygen defect, it seemed possible that Na_2O could displace 2CaO. This would lead to a composition of 54·92% CaO and 39·46% Al_2O_3 and a doubling of the slope of the line showing the theoretical displacement of free CaO in Figure 3. Both X-ray microprobe analysis and free-lime determination give results indicating that Na_2O replaces CaO. There is thus no evidence, in either the cubic solid-solution range or the orthorhombic for the replacement of 2CaO by Na_2O so this postulate should clearly be discarded.

In Figure 1 the change in lattice parameter is plotted against the percentage of Na_2O present in the sample. Semi-quantitative determination of the phases present in the samples containing 3·0% Na_2O and 3·75% Na_2O showed that the former contained about 50% cubic, 50% orthorhombic and the latter contained about 10% cubic, 90% orthorhombic. These results were used as a guide for determining the limits between which mixtures of the phases would be expected to occur. The limits are shown in Figure 1 as occurring between 2·0% and 4·0% of Na_2O in the sample.

The lattice dimension of C_3A appears to contract slightly until 2% Na_2O is reached. Mixtures of cubic and orthorhombic phases occur between 2·0 and 4·0% Na_2O. The orthorhombic lattice dimensions again change slightly between 4 and 5·9% Na_2O; beyond 5·9% Na_2O there is no significant change. This agrees with the limit of solid solution shown in Figure 3. The measured differences between the *a* and *b* parameters show some discrepancies, probably due to the difficulty of measuring the position of almost coincident reflections.

Conclusions

The solid solution of Na_2O in C_3A has been investigated. In preparations made at 1,350°C it was confirmed that Na_2O replaced CaO. The sodium calcium aluminate formed at the limit of solid solution has the composition 91·0 mol % C_3A, 9·0 mol % N_3A. This compound has been indexed on an orthorhombic system with cell dimensions $a = 15{\cdot}314$, $b = 15{\cdot}394$, $c = 15{\cdot}137$ Å. For preparations containing up to 2% Na_2O there is a slight contraction of the lattice dimension of the cubic C_3A; between 2 and 4% Na_2O a mixture of cubic and orthorhombic forms is found and at 4% Na_2O a single orthorhombic form occurs. Further solid solution causes a slight modification of the orthorhombic lattice dimension until the limit of solid solution is reached with 6% Na_2O. The X-ray diffraction pattern obtained when the phase contains between 4 and 6% Na_2O agrees well with that given by Moore for a new phase in Portland cements which she concluded to be a new C_3A phase in which additional oxides, Na_2O, K_2O, MgO or even Fe_2O_3 or traces of TiO_2 had lowered the symmetry from cubic to orthorhombic. It cannot, however, be concluded that the new phase is stabilized solely by Na_2O since the analyses of Moore appear to preclude the possibility of even 4% Na_2O being retained in the new phase in some of the cements investigated.

ACKNOWLEDGEMENTS

The authors would like to thank R. Filmer for writing the computer programme and L. J. Larner for carrying out the sodium analyses. The work described forms part of the research programmes of the Building Research Station and the Cement and Concrete Association and this paper is published by permission of the Director of Building Research and the Director of Research of the Cement and Concrete Association.

REFERENCES

1. BROWNMILLER, L. T. and BOGUE, R. H. System $CaO-Na_2O-Al_2O_3$. *Journal of Research of the National Bureau of Standards.* Vol. 8. 1932. pp. 289–307.
2. BOGUE, R. H. Constitution of Portland cement clinker. *Proceedings of the Symposium on the Chemistry of Cements, Stockholm* 1938. Stockholm, Ingeniørsvetenskapsakademien, 1939. pp. 59–140.
3. GREEN, K. T. and BOGUE, R. H. Phase equilibrium relations in a portion of the system $Na_2O-CaO-Al_2O_3-SiO_2$. *Journal of Research of the National Bureau of Standards.* Vol. 36. February 1946. pp. 185–207.
4. SUZUKAWA, Y. Die Alkaliphasen im Portlandzement 1: Natriumphasen. *Zement-Kalk-Gips.* Vol. 9, No. 8. August 1956. pp. 345–351.
5. MOORE, A. E. Evidence for new phase occurring in Portland cements. *Nature.* Vol. 199, No. 4892. 3 August 1963. pp. 480–481.
6. CONWICKE, J. A. and DAY, D. E. Crystalline solubility of soda in tricalcium aluminate. *Journal of the American Ceramic Society.* Vol. 47, No. 12. December 1964. pp. 654–655.
7. PRESSLER, E. E., BRUNAUER, S. and KANTRO, D. L. Investigation of the Franke method of determining free calcium hydroxide and free calcium oxide. *Analytical Chemistry.* Vol. 28, No. 5. 1956. pp. 896–902.

51-5009 HS LTD 6/66 5

CURRENT PAPERS

RESEARCH SERIES - recent issues

31. BUTTERWORTH, B.
The frost resistance of bricks and tiles: A review

32. NEWBERRY, C.W.
Measuring the sonic boom and its effect on buildings

33. MARSLAND, A. and A.G. LOUDON
The flow properties and yield gradients of bentonite groups in sands and capillaries

34. NUTTALL, J.F.
Control of repetitive construction

35. PARKIN, P.H. and K. MORGAN
'Assisted resonance' in the Royal Festival Hall, London

36. LACY, R.E.
Some measurements of snow density

37. LOUDON, A.G. and E. DANTER
Investigations of summer overheating at the Building Research Station

38. LANGDON, F.J.
A study of annoyance caused by noise in automatic data processing offices

39. PETHERBRIDGE, P.
Sunpath diagrams and overlays for solar heat gain calculations

40. LANGDON, F.J.
Design of card punches and the seating of operators

41. DAWS, L.F., PENWARDEN, A.D., and G.T. WATERS
A visualization technique for the study of air movement in rooms

42. GUTT, W. and B. HINKINS
Sulphide content in Portland blast-furnace cement

43. BOOT, A.R. and A. WATSON
Applications of centimetric radio waves in non-destructive testing

44. NURSE, R.W., WELCH, J.H., AND A.J. MAJUMDAR
The $12CaO.7Al_2O_3$ phase in the $CaO-Al_2O_3$ system

45. PRATT, A.W.
Variable heat flow through walls of cavity construction, naturally exposed

46. FLETCHER, K.E.
The polymorphism of tricalcium silicate - a comparison of the effect of the Fe^{3+} and Al^{3+} ions

47. PENMAN, A.D.M. and G.H. WATSON
The improvement of a tank foundation by the weight of its own test load

48. PARKIN, P.H. and W.E. SCHOLES
The horizontal propagation of sound from a jet engine close to the ground, at Hatfield

49. WARD, W.H. and H.S.H. THOMAS
The development of earth loading and deformation in tunnel linings in London clay

50. LACY, R.E.
Driving rain at Garston, United Kingdom

Dr. H. G. Midgley.—The differential thermal analysis (D.T.A.) method can be a very useful tool in the investigation of calcareous materials, but some warnings should be given in its use if full benefit from the method is to be obtained. 30

If the method is to be made quantitative, great care is required to keep the base line straight; this can be helped by making the

two compartments of the crucible symmetrical, keeping the thermocouples to a minimum size and if possible using only one in each compartment. The heat capacities of the two sides should be kept as nearly equal as possible, by using an inert material in both sides with the sample under investigation as a diluent in the sample side.

The position of the peak in relation to its area can be plotted as peak temperature vs. $\log_e$ area of peak as in Fig. 2. The smaller the area, i.e., the smaller the amount of substance in a mixture, the lower is the peak temperature.

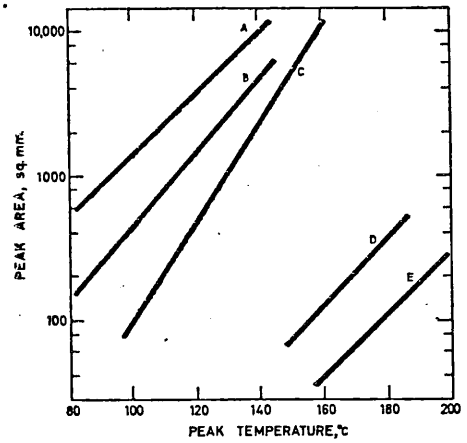

FIG. 2. *Relation between peak temperature and peak area*

A free water B tobermorite gel C $C_3A,CaSO_4,32H_2O$
D $C_4A,13H_2O$ E $C_3A,CaSO_4,13H_2O$

It can be seen from this diagram that it is possible for a phase, which in an undiluted state will have a peak temperature in excess of another phase, when diluted will have a lower peak temperature. Thus, the identity of a phase in a mixture may be established, in ideal circumstances, by determining the area and peak temperature and then finding on which line it lies. For example, a peak at 120° could be free water, tobermorite gel or ettringite ($C_3A,3CaSO_4,32\ H_2O$), but the peak areas would sort out which phase was present; viz., free water would have 4000 cm^2, tobermorite gel 2500 cm^2 and ettringite 440 cm^2.

The D.T.A. method is capable of great precision but must be used with care.

General discussion of the four preceding papers

Dr. H. G. Midgley.—The precision of the microscopical method of determining the quantities of the silicate phases in Portland cement clinker can be determined experimentally. The method in use in the Mineralogy Laboratory of the Building Research Station is the Gatgalov point counting method,[1] for which the clinker samples are prepared and etched with hydrofluoric acid by the Parker & Nurse method.[2]

So far we have determined the operator error, and error due to the size of the individual clinker pellets. The results are as follows:

	Coefficient of variation, %	
	$3CaO,SiO_2$	$2CaO,SiO_2$
Nine different observers	2·4	3·6
One observer, 6 times on same surface	1·7	3·0
Six samples, all same size	7·0	6·0
Six samples, all different sizes ..	14·0	15·0

These results show that variation from observer to observer is of the same order as that for one observer, although in this experiment the one observer was experienced, and of the nine observers, some had never used any form of microscope before.

The greatest variation is in sampling from the batch, for the size of clinker pellet used influences the result.

For average quantitative results for a clinker sample a method of 'quartering' will have to be evolved which will reduce the size error.

The microscopical point counting method shows great promise for the quantitative estimation of the silicate phases in Portland cement clinkers.

References

[1] Chayes, F., 'Petrographic Model Analysis', 1956 (New York)
[2] Parker, T. W., & Nurse, R. W., *J. Soc. chem. Ind., Lond.*, 1939, **58**, 1255